Hepatocelluar Carcinoma:
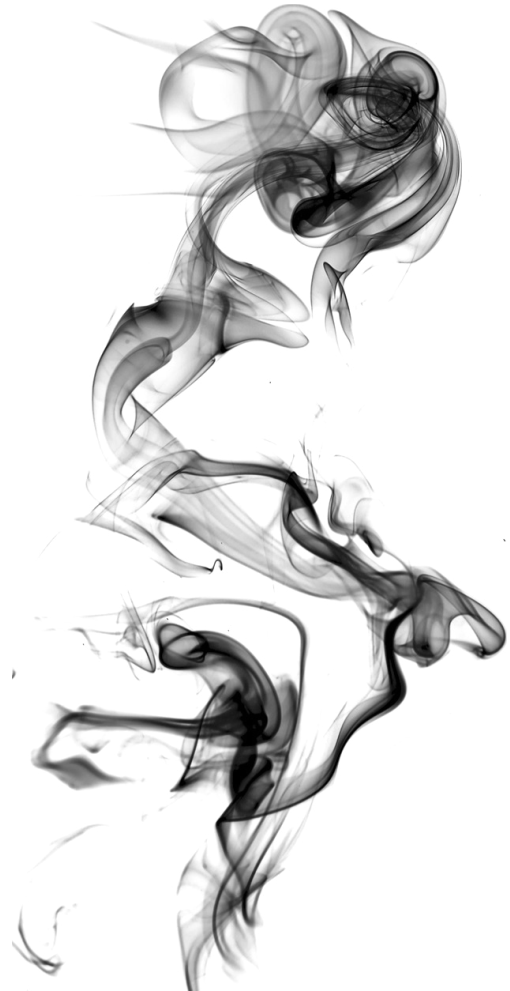# from Liquid Biopsy to Immunotherapy

Zhouhong Ge

Hepatocellular Carcinoma:
from Liquid Biopsy to Immunotherapy

Zhouhong Ge

Hepatocellular Carcinoma:
from Liquid Biopsy to Immunotherapy

Hepatocellulair carcinoom:

van vloeibare biopsie tot immunotherapie

Thesis

To obtain the degree of Doctor from the
Erasmus University Rotterdam
by command of the
rector magnificus

Prof. dr. F.A. van der Duijn Schouten

and in accordance with the decision of the Doctorate Board

The public defense shall be held on

Tuesday 1ˢᵗ June 2021 at 13:00

by

Zhouhong Ge

Born in Suzhou, Jiangsu Province, China

Doctoral Committee

Promotor:

Prof.dr. M.P. Peppelenbosch

Inner Committee:

Prof.dr. L.J.W. van der Laan

Prof.dr. W.N.M. Dinjens

Dr. L.L. Kodach

Copromotor:

Dr. D. Sprengers

Dr. Ing. J. Kraan

CONTENTS

CHAPTER 1

General introduction and aim of the thesis

Hepatocellular carcinoma (HCC)

Liver cancers was the sixth most commonly diagnosed cancer type and the fourth leading cause of cancer related death worldwide in 2018 [1]. Hepatocellular carcinoma (HCC) comprises 75%-85% of all liver cancer cases [1]. The main risk factors for HCC are chronic infection with hepatitis B virus (HBV) or hepatitis C virus (HCV), heavy alcohol intake, obesity, smoking and type 2 diabetes [2]. More than 80% of HCC patients are diagnosed at advanced stage (BCLC stage C) and their median survival is less than 2 years [3]. For patients at advanced stage, the FDA-approved first line treatments are the tyrosine inhibitors (TKIs,), sorafenib [4] or lenvatinib [5] which can prolong overall survival time by 3 months. The treatment options for late-stage HCC patients have been broadened with recent approval of additional TKIs (e.g. regorafenib [6] and cabozantinib [7]), as well as immunotherapies such as immune checkpoint inhibitors (nivolumab[8] and pembrolizumab[9]) and monoclonal IgG1 antibody targeting VEGFR2 (ramucirumab[10]). Nevertheless, a majority of patients will not respond to systemic agents or progress on these therapies. Both the current diagnosis and treatments of HCC remain to be improved.

Molecular diagnosis

The genetic landscape of hepatocellular carcinoma has been studied extensively. Recurrent somatic oncogenic drivers or tumor suppressors in several cellular pathways were identified (i.e, telomere maintenance, WNT signaling, cell-cycle control, chromatin remodeling, TP53, PI3K-TOR and MAPK pathways) [11-14] . Genomic pathway alterations in tumor cells were correlated with treatment response and outcome. HCC patients with vessels that encapsulate tumor clusters (VETC) pattern benefited more from sorafenib treatment (median overall survival (OS): 27.1 vs 12.7 months) [11]. In contrast, sorafenib is not effective for patients harboring activating mutations in the PI3K-mTOR pathway [15]. CTNNB1 mutated HCC does not show any inflammatory cell infiltration, which is thus considered as an immunologically cold tumor and thus less likely to benefit from immune therapy [11]. In apparent agreement, the presence of an activating WNT/beta-catenin mutation was also associated with tumor innate resistance to immune checkpoint inhibitors [11, 16, 17]. Thus, molecular profiling could facilitate the further understanding of tumor, the mechanism of primary resistance to treatments and better tailoring of therapeutic strategies.

Immunotherapy

Immunotherapy is a promising approach for the treatment of HCC[18]. The rationale for immunotherapy is based on the presence of high numbers of tumor-infiltrating T cells in HCC tissue[19], the correlation between the density of lymphocytic infiltrates in HCC lesions and prognosis[20] and most importantly, the finding that adoptive immunotherapy with interleukin (IL)-2/anti-CD3-stimulated autologous lymphocytes lowers postsurgical recurrence rate in humans [21].

HCC is shown to be immunogenic. In recent years, specific tumor associated antigens (TAAs) and their cytotoxic T lymphocytes (CTL) epitopes have been identified in HCC. TAA-specific CD8^{+} T cell responses to alpha-fetoprotein (AFP), glypican-3 (GPC-3), melanoma-associated antigen 1 (MAGE-A1), New York esophageal squamous cell carcinoma (NY-ESO-1) and human telomerase reverse transcriptase (hTERT) were detected in the circulation or tumor tissue of HCC patients[22-24]. Moreover, the presence of the responses correlates with patient survival [22]. However, in HCC these tumor-specific T cells become dysfunctional at the pre- and early malignant stage, possibly through a dynamic antigen-driven differentiation program in which T cells are exposed to chronic antigen stimulation[25]. Exhausted CD8^{+} T cells comprise heterogeneous cell populations with unique differentiation and functional states. A subset of these CD8^{+} T cells can be reinvigorated by immune checkpoint inhibitors (ICIs) (i.e. anti-PD-1/PDL-1 and anti CTLA4 monoclonal antibody) [26, 27]. Other strategies to restore function in exhausted CD8^{+} T cells are currently under evaluation—many in combination with PD-1-targeted therapy [26].

1. Liquid biopsies

Molecular diagnosis of HCC includes imaging-based approaches (e.g. EOB-MRI could identify *CTNNB1* mutated gene products), blood testing (e.g. AFP serum level) and histology. For advanced HCC, patients are not eligible for surgery and tumor tissue is usually obtained by needle biopsies. This procedure is invasive and the limited tissue collected cannot represent the heterogeneity of the whole tumor. Liquid biopsies, including circulating tumor cells (CTCs) and cell-free tumor DNA (cfDNA), have been explored to identify tumor-derived mutations for diagnosis and targeted therapies through non-invasive blood sampling.

4

1.1 Circulating tumor cells

CTCs are cells that have detached from a primary or secondary tumor and enter circulation [28], and are regarded as seeds for metastasis. There has been a technical challenge to capture them due to the extremely low frequency, estimated ≤1 CTC/ml of blood in billions of blood cells. CellSearch is a standardized and validated method to detect EpCAM+ CTCs from epithelial tumors not including HCC [29]. Nevertheless, many studies show that CellSearch identifies CTCs in 16%-67% HCC patients in both early or late stage disease [30-37]. Other enrichment methods include size-based enrichment [38], density-based RosetteSep negative selection [39], magnetic negative selection[40], flowcytometric detection[41] and microfluidic enrichment[42]. Most CTCs studies report prognostic value of CTC numbers in HCC [30, 33-35, 37, 38, 43, 44]. The CTC-positive rate in peripheral blood was associated with the tumor size, AFP, vascular invasion and overall survival [30, 35, 36, 38, 44]. A preoperative CTC positivity is a predictor for tumor recurrence in HCC patients after surgery [33, 34]. The increase in postoperative CTC counts was significantly associated with the macroscopic tumor thrombus and shorter overall survival [37]. Moreover, to help guide treatment decisions, for instance to initiate or switch targeted therapy, it is important to determine the nature of the somatic mutations present in the cancer. Because of the risks associated with repeated tumor biopsies, it is attractive to use liquid biopsies for this purpose. Mutational analysis in CTCs can be performed by DNA sequencing [36, 45]. However, CTCs found by numerous methods have often not been analyzed for DNA mutations, likely due to limited numbers and inefficiency of single cell isolation techniques.

1.2 Circulating tumor DNA

Circulating tumor DNA (ctDNA) is the fraction of cell-free DNA that is derived from primary or metastatic tumors. The fraction of circulating mutant DNA fragments is very small, sometimes less than 0.01% [46], compared to circulating wildtype DNA fragments, making it difficult to detect and quantify [47]. The development of next generation sequencing (NGS), especially deep sequencing, and droplet digital PCR (ddPCR) have facilitated the identification of genetic variants in ctDNA. Chan et al. was the first to report analysis of ctDNA by shotgun sequencing of plasma samples from HCC patients in the early stage of the disease. The ctDNA concentration, determined by single nucleotide variants (SNVs) analysis, was found to range from 2.1% to 53% before surgery and from 0.4% -1.3% after surgery [48]. Frequent HCC-associated

mutations (e.g. *TP53*, *TERT*, *CTNNB1*, *APC*, *EGFR*, *MET* and *ARID1A*) were detected in cfDNA by NGS sequencing in advanced [49, 50] and operable HCC [51, 52]. The presence of somatic mutations in ctDNA before surgery could predict microvascular invasion in resectable HCC patients[51, 52]. Moreover, postoperative residual ctDNA was an independent risk factor for recurrence and poor disease-free survival in HCC patients[53]. Somatic mutations detected in ctDNA can guide treatment decisions with regard to targeted therapies. Mutation analysis of NRAS/KRAS/BRAF, PIK3CA and CSF-1R in plasma has been applied in a phase 2 clinical trial to assess response to a mitogen-activated protein kinase kinase (MEK) inhibitor (refametinib) in advanced HCC patients[54].

2. Immune checkpoints

Primary T cell activation involves the integration of three distinct signals: (1) antigen recognition, (2) costimulation, and (3) cytokine-mediated differentiation and expansion [55]. Immune checkpoints are molecules that either turn-up (co-stimulatory) or turn-down immune signals (co-inhibitory). Inhibitory checkpoint receptors, such as cytotoxic T-lymphocyte-associated protein 4 (CTLA-4), programmed cell death protein 1 (PD-1), lymphocyte-activation gene 3 protein (LAG-3), T cell immunoglobulin and mucin 3 domain (TIM-3), T cell immunoreceptor with Ig and ITIM domains (TIGIT), and others, are immunosuppressive molecules, as they negatively regulate activation of the immune effector cells. In cancer, these molecule can be upregulated on intratumoral T cells and NK cells and responsible for immune exhaustion of the effector cells and downregulation of antitumor response. Many cancers are able to evade the immune system, mainly by overexpressing inhibitory ligands to evade T cell attack[56].

Increased expression of inhibitory checkpoints on T cells was observed in HCC and correlated to HCC outcome. Tumors with a PD1^{high} signature were associated with poorer survival outcomes in HCC patients in the The Cancer Genome Atlas (TCGA) cohort [57]. PD1^{high} or PD1^{high} TIM3$^+$ CD8$^+$ T cells were significantly correlated with poor OS and RFS, and PD1^{high} TIM3$^+$ CD8$^+$ T cell subset was located closely to PD-L1$^+$ tumor associated macrophages [58]. Higher number of Tim-3$^+$ tumor-infiltrating T cells (TILs) or higher levels of serum soluble TIM3 were associated with poorer survival in patients with HBV-associated HCC [59, 60]. Blocking the Tim-3 signaling pathway is able to reverse the impaired function of CD8$^+$ or CD4$^+$ TILs in HCC [59, 61]. Expression of

6

LAG3 was found to be significantly higher on TAA-specific CD8^{+} tumor-infiltrating T helper cells and CD8^{+} cytotoxic T cells in tumors than those in tumor-free liver tissues of HCC patients [61]. Combined blockade of PD-L1 with TIM3, LAG3, or CTLA-4 further restored responses of human HCC tumor-derived T cells to TAAs in *ex vivo* assays compared to PD-L1 blockade alone[61]. The expression of TIGIT on intratumoral T cells correlates with PD-1 expression and marks intratumoral T cells with reduced effector functions [62-64]. A recent global phase II trial (CITYSCAPE) showed the improved efficacy of tiragolumab (anti-TIGIT hIgG1 antibody) in combination with atezolizumab (anti-PD-L1 hIgG1 antibody) compared to atezolizumab alone in PD-L1-positive metastatic NSCLC patients [65]. Thus, inhibitory checkpoints are promising immunotherapeutic targets for HCC.

3. Cancer testis antigens

Cancer testis antigens (CTAs) are a family of proteins that are highly expressed in immune-privileged germ cells and in cancer cells of various histological subtypes [66]. As CTAs have also shown to be immunogenic, these antigens are considered as suitable shared tumor antigens for cancer immunotherapy, including therapeutic vaccination [66, 67]. Based on their expression profile in adult healthy tissues, they are classified into testis-restricted, testis/brain-restricted and testis-selective CTAs, the last group having additional expression in somatic tissues [68]. As testis-restricted CTAs are solely expressed in immune-privileged germ cells, they can therefore be safely applied for cancer immunotherapy [68, 69].

Several CTAs such as the MAGE-family members, testis-specific Y-encoded protein (TSPY) and cancer antigen 1 (CAGE1), are functionally involved in inhibiting cancer cell growth and metastasis formation by modulating gene expression, regulating mitosis and tumorigenic signaling [66, 67]. In HCC, MAGE-A9 expression was related to the presence of portal vein invasion and distant metastasis and was an independent negative prognostic factor for disease-free survival and overall survival [70]. MAGE-C2 is the most studied CTA in HCC and its protein expression was detected in 19.5% - 47.4% HCC patients [71-73]. High MAGE-C2 expression could be an independent prognostic factor for overall survival in HCC [71]. MAGE-C1 and G antigen (GAGE) protein were expressed in around 12% of HCC patients and the positivity of MAGE-C1 or GAGE was correlated with reduced overall survival in patients with HCC [72]. TSPY

mRNA was expressed in 35.1% HCC samples and 6.6% HCC patients had serum Ab responses specific to recombinant TSPY protein [74]. In addition, NY-ESO-1 was detected in 24% of HCC-patients and 12% of HCC patients showed serum Ab responses to this antigen[75]. Immunotherapeutic targeting of CTA-expressing tumor cells by vaccination or other immunotherapeutic strategies, such as bispecific antibodies, TCR-engineered T cells or CAR T cells, are being explored.

4. Aim and outline of this thesis

From the above it is clear that there is a significant clinical need with regard to HCC for better therapy and for better targeted therapy. Addressing these concerns has been the aim of this thesis. To this end I first aim to explore a fluorescence-activated cell sorting(FACS) method to maximally enrich for CTCs from HCC patients and compare this strategy with the FDA-approved CellSearch method which can only enrich EpCAM+ CTCs, in the hope that better sorting strategies for CTCs will yield sufficient material of acceptable purity as to develop targeted therapies. The efforts involved are described in **Chapter 2** but unfortunately I am forced to conclude that the low number of CTCs do not allow meaningful success of such a strategy. Nevertheless, targeted therapy is still best hope for the first line treatment for patients with advanced HCC. Thus my second aim is to explore feasibility of detection of tumor-associated mutations in paired CTCs and cfDNA in a western cohort of HCC patients (**Chapter 3**), which proved more promising but also showed that novel therapeutic modalities are required. Encouragingly, immunotherapy is shifting the paradigm of HCC treatment and I decided to investigate the potential of making relevant contributions in this area. Thus in **Chapter 5**, I aim to investigate whether targeting the immunomodulatory molecule TIGIT has added value when compared to PD-1 monotherapy employing a model system in which I use the TILs of patients in *ex vivo* assays and I show promise of this strategy. Thus encouraged to further explore immunity-related strategies in HCC, in **Chapter 6**, I aim to evaluate the expression of cancer testis antigens (which can be attractive immune targets in the treatment of cancer) in HCC tumors and I compare these results to tumor-free liver. Additionally, I correlate their expression to patient prognosis. Furthermore, I attempt to screen a panel of CTAs that are frequently expressed in tumors of HCC patients but not in any healthy tissue except testis, with the aim purposing such CTAs for therapeutic vaccination. In conjunction, I hope that

the body of the work involved provides a meaningful contribution to the fight of humankind against HCC.

References

1. Bray F, Ferlay J, Soerjomataram I, et al. Global cancer statistics 2018: GLOBOCAN estimates of incidence and mortality worldwide for 36 cancers in 185 countries. CA Cancer J Clin 2018;68:394-424.
2. McGlynn KA, Petrick JL, London WT. Global Epidemiology of Hepatocellular Carcinoma: An Emphasis on Demographic and Regional Variability. Clinics in Liver Disease 2015;19:223-238.
3. European Association For The Study Of The L. EASL clinical practice guidelines: management of hepatocellular carcinoma. Journal of hepatology 2018;69:182-236.
4. Llovet JM, Ricci S, Mazzaferro V, et al. Sorafenib in Advanced Hepatocellular Carcinoma. New England Journal of Medicine 2008;359:378-390.
5. Kudo M, Finn RS, Qin S, et al. Lenvatinib versus sorafenib in first-line treatment of patients with unresectable hepatocellular carcinoma: a randomised phase 3 non-inferiority trial. The Lancet 2018;391:1163-1173.
6. Bruix J, Qin S, Merle P, et al. Regorafenib for patients with hepatocellular carcinoma who progressed on sorafenib treatment (RESORCE): a randomised, double-blind, placebo-controlled, phase 3 trial. Lancet 2017;389:56-66.
7. Abou-Alfa GK, Meyer T, Cheng AL, et al. Cabozantinib in Patients with Advanced and Progressing Hepatocellular Carcinoma. N Engl J Med 2018;379:54-63.
8. El-Khoueiry AB, Sangro B, Yau T, et al. Nivolumab in patients with advanced hepatocellular carcinoma (CheckMate 040): an open-label, non-comparative, phase 1/2 dose escalation and expansion trial. Lancet 2017;389:2492-2502.
9. Zhu AX, Finn RS, Edeline J, et al. Pembrolizumab in patients with advanced hepatocellular carcinoma previously treated with sorafenib (KEYNOTE-224): a non-randomised, open-label phase 2 trial. Lancet Oncol 2018;19:940-952.
10. Zhu AX, Park JO, Ryoo BY, et al. Ramucirumab versus placebo as second-line treatment in patients with advanced hepatocellular carcinoma following first-line therapy with sorafenib (REACH): a randomised, double-blind, multicentre, phase 3 trial. Lancet Oncol 2015;16:859-70.
11. Harding JJ, Nandakumar S, Armenia J, et al. Prospective Genotyping of Hepatocellular Carcinoma: Clinical Implications of Next-Generation Sequencing for Matching Patients to Targeted and Immune Therapies. Clinical Cancer Research 2019;25:2116.
12. Ally A, Balasundaram M, Carlsen R, et al. Comprehensive and integrative genomic characterization of hepatocellular carcinoma. Cell 2017;169:1327-1341. e23.
13. Zucman-Rossi J, Villanueva A, Nault J-C, et al. Genetic landscape and biomarkers of hepatocellular carcinoma. Gastroenterology 2015;149:1226-1239. e4.
14. Fujimoto A, Totoki Y, Abe T, et al. Whole-genome sequencing of liver cancers identifies etiological influences on mutation patterns and recurrent mutations in chromatin regulators. Nature genetics 2012;44:760-764.
15. Lindblad O, Cordero E, Puissant A, et al. Aberrant activation of the PI3K/mTOR pathway promotes resistance to sorafenib in AML. Oncogene 2016;35:5119-5131.
16. Spranger S, Bao R, Gajewski TF. Melanoma-intrinsic β-catenin signalling prevents anti-tumour immunity. Nature 2015;523:231-235.
17. Xiao Q, Wu J, Wang W-J, et al. DKK2 imparts tumor immunity evasion through β-catenin-independent suppression of cytotoxic immune-cell activation. Nature medicine 2018;24:262.
18. Mellman I, Coukos G, Dranoff G. Cancer immunotherapy comes of age. Nature 2011;480:480-489.
19. Yoong KF, McNab G, Hübscher SG, et al. Vascular adhesion protein-1 and ICAM-1 support the adhesion of tumor-infiltrating lymphocytes to tumor endothelium in human hepatocellular carcinoma. The Journal of Immunology 1998;160:3978-3988.
20. Gabrielson A, Wu Y, Wang H, et al. Intratumoral CD3 and CD8 T-cell densities associated with relapse-free survival in HCC. Cancer immunology research 2016;4:419-430.

21. Takayama T, Sekine T, Makuuchi M, et al. Adoptive immunotherapy to lower postsurgical recurrence rates of hepatocellular carcinoma: a randomised trial. The Lancet 2000;356:802-807.
22. Flecken T, Schmidt N, Hild S, et al. Immunodominance and functional alterations of tumor-associated antigen-specific CD8+ T-cell responses in hepatocellular carcinoma. Hepatology 2014;59:1415-26.
23. Mizukoshi E, Nakamoto Y, Marukawa Y, et al. Cytotoxic T cell responses to human telomerase reverse transcriptase in patients with hepatocellular carcinoma. Hepatology 2006;43:1284-1294.
24. Mizukoshi E, Nakamoto Y, Arai K, et al. Comparative analysis of various tumor-associated antigen-specific t-cell responses in patients with hepatocellular carcinoma. Hepatology 2011;53:1206-16.
25. Schietinger A, Philip M, Krisnawan VE, et al. Tumor-Specific T Cell Dysfunction Is a Dynamic Antigen-Driven Differentiation Program Initiated Early during Tumorigenesis. Immunity 2016;45:389-401.
26. Masao H, Alice OK, Se Jin I, et al. CD8 T Cell Exhaustion in Chronic Infection and Cancer: Opportunities for Interventions. Annual Review of Medicine 2018;69:301-318.
27. Blackburn SD, Shin H, Freeman GJ, et al. Selective expansion of a subset of exhausted CD8 T cells by αPD-L1 blockade. Proceedings of the National Academy of Sciences 2008;105:15016-15021.
28. Ashworth TR. A case of cancer in which cells similar to those in the tumours were seen in the blood after death. Aust Med J 1869;14:146.
29. Millner LM, Linder MW, Valdes R. Circulating tumor cells: a review of present methods and the need to identify heterogeneous phenotypes. Annals of Clinical & Laboratory Science 2013;43:295-304.
30. Schulze K, Gasch C, Staufer K, et al. Presence of EpCAM-positive circulating tumor cells as biomarker for systemic disease strongly correlates to survival in patients with hepatocellular carcinoma. Int J Cancer 2013;133:2165-71.
31. Morris KL, Tugwood JD, Khoja L, et al. Circulating biomarkers in hepatocellular carcinoma. Cancer Chemother Pharmacol 2014;74:323-32.
32. Zee BC, Wong C, Kuhn T, et al. Detection of circulating tumor cells (CTCs) in patients with hepatocellular carcinoma (HCC). Journal of Clinical Oncology 2007;25:15037-15037.
33. Sun Y-F, Xu Y, Yang X-R, et al. Circulating stem cell–like epithelial cell adhesion molecule–positive tumor cells indicate poor prognosis of hepatocellular carcinoma after curative resection. Hepatology 2013;57:1458-1468.
34. von Felden J, Schulze K, Krech T, et al. Circulating tumor cells as liquid biomarker for high HCC recurrence risk after curative liver resection. Oncotarget 2017;8:89978.
35. Fang Z-T, Zhang W, Wang G-Z, et al. Circulating tumor cells in the central and peripheral venous compartment–assessing hematogenous dissemination after transarterial chemoembolization of hepatocellular carcinoma. OncoTargets and therapy 2014;7:1311.
36. Kelley RK, Magbanua MJM, Butler TM, et al. Circulating tumor cells in hepatocellular carcinoma: a pilot study of detection, enumeration, and next-generation sequencing in cases and controls. BMC cancer 2015;15:206.
37. Yu J-j, Xiao W, Dong S-l, et al. Effect of surgical liver resection on circulating tumor cells in patients with hepatocellular carcinoma. BMC Cancer 2018;18:835.
38. Vona G, Estepa L, Béroud C, et al. Impact of cytomorphological detection of circulating tumor cells in patients with liver cancer. Hepatology 2004;39:792-797.
39. Guo W, Yang X-R, Sun Y-F, et al. Clinical significance of EpCAM mRNA-positive circulating tumor cells in hepatocellular carcinoma by an optimized negative enrichment and qRT-PCR–based platform. Clinical cancer research 2014;20:4794-4805.
40. Lapin M, Tjensvoll K, Oltedal S, et al. MINDEC-an enhanced negative depletion strategy for circulating tumour cell enrichment. Scientific reports 2016;6:28929.
41. Ogle LF, Orr JG, Willoughby CE, et al. Imagestream detection and characterisation of circulating tumour cells - A liquid biopsy for hepatocellular carcinoma? J Hepatol 2016;65:305-13.

42. Kalinich M, Bhan I, Kwan TT, et al. An RNA-based signature enables high specificity detection of circulating tumor cells in hepatocellular carcinoma. Proceedings of the National Academy of Sciences 2017;114:1123-1128.

43. Xu W, Cao L, Chen L, et al. Isolation of circulating tumor cells in patients with hepatocellular carcinoma using a novel cell separation strategy. Clinical Cancer Research 2011;17:3783-3793.

44. Ogle LF, Orr JG, Willoughby CE, et al. Imagestream detection and characterisation of circulating tumour cells–A liquid biopsy for hepatocellular carcinoma? Journal of hepatology 2016;65:305-313.

45. Boral D, Vishnoi M, Liu HN, et al. Molecular characterization of breast cancer CTCs associated with brain metastasis. Nature communications 2017;8:1-10.

46. Diehl F, Li M, Dressman D, et al. Detection and quantification of mutations in the plasma of patients with colorectal tumors. Proceedings of the National Academy of Sciences 2005;102:16368-16373.

47. Diehl F, Schmidt K, Choti MA, et al. Circulating mutant DNA to assess tumor dynamics. Nature Medicine 2008;14:985-990.

48. Chan KCA, Jiang P, Zheng YWL, et al. Cancer Genome Scanning in Plasma: Detection of Tumor-Associated Copy Number Aberrations, Single-Nucleotide Variants, and Tumoral Heterogeneity by Massively Parallel Sequencing. Clinical Chemistry 2013;59:211-224.

49. Ikeda S, Tsigelny IF, Skjevik ÅA, et al. Next-Generation Sequencing of Circulating Tumor DNA Reveals Frequent Alterations in Advanced Hepatocellular Carcinoma. The oncologist 2018;23:586-593.

50. Kaseb AO, Sánchez NS, Sen S, et al. Molecular Profiling of Hepatocellular Carcinoma Using Circulating Cell-Free DNA. Clinical Cancer Research 2019;25:6107.

51. Wang J, Huang A, Wang YP, et al. Circulating tumor DNA correlates with microvascular invasion and predicts tumor recurrence of hepatocellular carcinoma. Ann Transl Med 2020;8:237.

52. Wang D, Xu Y, Goldstein JB, et al. Preoperative evaluation of microvascular invasion with circulating tumor DNA in operable hepatocellular carcinoma. Liver Int 2020.

53. An Y, Guan Y, Xu Y, et al. The diagnostic and prognostic usage of circulating tumor DNA in operable hepatocellular carcinoma. American journal of translational research 2019;11:6462-6474.

54. Kim R, Tan E, Wang E, et al. A Phase I Trial of Trametinib in Combination with Sorafenib in Patients with Advanced Hepatocellular Cancer. The oncologist 2020;25:e1893-e1899.

55. Sckisel GD, Bouchlaka MN, Monjazeb AM, et al. Out-of-sequence signal 3 paralyzes primary CD4+ T-cell-dependent immunity. Immunity 2015;43:240-250.

56. Xu F, Jin T, Zhu Y, et al. Immune checkpoint therapy in liver cancer. Journal of Experimental & Clinical Cancer Research 2018;37:1-12.

57. Kim HD, Song GW, Park S, et al. Association Between Expression Level of PD1 by Tumor-Infiltrating CD8(+) T Cells and Features of Hepatocellular Carcinoma. Gastroenterology 2018;155:1936-1950 e17.

58. Ma J, Zheng B, Goswami S, et al. PD1 Hi CD8+ T cells correlate with exhausted signature and poor clinical outcome in hepatocellular carcinoma. Journal for immunotherapy of cancer 2019;7:1-15.

59. Li H, Wu K, Tao K, et al. Tim-3/galectin-9 signaling pathway mediates T-cell dysfunction and predicts poor prognosis in patients with hepatitis B virus-associated hepatocellular carcinoma. Hepatology 2012;56:1342-1351.

60. Li F, Li N, Sang J, et al. Highly elevated soluble Tim-3 levels correlate with increased hepatocellular carcinoma risk and poor survival of hepatocellular carcinoma patients in chronic hepatitis B virus infection. Cancer management and research 2018;10:941.

61. Zhou G, Sprengers D, Boor PPC, et al. Antibodies Against Immune Checkpoint Molecules Restore Functions of Tumor-Infiltrating T Cells in Hepatocellular Carcinomas. Gastroenterology 2017;153:1107-1119 e10.

62. Johnston RJ, Comps-Agrar L, Hackney J, et al. The immunoreceptor TIGIT regulates antitumor and antiviral CD8(+) T cell effector function. Cancer Cell 2014;26:923-937.

63. Josefsson SE, Huse K, Kolstad A, et al. T cells expressing checkpoint receptor TIGIT are enriched in follicular lymphoma tumors and characterized by reversible suppression of T-cell receptor signaling. Clinical Cancer Research 2018;24:870-881.

64. Josefsson SE, Beiske K, Blaker YN, et al. TIGIT and PD-1 mark intratumoral T cells with reduced effector function in B-cell non-Hodgkin lymphoma. Cancer immunology research 2019;7:355-362.

65. Rodriguez-Abreu D, Johnson ML, Hussein MA, et al. Primary analysis of a randomized, double-blind, phase II study of the anti-TIGIT antibody tiragolumab (tira) plus atezolizumab (atezo) versus placebo plus atezo as first-line (1L) treatment in patients with PD-L1-selected NSCLC (CITYSCAPE): American Society of Clinical Oncology, 2020.

66. Gjerstorff MF, Andersen MH, Ditzel HJ. Oncogenic cancer/testis antigens: prime candidates for immunotherapy. Oncotarget 2015;6:15772.

67. Whitehurst AW. Cause and consequence of cancer/testis antigen activation in cancer. Annual review of pharmacology and toxicology 2014;54:251-272.

68. Hofmann O, Caballero OL, Stevenson BJ, et al. Genome-wide analysis of cancer/testis gene expression. Proceedings of the National Academy of Sciences 2008;105:20422-20427.

69. Djureinovic D, Hallström BM, Horie M, et al. Profiling cancer testis antigens in non–small-cell lung cancer. JCI insight 2016;1.

70. Gu X, Fu M, Ge Z, et al. High expression of MAGE-A9 correlates with unfavorable survival in hepatocellular carcinoma. Scientific reports 2014;4:6625.

71. Gu X, Mao Y, Shi C, et al. MAGEC2 Correlates With Unfavorable Prognosis And Promotes Tumor Development In HCC Via Epithelial-Mesenchymal Transition. Onco Targets Ther 2019;12:7843-7855.

72. Riener M-O, Wild PJ, Soll C, et al. Frequent expression of the novel cancer testis antigen MAGE-C2/CT-10 in hepatocellular carcinoma. International Journal of Cancer 2009;124:352-357.

73. Sideras K, Bots SJ, Biermann K, et al. Tumour antigen expression in hepatocellular carcinoma in a low-endemic western area. Br J Cancer 2015;112:1911-20.

74. Yin YH, Li YY, Qiao H, et al. TSPY is a cancer testis antigen expressed in human hepatocellular carcinoma. British Journal of Cancer 2005;93:458-463.

75. Korangy F, Ormandy LA, Bleck JS, et al. Spontaneous tumor-specific humoral and cellular immune responses to NY-ESO-1 in hepatocellular carcinoma. Clinical cancer research 2004;10:4332-4341.

12

CHAPTER 2

Isolation of circulating tumor cells by RosetteSep enrichment and fluorescence-activated cell sorting (FACS) in patients with hepatocellular carcinoma

Zhouhong Ge[1], Patrick P.C.Boor[1], Maikel Peppelenbosch[1], Jaap Kwekkeboom[1], Jaco Kraan[2], Dave Sprengers[1].

Departments of [1]Gastroenterology and Hepatology, [2]Medical Oncology, Erasmus MC-University Medical Center, Rotterdam, the Netherlands

Abstract

Background and aims: Circulating tumor cells (CTCs) are proposed to constitute an attractive source of cancer material that can guide clinical decision-making in. hepatocellular carcinoma (HCC). A number of approaches have been developed to detect CTCs in HCC patients but their usefulness in clinical practice has not been demonstrated. Hence, here we investigated the feasibility of pre-enrichment combined with fluoresecne-activated cell sorting (FACS) for isolation of CTCs from the blood of HCC patients.

Methods: Expression of ASGPR1, GPC3 and EpCAM by tumor cells was determined using tissue microarrays (TMAs) with cores of normal liver tissue, tumors and paired tumor-free liver tissues from 133 HCC-patients by immunohistochemistry (IHC). Fifteen HCC patients were enrolled and 22.5 mL peripheral blood from each patient was obtained. RosetteSep CD45 depletion combined with FACS was optimized to allow CTC isolation from patient blood. From each patient, the single cell fraction that was either CD45- DRAQ5+CK+ or ASGPR1+ or GPC3+ or EpCAM+ was isolated by FACS and evaluated by PCR.

Results: IHC on TMAs demonstrates that in 98% of HCC patient tumors express either ASGPR1, GPC3 or EpCAM and only 2% of patients express non of the three markers. The recovery rate of RosetteSep ranges from 43.9% to 51% and the recovery rate of FACS ranges from 56% to 64%. The combination of RosetteSep enrichment with flow sorting using anti-ASGPR1, GPC3 and EpCAM antibodies resulted in a final recovery of 6% to 12% of spiked target cells. We detected low numbers of CTCs (1-21 in 22.5ml blood) in blood of all HCC patients but failed to isolate DNA from these potential CTCs.

Conclusions: We established a panel of ASGPR1, GPC3, EpCAM and CK for capturing CTCs and this panel can potentially detect cancer cells in 98% of HCC patients. We did not observe a strong increase of CTCs using a panel of multiple markers. We sorted the low numbers of putative CTC events but we failed to isolate DNA from these cells, hence FACS of CTCs is not a promising avenue for precision medicine in HCC.

Key words: RosetteSep™ immunodensity cell separation; fluorescence-activated cell sorting; single cell analysis

14

Introduction

Currently, very little is known about the biology and molecular characteristics of circulating tumor cells (CTCs). This paucity of information can be attributed to the technical challenges associated with isolating these rare cells, of which the frequency is estimated to be ≤1 per mL of blood. There is a need to elucidate the biology of the tumor cells, including their role in tumor metastasis and progression. It has been shown in breast[1] and prostate cancer[2] there is a clonal relationship between CTCs and matched archival primary tumors via genome-wide copy number variation (CNV) analysis. In addition, the genetic alteration information may have more accurate prognostic value as well as therapeutic value.

A number of approaches have been developed to detect and enumerate tumor cells in blood samples. CellSearch is still the first and only clinically validated FDA-approved test to capture and enumerate EpCAM$^+$ CTCs from epithelial tumors and this assay has shown prognostic and predictive significance in breast [3], colorectal [4] and prostate cancer patients [5]. However, this approach may miss EpCAM- CTCs. In Western hepatocellular carcinoma (HCC) patients, EpCAM is expressed in less than 20% of tumors[6, 7] and so in this disease there is a need for additional techniques to isolate CTCs from blood. Alternative strategies for CTC isolation consists of the combination of less specific enrichment steps including negative selection (density [8], size [9] or magnetism-based [10]) or positive selection (magnetism-based[11]), followed by more specific characterization of enriched cells with techniques like immunocytochemistry (ICC) [12-14] and nucleic acid-based assays using reverse transcriptase-polymerase chain reaction (RT-PCR) [15, 16] or sequencing [17]. However, none of these approaches lead to direct isolation of CTCs. RT-PCR based methods detect cancer-related genes in bulk cells and have high noise to signal ratio, which means that it is difficult to acquire true signals of those rare tumor cells. With ICC and other slides-based methods, usually enumeration of CTCs is performed, whereas isolating CTCs by micromanipulation is technically demanding. All CTC enrichment methods are hampered by contamination with normal cells, which mandates a further step of purification to enable reliable downstream genetic analysis. It is important to verify that the isolated single and pooled putative CTCs are bona fide cancer cells by DNA analysis for mutation[18, 19], methylation[20, 21] or copy number variation (CNV) [22, 23].

The combination of pre-enrichment (not CellSearch based) with FACS for CTC isolation has been demonstrated to be promising in breast cancer [1, 24] or prostate cancer [2]. However, its usefulness in the setting of HCC has not been explored yet. Considering the observed relatively low EpCAM expression in HCC, we searched for alternative cell surface markers that can be used to identify and isolate CTCs from peripheral blood of HCC patients, using FACS. In this study, we investigated the feasibility of the combination of pre-enrichment from whole blood of these target cells by negative selection and standard density gradient centrifugation, followed by flow cytometric analysis and subsequent cell sorting. Eventually, we aim to perform genomic analysis using the purified CTCs.

Material and Methods

Patients and blood collection

A total of 15 advanced HCC-patients were enrolled in the study between May 2018 and July 2019. Peripheral blood samples (22.5 mL) from each patient were collected into Cellsave tubes. The study was approved by the local ethics committee, and written informed consent was obtained from each patient. The clinical characteristics of the 16 patients are summarized in **Table S1**.

Blood processing

Blood samples were processed within 24 hours after collection. Blood was first centrifuged at 1700g for 10min to separate plasma and blood cells. The blood cells from the first centrifugation were used to isolate CTCs using RosetteSep enrichment combined with FACS. Potential CTC events from each patient that were CD45-DRAQ5+CK+/ASGPR1+/ GPC3+/EpCAM+ were sorted and pooled to a PCR vial for further analysis.

Cell line

The human HCC cell line HepG2 was purchased from ATCC and used in spiking experiments. The cell line was maintained in DMEM (Gibco) supplemented with 10% fetal calf serum (FCS)(Gibco), 1% penicillin-streptomycin, at 37°C under 5% CO_2 in incubator. The cell line was routinely screened for the presence of mycoplasma during experiments.

16

Optimization of RosetteSep enrichment combined with FACS

To determine the recovery rate of RosetteSep enrichment, HepG2 cells were spiked into 2-7.5mL of blood from a healthy donor. These samples were processed by negative selection method using RosetteSep[TM] Human CD45 depletion cocktail (StemCell, Vancouver, Canada) according to manufacturer's instructions. After enrichment, HepG2 cells were counted using CellSearch system to calculate the recovery of RosetteSep enrichment. To determine the recovery rate of FACS, HepG2 cells were spiked directly in 2×10^5 PBMC and stained with DRAQ5, anti-CK, CD45, ASGPR1, GPC-3 and EpCAM antibodies (**Table S2**). HepG2 cells were flow-sorted to 96-well flat bottom plates and counted using fluorescence microscope. To further determine the recovery rate of combining RosetteSep and FACS, RosetteSep enriched cells were stained with DRAQ5, CK, CD45, ASGPR1, GPC3 and EpCAM, then flow-sorted to 96-well flat bottom plate and counted under fluorescence microscope. The recovery rate was calculated as following: recovered rate (%) = (number of cells recovered/number of cells spiked) x 100%.

Statistical analysis

The distribution of all data sets was analyzed for normality using the Shapiro-Wilk test. The differences between paired groups of data were analyzed according to their distribution via paired *t* test or Wilcoxon matched pairs test. Differences between different groups of patients were analyzed via *t* test or Mann-Whitney test. Statistical analysis was performed using Graphpad Prism 8.0. *P* value less than 0.05 was considered statistically significant (*$P < 0.05$; **$P < 0.01$; ***$P < 0.001$; ****$P < 0.0001$).

A detailed description of other methods is provided in the **Supplemental information**.

Results

Expression of liver and HCC-specific markers in HCC tissue

EpCAM[+] CTCs have been detected in only a minority of HCC patients in Western cohorts by CellSearch [17, 25, 26], and CTCs may lose EpCAM during epithelial to mesenchymal transition (EMT). Hence, we searched for additional proteins that are expressed on the cell surface of HCC cells and that can therefore be targeted to detect these cells in circulating blood. A literature search identified multiple proteins that are expressed on the surface of hepatocytes or upregulated in HCC (**Table 1**). Among these markers, Villin and alpha fetoprotein (AFP) were excluded as they were expressed in less than 50% of HCC tumor cells. pCEA (carcinoembryonic antigen CEA) was excluded as it can be expressed by colon cancer tissue [27, 28]. HepPar1 (Hepatocyte Paraffin 1) was excluded as its expression is decreased by more than 50% of tumor cells in poorly differentiated HCC. Arginase1 was excluded as it is also expressed by neutrophils [29], myeloid-derived suppressor cells (MDSC) as well as tumor associated macrophages [30]. Eventually, we selected ASGPR1, and GPC3 to be together with EpCAM for further validation. Expression of ASGPR1, GPC3 and EpCAM by tumor cells was determined using tissue microarrays with cores of normal liver tissue, tumors and paired tumor-free liver tissues from 133 HCC-patients by immunohistochemistry (cohort and tissue micro-arrays were described previously in [31, 32]. ASGPR1 was significantly downregulated in tumor cells compared to hepatocytes in TFL (**Figure 1A and 1C**).The downregulation of ASGPR1 was correlated with higher tumor grade and cirrhosis (**Figure 1D and 1E**). EpCAM and GPC3 (see our recent publication by K. Sideras et al.) [31] were upregulated in tumor compared to TFL (**Figure 1B and 1F**). ASGPR1 was expressed in 98% of HCC patient tumor tissue, followed by GPC3 in 39% (see K. Sideras et al.) [31] and EpCAM in 6% of HCC patient tumor tissue. 98% of HCC patient tumors express either one of the three markers and 43% of patients coexpress either two of the markers, 6% of patients co-expressed all three markers. Only 2% of patients express none of the three markers (**Figure 1G and 1H**).

Together, ASGPR1, GPC3 and EpCAM are expressed on the surface of HCC cells from 98% of our HCC patients, suggesting that a combination of antibodies that targets these proteins can potentially be used to detect and isolate circulating tumor cells in a majority of HCC patients.

18

Table 1. Expression of liver and HCC-specific markers in HCC tissue

	HCC differentiation	Positive rate	Ref.
AFP		52% (13/25)	Takao Tsuiji et al. Hepatology.1988.
		29% (12/42)	Lau SK et al. Hum Pathol.2002.
		7% (9/133)	K.Sideras et al. Br J Cancer.2015.
ASGPR1		75% (133/177)	Bin Shi et al. J Histochem Cytochem.2013.
Arginase1		96% (145/151)	C.Yan et al. Am J Clin Pathol.2010.
	Well	100% (70/70)	
	Moderate	96%(51/53)	
	Poor	86%(24/28)	
GPC-3		72% (21/29)	Capurro M et al. Gastroenterology.2003.
		39% (52/133)	Sideras et al. Br J Cancer.2015.
		77% (50/65)	Yao et al. J Histochem Cytochem.2013.
EpCAM		56%(46/82)	Sung et al. J Pathol Transl Med.2015.
		39%(39/101)	Yamashita et al. Cancer Research.2008.
HepPar-1		84% (127/151)	C.Yan et al. Am J Clin Pathol.2010.
	Well	100%(70/70)	
	Moderate	83% (44/53)	
	Poor	46% (13/28)	
		82% (53/65)	Minervini MI et al. Mod Pathol.1997.
		93% (39/42)	Kakar S et al. Am J Clin Pathol.2003.
		73% (35/48)	Lugli et al. Am J Clin Pathol.2004.
pCEA		48% (32/68)	Karabork et al.Pathology.2010.
		93% (39/42)	K.Lau et al. Hum Pathol.2002.
Villin		24% (16/68)	Karabork et al.Pathology.2010.
		31%(13/42)	K.Lau et al. Hum Pathol.2002.
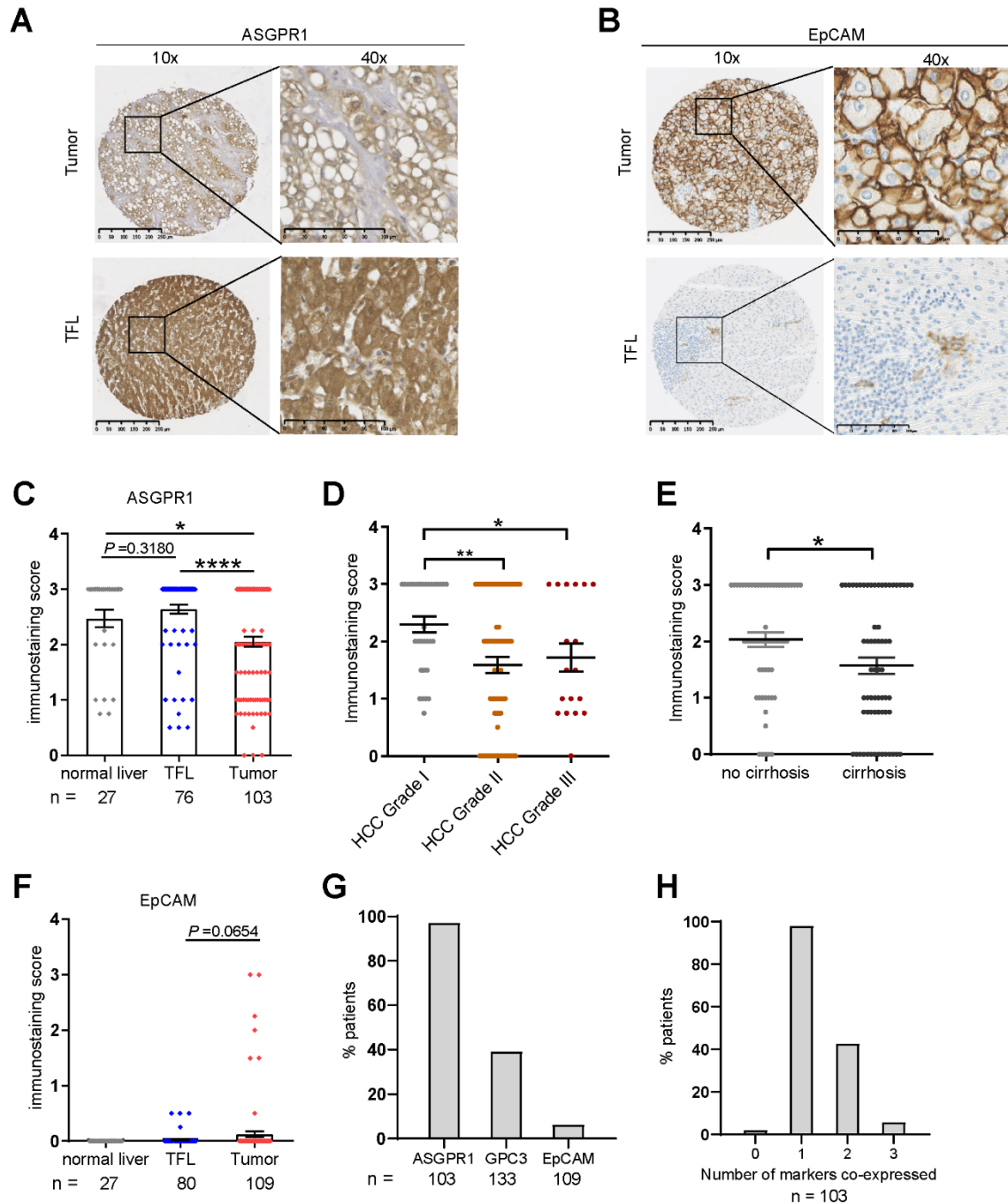
Figure 1. Expression of HCC and liver specific markers in HCC tissue. (A-B) Representative images of immunohistochemistry staining show ASGPR1 and EpCAM expression in HCC tumor and paired TFL tissue. The immunostaining score for ASGPR1 was 3D in tumor and 1D in TFL, and for EpCAM was 3D in tumor and 0 in TFL. Scale bars are presented in each image. (C-F) The immunostaining score of ASGPR1 and EpCAM in individual patients is presented. Significance was assessed by Wilcoxon matched-pairs signed rank test for tumor and TFL, Mann-Whitney test for tumor and normal, TFL and normal. Data are presented as mean ± SEM. *$P < 0.05$, ****$P < 0.0001$. (G) Frequencies of HCC patients expressing ASGPR1, GPC3 and EpCAM. (H) Distribution of total number of antigens expressed in the tumors of HCC-patients.

Optimization of RosetteSep enrichment combined with FACS

We next evaluated the recovery of target cells from whole blood by the combination of enrichment through RosetteSep CD45 depletion combined with FACS. HepG2, a HCC cell line, was used as a model cell line for spiking experiments because HepG2 cells expressed high levels of CK, EpCAM, ASGPR1 and GPC3 (**Figure 2A**). We spiked 1000 HepG2 cells in 2ml or 7.5ml of blood from a healthy volunteer to test the recovery rate of RosetteSep enrichment. To accurately monitor the HepG2 cells recovered from RosetteSep, HepG2 cells were counted by CellSearch system before and after RosetteSep isolation. The recovery rate of RosetteSep ranges from 43.9% to 51% and did not differ much when the same number of HepG2 cells were spiked in a different volume of blood (**Figure 2B**). Next we evaluated the recovery of FACS. We spiked 50 and 100 HepG2 cells respectively in $2x10^5$ PBMC which represents the amount of leukocytes remaining after RosetteSep enrichment. HepG2 cells were stained with CK and GPC3 only and were flow-sorted to 96-well flat bottom plates and counted under fluorescence microscope. Flowcytometric gating strategy is shown in **Figure S2A**. The recovery rate of flow sorting ranges from 56% to 64% (**Figure 2C**). Next we evaluated the recovery rate of RosetteSep combined with FACS. Fifty or 100 HepG2 cells were spiked into 5.5 mL blood from a healthy donor and enriched by RosetteSep. Enriched cells were stained with DRAQ5, CK, CD45, ASGPR1, GPC3 and EpCAM, and flow-sorted to 96-well plate for counting as aforementioned. Strikingly, the recovery rate drops dramatically, ranging from 6%-12%, albeit in a limited number of experiments (**Figure 2C-2D**).

Collectively, these data suggest that RosetteSep CD45 depletion combined with flow sorting gives a relatively low recovery.
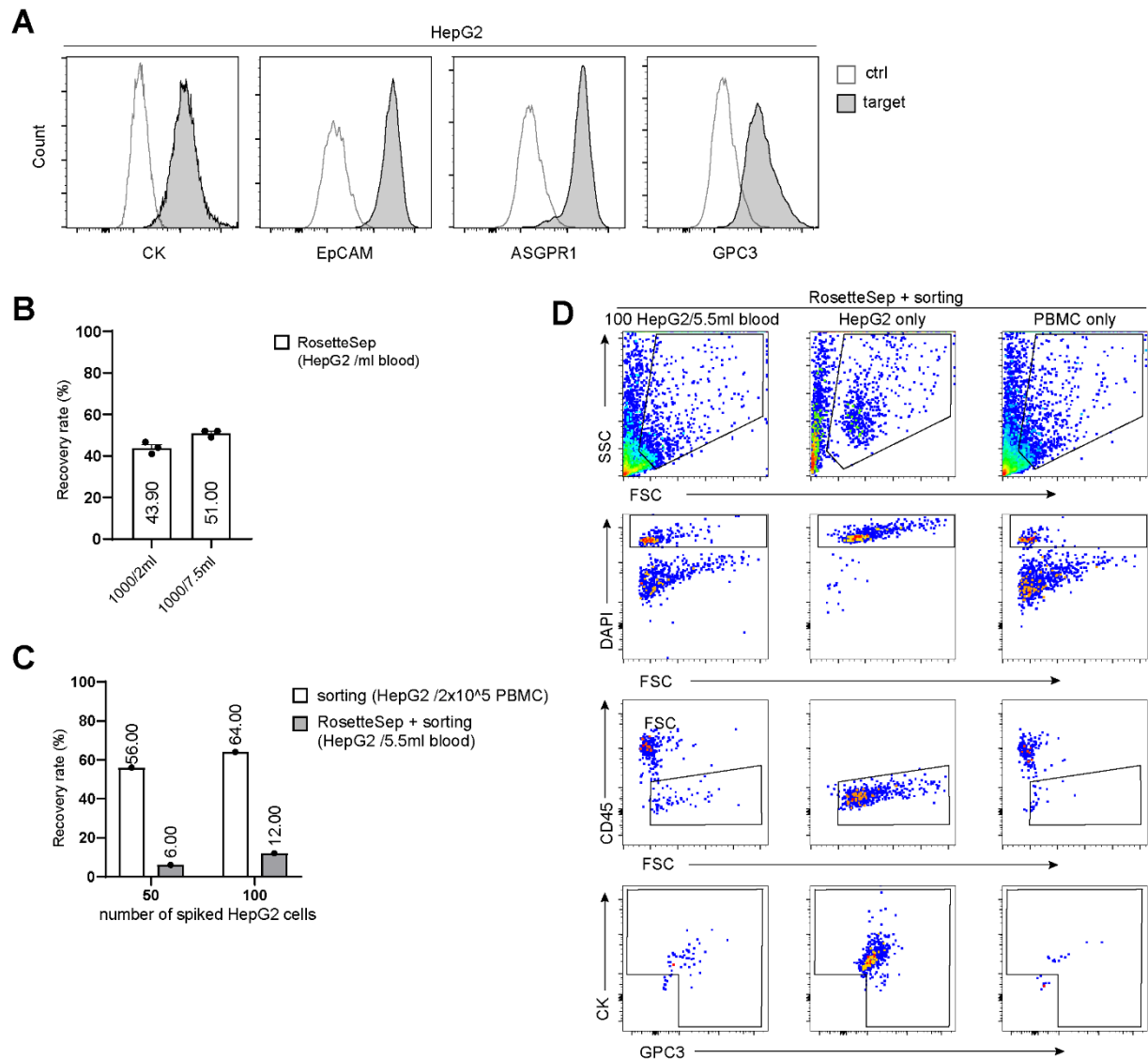
Figure 2. Optimization of RosetteSep enrichment combined with FACS. (A) Flow-cytometry plots of CK, EpCAM, ASGPR1 and GPC3 on HepG2 cells. (B) Recovery rate of RosetteSep enrichment method. (C) Recovery rate of HepG2 enriched by FACS or by combining RosetteSep and FACS. (D) Flow-cytometry plots of HepG2 during flow sorting after spiked in blood and enriched by RosetteSep.

CTCs detection in HCC patients

We next evaluated the combination of RosetteSep enrichment followed by flow cytometric analysis and subsequent FACS to detect CTCs in patient blood samples using antibodies directed at the surface proteins (e.g. ASGPR1, GPC3 and EpCAM) that were identified to be expressed by the majority of HCC. 22.5ml blood from each advanced HCC patient was used for CTC detection using our method and flowchart of the experimental set-up is shown in **Figure 3A**.To help localize our cells of interest

22

within the large number of non-target blood cells, we included stained HepG2 and unstained HepG2 controls in each sorting experiment with patient materials. A nucleic acid dye DRAQ5 combined with FSC was used to gate on nucleated cells. Then a dump channel using the unstained PE-Cy7 channel (to exclude autofluoresecent events) combined with CD45 was used to exclude unspecific events like rosettes (which may form because–of CD45 antibody binding to erythrocytes and CD45^{+} leukocytes). Then each targeted surface marker was plotted against CD45 to gate on putative CTCs. Representative data are provided in **Figure 3B-3D**. Numbers of CTCs detected with both our method and CellSearch System (method described in **Chapter 3**) are listed in **Table 2**. Despite including multiple markers and a three times higher sample volume (7.5 vs 22.5 mL) there is no clear CTC events cluster visible in all 15 advanced HCC patients or a subtantial increase compared to the CellSearch System.

A major advantage of FACS analysis is the ease of collecting cells into reaction tubes allowing for a convenient PCR-based down-stream analysis. To prevent loss of cells and nucleic acids, any liquid transfer after cell sorting must be avoided. Putative CTC events that were positive for either CK/ASGPR1/GPC3 or EpCAM were sorted and pooled into one PCR tube prefilled with lysis buffer (250uL) for further DNA analysis (**Figure 3B-3D**). CD45^{+} leukocytes were sorted in another vial and served as positive control for DNA analysis.

Table 2. Numbers of CTCs detected with both methods

Patients	CellSearch (CTCs/7.5ml)	RosetteSep + FACS (CTCs/22.5ml)			
	EpCAM+CK+	CK+	ASGPR1+	EpCAM+	GPC3+
1	0	4	4	1	2
2	4	1	0	1	4
3	0	5	1	3	2
4	0	4	21	0	4
5	0	2	0	0	2
6	0	2	1	0	3
7	15	11	0	16	11
8	0	0	3	4	7
9	0	2	2	1	1
10	0	1	2	0	3
11	2	0	2	1	1
12	3	0	0	0	4
13	0	5	6	5	5
14	0	0	1	0	1
15	0	1	0	0	0
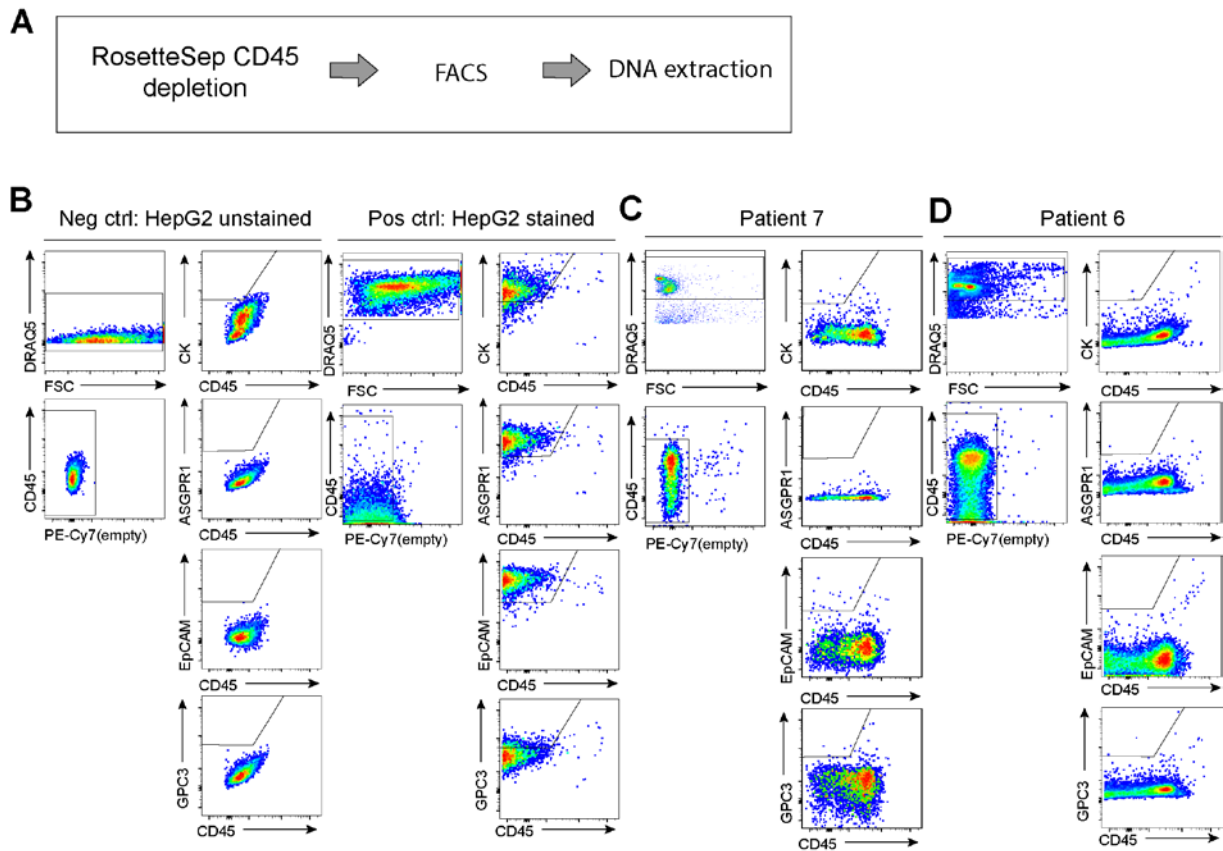
Figure 3. CTCs detected by our method. (A) Flowchart of our method. (B-D)Flow-cytometry plots of patient samples show gated potential CTC events. Unstained HepG2 cells served as negative control and stained HepG2 served as positive control.

DNA isolation of sorted CTCs

PCR amplification may involve the targeted amplification of specific transcripts or DNA regions of interest (e.g. mutational hotspots), or whole genome or whole transcriptome amplification. The amplified products can then be subjected to different types of analyses, such as single/multiplexed PCR analyses. Here we fixed cells already, so it is not possible to do RNA analysis thereby we focused on DNA analysis. However, we failed to isolate any DNA from sorted patient and control samples.

24

Discussion

For advanced HCC patients, tumor biopsy specimens are difficult to obtain or unobtainable. Moreover, the tumor biopsies may not recapitulate the whole tumor. Liquid biopsies such as CTC can be obtained repetitively and may be used as a surrogate for regular biopsies. The detection of CTC may hold prognostic value and it may be used in treatment decisions, for instance when DNA analysis reveals druggable targets.

Gene expression profiling and IHC staining have shown that GPC3 is significantly overexpressed in CD90^{+} cancer stem cells in HCC[33]. EpCAM is a validated marker of (cancer) stem cells in the liver[34-37]. GPC3[31, 38] or EpCAM[39] expression is associated with high AFP, worse tumor differentiation and vascular invasion. In contrast, ASGPR1 is associated with high tumor differentiation [40]. Therefore, a combination of antibodies that targets EpCAM, GPC3 and ASGPR1 to identify HCC cells seems to be able to detect cancer cells from both well and poorly differentiated HCC tumors. Indeed, we found that 98% of HCC patient tumors express either one of the three markers and 43% of patients co-express either two of the markers, 6% of patients co-expressed all three markers. Only 2% of patients express none of the three markers. As these data was collected using early stage HCC tumors, the co-expression pattern of these markers on advanced HCC tumors might be a bit different but still CTC isolation for most HCCs should still be amenable to a strategy employing these markers.

Many studies have explored CTC detection methods, with some being based on cell size, cell density or cell markers or the combination of either two, such as filtration, centrifugation or fluorescent imaging. Most CTC isolation systems are not validated in the clinic and only enrich a subgroup of cancer cells. Marker-based systems such as CellSearch can only capture CTCs through a single surface marker, EpCAM, which can easily be lost on CTCs during EMT transition, whereas most HCC cells do not express EpCAM. We tested the cell recovery rates of several commercial systems, such as size-based microfluidics (the Parsortix™ cell separation system) and sized-based filtration system (VyCAP's CTC enumeration chip). Using HCC cell lines, both systems showed a low recovery rate which is less than 20% (data not shown) and low reproducibility. Our method to combine negative selection and positive sorting based on multiple HCC or liver-specific markers is reproducible and theoretically should

enrich many diverse types of CTCs. In practice, however, the recovery rate is actually very low, hence the CTC compartment in advanced HCC appears not sufficient in size as to allow meaningful guidance of clinical decision making.

Despite including multiple markers and large sample input, there is no clear CTC events cluster from 15 advanced HCC patients. We thus infer that the frequency of diverse CTCs in HCC patients must be very low. Few studies discuss the true frequencies of CTCs in advanced HCC patients. An example in the case are EpCAM+ CTCs. EpCAM-positive tumor cells in HCC appear to be stem cell like and are related to a more aggressive tumor type [34]. Aggressive tumor is more likely to invade vessels thus more likely to shed tumor cells. EpCAM+ CTCs have previously been detected in 28%-35% of advanced HCC patients in Western cohorts by the CellSearch system [17, 25, 26]. The expression of EpCAM is always spatially prominent in full section staining of tumors. When the tumor expresses EpCAM the whole tumor may be EpCAM+ and the reported detectable CTCs range from 1-15/7.5mL (median 3-4 cells), then this frequency is likely to be the true frequency of CTCs in advanced HCC patients. For the HCC positive with ASGPR1 marker, the frequency of ASGPR1+ CTCs might be even lower because ASGPR1+ tumors (ASGPR expression is associated with higher tumor differentiation[40]) are not as aggressive as EpCAM+ or GPC3+ tumors [31].

The low detection rate of CTCs using our isolation method may be partly due to the cell loss during multiple washing and staining steps, especially the intracellular staining protocol is cumbersome. Additionally, DNA isolation from these sorted rare cell events, which is currently technically too challenging to be implemented in daily clinical practice.

In conclusion, we established a panel of antigens that are expressed on the surface of cancer cells of 98% of HCC patients. We demonstrate that these markers can be used to identify and isolate putative CTC from the blood of these patients by combining RosetteSep and flow cytometry. However, the observed frequency is low and we failed to isolate DNA from these cells, which implies that this liquid biopsy technique in particular, but possibly also in general currently avaible CTC-based strategies hold little promise with regard to the detailed analysis of HCC biology or with regard to guiding clinical decision making.

References

1.   Magbanua MJM, Sosa EV, Roy R, et al. Genomic profiling of isolated circulating tumor cells from metastatic breast cancer patients. Cancer research 2013;73:30-40.
2.   Magbanua MJM, Sosa EV, Scott JH, et al. Isolation and genomic analysis of circulating tumor cells from castration resistant metastatic prostate cancer. BMC cancer 2012;12:78.
3.   Cristofanilli M, Budd GT, Ellis MJ, et al. Circulating tumor cells, disease progression, and survival in metastatic breast cancer. New England Journal of Medicine 2004;351:781-791.
4.   Negin BP, Cohen SJ. Circulating tumor cells in colorectal cancer: past, present, and future challenges. Current treatment options in oncology 2010;11:1-13.
5.   Punnoose EA, Atwal SK, Spoerke JM, et al. Molecular biomarker analyses using circulating tumor cells. PloS one 2010;5:e12517.
6.   de Boer CJ, van Krieken JH, Janssen-van Rhijn CM, et al. Expression of Ep-CAM in normal, regenerating, metaplastic, and neoplastic liver. J Pathol 1999;188:201-6.
7.   Went PT, Lugli A, Meier S, et al. Frequent EpCam protein expression in human carcinomas. Hum Pathol 2004;35:122-8.
8.   Guo W, Yang X-R, Sun Y-F, et al. Clinical significance of EpCAM mRNA-positive circulating tumor cells in hepatocellular carcinoma by an optimized negative enrichment and qRT-PCR–based platform. Clinical cancer research 2014;20:4794-4805.
9.   Vona G, Estepa L, Béroud C, et al. Impact of cytomorphological detection of circulating tumor cells in patients with liver cancer. Hepatology 2004;39:792-797.
10.   Lapin M, Tjensvoll K, Oltedal S, et al. MINDEC-an enhanced negative depletion strategy for circulating tumour cell enrichment. Scientific reports 2016;6:28929.
11.   Xu W, Cao L, Chen L, et al. Isolation of circulating tumor cells in patients with hepatocellular carcinoma using a novel cell separation strategy. Clinical Cancer Research 2011;17:3783-3793.
12.   Ogle LF, Orr JG, Willoughby CE, et al. Imagestream detection and characterisation of circulating tumour cells - A liquid biopsy for hepatocellular carcinoma? J Hepatol 2016;65:305-13.
13.   Nel I, Baba HA, Ertle J, et al. Individual profiling of circulating tumor cell composition and therapeutic outcome in patients with hepatocellular carcinoma. Translational oncology 2013;6:420-428.
14.   Wu S, Liu S, Liu Z, et al. Classification of circulating tumor cells by epithelial-mesenchymal transition markers. PloS one 2015;10:e0123976.
15.   Guo W, Sun Y-F, Shen M-N, et al. Circulating tumor cells with stem-like phenotypes for diagnosis, prognosis, and therapeutic response evaluation in hepatocellular carcinoma. Clinical Cancer Research 2018;24:2203-2213.
16.   Miyamoto DT, Lee RJ, Kalinich M, et al. An RNA-based digital circulating tumor cell signature is predictive of drug response and early dissemination in prostate cancer. Cancer discovery 2018;8:288-303.
17.   Kelley RK, Magbanua MJM, Butler TM, et al. Circulating tumor cells in hepatocellular carcinoma: a pilot study of detection, enumeration, and next-generation sequencing in cases and controls. BMC cancer 2015;15:206.
18.   Shaw JA, Guttery DS, Hills A, et al. Mutation analysis of cell-free DNA and single circulating tumor cells in metastatic breast cancer patients with high circulating tumor cell counts. Clinical Cancer Research 2017;23:88-96.
19.   Sundaresan TK, Sequist LV, Heymach JV, et al. Detection of T790M, the acquired resistance EGFR mutation, by tumor biopsy versus noninvasive blood-based analyses. Clinical Cancer Research 2016;22:1103-1110.
20.   Gkountela S, Castro-Giner F, Szczerba BM, et al. Circulating Tumor Cell Clustering Shapes DNA Methylation to Enable Metastasis Seeding. Cell 2019;176:98-112.e14.
21.   Mastoraki S, Strati A, Tzanikou E, et al. ESR1 methylation: A liquid biopsy–based epigenetic assay for the follow-up of patients with metastatic breast cancer receiving endocrine treatment. Clinical Cancer Research 2018;24:1500-1510.
22.   Paoletti C, Cani AK, Larios JM, et al. Comprehensive mutation and copy number profiling in archived circulating breast cancer tumor cells documents heterogeneous resistance mechanisms. Cancer research 2018;78:1110-1122.

23. Ni X, Zhuo M, Su Z, et al. Reproducible copy number variation patterns among single circulating tumor cells of lung cancer patients. Proceedings of the National Academy of Sciences 2013;110:21083-21088.

24. Magbanua MJM, Park JW. Isolation of circulating tumor cells by immunomagnetic enrichment and fluorescence-activated cell sorting (IE/FACS) for molecular profiling. Methods 2013;64:114-118.

25. Morris KL, Tugwood JD, Khoja L, et al. Circulating biomarkers in hepatocellular carcinoma. Cancer Chemother Pharmacol 2014;74:323-32.

26. Schulze K, Gasch C, Staufer K, et al. Presence of EpCAM-positive circulating tumor cells as biomarker for systemic disease strongly correlates to survival in patients with hepatocellular carcinoma. Int J Cancer 2013;133:2165-71.

27. Thomas SN, Zhu F, Schnaar RL, et al. Carcinoembryonic antigen and CD44 variant isoforms cooperate to mediate colon carcinoma cell adhesion to E-and L-selectin in shear flow. Journal of biological chemistry 2008;283:15647-15655.

28. Thomas SN, Tong Z, Stebe KJ, et al. Identification, characterization and utilization of tumor cell selectin ligands in the design of colon cancer diagnostics. Biorheology 2009;46:207-225.

29. Jacobsen LC, Theilgaard-Monch K, Christensen EI, et al. Arginase 1 is expressed in myelocytes/metamyelocytes and localized in gelatinase granules of human neutrophils. Blood 2007;109:3084-7.

30. Mantovani A, Sica A, Allavena P, et al. Tumor-associated macrophages and the related myeloid-derived suppressor cells as a paradigm of the diversity of macrophage activation. Hum Immunol 2009;70:325-30.

31. Sideras K, Bots SJ, Biermann K, et al. Tumour antigen expression in hepatocellular carcinoma in a low-endemic western area. Br J Cancer 2015;112:1911-20.

32. Sideras K, Biermann K, Verheij J, et al. PD-L1, Galectin-9 and CD8(+) tumor-infiltrating lymphocytes are associated with survival in hepatocellular carcinoma. Oncoimmunology 2017;6:e1273309.

33. Ho DW, Yang ZF, Yi K, et al. Gene expression profiling of liver cancer stem cells by RNA-sequencing. PLoS One 2012;7:e37159.

34. Yamashita T, Forgues M, Wang W, et al. EpCAM and α-fetoprotein expression defines novel prognostic subtypes of hepatocellular carcinoma. Cancer research 2008;68:1451-1461.

35. Kim H, Choi GH, Na DC, et al. Human hepatocellular carcinomas with "Stemness"-related marker expression: keratin 19 expression and a poor prognosis. Hepatology 2011;54:1707-17.

36. Guo Z, Li LQ, Jiang JH, et al. Cancer stem cell markers correlate with early recurrence and survival in hepatocellular carcinoma. World J Gastroenterol 2014;20:2098-106.

37. Breuhahn K, Baeuerle PA, Peters M, et al. Expression of epithelial cellular adhesion molecule (Ep-CAM) in chronic (necro-)inflammatory liver diseases and hepatocellular carcinoma. Hepatol Res 2006;34:50-6.

38. Yorita K, Takahashi N, Takai H, et al. Prognostic significance of circumferential cell surface immunoreactivity of glypican-3 in hepatocellular carcinoma. Liver Int 2011;31:120-31.

39. Sung JJ, Noh SJ, Bae JS, et al. Immunohistochemical Expression and Clinical Significance of Suggested Stem Cell Markers in Hepatocellular Carcinoma. J Pathol Transl Med 2016;50:52-7.

40. Shi B, Abrams M, Sepp-Lorenzino L. Expression of asialoglycoprotein receptor 1 in human hepatocellular carcinoma. Journal of Histochemistry & Cytochemistry 2013;61:901-909.

28

Supplemental data for:

Isolation of circulating tumor cells by RosetteSep enrichment and fluorescence-activated cell sorting (FACS) in patients with hepatocellular carcinoma

Table of contents

Supplemental material and methods

Immunohistochemistry (IHC)

The construction of tissue microarrays (TMA) of tumor and tumor-free liver tissues has been described previously [1, 2]. The TMAs were then immunohistochemically stained by the department of pathology of Erasmus MC, using anti-EpCAM (provided by pathology) and anti-ASGPR1 (rabbit, polyclone, 1:500, Sigma Life Sciences) antibodies. IHC was performed with an automated, validated and accredited staining system (Ventana Benchmark ULTRA, Ventana Medical Systems, Tucsen, AZ, USA) using Optiview universal DAB detection Kit (#760-700). In brief, following deparaffinization and heat-induced antigen retrieval the tissue samples were incubated according to their optimized time with each antibody. Incubation was followed by hematoxylin II counter stain for 12 minutes and then a blue coloring reagent for 8 minutes according to the manufactures instructions (Ventana). The immunohistochemically stained TMAs were then scanned using NanoZoomer 2.0HT (Hamamatsu) and scored blindly by two researchers, based on the intensity of staining (0[none],1[low], 2[intermediate], 3[strong]) and the frequency of positive tumor cells or hepatocytes (A[<10%], B[10-50%], C[50-90%], D[>90%]). The score per core was calculated by multiplying the intensity by the frequency of positive cells (A=0.1, B=0.3, C=0.7 and D=1), and then the average score per tissue was calculated by taking the average of the three scores.

Supplemental References

1. Sideras K, Bots SJ, Biermann K, Sprengers D, Polak WG, JN IJ, de Man RA, Pan Q, Sleijfer S, Bruno MJ, Kwekkeboom J. Tumour antigen expression in hepatocellular carcinoma in a low-endemic western area. Br J Cancer 2015;112:1911-20.
2. Sideras K, Biermann K, Verheij J, Takkenberg BR, Mancham S, Hansen BE, Schutz HM, de Man RA, Sprengers D, Buschow SI, Verseput MC, Boor PP, Pan Q, van Gulik TM, Terkivatan T, Ijzermans JN, Beuers UH, Sleijfer S, Bruno MJ, Kwekkeboom J. PD-L1, Galectin-9 and CD8(+) tumor-infiltrating lymphocytes are associated with survival in hepatocellular carcinoma. Oncoimmunology 2017;6:e1273309.

Supplemental Table 1. Patient Characteristics

	HCC patients (n=15)
Gender	
Male	14
Female	1
Age at sampling (years)	
<60	5
≥60	10
Mean ± SD	65 ± 3.4
Race	
Caucasian	13
Asian	1
African	1
Etiology	
No known liver disease	4
Hepatitis B/C	2/2
Alcohol-related liver disease	4
NASH/NAFLD*	2/1
Cirrhosis	
No	6
Yes	9
Size of largest lesion (cm)	
<10	4
≥10	11
Mean ± SD	13.6 ± 5.6
Tumor number	
1	11
>1	4
Macrovascular invasion	
No	6
Yes	9
Staging based on TNM	
1	2
2	0
3	11
4	2
AFP level (ug/L)	
<20	5
20-400	1
>400	9

* NASH, non-alcoholic steatohepatitis (NASH);

NAFLD, non-alcoholic fatty liver disease (NAFLD)

Supplemental Table 2. Anti-human Antibodies Used in Flow Cytometry, FACS and /or CellSearch system

Antibody	Clone	Supplier
Pan CK8,18,19-PE	C11 and A53-B/A2	CellSearch
CD45-APC	HI30	CellSearch
EpCAM (coupled to ferrofluids)	VU1D9	CellSearch
EpCAM-PercpCy5.5	VU1D9	Abcam
ASGPR1-Alexa488	8D7	Santa Cruz
ASGPR1-PE	8D7	BD Biosciences
GPC3-Alexa405	307801	R&D systems
DRAQ5 (Far red nucleus dye)	-	BioStatus

CHAPTER 3

Detection of oncogenic mutations in paired circulating tumor DNA and circulating tumor cells in in patients with hepatocellular carcinoma

Zhouhong Ge[1], Jean C.A.Helmijr[2], Maurice P.H.M.Jansen[2], Patrick P.C.Boor[1], Lisanne Noordam[1], Maikel Peppelenbosch[1], Jaap Kwekkeboom[1], Jaco Kraan*[,2], Dave Sprengers*[,1]. (*shared senior authors)

Departments of [1]Gastroenterology and Hepatology, [2]Medical Oncology, Erasmus MC-University Medical Center, Rotterdam, the Netherlands

Abstract

Background and aims: Circulating tumor cells (CTCs) or circulating tumor DNA (ctDNA) may be used for diagnostic or prognostic purposes in patients with hepatocellular carcinoma (HCC). We aim to determine whether CTCs or ctDNA are suitable to determine oncogenic mutations in HCC patients.

Methods: Twenty-six, predominantly advanced, HCC patients were enrolled. 30 mL peripheral blood from each patient was obtained. CellSearch system was used for CTC detection. A sequencing panel covering 14 cancer-relevant genes was used to identify oncogenic mutations. *TERT* promoter C228T and C250T mutations were determined by droplet digital PCR.

Results: CTCs were detected in 27% (7/26) of subjects but at low numbers (median: 2 cells, range: 1-15 cells) while ctDNA was found in 77% (20/26) of patients. Mutations in ctDNA were identified in several genes: *TERT* promoter C228T (77%, 20/26), *TP53* (23%, 6/26), *CTNNB1* (12%, 3/26), *PIK3CA* (12%, 3/26) and *NRAS* (4%, 1/26). The *TERT* C228T mutation was present in all patients in which mutations were found in ctDNA, or with detectable CTCs. The *TERT* C228T and *TP53* mutations detected in ctDNA were present in matched primary HCC tumor tissue. The maximal variant allele frequency (VAF) of ctDNA showed linear correlation with tumor size and AFP level (Log10). ctDNA positivity (including *TERT* C228T) was associated with macrovascular invasion, and ctDNA positivity (including *TERT* C228T) or CTCs ($\geq$2) correlated with poor patient survival.

Conclusions: Oncogenic mutations could be detected in ctDNA from advanced HCC patients and predicts prognosis. ctDNA analysis of liquid biopsies appears promising for identifying druggable mutations.

Key words: circulating tumor DNA; circulating tumor cells; *TERT* promoter mutations; macrovascular invasion

Introduction

Hepatocellular carcinoma is the 4th leading cause of cancer-related death worldwide[1]. Treatments options for advanced disease are limited. Most patients are diagnosed at a late stage in which surgery is no longer a viable option and median survival is less than 2 years [2]. In advanced patients, tumor tissue is usually obtained by needle biopsies, which are invasive and does not capture the heterogeneity of the whole tumor. Liquid biopsies, including circulating tumor cells (CTCs) and cell-free DNA (ctDNA), have been suggested to allow identification of tumor-derived mutations for use in diagnosis and rational application of targeted therapies while patient burden associated with such sampling is minimal. The feasibility, however, of such approaches in advanced HCC remains for now largely obscure.

CTCs are cells that have detached from a primary or secondary tumor and enter circulation [3], and are regarded as seeds for metastasis. There has been a technical challenge to capture them due to the extremely low frequency, estimated ≤1 CTC/ml of blood in billions of blood cells. CellSearch is a standardized and validated method to detect EpCAM+ CTCs from epithelial tumors not including HCC [4]. Nevertheless, many studies show that CellSearch identifies CTCs in 16%-67% HCC patients in early or late stage [5-12]. Other enrichment methods include size-based enrichment [13], density-based RosetteSep negative selection [14], magnetic negative selection[15], flowcytometric detection[16] and microfluidic enrichment[17]. Most CellSearch studies report prognostic value of CTC numbers in HCC [5, 8-10, 12]. The CTC-positive rate in peripheral blood was associated with tumor size, serum alpha-fetoprotein level (AFP), vascular invasion and overall survival [5, 10, 11]. A preoperative CTC positivity is a predictor for tumor recurrence in HCC patients after surgery [8, 9]. The increase in postoperative CTC counts was significantly associated with the macroscopic tumor thrombus and shorter overall survival [12]. Moreover, to help guide treatment decisions, for instance to initiate or switch targeted therapy, it is important to determine acquisition of somatic mutations. Because of the risks associated with repeated tumor biopsies, it is attractive to use liquid biopsies for this purpose. Mutational analysis in CTCs can be performed by DNA sequencing [11, 18]. However, CTCs found by numerous methods have often not been analyzed for DNA mutations in HCC, likely due to limited numbers and inefficiency of single cell isolation techniques.

Circulating tumor DNA (ctDNA) is the fraction of cell-free DNA that is derived from primary or metastatic tumors. The fraction of circulating mutant DNA fragments is very small, sometimes less than 0.01% [19], compared to circulating wildtype DNA fragments, making it difficult to detect and quantify [20]. The development of next generation sequencing (NGS), especially deep sequencing, and droplet digital PCR (ddPCR) have facilitated the identification of genetic variants in ctDNA. Chan et al. was the first to report analysis of ctDNA by shotgun sequencing of plasma samples from HCC patients in early stage. The ctDNA concentration, determined by single nucleotide variants (SNVs) analysis, was found to range from 2.1% to 53% before surgery and from 0.4% -1.3% after surgery [21]. HCC-associated mutations (e.g. *TP53*, *TERT*, *CTNNB1*, *APC*, *EGFR*, *MET*, *ARID1A*) were detected in ctDNA by NGS sequencing in advanced [22, 23] and operable HCC [24, 25]. The presence of somatic mutations in ctDNA before surgery could predict microvascular invasion in resectable HCC patients[24, 25]. Moreover, postoperative residual ctDNA was an independent risk factor for recurrence and poor disease-free survival in HCC patients [26]. Very recently, TERT promotor mutated ctDNA was described to be a prognostic biomarker for HCC [27, 28], but this observation requires further validation.

The apparent promise of liquid biopsies for guiding management of HCC prompts studies in which the feasibility of such approaches is tested in real life cohorts. Hence, in this study, we used paired samples of CTCs and ctDNA to explore feasibility to detect oncogenic mutations in HCC patients.

Material and Methods

Patients and blood collection

A total of sequential 26 HCC-patients with advanced disease were enrolled in the study between May 2018 and July 2019. Patients who did not sign the written informed consent were exluded. Peripheral blood samples (30 mL) from each patient were collected before any anti-tumor treatment and were collected into Cellsave tubes (Menarini Silicon Biosystems, Huntington Valley, PA). Matched FFPE primary tumor tissue biopsies were obtained from department of Pathology in Erasmus MC. The study was approved by the local ethics committee (METC), Erasmus MC, Rotterdam (METC number: 17-238), and written informed consent was obtained from each patient. The clinical characteristics of the 26 patients are summarized in **Table 1**.

Plasma separation and ctDNA extraction

Blood samples were processed within 24 hours after collection. Blood was first centrifuged at 1700g for 10min to separate plasma and blood cells. The separated plasma was centrifuged at 12,000g for another 10min to remove cellular debris. The plasma was collected and aliquoted in vials per 2ml and stored at -80°C until further processing. ctDNA was isolated from 440µL-4mL (median 3.95mL) plasma using QIA-amp Circulating Nucleic Acid kit (Qiagen, Venlo, the Netherlands) and eluted in 30µL elution buffer. CtDNA concentrations were determined by Qubit^{TM} 1X dsDNA HS Assay kit (Thermo Fisher scientific, Waltham, MA) using 2µL of ctDNA.

Enrichment of CTCs and single cell isolation

7.5mL whole blood was used to detect EpCAM$^+$ CTCs by CellSearch system (Menarini Silicon Biosystems). The cells were isolated by EpCAM positive selection using the CellSearch Circulating Tumor Cell kit $^®$ and defined as CD45$^-$ CK(8/18/19)$^+$ DAPI$^+$. The stained and scanned CTCs were scored blindly by two certified researchers. Single CTC were isolated from the CellSearch cartridge with the VyCAP cell puncher system (VyCAP, Enschede, The Netherlands) using an isolation chip, which consists of 6400 microwells [29]. Single cells were subjected to whole-genome amplification (WGA) by the Ampli1 WGA kit (Menarini Silicon Biosystems) and the DNA quality of the WGA-products was determined with the WGA Quality control kit (VyCAP) according to manufactures instructions.

Amplification of ctDNA

The extracted ctDNA was pre-amplified for the targets *TERT* C228T and *TERT* C250T by PCR. In brief, a pre-amp reaction mix (total volume: 8µL) was prepared for each target using: 4µL Taqman PreAMP Master Mix (Thermo Fisher Scientific), 2µL ctDNA sample and 2µL of 100x diluted *TERT* C228T-113 or *TERT* C250T-113 assay (Bio-Rad, Herucles, CA). Then PCR was performed using the following cycle conditions: 1 cycle of 10min at 95°C,15 cycles of 15 sec at 95°C and 4 min at 60°C and finally hold at 4°C. After pre-amplification PCR 72µL ultrapure DNAse/RNAse free H_2O (Thermo Fischer Scientific/Gibco) was added to the reaction for a final volume of 80µL.

Droplet digital PCR (ddPCR)

For the quantification of the *TERT* C228T and C250T mutations in ctDNA from HCC patients, ddPCR was performed using the Naica Crystal PCR system (Stilla Technologies, Beverly, MA). Prior to the ddPCR, pre-amplified ctDNA samples were diluted 20x for every 0.5ng of ctDNA input in the pre-amplification reaction to prevent saturation with DNA copies of the ddPCR Sapphire chips (Stilla Technologies) with copies. Based on the resulting amount of target copies of the first ddPCR (low sample concentration input), a second ddPCR (high sample concentration input) was performed with an input of at least 2500 target copies. For each target the following ddPCR reaction mix was prepared: 1 µL of diluted pre-amplified ctDNA sample, 14 µL ddPCR™ supermix for probes (Bio-Rad), 2.8 µL of 5M Betaine (Sigma Aldrich, Darmstadt, Germany), 1µL of 28mM EDTA (Thermo Fisher Scientific), 1.4µL of *TERT* C228T-113 or *TERT* C250T-113 assay (Bio-Rad) [30], 2.8µL of 1 µM Fluorescein (VWR, Radnor, PA) and finally ultrapure DNAse/RNAse free H_2O (Thermo Fischer Scientific/Gibco) was added to bring up the total volume to 28 µL. Then 26µL of the reaction mix was then loaded unto the Sapphire chips (Stilla Technologies) and ddPCR was performed using the following cycle conditions: 1 cycle of 10 min at 95°C, 50 cycles of 30 sec at 96°C and 1 min at 62°C, 1 cycle of 10 min at 98°C and finally hold at 4°C. The Sapphire Chips were scanned using Naica Prism3 system with default exposure times for the FAM-labeled mutant probe (50ms) and the HEX-labeled wildtype probe (250ms). Then, data was analyzed using the Stilla Crystal Miner v2.4.0.3 software and thresholds were set based on positive and negative controls for each mutation assay.

To exclude false positive samples, all ctDNA were analyzed at low and high concentrations. An increase in sample concentration should result in an elevated number of mutant copies compared to the lower concentrated sample. If mutant copies were detected and no increase was observed in the higher concentrated sample of the same patient, the patient was regarded negative for either the *TERT* C228T or C250T mutation. Finally, a minimum threshold of 5 detected mutant copies was established to discriminate between *TERT* mutation positive and negative patients. The variant allele fraction (VAF) was calculated as the proportion of ctDNA harboring the variant in a background of wild-type cell-free DNA.

Targeted next-generation sequencing (NGS)

Sequencing was performed by Ion semiconductor sequencing on the Ion Torrent S5XL Next generation sequencing (NGS) system using the Oncomine ctDNA Assay with molecular barcoding loaded on Ion 540 chips. Experiments were performed according to the manufacturer's protocol (Thermo Fisher Scientific/Life Technologies). Since there is no customized oncopanel for HCC in EMC, we chose the Oncomine™ Colon ctDNA panel (Thermo Fisher/Life Technologies) which contains the most frequently mutated driver genes in HCC. This panel comprises of 14 colon cancer-related genes (*TP53*, *CTNNB1*, *APC*, BRAF, AKT1, PIK3CA, *EGFR*, ERBB2, KRAS, NRAS, GNAS, MAD4, MAP2K1, FBXW7) covering >240 mutational hotspots. Sample input ranged between 2.8-20.7ng DNA in 13ul for the sequence reaction. Basecalling was performed using the Ion Torrent Suite Software 5.10 plugin (Thermo Fisher Scientific/Life Technologies) according the manufactures protocol with default basecalling settings. Variant calling was performed using the Ion Torrent Suite software and Variant caller plugin (Thermo Fisher Scientific/Life Technologies) and the variant caller parameters can be found in **supplementary table 5**. Additionally, the following post-variant caller filters were used to eliminate false positive variants: only known hotspot variants were selected when detected in at least 3 independent mutant molecules, with a variant allele frequency of at least 0.2% and the total sequencing depth at that the variant position (wildtype and mutant) was at least 500 independent (wildtype and mutant) molecules.

Statistical analysis

Spearman's rank correlation test for nonparametric data was used to analyze the correlation between two factors. Kaplan-Meier analysis is used to evaluate the survival differences. Clinical parameters in different groups were compared using Chi-Square test. Cox regression model was used for univariate and multivariate analysis. Statistical analysis was performed using Graphpad Prism 8.0 or IBM SPSS statistics 25. P value less than 0.05 was considered statistically significant (*P < 0.05; **P < 0.01; ***P < 0.001; ****P < 0.0001).

A detailed description of other methods is provided in the **Supplemental information**.

Results

Description of study cohort

In total 26 patients diagnosed with HCC were enrolled. The patient characteristics are summarized in **Table 1**. With the exception of one patient who could undergo curative surgery, all patients were treated with palliative therapy because of comorbidity, severity of liver disease and/or advanced tumor stage. Male individuals accounted for the majority (88%, 23/26) of subjects included. The median diagnostic age of enrolled HCC patients was 68.5 years (ranged from 40-85). Most of patients are Caucasian (88%, 23/26). In 9/26 (35%) patients there was no known liver disease, almost half of patients had alcohol-related liver disease or NASH/NAFLD (46%, 12/26), and a small percentage of patients had a chronic hepatitis B/C infection (19%, 5/26). Cirrhosis existed in 15 patients (58%). The largest tumor diameter was more than or equal to 10cm in 73% (19/26) of patients. Nine patients (35%) had multiple malignant tumor foci. Macrovascular invasion was detected in 14 patients (54%). Fifteen of 26 pts (58%) were cirrhotic (BCLC stage A/B/C: 3/5/7 respectively). Elevated AFP (>400ug/L) was seen in 11 patients (42%).

Table 1. Patient Characteristics

	HCC patients (n=26)
Gender	
Male	23
Female	3
Age at sampling (years)	
<60	6
≥60	20
Mean ± SD	67 ± 11.6
Race	
Caucasian	23
Asian	2
African	1
Etiology	
No known liver disease	9
Hepatitis B/C	3/2
Alcohol-related liver disease	7
NASH/NAFLD*	4/1
Cirrhosis	
No	11
Yes	15
BCLC stage (A/B/C)	3/5/7
Size of largest lesion (cm)	
<10	7
≥10	19
Mean ± SD	13 ± 5.2
Tumor number	
1	17
>1	9
Macrovascular invasion	
No	12
Yes	14
AFP level (ug/L)	
<20	12
20-400	3
>400	11
Treatment	
Surgery	1
TACE/SIRT **	5
Systemic therapy (Sorafenib)	10
BSC***	10

* NASH, non-alcoholic steatohepatitis;

   NAFLD, non-alcoholic fatty liver disease

** TACE, transarterial chemoembolization;

   SIRT, selective internal radiation therapy

***BSC, best supportive care

CTC count and mutation profiling of CTC

As CellSearch based on EpCAM positive selection is the only U.S. FDA-approved technique for CTC detection, an important prerequisite for a diagnostic tool to be implemented in clinical practice, we used the CellSearch system to detect CTCs in HCC patients. For CTC analysis, twenty-six patients were enrolled and 7.5 mL peripheral blood from each patient was used. The number of CTCs detected by CellSearch ranged from 1-15/7.5mL blood and 27% (7/26) of patients were CTC-positive (**Figure 1A and 1B**). Among CTC-positive patients, 4 out of 7 had ≥2 CTCs. Using the Vycap system, we managed to isolate 8 single CTC (53% recovery) from the CellSearch enriched CTC fraction from the patient that had 15 CTCs (patient 12). We did whole genome amplification for each single CTC and only one CTC had good quality of the WGA and could be analyzed for the oncogenic mutations by ddPCR and NGS sequencing. However, we did not find any mutations in this CTC. Importantly, we also did not detect any oncogenic mutation in ctDNA from the plasma of this patient.

Since CellSearch is dependent on EpCAM expression by CTC, we analyzed the expression of EpCAM on tumor cells using tissue microarrays with cores of resected tumors from 109 early-stage HCC patients (surgery candidates as described previously in [31, 32]) by immunohistochemistry (IHC) staining. EpCAM expression in tumor tissue was found in only 7% (7/109) of these HCC patients (**Figure S1A-S1D**).

Collectively, we detected CTCs in a minority of our cohort of mostly advanced HCC patients and we could not isolate sufficient single CTC cells for mutational analysis.
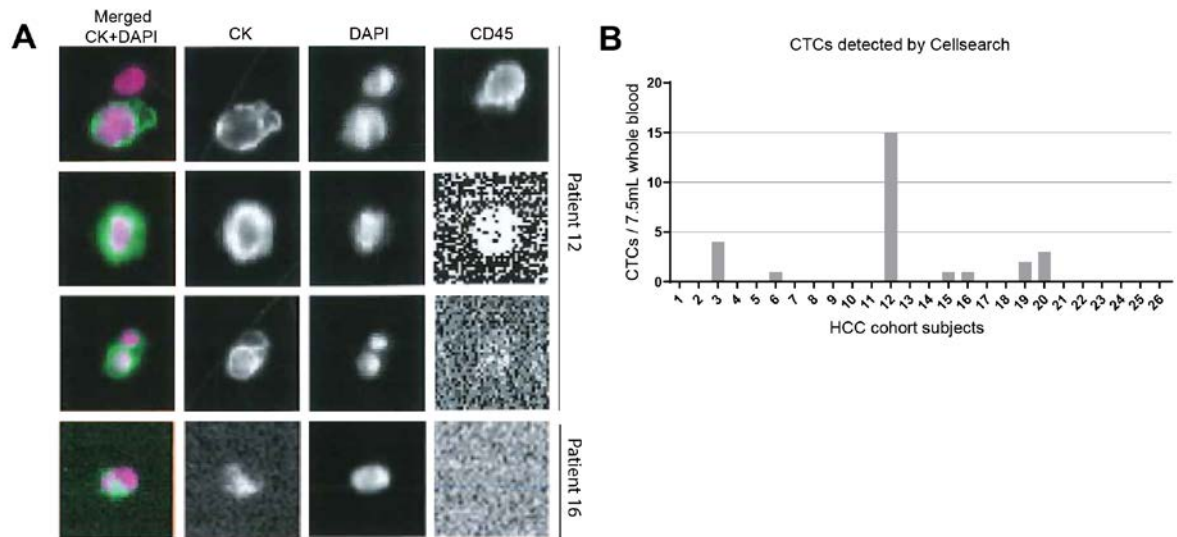
42

Figure 1.

Figure 1. CTC counts in advanced HCC patients. (A) Representative images of CellSearch show EpCAM enriched CTCs which are CK⁺ DAPI⁺CD45⁻. (B) The number of CTCs in individual HCC patient identified by the CellSearch system (n=26).

Mutational landscape in HCC by ctDNA profiling

As *TERT* promoter mutations are the most common mutations present in around 60% of HCC patients[33], we analyzed *TERT* promoter mutations C228T and C250T by ddPCR in order to estimate the ctDNA amount in blood from HCC patients. We additionally analyzed somatic mutations with a NGS panel covering 14 oncogenic genes. The amount of ctDNA that we isolated ranged from 7-282.4 ng per ml of plasma (mean 45.52 ng/ml plasma) (**Figure S2A**). The majority of patients (77%, 20/26) had at least one mutation in ctDNA, only six (23%, 6/26) had no detectable mutations (**Table S1 and S2**). The *TERT* C228T mutation (20/26, 77%) was the most frequently detected mutation whereas the *TERT* C250T mutation was absent in all patients (**Figure 2A**). *TP53* (6/26, 23%) was the second most frequently detected mutation, followed by *CTNNB1* (3/26, 12%), *PIK3CA* (3/26, 12%) and *NRAS* (4%, 1/26) (**Figure 2A**). The median VAF for ctDNA mutations are 2.76% (range: 0.3%-17.92%) for *TERT* C228T, 7.21% (range: 0.28%-14.05%) for *TP53*, 5.63% (range: 5.63%-14.68%) for *CTNNB1* and 13.09% (0.35%-13.99%) for *PIK3CA* (**Figure 2B**). Interestingly, the *TERT* C228T mutation was present in all patients with one or more ctDNA mutations, and this mutation was detectable in all patients of which CTCs were detectable (**Figure 2C**). However, ctDNA maximal VAF did not correlate with CTC count (**Figure S2B**).

43

Subsequently, we explored the concordance of these mutations in ctDNA and matched tumor tissue. There were two matched primary tumor biopsies available (patient 14 and 16) for mutational analysis, and in those tissues *TERT* C228T and *TP53* (hotspot p.R249S) mutations were present at much higher frequency in tumor compared to ctDNA (**Figure 2D**).

Collectively, ctDNA mutations can be detected in our HCC patients and the mutational landscape in ctDNA matches the published HCC mutation landscape acquired by bulk sequencing of tumor tissues [34].
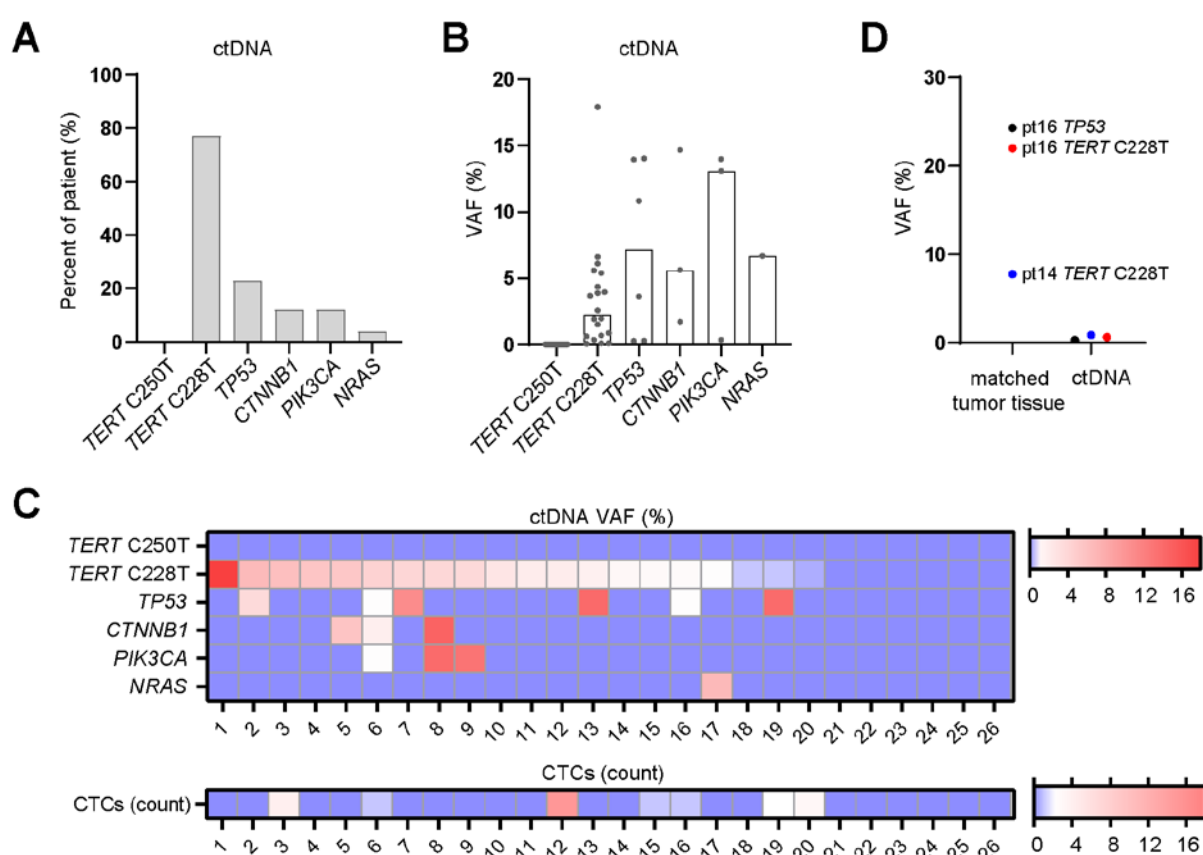
Figure 2. Mutational landscape in advanced HCC by ctDNA profiling. (A) The percentages of HCC patients that were positive for each mutated gene detected in ctDNA. TERT mutations were detected by ddPCR and other mutations were detected by NGS sequencing. (B) The VAF for each mutated gene in each HCC patient. Bars show median value of VAF. (C) Heat map shows ctDNA VAF and CTC count in each of the 26 HCC patients. VAF, variant allele frequency. (D) The VAF of mutated genes in ctDNA and matched tumor tissue.

ctDNA positively correlated with macrovascular invasion, tumor size and AFP level

We analyzed whether ctDNA status or CTC count correlated with clinicopathologic parameters known to be associated with prognosis. Clinical parameters in different groups were compared using Chi-Square test. We found that ctDNA positivity (or *TERT* C228T positivity) correlated with macrovascular invasion (MVI) as determined on imaging with CT/MRI, whereas for CTCs we did not observe such correlation (**Table 2**). We next performed a linear regression analysis to further explore the correlation between clinicopathologic parameters and ctDNA VAF or CTC counts. Results showed that maximal ctDNA VAF was positively correlated with the size of the largest tumor (r=0.44, *P*=0.024) and AFP level (r=0.53, *P*=0.005) (**Figure 3A and 3B**). Also *TERT* C228T VAF significantly correlated with largest tumor diameter (r=0.41, *P*=0.037) and AFP (Log10) level (r=0.55, *P*=0.004) (**Figure 3C and 3D**). In contrast, the CTC count did not show such correlations with largest tumor diameter or AFP (Log10) level (**Figure 3E and 3F**).

Table 2. Comparison of the clinical parameters between classified ctDNA or CTC groups

Clinicopathologic parameters	ctDNA pos (n=20)	ctDNA neg (n=6)	*P* value	CTC ≥2 (n=4)	CTC <2 (n=22)	*P* value
	N (%)	N (%)		N (%)	N (%)	
Age, years						
<60	6 (23.1)	1 (3.8)	1.000	2 (7.7)	5 (19.2)	0.287
≥60	14 (53.8)	5 (19.2)		2 (7.7)	17 (65.4)	
Cirrhosis						
No	9 (34.6)	2 (7.7)	1.000	1 (3.8)	10 (38.5)	0.614
Yes	11 (42.3)	4 (15.4)		3 (11.5)	12 (46.2)	
Tumor size						
<10	4 (15.4)	3 (11.5)	0.293	0 (0)	7 (26.9)	0.546
≥10	16 (61.5)	3 (11.5)		4 (15.4)	15 (57.7)	
Tumor number						
1	14 (53.8)	3 (11.5)	0.628	3 (11.5)	14 (53.8)	1.000
>1	6 (23.1)	3 (11.5)		1 (3.8)	8 (30.8)	
Macrovascular invasion						
No	6 (23.1)	6 (23.1)	0.004	0 (0)	12 (46.2)	0.100
Yes	14 (53.8)	0 (0)		4 (15.4)	10 (38.5)	
AFP (ng/mL)						
<20	8 (30.8)	4 (15.4)	0.365	1 (3.8)	11 (42.3)	0.598
≥20	12 (46.2)	2 (7.7)		3 (11.5)	11 (42.3)	

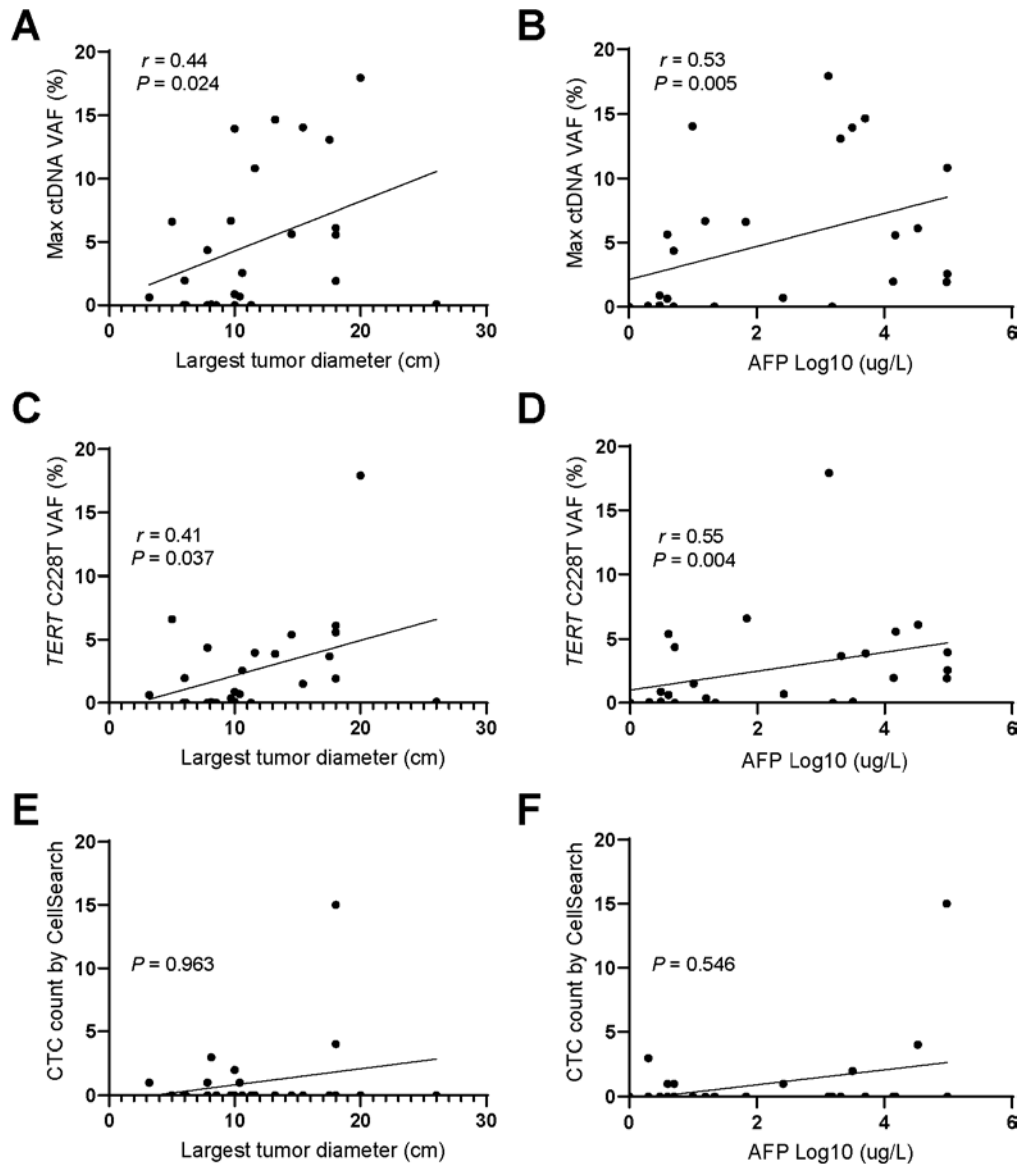**Figure 3.** ctDNA positively correlated with macrovascular invasion, tumor size and AFP level. (A-D) Linear correlations between maximal ctDNA VAF or *TERT* C228T VAF and largest tumor diameter or AFP level. (E-F) Absence of correlations between CTC count and tumor size or AFP (Log10). Spearman's rank correlation test is used to analyze the correlation between two factors. VAF, variant allele frequency.

ctDNA positivity or CTC count correlated with HCC patient survival

We next investigated whether ctDNA status or CTC count correlated with overall survival (OS) or tumor specific survival. Patients with one or more ctDNA mutations (*TERT* C228T positive patients) had a significantly worse overall survival than patients without ctDNA mutations (median OS 3 vs 17.5 months, *P*=0.016) (**Figure 4A**). Patients with CTC≥2 tended to have a worse overall survival than patients with CTC≤2 (median OS 3.5 vs 5 months, *P*=0.052) (**Figure 4B**). Moreover, patients that were ctDNA+ (or *TERT* C228T+) or with CTC≥2 had significantly worse tumor-specific survival (**Figure 4C and 4D**). We performed cox regression analysis to reveal the risk factors for overall survival. Univariate analysis revealed that ctDNA positivity and MVI were risk factors for overall survival, whereas multivariate analysis demonstrated that these two factors were dependent on each other (**Table S3**). This result was validated in chi-square test, which shows that ctDNA positivity was significantly associated with MVI (*P*=0.004) (**Table 2**).
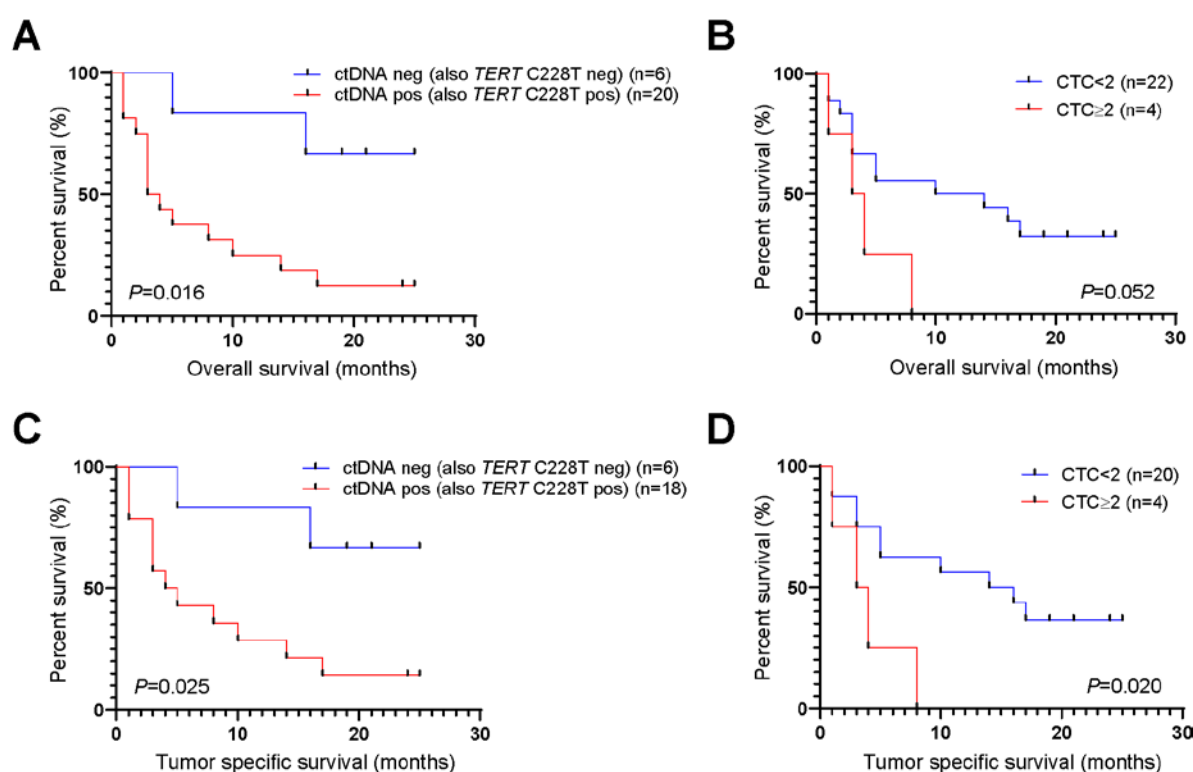

Figure 4. ctDNA positivity or CTC count correlated with HCC patient survival. (A) Patients with positive ctDNA (or *TERT* C228T) and negative ctDNA (or *TERT* C228T) demonstrated differentiated overall survival. (B) Survival curve for patients with CTC count <2 and ≥ 2. Kaplan-Meier analysis is used to evaluate the survival differences. *P* < 0.05 is considered significant.

Discussion

Liquid biopsies, including CTCs and ctDNA, may potentially be used to identify tumor-derived mutations for HCC diagnosis and to guide decisions with regard to targeted therapies. In this study, we compare CTCs and ctDNA from the same patient for oncogenic mutational profiling in a cohort of mostly advanced HCC.

EpCAM[+] CTCs have previously been detected in 28%-35% of advanced HCC patients in Western cohorts by CellSearch [5, 6, 11], which is lower than the frequencies reported in Asian cohorts (EpCAM[+] CTCs: 44%-74%) of mostly on resectable HCC patients [8, 10, 12]. In line with these findings, we found CTCs in 27% of a Western cohort of advanced HCC patients using this method. Moreover, in 43% (3/7) of CTCs+ patients only 1 CTC/7.5ml blood could be detected. Such low detection rate limits the use of this technique for mutational analysis. There can be several explanations for the low CTC detection rate: CTCs are simply not present (the frequency is < 1 in 7.5 mL blood), or they cannot be detected by this assay because the expression of capture (EpCAM) and/or identification (CK) markers is too low or lacking in a subset of patients. EpCAM was expressed in tumors of only 7% of HCC patients in our IHC analysis, and moreover has been reported to be downregulated during epithelial-mesenchymal transition (EMT) [35, 36]. The frequency of EpCAM expression in our western HCC cohort was lower compared to Asian cohorts in which its frequency ranges from 15% to 56% of patients [37-43]. This might be due to the difference in etiology of liver disease. EpCAM expression is reported to correlate with HBV infection [37, 38, 42]. However, in our cohort only 8% HBV+ patients were EpCAM[+] (2/24). Although IHC may be less sensitive to detect EpCAM expression compared to immunomagnetic capture with ferrofluids and the CellSearch enhanced aggregation technique, xour data emphasize the limitations of EpCAM-based detection of circulating tumor cells in HCC for mutational analysis due to the low frequency of CTCs in our patient cohort. Several other techniques for CTC detection have been described [4], but they have as far as we know not been FDA approved, which hampers widespread implementation in clinical practice.

In contrast, HCC-associated mutations could be detected in 77% of patients using ctDNA. In our cohort, 77% of patients have *TERT* promoter mutations, 23% have *TP53* and 12% have *CTNNB1* or *PIK3CA* mutations. Moreover, in all ctDNA+ patients the *TERT* promotor C228T mutation was present, whereas one or more additional

48

oncogenic mutation(s) was/were present in 50% of these patients. Overall the observed frequencies of mutations are consistent with NGS results of HCC tumors [34]: Totoki et al detected in HCC histology: 55% *TERT* promoter mutations, 31% *TP53*, 31% *CTNNB1* and 1% *PIK3CA* mutations respectively (a comparison of all oncogenic mutations analyzed is provided in supplementary table 4). Our data are also in line with other studies reporting that oncogenic alteration in ctDNA can be detected in 57% (8/14) - 88% (181/206) of advanced HCC patients [22, 23]. Discrepancies in reported frequencies may be related to differences in clinical characteristics of the populations studied since genomic differences along ethnic lines may influence presentation of HCC in this respect[22, 23]; we have included mostly Caucasian patients with unknown or alcoholic liver disease, whereas the above mentioned studies include more patients with viral etiology of their liver disease. In our experimental design there can be two possible explanations for ctDNA negativity: 1) the absence of any targeted mutation in the primary tumor, 2) the targeted oncogenic mutation was present in the primary tumor but it could not be detected in blood. To illustrate, recently, TERT promotor mutation in paired plasma and tissue biopsy were concordant in 21/34 patients (62%). In the 12 of 13 non-concordant samples, the TERT mutation was found in tumor but not in plasma[27]. In agreement with other studies [26, 44-46], we found mutation concordance between ctDNA and primary tumor tissue in two patients but since in our clinic routine tumor biopsies are uncommon in advanced HCC patients (in context of cirrhosis) our dataset of matched tissues is too small to draw conclusions.

In our cohort presence of ctDNA was associated with clinicopathologic parameters of advanced disease. Maximal ctDNA VAF correlated with tumor size and AFP level, and ctDNA positivity was associated with macrovascular invasion. Moreover we showed that ctDNA positivity was associated with overall and tumor-specific survival in our HCC patients and *TERT* C228T mutation alone is a significant predictor of survival. These findings are in line with recent findings by others, that have correlated TERT promotor mutation in plasma with macrovascular invasion and overall survival[27, 28]. The ddPCR technique used in our study for TERT promoter mutation analysis is a relatively easy, fast and affordable assay, that can be used in clinical care for detection of this biomarker, for instance as an additional tool in the early detection of HCC, as was suggested by others [47, 48]. Previously, ctDNA mutations in early-stage HCC patients have been associated with microvascular invasion and recurrence by others

[44, 45]. ctDNA positivity in postoperative plasma predicted poor disease-free survival after tumor resection in early HCC-patients [26].

Somatic mutations detected in ctDNA can guide treatment decisions with regard to targeted therapies. Mutation analysis of *NRAS/KRAS/BRAF*, *PIK3CA* and *CSF-1R* in plasma has been applied in a phase 2 clinical trial to assess response to a mitogen-activated protein kinase kinase (MEK) inhibitor (refametinib) in advanced HCC patients [49]. Ikeda et al.[22] evaluated 14 patients with advanced HCC and detected druggable mutations in 79% of patients. Based on their findings patients were treated with customized therapies. A patient with a *CDKN2A*-inactivating and a *CTNNB1*-activating mutation received palbociclib (CDK4/6 inhibitor) and celecoxib (COX-2/Wnt inhibitor) treatment and found declined des-gamma-carboxy prothrombin (DCP) level after 2 months of treatment. Another patient with a *PTEN*-inactivating and a *MET*-activating mutation received sirolimus (mechanistic target of rapamycin inhibitor) and cabozantinib (*MET* inhibitor) and demonstrated signs of clinical efficacy. The ease-of-use of mutational analyses using ctDNA as opposed to the more cumbersome CTC isolation allows for repeated, longitudinal analysis for prognostic and therapeutic decision making in HCC patients. In our cohort, we detected druggable mutations in 5 patients, including 3 patients with *CTNNB1*, 3 patients with *PIK3CA* and 1 patient with *NRAS* mutations.

Our study has several limitations: (1) we have a relatively small cohort of patients; (2) as mentioned, we lack sufficient matched primary tumor tissue biopsies for comparison; and (3) we did not perform paired leukocyte DNA sequencing thus we could not fully exclude that *TP53* mutations were derived from leukocyte DNA, because somatic variants in *TP53* found in ctDNA could be derived from clonal hematopoiesis [50, 51]; (4) the ctDNA panel that we used is limited and does not contain all known actionable somatic alterations (e.g. mutation in *TSC1*/*TSC2*, amplification in *EGFR* and *MET*).

In conclusion, we compared CTC and ctDNA for detecting tumor mutations in a cohort of mostly advanced HCC patients. CTCs as detected by CellSearch are present in low frequency and it is challenging to isolate single CTC for mutational analysis. In contrast, ctDNA is detectable in 77% of our HCC patients. CtDNA detection is associated with known prognostic markers for disease survival. Our study illustrates that analysis of

ctDNA may serve as a liquid biopsy to identify druggable mutations in advanced HCC patients.

References

[1]   Bray F, Ferlay J, Soerjomataram I, Siegel RL, Torre LA and Jemal A. Global cancer statistics 2018: GLOBOCAN estimates of incidence and mortality worldwide for 36 cancers in 185 countries. CA Cancer J Clin 2018; 68: 394-424.

[2]   El-Serag HB, Marrero JA, Rudolph L and Reddy KR. Diagnosis and treatment of hepatocellular carcinoma. Gastroenterology 2008; 134: 1752-1763.

[3]   Ashworth TR. A case of cancer in which cells similar to those in the tumours were seen in the blood after death. Aust Med J 1869; 14: 146.

[4]   Millner LM, Linder MW and Valdes R. Circulating tumor cells: a review of present methods and the need to identify heterogeneous phenotypes. Annals of Clinical & Laboratory Science 2013; 43: 295-304.

[5]   Schulze K, Gasch C, Staufer K, Nashan B, Lohse AW, Pantel K, Riethdorf S and Wege H. Presence of EpCAM-positive circulating tumor cells as biomarker for systemic disease strongly correlates to survival in patients with hepatocellular carcinoma. Int J Cancer 2013; 133: 2165-2171.

[6]   Morris KL, Tugwood JD, Khoja L, Lancashire M, Sloane R, Burt D, Shenjere P, Zhou C, Hodgson C, Ohtomo T, Katoh A, Ishiguro T, Valle JW and Dive C. Circulating biomarkers in hepatocellular carcinoma. Cancer Chemother Pharmacol 2014; 74: 323-332.

[7]   Zee BC, Wong C, Kuhn T, Howard R, Yeo W, Koh J, Hui E and Chan AT. Detection of circulating tumor cells (CTCs) in patients with hepatocellular carcinoma (HCC). Journal of Clinical Oncology 2007; 25: 15037-15037.

[8]   Sun Y-F, Xu Y, Yang X-R, Guo W, Zhang X, Qiu S-J, Shi R-Y, Hu B, Zhou J and Fan J. Circulating stem cell–like epithelial cell adhesion molecule–positive tumor cells indicate poor prognosis of hepatocellular carcinoma after curative resection. Hepatology 2013; 57: 1458-1468.

[9]   von Felden J, Schulze K, Krech T, Ewald F, Nashan B, Pantel K, Lohse AW, Riethdorf S and Wege H. Circulating tumor cells as liquid biomarker for high HCC recurrence risk after curative liver resection. Oncotarget 2017; 8: 89978.

[10]   Fang Z-T, Zhang W, Wang G-Z, Zhou B, Yang G-W, Qu X-D, Liu R, Qian S, Zhu L and Liu L-X. Circulating tumor cells in the central and peripheral venous compartment–assessing hematogenous dissemination after transarterial chemoembolization of hepatocellular carcinoma. OncoTargets and therapy 2014; 7: 1311.

[11]   Kelley RK, Magbanua MJM, Butler TM, Collisson EA, Hwang J, Sidiropoulos N, Evason K, McWhirter RM, Hameed B and Wayne EM. Circulating tumor cells in hepatocellular carcinoma: a pilot study of detection, enumeration, and next-generation sequencing in cases and controls. BMC cancer 2015; 15: 206.

[12]   Yu J-j, Xiao W, Dong S-l, Liang H-f, Zhang Z-w, Zhang B-x, Huang Z-y, Chen Y-f, Zhang W-g, Luo H-p, Chen Q and Chen X-p. Effect of surgical liver resection on circulating tumor cells in patients with hepatocellular carcinoma. BMC Cancer 2018; 18: 835.

[13]   Vona G, Estepa L, Béroud C, Damotte D, Capron F, Nalpas B, Mineur A, Franco D, Lacour B and Pol S. Impact of cytomorphological detection of circulating tumor cells in patients with liver cancer. Hepatology 2004; 39: 792-797.

[14]   Guo W, Yang X-R, Sun Y-F, Shen M-N, Ma X-L, Wu J, Zhang C-Y, Zhou Y, Xu Y and Hu B. Clinical significance of EpCAM mRNA-positive circulating tumor cells in hepatocellular carcinoma by an optimized negative enrichment and qRT-PCR–based platform. Clinical cancer research 2014; 20: 4794-4805.

[15]   Lapin M, Tjensvoll K, Oltedal S, Buhl T, Gilje B, Smaaland R and Nordgård O. MINDEC-an enhanced negative depletion strategy for circulating tumour cell enrichment. Scientific reports 2016; 6: 28929.

[16]   Ogle LF, Orr JG, Willoughby CE, Hutton C, McPherson S, Plummer R, Boddy AV, Curtin NJ, Jamieson D and Reeves HL. Imagestream detection and characterisation of circulating tumour cells - A liquid biopsy for hepatocellular carcinoma? J Hepatol 2016; 65: 305-313.

[17]   Kalinich M, Bhan I, Kwan TT, Miyamoto DT, Javaid S, LiCausi JA, Milner JD, Hong X, Goyal L and Sil S. An RNA-based signature enables high specificity detection of circulating tumor cells in hepatocellular carcinoma. Proceedings of the National Academy of Sciences 2017; 114: 1123-1128.

52

[18]   Boral D, Vishnoi M, Liu HN, Yin W, Sprouse ML, Scamardo A, Hong DS, Tan TZ, Thiery JP and Chang JC. Molecular characterization of breast cancer CTCs associated with brain metastasis. Nature communications 2017; 8: 1-10.

[19]   Diehl F, Li M, Dressman D, He Y, Shen D, Szabo S, Diaz LA, Goodman SN, David KA and Juhl H. Detection and quantification of mutations in the plasma of patients with colorectal tumors. Proceedings of the National Academy of Sciences 2005; 102: 16368-16373.

[20]   Diehl F, Schmidt K, Choti MA, Romans K, Goodman S, Li M, Thornton K, Agrawal N, Sokoll L, Szabo SA, Kinzler KW, Vogelstein B and Diaz Jr LA. Circulating mutant DNA to assess tumor dynamics. Nature Medicine 2008; 14: 985-990.

[21]   Chan KCA, Jiang P, Zheng YWL, Liao GJW, Sun H, Wong J, Siu SSN, Chan WC, Chan SL, Chan ATC, Lai PBS, Chiu RWK and Lo YMD. Cancer Genome Scanning in Plasma: Detection of Tumor-Associated Copy Number Aberrations, Single-Nucleotide Variants, and Tumoral Heterogeneity by Massively Parallel Sequencing. Clinical Chemistry 2013; 59: 211-224.

[22]   Ikeda S, Tsigelny IF, Skjevik ÅA, Kono Y, Mendler M, Kuo A, Sicklick JK, Heestand G, Banks KC, Talasaz A, Lanman RB, Lippman S and Kurzrock R. Next-Generation Sequencing of Circulating Tumor DNA Reveals Frequent Alterations in Advanced Hepatocellular Carcinoma. The oncologist 2018; 23: 586-593.

[23]   Kaseb AO, Sánchez NS, Sen S, Kelley RK, Tan B, Bocobo AG, Lim KH, Abdel-Wahab R, Uemura M, Pestana RC, Qiao W, Xiao L, Morris J, Amin HM, Hassan MM, Rashid A, Banks KC, Lanman RB, Talasaz A, Mills-Shaw KR, George B, Haque A, Raghav KPS, Wolff RA, Yao JC, Meric-Bernstam F, Ikeda S and Kurzrock R. Molecular Profiling of Hepatocellular Carcinoma Using Circulating Cell-Free DNA. Clinical Cancer Research 2019; 25: 6107.

[24]   Wang J, Huang A, Wang YP, Yin Y, Fu PY, Zhang X and Zhou J. Circulating tumor DNA correlates with microvascular invasion and predicts tumor recurrence of hepatocellular carcinoma. Ann Transl Med 2020; 8: 237.

[25]   Wang D, Xu Y, Goldstein JB, Ye K, Hu X, Xiao L, Li L, Chang L, Guan Y, Long G, He Q, Yi X, Zhang J, Wang Z, Xia X and Zhou L. Preoperative evaluation of microvascular invasion with circulating tumor DNA in operable hepatocellular carcinoma. Liver Int 2020;

[26]   An Y, Guan Y, Xu Y, Han Y, Wu C, Bao C, Zhou B, Wang H, Zhang M, Liu W, Qiu L, Han Z, Chen Y, Xia X, Wang J, Liu Z, Huang W, Yi X and Huang J. The diagnostic and prognostic usage of circulating tumor DNA in operable hepatocellular carcinoma. American journal of translational research 2019; 11: 6462-6474.

[27]   Oversoe SK, Clement MS, Pedersen MH, Weber B, Aagaard NK, Villadsen GE, Grønbæk H, Hamilton-Dutoit SJ, Sorensen BS and Kelsen J. TERT promoter mutated circulating tumor DNA as a biomarker for prognosis in hepatocellular carcinoma. Scandinavian Journal of Gastroenterology 2020; 55: 1433-1440.

[28]   Hirai M, Kinugasa H, Nouso K, Yamamoto S, Terasawa H, Onishi Y, Oyama A, Adachi T, Wada N and Sakata M. Prediction of the prognosis of advanced hepatocellular carcinoma by TERT promoter mutations in circulating tumor DNA. Journal of Gastroenterology and Hepatology 2020;

[29]   Stevens M, Oomens L, Broekmaat J, Weersink J, Abali F, Swennenhuis J and Tibbe A. VyCAP's puncher technology for single cell identification, isolation, and analysis. Cytometry A 2018; 93: 1255-1259.

[30]   Corless BC, Chang GA, Cooper S, Syeda MM, Shao Y, Osman I, Karlin-Neumann G and Polsky D. Development of Novel Mutation-Specific Droplet Digital PCR Assays Detecting TERT Promoter Mutations in Tumor and Plasma Samples. J Mol Diagn 2019; 21: 274-285.

[31]   Sideras K, Bots SJ, Biermann K, Sprengers D, Polak WG, JN IJ, de Man RA, Pan Q, Sleijfer S, Bruno MJ and Kwekkeboom J. Tumour antigen expression in hepatocellular carcinoma in a low-endemic western area. Br J Cancer 2015; 112: 1911-1920.

[32]   Sideras K, Biermann K, Verheij J, Takkenberg BR, Mancham S, Hansen BE, Schutz HM, de Man RA, Sprengers D, Buschow SI, Verseput MC, Boor PP, Pan Q, van Gulik TM, Terkivatan T, Ijzermans JN, Beuers UH, Sleijfer S, Bruno MJ and Kwekkeboom J. PD-L1, Galectin-9 and CD8(+) tumor-infiltrating lymphocytes are associated with survival in hepatocellular carcinoma. Oncoimmunology 2017; 6: e1273309.

[33]   Zucman-Rossi J, Villanueva A, Nault JC and Llovet JM. Genetic Landscape and Biomarkers of Hepatocellular Carcinoma. Gastroenterology 2015; 149: 1226-1239 e1224.

[34] Totoki Y, Tatsuno K, Covington KR, Ueda H, Creighton CJ, Kato M, Tsuji S, Donehower LA, Slagle BL and Nakamura H. Trans-ancestry mutational landscape of hepatocellular carcinoma genomes. Nature genetics 2014; 46: 1267.

[35] Gorges TM, Tinhofer I, Drosch M, Röse L, Zollner TM, Krahn T and Von Ahsen O. Circulating tumour cells escape from EpCAM-based detection due to epithelial-to-mesenchymal transition. BMC cancer 2012; 12: 178.

[36] Gabriel MT, Calleja LR, Chalopin A, Ory B and Heymann D. Circulating Tumor Cells: A Review of Non–EpCAM-Based Approaches for Cell Enrichment and Isolation. Clinical Chemistry 2016; 62: 571-581.

[37] Sung JJ, Noh SJ, Bae JS, Park HS, Jang KY, Chung MJ and Moon WS. Immunohistochemical expression and clinical significance of suggested stem cell markers in hepatocellular carcinoma. Journal of pathology and translational medicine 2016; 50: 52.

[38] Yamashita T, Forgues M, Wang W, Kim JW, Ye Q, Jia H, Budhu A, Zanetti KA, Chen Y and Qin L-X. EpCAM and α-fetoprotein expression defines novel prognostic subtypes of hepatocellular carcinoma. Cancer research 2008; 68: 1451-1461.

[39] Kim H, Choi GH, Na DC, Ahn EY, Kim GI, Lee JE, Cho JY, Yoo JE, Choi JS and Park YN. Human hepatocellular carcinomas with "Stemness"-related marker expression: keratin 19 expression and a poor prognosis. Hepatology 2011; 54: 1707-1717.

[40] Guo Z, Li LQ, Jiang JH, Ou C, Zeng LX and Xiang BD. Cancer stem cell markers correlate with early recurrence and survival in hepatocellular carcinoma. World J Gastroenterol 2014; 20: 2098-2106.

[41] Shan YF, Huang YL, Xie YK, Tan YH, Chen BC, Zhou MT, Shi HQ, Yu ZP, Song QT and Zhang QY. Angiogenesis and clinicopathologic characteristics in different hepatocellular carcinoma subtypes defined by EpCAM and α-fetoprotein expression status. Med Oncol 2011; 28: 1012-1016.

[42] Kimura O, Kondo Y, Kogure T, Kakazu E, Ninomiya M, Iwata T, Morosawa T and Shimosegawa T. Expression of EpCAM increases in the hepatitis B related and the treatment-resistant hepatocellular carcinoma. Biomed Res Int 2014; 2014: 172913.

[43] Govaere O, Komuta M, Berkers J, Spee B, Janssen C, de Luca F, Katoonizadeh A, Wouters J, van Kempen LC, Durnez A, Verslype C, De Kock J, Rogiers V, van Grunsven LA, Topal B, Pirenne J, Vankelecom H, Nevens F, van den Oord J, Pinzani M and Roskams T. Keratin 19: a key role player in the invasion of human hepatocellular carcinomas. Gut 2014; 63: 674-685.

[44] Ono A, Fujimoto A, Yamamoto Y, Akamatsu S, Hiraga N, Imamura M, Kawaoka T, Tsuge M, Abe H and Hayes CN. Circulating tumor DNA analysis for liver cancers and its usefulness as a liquid biopsy. Cellular and molecular gastroenterology and hepatology 2015; 1: 516-534.

[45] Liao W, Yang H, Xu H, Wang Y, Ge P, Ren J, Xu W, Lu X, Sang X and Zhong S. Noninvasive detection of tumor-associated mutations from circulating cell-free DNA in hepatocellular carcinoma patients by targeted deep sequencing. Oncotarget 2016; 7: 40481.

[46] Huang A, Zhang X, Zhou SL, Cao Y, Huang XW, Fan J, Yang XR and Zhou J. Detecting Circulating Tumor DNA in Hepatocellular Carcinoma Patients Using Droplet Digital PCR Is Feasible and Reflects Intratumoral Heterogeneity. J Cancer 2016; 7: 1907-1914.

[47] Jiao J, Watt GP, Stevenson HL, Calderone TL, Fisher-Hoch SP, Ye Y, Wu X, Vierling JM and Beretta L. Telomerase reverse transcriptase mutations in plasma DNA in patients with hepatocellular carcinoma or cirrhosis: Prevalence and risk factors. Hepatol Commun 2018; 2: 718-731.

[48] Akuta N, Kawamura Y, Kobayashi M, Arase Y, Saitoh S, Fujiyama S, Sezaki H, Hosaka T, Kobayashi M, Suzuki Y, Suzuki F, Ikeda K and Kumada H. TERT Promoter Mutation in Serum Cell-Free DNA Is a Diagnostic Marker of Primary Hepatocellular Carcinoma in Patients with Nonalcoholic Fatty Liver Disease. Oncology 2021; 99: 114-123.

[49] Lim HY, Heo J, Choi HJ, Lin CY, Yoon JH, Hsu C, Rau KM, Poon RT, Yeo W, Park JW, Tay MH, Hsieh WS, Kappeler C, Rajagopalan P, Krissel H, Jeffers M, Yen CJ and Tak WY. A phase II study of the efficacy and safety of the combination therapy of the MEK inhibitor refametinib (BAY 86-9766) plus sorafenib for Asian patients with unresectable hepatocellular carcinoma. Clin Cancer Res 2014; 20: 5976-5985.

54

[50]   Razavi P, Li BT, Brown DN, Jung B, Hubbell E, Shen R, Abida W, Juluru K, De Bruijn I, Hou C, Venn O, Lim R, Anand A, Maddala T, Gnerre S, Vijaya Satya R, Liu Q, Shen L, Eattock N, Yue J, Blocker AW, Lee M, Sehnert A, Xu H, Hall MP, Santiago-Zayas A, Novotny WF, Isbell JM, Rusch VW, Plitas G, Heerdt AS, Ladanyi M, Hyman DM, Jones DR, Morrow M, Riely GJ, Scher HI, Rudin CM, Robson ME, Diaz LA, Solit DB, Aravanis AM and Reis-Filho JS. High-intensity sequencing reveals the sources of plasma circulating cell-free DNA variants. Nature Medicine 2019; 25: 1928-1937.
[51]   Leal A, van Grieken NCT, Palsgrove DN, Phallen J, Medina JE, Hruban C, Broeckaert MAM, Anagnostou V, Adleff V, Bruhm DC, Canzoniero JV, Fiksel J, Nordsmark M, Warmerdam FARM, Verheul HMW, van Spronsen DJ, Beerepoot LV, Geenen MM, Portielje JEA, Jansen EPM, van Sandick J, Meershoek-Klein Kranenbarg E, van Laarhoven HWM, van der Peet DL, van de Velde CJH, Verheij M, Fijneman R, Scharpf RB, Meijer GA, Cats A and Velculescu VE. White blood cell and cell-free DNA analyses for detection of residual disease in gastric cancer. Nature Communications 2020; 11: 525.

Supplemental data for:

Detection of oncogenic mutations in paired circulating tumor DNA and circulating tumor cells in in patients with hepatocellular carcinoma

Table of contents

56

Supplemental material and methods

Immunohistochemistry (IHC)

To estimate the frequency of HCC patients with EpCAM expressing tumors cells, expression of EpCAM was determined on tumor cells using tissue microarrays with cores of normal liver tissue (obtained from livers of multi-organ donors), tumors and paired tumor-free liver tissues from 109 HCC-patients by immunohistochemistry (cohort and tissue micro-arrays were described previously) [1, 2]. The TMAs were immunohistochemically stained by the department of pathology of Erasmus MC. IHC was performed with an automated, validated and accredited staining system (Ventana Benchmark ULTRA, Ventana Medical Systems, Tucsen, AZ, USA) using Optiview universal DAB detection Kit (#760-700). In brief, following deparaffinization and heat-induced antigen retrieval the tissue samples were incubated according to their optimized time with CD155. Incubation was followed by hematoxylin II counter stain for 12 minutes and then a blue coloring reagent for 8 minutes according to the manufactures instructions (Ventana). The immunohistochemically stained TMAs were then scanned using NanoZoomer 2.0HT (Hamamatsu) and scored blindly by two researchers, based on the intensity of staining (0[none],1[low], 2[intermediate], 3[strong]) and the frequency of positive tumor cells or hepatocytes (A[<10%], B[10-50%], C[50-90%], D[>90%]). The score per core was calculated by multiplying the intensity by the frequency of positive cells (A=0.1, B=0.3, C=0.7 and D=1), and then the average score per tissue was calculated by taking the average of the three scores.

References

1. Sideras K, Bots SJ, Biermann K, et al. Tumour antigen expression in hepatocellular carcinoma in a low-endemic western area. Br J Cancer 2015;112:1911-20.

2. Sideras K, Biermann K, Verheij J, et al. PD-L1, Galectin-9 and CD8(+) tumor-infiltrating lymphocytes are associated with survival in hepatocellular carcinoma. Oncoimmunology 2017;6:e1273309.
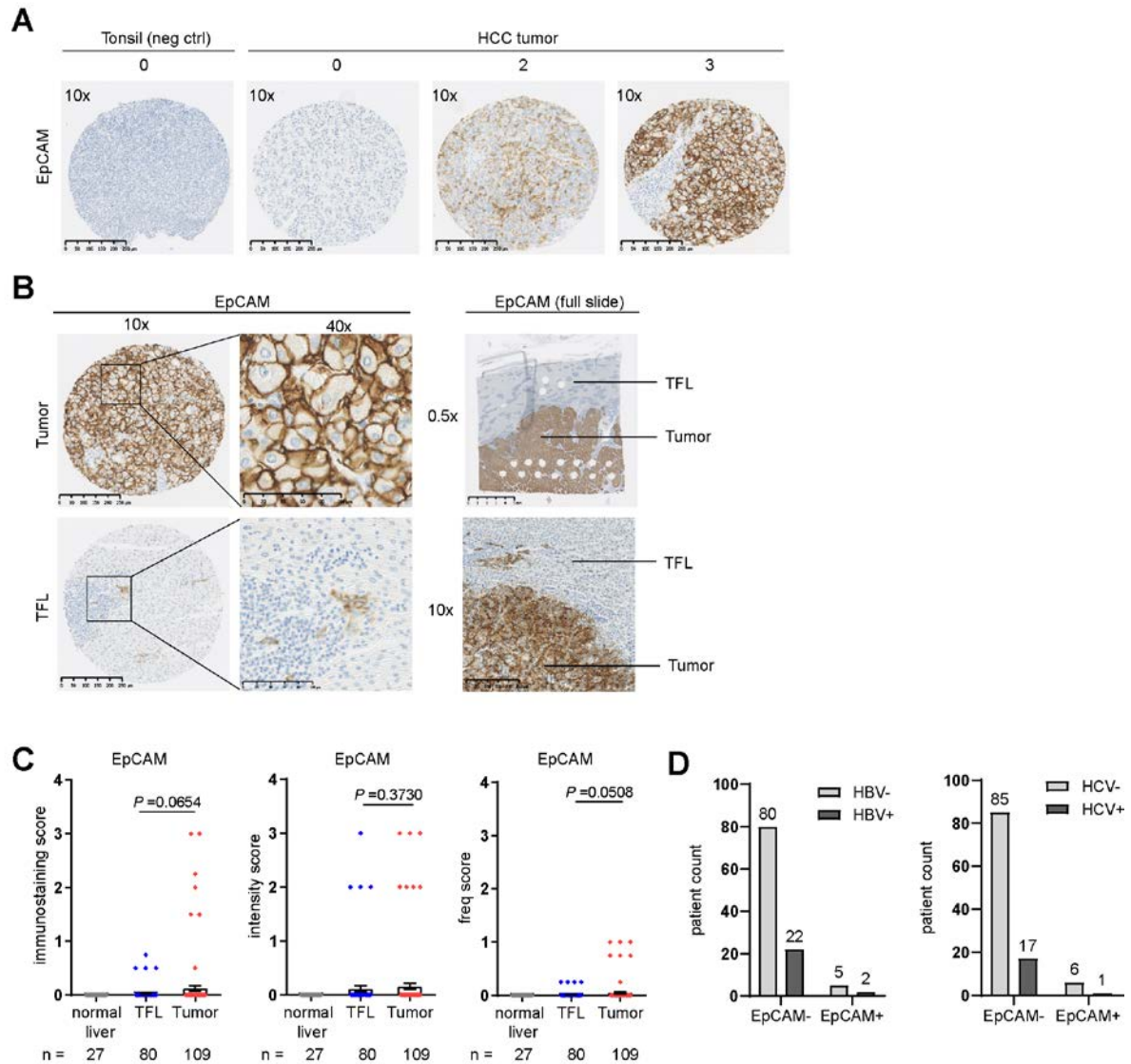
Supplemental Figure 1. EpCAM expression in HCC tumors. (A) Representative images of immunohistochemistry staining show EpCAM intensity scoring in tissue microarrays. Tonsil serves as negative control tissue. (B) Representative images of immunohistochemistry staining show EpCAM expression in HCC tumor and paired surrounding tumor-free liver (TFL) tissue. The immunostaining score for tumor is 3D and for TFL is 0. The full tissue section of this patient is also shown. Scale bars are presented in each image. (C) The immunostaining score, intensity score and frequency score of EpCAM in individual patients is presented (n=109). Significance was assessed by Wilcoxon matched-pairs signed rank test. P<0.05 is considered statistically significant. (D) The associations of EpCAM positivity of tumors with HBV/HCV infections are shown.
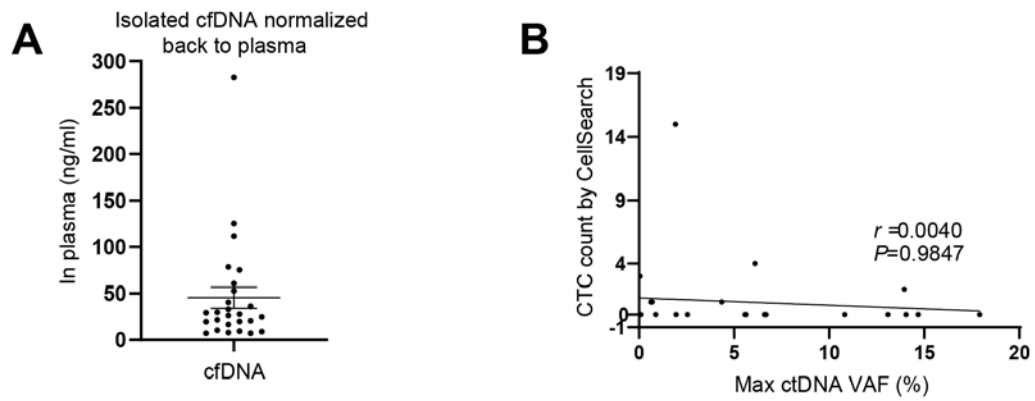
Supplemental Figure 2. CfDNA amount and the correlation between ctDNA VAF and CTC count. (A) The isolated cfDNA amount normalized to per ml plasma. (B) The correlation between CTC count and maximal ctDNA VAF.

Supplemental Table 1. An overview of ctDNA mutations and CTC count in advanced HCC patients

Patients	Total no. of mutations in cfDNA	Mutated Genes VAF (%)					Count
		TERT C228T	TP53	CTNNB1	PIK3CA	NRAS	EpCAM+ CTCs
1	1	17.92					0
2	2	6.61	3.61				0
3	1	6.11					4
4	1	5.57					0
5	2	5.39		5.63			0
6	4	4.35	0.29	1.73	0.35		1
7	2	3.95	10.82				0
8	3	3.87		14.68	13.99		0
9	2	3.67			13.09		0
10	1	2.55					0
11	1	1.95					0
12	1	1.92					15
13	2	1.50	14.05				0
14	1	0.88					0
15	1	0.69					1
16	2	0.63	0.28				1
17	2	0.35				6.68	0
18	1	0.09					0
19	2	0.09	13.95				2
20	1	0.05					3
21	0						0
22	0						0
23	0						0
24	0						0
25	0						0
26	0						0
	Total	20	6	3	3	1	7

Color scale: stronger color indicates higher frequency or number.

60

Supplemental Table 2. An overview of ctDNA mutation hotspots detected in HCC by NGS

Patient	Gene ID	Allele name	Mutation	VAF(%)	Chromosome location
2	TP53	p.R283P	C->G	3.61	Chr17_7577118
7	TP53	p.P278T	G->T	10.82	Chr17_7577118
13	TP53	p.R248W	G->A	14.05	Chr17_7577547
16	TP53	p.R249S	C->A	0.28	Chr17_7577547
19	TP53	p.R249S	C->A	13.95	Chr17_7577547
5	CTNNB1	p.T41A	A->G	5.63	Chr3_41266125
6	CTNNB1	p.T41A	A->G	1.73	Chr3_41266125
	PIK3CA	p.Q546R	A->G	0.35	SP_27.58329
	TP53	p.R282W	G->A	0.29	Chr17_7577118
8	CTNNB1	p.S45P	T->C	14.68	Chr3_41266125
	PIK3CA	p.Q546K	C->A	13.99	SP_27.58329
9	PIK3CA	p.E542K	G->A	13.09	SP_27.58329
17	NRAS	p.Q61K	G->T	6.68	SP_1.225761

Supplemental Table 3. Univariate and multivariate analysis of overall survival by Cox regression model

Clinicopathologic parameters	Univariate		Multivariate	
	HR (95% CI)	*P* value	HR (95%CI)	*P* value
ctDNA status: neg vs pos	5.382 (1.215-23.849)	0.027	3.996 (0.727-21.955)	0.111
CTC count: <2 vs ≥2	2.195 (0.679-7.093)	0.189		
Age, y: <60 vs ≥60	0.415 (0.156-1.102)	0.077		
Cirrhosis: yes vs no	0.499 (0.187-1.331)	0.165		
Tumor size:<10 vs ≥10	2.401 (0.685-8.416)	0.171		
Tumor number: 1 vs >1	0.578 (0.214-1.561)	0.280		
MVI: yes vs no	3.101 (1.111-8.654)	0.031	1.567 (0.489-5.023)	0.450
AFP: < 20 vs ≥20	1.586 (0.615-4.088)	0.340		

62

Supplementary Table 4. Comparison of genes in current study to Totoki's study[a]

gene	Ge (n=26)	Totoki (n=452)
TERT promoter	77%	55%
TP53	23%	31%
CTNNB1	12%	31%
PIK3CA	12%	1%
NRAS	4%	NA[b]
APC	0%	2%
BRAF	0%	NA
AKT1	0%	NA
EGFR	0%	NA
ERBB2	0%	NA
KRAS	0%	NA
GNAS	0%	NA
MAD4	0%	NA
MAP2K1	0%	NA
FBXW7	0%	<1%

a. Study represented here: Totoki et al. Nature Genetics 2014.
b. NA, not available. Because the frequency is not reported in the paper.

Supplementary table 5: Torrent Variant Caller parameter settings

Parameter *	Value
snp_min_allele_freq	0.0005
snp_strand_bias	1
hotspot_min_coverage	3
sse_prob_threshold	1
try_few_restart_freq	1
hotspot_min_cov_each_strand	0
indel_min_var_coverage	2
hotspot_min_allele_freq	0.0005
report_ppa	0
mnp_min_variant_score	6
indel_func_size_offset	0
hotspot_strand_bias	1
filter_insertion_predictions	0.2
indel_min_variant_score	10
indel_min_coverage	3
heavy_tailed	3
snp_strand_bias_pval	0
outlier_probability	0.001
position_bias_ref_fraction	0.05
indel_strand_bias_pval	0
data_quality_stringency	20
snp_min_cov_each_strand	0
tag_sim_max_cov	10
indel_as_hpindel	0
hp_max_length	5
mnp_strand_bias	1
snp_min_coverage	3
use_fd_param	0
hotspot_min_var_coverage	2
mnp_strand_bias_pval	0
min_ratio_for_fd	0.1
hotspot_strand_bias_pval	0
hotspot_min_variant_score	3
max_flows_to_test	10
mnp_min_var_coverage	2
indel_strand_bias	1
position_bias	0.75
downsample_to_coverage	20000
filter_unusual_predictions	0.1
indel_min_allele_freq	0.0005
mnp_min_allele_freq	0.0005
mnp_min_coverage	3

mnp_min_cov_each_strand	0
fd_nonsnp_min_var_cov	1
tag_trim_method	sloppy-trim
prediction_precision	1
indel_min_cov_each_strand	0
filter_deletion_predictions	0.2
min_tag_fam_size	3
snp_min_variant_score	6
suppress_recalibration	0
position_bias_pval	0.05
use_position_bias	0
snp_min_var_coverage	2
* For detailed description of each parameter please read the Torrent Suite software user Guide 5.10: *https://assets.thermofisher.com/TFS-Assets/LSG/manuals/MAN0017598_TorrentSuiteSoftware_5_10_UG.pdf*	

CHAPTER 4

TIGIT, the next step towards successful combination immune checkpoint therapy in cancer

Zhouhong Ge[1], Maikel P.Peppelenbosch[1], Dave Sprengers*[1], Jaap Kwekkeboom*[1]

Department of [1] Gastroenterology and Hepatology, Erasmus MC-University Medical Center, Rotterdam, the Netherlands

Highlights

- TIGIT blockade synergizes with PD-1/PD-L1 blockade to enhance anti-tumor effects of CD8$^+$ T cells.

- TIGIT blockade does not only reinvigorate anti-tumor T cell responses but also enhances anti-tumor NK cell responses.

- TIGIT blockade reduces the suppressive capacity of tumor-infiltrating regulatory T cells.

Summary

T cell immunoreceptor with Ig and ITIM domains (TIGIT) is an inhibitory receptor expressed on several types of lymphocytes. Efficacy of antibody blockade of TIGIT in cancer immunotherapy is currently widely being investigated in both pre-clinical and clinical studies. In multiple cancers TIGIT is expressed on tumor-infiltrating cytotoxic T cells, helper T cells, regulatory T cells and NK cells, and its main ligand CD155 is expressed on tumor-infiltrating myeloid cells and upregulated on cancer cells, which contributes to local suppression of immune-surveillance. While single TIGIT blockade has limited anti-tumor efficacy, pre-clinical studies indicate that co-blockade of TIGIT and PD-1/PD-L1 pathway leads to tumor rejection, notably even in anti-PD-1 resistant tumor models. Among inhibitory immune checkpoint molecules, a unique property of TIGIT blockade is that it enhances not only anti-tumor effector T-cell responses, but also NK-cell responses, and reduces the suppressive capacity of regulatory T cells. Numerous clinical trials on TIGIT-blockade in cancer have recently been initiated, predominantly combination treatments. The first interim results show promise for combined TIGIT and PD-L1 co-blockade in solid cancer patients. In this review, we summarize the current knowledge and identify the gaps in our current understanding of TIGIT's roles in cancer immunity, and provide, based on these insights, recommendations for its positioning in cancer immunotherapy.

Key words: Immunotherapy; T cells; NK cells; CD226; CD155

Introduction

Therapeutic immune checkpoint inhibitors (ICIs) aimed to restore the functionality of tumor-specific T-cells to combat malignant tumors have been shown to be effective in many cancer types. Specifically, anti-PD-1/PD-L1 therapies have been approved by FDA for treating more than ten cancer entities, including melanoma, non-small cell lung carcinoma (NSCLC), advanced hepatocellular carcinoma (HCC) and all types of deficient mismatch repair(dMMR) tumors[1-3].

However, only a subset of patients with these types of cancer showed durable clinical responses [4, 5], and numerous other types of cancer, among which MMR-proficient CRC, are resistant to anti-PD1-/PD-L1 therapies [6, 7], suggesting that in these patients mechanisms are present that limit the effects of anti-PD-1/PD-L1 antibodies. An immunosuppressive tumor microenvironment, a paucity of T cells in tumors (so called immunologically "cold" tumors) and low tumor-mutational burden have all been suggested to contribute to the observed suboptimal therapeutic effects of anti-PD-1/PD-L1 therapies [8]. In addition, although the PD-1/PD-L1 axis plays a central role in regulating T cell functions, there are many other co-inhibitory receptor-ligand interactions that can restrain anti-tumor functions of CD8$^+$ T cells in the tumor micro-environment, either directly or indirectly. These co-inhibitory receptors include T cell immunoglobulin mucin domain 3 (TIM3) [9], lymphocyte-activation gene 3 (LAG3) [10], cytotoxic T-lymphocyte associated protein 4 (CTLA-4) [11] and T cell immunoreceptor with Ig and ITIM domains (TIGIT) [12]. Their ligands are expressed on cancer cells and/or immune cells in many tumors. These inhibitory receptor-ligand interactions collaborate to achieve fine tuning of T-cell functions throughout the different phases of T-cell activation, and can contribute to resistance of tumors against PD-1/PD-L1 blockade.

In preclinical and subsequent clinical studies, it has been demonstrated that co-blockade of PD-1 and a second co-inhibitory receptor is able to augment the antitumor immunity versus single PD-1 blockade. Indeed, blockade of both PD-1 and CTLA-4 showed improved clinical efficacy in patients with, amongst others, melanoma [13] and advanced non-small-cell lung cancer [14] and hepatocellular carcinoma [15]. However, combine PD-1 and CTLA-4 blockade is hampered by a high frequency of severe immune-related systemic adverse effects [16], therefore other less toxic combinations are urgently needed. Theoretically, TIGIT-blockade may be an interesting alternative

for CTLA-4 blockade, because TIGIT knockout mice do not develop autoimmunity [17, 18], while CTLA-4 knockout mice die within 2-3 weeks due to severe autoimmunity [19].

Here we review the current knowledge of the immunomodulatory activity of TIGIT in anti-cancer immunity and its potential as a target for cancer immune checkpoint therapy. We identify gaps in our current understanding of TIGIT's roles in cancer immunity that require further study and, based on current insights, we provide recommendations for its positioning in cancer immune checkpoint therapy.

TIGIT structure, expression and ligands

TIGIT (also identified as WUCAM [20], VSTM3 [17]) is a co-inhibitory molecule that was first identified in 2009 [21]. Similar to LAG3 and TIM3, TIGIT belongs to the immunoglobulin superfamily [22]. It consists of an extracellular immunoglobulin variable (IgV) domain, a type 1 transmembrane domain and a cytoplasmic tail with an immunoreceptor tyrosine-based inhibitory motif (ITIM) and an Ig tail-tyrosine (ITT)-like motif [21-24]. TIGIT is exclusively expressed on lymphocytes, including CD8$^+$ T cells, memory and regulatory CD4$^+$ T cells, follicular CD4$^+$ T cells and NK cells [20-22].

TIGIT binds to at least two nectin family members, CD155 (PVR, Necl-5) and CD112 (PVRL2, Nectin-2), but with much higher affinity to CD155 (Kd=1-3 nM) than to CD112 (Kd unmeasurable) [21]. TIGIT shares these ligands with two other receptors; CD226 (DNAM-1) and CD96 (TACTILE), which deliver co-stimulatory and co-inhibitory signals, respectively. TIGIT competes with the costimulatory receptor CD226 for binding to CD155, but TIGIT has a higher affinity for CD155 (Kd=1-3 nM) compared to CD226 (Kd=119 nM) [21]. A recent paper shows that TIGIT also binds to nectin-4 and that nectin-4 interacts only with TIGIT, and not with CD226 and CD96 [25], but little is known about the functional role of TIGIT-nectin-4 interaction in anti-tumor immunity.

CD155 is expressed on monocytes, dendritic cells (DCs), fibroblasts and endothelial cells, both in healthy tissues and in tumors. Additionally, CD155 is over-expressed on cancer cells in human malignancies including colon cancer [26], lung adenocarcinoma [27], melanoma [28], pancreatic cancer [29], glioblastoma [30] and hepatocellular carcinoma [31]. Apart from its normal function in establishing cell-cell adhesion [32, 33], it also functions as the receptor of polio virus [34]. Expression of CD155 on tumor cells facilitates tumor cell growth and migration by tumor-intrinsic mechanisms [30] and its overexpression is

correlated with tumor progression and unfavorable prognosis [27-29]. However, loss of CD155 on tumor cells not only reduces tumor growth by tumor-intrinsic mechanisms, but also improves response to anti-PD-1 antibody therapy in mouse tumor models [35]. In addition, high CD155 expression in tumors is associated with resistance to anti-PD-1 therapy in metastatic melanoma patients [36]. Moreover, PVRL1 (CD111, nectin-1) promotes TIGIT-mediated T cell suppression by stabilizing CD155 on the surface of HCC tumor cells, and PVRL1 knockdown in tumor cells in an HCC mouse model resulted in reduced tumor growth in a CD8$^+$ T cell-dependent manner [37]. These data show that CD155 expression in tumors has dual tumor-promoting effects, both tumor-intrinsic and by inhibition of anti-tumor immunity.

CD112 is expressed by DCs and monocytes [38] and over-expressed in different types of cancers such as acute myeloid leukemia [39], multiple myeloma [40-42] and epithelial cancers [43, 44]. CD112 has higher affinity for CD112R (PVRIG) than for TIGIT, and suppresses T cells mainly via binding to CD112R [45, 46] and not via TIGIT [47]. Therefore, it is reasonable to consider that modulation of T cell and NK cell functions via TIGIT is mainly by mediated by interaction with CD155.

The mechanisms of TIGIT co-inhibition

While all co-inhibitory receptors have the ability to suppress T cell activation, they differ in potency, kinetics of expression and with respect to the cellular signaling pathways they alter. Whereas the co-inhibitory checkpoint CTLA-4 acts downstream of TCR-induced signaling by targeting downstream effectors of PI3K through activation of the serine/threonine phosphatase PP2A [48], TIGIT acts more upstream [49]. TIGIT can inhibit CD8$^+$ T cell proliferation and activation by directly acting on TCR expression itself as engagement of TIGIT induces a down-regulation of the TCR-α chain and molecules that comprise the TCR complex [18]. In addition, TIGIT can reduce TCR-induced p-ERK signaling in CD8$^+$ T cells [49]. Binding of TIGIT on NK cells to its ligand CD155 suppresses NK-cell mediated cytotoxicity and IFN-γ production through signaling cascades generated by ITIM and ITT-like motifs in its cytoplasmic tail [22-24]. However, TIGIT exerts its functions not only by direct cell-intrinsic inhibitory signaling, but like CTLA4 which blocks binding of its co-stimulatory counterpart CD28 to their shared ligands CD80 and CD86, also in an indirect way. TIGIT can compete for ligand binding with CD226 thereby reducing T-cell co-stimulation via CD226 [50]. In addition, TIGIT can

prevent co-stimulatory signaling via CD226 by blocking CD226 homo-dimerization [51]. Finally, TIGIT can suppress T-cells indirectly by modulating functions of cells expressing its ligand CD155. TIGIT expressed on CD4$^+$ T cells induces IL-10 and suppresses IL-12 production by DCs via CD155 ligation and thereby inhibits CD4$^+$ T cell proliferation and IFN-γ production [21]. The mechanisms of TIGIT co-inhibition of T cells are illustrated in **Figure 1.**
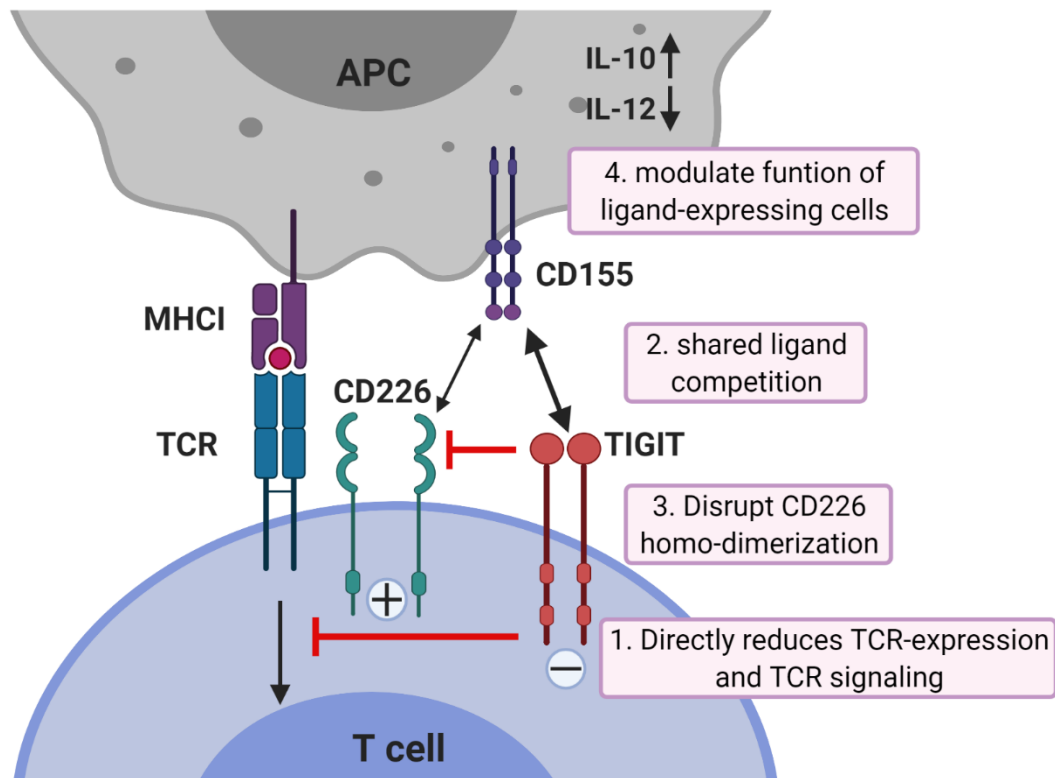
Figure 1. Mechanisms of TIGIT inhibition in T cells. TIGIT displays multiple inhibitory mechanisms in T cells. 1) TIGIT binds to CD155 and delivers intracellular inhibitory signals which directly reduces TCR-expression and TCR signaling. 2) TIGIT binds to CD155 with much higher affinity than its co-stimulatory counterpart CD226 and thereby can replace CD226 from CD155 binding; 3) or disrupts CD226 homo-dimerization to inhibit CD226-mediated T cell activation. 4) TIGIT binds to CD155 on APCs to induce IL-10 production and decrease IL-12 production which indirectly inhibits T cells. APCs, antigen-presenting cells. The figure is adapted based upon the cartoon from Pauken KE et al.[101]

TIGIT's role in anti-cancer immunity

TIGIT is expressed on human tumor-infiltrating CD8^{+} T cells, NK cells, Th and Treg cells in melanoma [52, 53], NSCLC [54, 55], colon cancer [51], HCC [31, 56], gastric cancer [57], glioblastoma [58] and hematological malignancies [41, 59, 60]. Increased numbers of intra-tumoral TIGIT^{+}CD4^{+} and CD8^{+} T cells are associated with inferior patient outcomes and poor survival in follicular lymphoma patients [59]. High TIGIT expression on peripheral CD8^{+} T cells is associated with primary refractory disease in acute myelogenous leukemia (AML) patients [61]. Circulating PD-1^{+}TIGIT^{+}CD8^{+} T-cell populations are negatively correlated with overall survival rate and progression-free survival rates in patients with hepatitis B virus associated HCC (HBV-HCC) [62]. These data suggest a suppressive role of TIGIT in anti-tumor immunity in cancer patients. In the next four paragraphs, we will discuss via which tumor-infiltrating immune cell populations TIGIT may inhibit anti-tumor immunity, and how such inhibition could be overcome.

TIGIT blockade synergizes with PD-1 blockade to enhance anti-tumor effects of intra-tumoral CD8^{+} T cells

Generating CD8^{+} T cell antitumor responses is the major goal of most cancer immunotherapies because it is considered that CD8^{+} T cells not only provide effective immediate cytotoxicity against tumor cells, but also generate immunological memory to sustain anti-tumor immunity. Knockdown of TIGIT was able to restore *in vitro* IFN-γ and TNF-α production by circulating CD8^{+} T cells from AML patients [61]. Nevertheless, single TIGIT blockade achieved no or moderate anti-tumor efficacy in experimental tumor models [37, 51, 56, 63] and in enhancing *in vitro* functionality of human tumor-infiltrating CD8^{+} T cells [31]. However, since CD155-TIGIT interaction contributes to cancer resistance to PD-1 blockade [35, 36], inhibition of TIGIT may be a promising strategy to increase the efficacy of PD-1 blockade therapy, especially to combat PD-1 inhibitor resistant tumors [37].

TIGIT is coordinately expressed with PD-1 on human and murine CD8^{+} TILs [51, 52, 56, 64, 65], whereas CD226 expression is negatively associated with PD-1 expression on CD8^{+} TILs [31, 52]. In mouse tumors, TIGIT marks a dysfunctional subset of CD8^{+} TILs that co-expresses high levels of PD-1 and TIM3 [65, 66]. Similarly, co-expression of TIGIT and PD-1 identifies dysfunctional CD4^{+} and CD8^{+} TIL subsets in human B-cell lymphoma

74

[64]. We recently showed that in HCC patients TIGIT expression is up-regulated whereas CD226 expression is down-regulated on CD8$^+$ TILs that display high PD-1 expression. These TIGIT$^+$PD-1^{hi}CD8$^+$ T cells co-express exhaustion markers TIM3 and LAG3, show functional defects in IFN-γ and TNF-α production, and demonstrate higher TOX expression and lower TCF-1 expression compared to TIGIT$^+$PD-1^{int} CD8$^+$ TILs, together characterizing them as exhausted dysfunctional CD8$^+$ TILs [31]. While CD8$^+$PD1^{int}TIGIT$^+$ T cells are found in tumors of all HCC patients, TIGIT-expressing CD8$^+$PD1^{hi} TILs are present in a subset of HCC patients [31] and are associated with poor prognosis [67], supporting their poor anti-tumor functions. Interestingly, it has been demonstrated that *in vitro* PD-1 blockade upregulates TIGIT expression on NY-ESO-1$^+$ CD8$^+$ T cells from melanoma patients [52], and that TIGIT is the most-upregulated immune checkpoint on CD8$^+$ TILs upon anti-PD-1 treatment in a PD-1 non-responsive HCC mouse model [37], suggesting TIGIT as a plausible target to improve efficacy of anti-PD-1 treatment.

In the MC38 colon carcinoma mouse model, TIGIT blockade alone led to a small but uniform retardation of tumor growth. Anti-PD-1 treatment alone resulted in a variable response with most mice showing initial tumor regression followed by escape and only one mouse showing complete tumor regression. However, anti-TIGIT/anti-PD-1 co-blockade increased IFN-γ, TNF-α and IL-2 in CD8$^+$ TILs and resulted in complete tumor regression in all mice [68]. Likewise, in the CT26 colon carcinoma [51] and glioblastoma[63] mouse models, co-blockade of TIGIT and PD-1/PD-L1 pathway synergistically decreased tumor burden and improved survival by increasing IFN-γ^+ CD8$^+$ TILs[51]. In HCC-bearing mice which were resistant to PD-1 blockade, dual blockade of TIGIT and PD-1 expanded the effector memory CD8$^+$ T cell population and increased ratio of cytotoxic T cells to Treg in tumors, resulting in suppressed tumor growth and prolonged survival [37]. Combined PD-1/TIGIT blockade resulted also in another mouse HCC model in synergistic inhibition of tumor growth and significantly prolonged mice survival [56]. Furthermore, co-blockade of PD-1 and TIGIT increased the *in vitro* proliferation, cytokine production and anti-tumor function of CD8$^+$ TILs from HCC and melanoma patients [31, 52].

The balance of TIGIT/CD226 expression on CD8$^+$ T cells is important for proper CD8$^+$ function, and the effect of TIGIT blockade is abrogated by CD226-blockade [31, 51, 69, 70],

demonstrating that co-stimulation via CD226 is required for stimulatory effect of TIGIT blockade on CD8^{+} T cells. CD226^{hi} CD8^{+} T cells but not CD226^{lo} CD8^{+} T cells are required for anti-TIGIT or anti-PD-1 responses [70]. Unfortunately, CD226 expression is down-regulated on CD8^{+} TILs [52, 70], especially on CD8^{+}PD1^{hi} exhausted dysfunctional CD8^{+} TILs [31] which have been shown to contain the majority of tumor-reactive cells[55, 71]. Moreover, PD-1 signaling suppresses CD226 signaling [69]. These mechanisms may explain the limited effect of single TIGIT blockade on CD8^{+} TIL anti-tumor functions. Interestingly, blockade of PD-1 restores CD226 co-stimulatory signaling [69], and this observation may explain the synergy between PD-1 and TIGIT blockade in enhancing CD8^{+} TIL responses.

Together with pre-clinical [35, 37] and clinical data [36] showing that CD155 expression on tumor cells contributes critically to resistance to anti-PD-1 immunotherapy, the pre-clinical data that demonstrate and mechanistically explain synergy between TIGIT-blockade and PD-1 blockade to enhance anti-tumor CD8^{+} T cell immunity, argue that dual PD-1 and TIGIT blockade is a promising combinatorial approach to overcome resistance to PD-1/PD-L1 single blockade. The interactions between the mechanisms of T cell co-inhibition by TIGIT and PD-1 interactions are depicted in **Figure 2**.
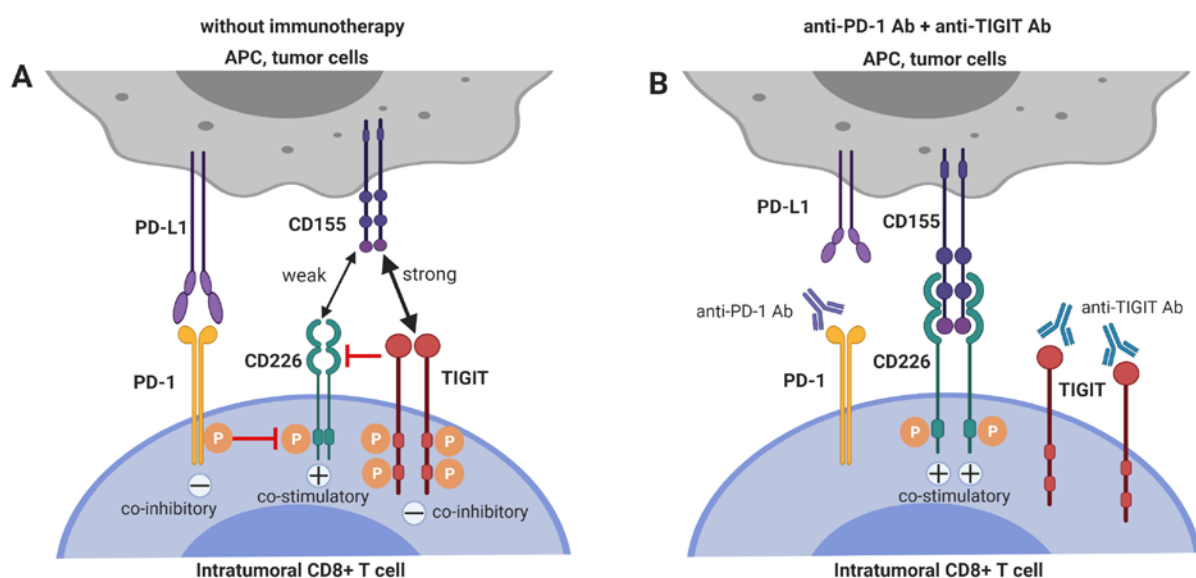

Figure 2. Dual blockade of TIGIT and PD-1 has synergistic effects on intra-tumoral CD8+ T cells. (A) CD226 co-stimulatory signaling is suppressed by both TIGIT and PD-1 signaling. (B) Co-blockade of PD-1 and TIGIT synergizes to restore CD226 co-stimulatory signaling.

Blockade of TIGIT on Tregs reduces their immunosuppressive functions

Tregs play a dominant role in the regulation of antitumor immunity, and suppress multiple steps of the cancer immunity cycle. In contrast to the dampening action that TIGIT ligation has on CD8^{+} T- and NK cell functions, the suppressive function of Treg is enhanced by engagement of TIGIT on Treg. TIGIT is constitutively expressed in most Tregs in humans [31, 72-74] and mice [72], and agonistic TIGIT ligation augments the suppressive function and stability of these cells [72, 74]. Conversely, agonistic ligation of CD226 on Tregs disrupts their suppression [74]. High TIGIT expression marks highly active suppressive Tregs. Compared to TIGIT[-] Tregs, TIGIT[+] Tregs express higher levels of FoxP3, co-inhibitory molecules (ICOS, CTLA4, PD-1 and TIM3) as well as the immunosuppressive cytokine IL-10, indicating that TIGIT[+] Treg might be optimally equipped for mediating immunosuppression [66, 72, 74]. TIGIT[+] Treg specifically suppress pro-inflammatory T helper 1 (Th1) and Th17 cells, but not Th2 cell responses, and ligation of TIGIT on Treg induces production of fibrinogen-like protein 2 which suppresses effector T cell proliferation [72]. Additionally, TIGIT signaling in Tregs upregulates CCR8 which may promote Treg migration and retention in tumor tissue [66, 75, 76] (**Figure 3A**).

TIGIT[+] Treg have been demonstrated to accumulate both in mouse tumors [66] and in several types of human tumors [74, 77]. In HCC TILs, Treg represent the population of lymphocytes with highest TIGIT expression [31]. In contrast, CD226 is down-regulated on tumor-infiltrating Treg, and a high TIGIT/CD226 expression ratio on tumor-infiltrating Tregs correlates with high Treg frequencies in tumors and poor clinical outcome in melanoma patients treated with anti-PD1 and/or anti-CTLA4 immune checkpoint blockade, suggesting that the TIGIT/CD226 ratio in Tregs is a marker of Treg stability[74]. In an *in vitro* study, TIGIT blockade depleted FoxP3^{+} Tregs while increasing proliferation of IFNγ-producing CD4^{+} T cells from peripheral blood from patients with multiple myeloma[41]. Adoptive transfer experiments in mouse tumor models have even suggested that TIGIT ligation dampens anti-tumor immunity predominantly via regulatory T cells, rather than through a direct effect on TIGIT^{+}CD8^{+} T cells [66]. However, a study in which different T-cell subsets were depleted by specific antibodies found that CD8^{+} T cell depletion as well as Treg depletion could abrogate the anti-tumor effects of TIGIT-blockade in a mouse cancer model [65].

Whether PD-1-blockade might synergize with TIGIT-blockade in reducing suppression of intra-tumoral immunity Treg has not yet been investigated. The functional effects of PD-1 expression on Tregs is still a matter of debate. On the one hand, PD-1-deficient mouse Tregs have an enhanced suppressive capacity [78] and *in vitro* PD-L1 blockade augmented the suppressive capacity of Treg from HCV-infected patients [79]. Moreover, PD-1 blockade enhanced the suppressive function PD-1+ Treg isolated from human tumors [80]. On the other hand, interaction between PD-1 on Tregs from mice with chronic LMCV-infection with PD-L1 expressed on CD8+ T cells was found to contribute to their capacity to suppress CD8+ T cell functions [81] and blockade of PD-L1 has been shown to reduce the *in vitro* suppressive function of human tumor-infiltrating Treg [77].

Therefore, PD-1/PD-L1 blockade may either enhance or reduce the suppressive capacity of PD-1-expressing Treg in the tumor micro-environment. In both cases, co-blockade of TIGIT may be beneficial. If PD-1/PD-L1 blockade enhances intra-tumoral Treg immunosuppression, this mechanism may serve as a resistance mechanism against PD-1/PD-L1 blockade, which is supported by recent data in cancer patients treated with anti-PD-1 antibody [80]. In this case, co-treatment with a blocking anti-TIGIT antibody may counteract this resistance mechanism (**Figure 3B**). Alternatively, if PD-1 and TIGIT expressed on chronically activated Treg present within the tumor micro-environment both contribute to their strong suppressive capacity, PD-1 blockade may synergize with TIGIT-blockade in reducing local immune-suppression exerted by tumor-infiltrating Treg functions. Both mechanisms may contribute to the synergistic effect of dual TIGIT/PD-1 blockade on anti-tumor immunity observed in pre-clinical models, and both hypotheses are worth to be investigated.

The role of TIGIT in regulation of memory CD4+ T cells in cancer is under-investigated

The requirement for CD4+ T cells in anti-tumor responses has been attributed to providing help during priming to achieve full activation and effector function of tumor-specific CD8+ T cells [82]. Mouse TIGIT$^{-/-}$ CD4+ T cells showed increased proliferation upon re-stimulation with antigenic peptide, and produced higher amounts of IFN-γ and lower amounts of IL-10, indicating a T cell intrinsic opposite effect in regulating IFN-γ versus IL-10 production in CD4+ T cells [18]. Moreover, the interaction of TIGIT on mouse Th with CD155 on DCs induced phosphorylation of CD155 and consequently

upregulation of IL-10 production and downregulation of IL-12 production by DC, which suggests the existence of an IL-10-driven feedback loop for TIGIT-mediated Th cell suppression [21]. TIGIT is expressed on around 20% of intra-tumoral Th in HCC patients, but not over-expressed compared to Th in tumor-free liver tissue and in the circulation [31]. Similar to CD8+ T cells and Treg, CD226 is downregulated on intra-tumoral Th in HCC patients. In contrast, TIGIT is highly expressed on effector memory (around 80%), effector (around 50%) and central memory (around 40%) CD4+ T cells in follicular lymphoma patients[49]. PD-1+TIGIT+ CD4+ T cells from non-hodgkin lymphoma patients produced lower amounts of IL2, IFN-γ and TNF-α compared to other subsets after re-stimulation [64], suggesting loss of poly-functionality. Indeed, tumor-infiltrating CD4+ T cells expressing IL2 were increased after TGIT blocking mAb treatment in a head and neck squamous cell carcinoma mouse model [65]. Moreover, animals treated with dual anti-TIGIT/PD-1 antibodies showed increased IFN-γ secretion by CD4+ TILs in the MC38 colon tumor mouse model, compared to single anti-PD-1 treatment [68]. There are few studies which investigated TIGIT function in regulation of T helper cells in tumors, and this requires further investigation.
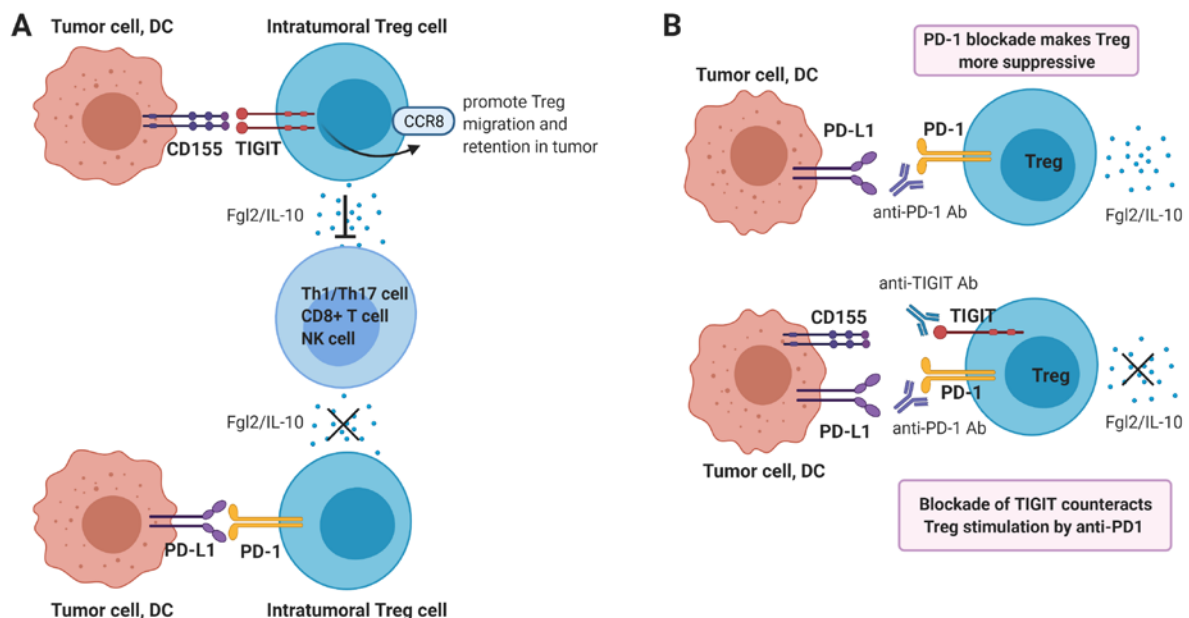
Figure 3. Ligation of TIGIT on Tregs contributes to dampening of anti-tumor immunity. (A) Ligation of TIGIT augments suppressive function of Tregs, which inhibits Th1/17 cell, CD8+ T cell or NK responses via production of Fgl2 and IL-10. On the contrary, PD-1 ligation may reduce Treg suppressive function. (B) Single blockade of PD-1 may enhance Treg immunosuppression, whereas dual blockade of TIGIT and PD-1 may counteract this resistance mechanism.

Blockade of TIGIT on NK cells augments anti-tumor immunity

NK cells not only detect and identify malignant cancer cells, but they also induce cancer cell death [83, 84], e.g. by destroying MHC class I-deficient tumor cells which are refractory to CD8^{+} T cell-mediated immunity. In contrast, lack of MHC class I expression renders cells vulnerable to NK cell killing, because they are devoid of a major NK-cell inhibitory mechanism exerted by binding of self-MHC class I to inhibitory Killer Immunoglobulin Receptors (KIR) and NKG2A/CD94. Interestingly, defects in MHC class I presentation are relatively frequent in cancer cells. Moreover, mutations in β2-microglobulin which cause lack of surface MHC class I expression are also involved in acquired resistance to anti-PD-1 therapy [85, 86]. For these tumors, appropriate activation of NK cells in the tumor microenvironment may be a promising alternative therapeutic option [87]. In addition, NK cells help to trigger a more robust anti-tumor T-cell response by engaging other immune cells [88, 89]. For example, CD8^{+} T cell responses against tumor cells are stimulated by NK-initiated cytokine production [89-91].

TIGIT expression on tumor-infiltrating NK cells is associated with tumor progression and is linked to functional exhaustion of NK cells in multiple cancer models [92]. NK cell functions are regulated by the net balance of signals perceived by their activating and inhibiting receptors. The CD226 activating receptor and the TIGIT and CD96 inhibitory receptors have been shown to be key regulators of anti-tumor immune responses by NK cells. They share the same ligand CD155 [93]. In this review, we will focus on the role of TIGIT in regulating anti-tumor functions of NK cells. In the B16 melanoma mouse model, NK cell-specific TIGIT-deficiency led to improved survival. Additionally, it induced a lower frequency of tumor-infiltrating CD8^{+} T cells expressing TIGIT and TIM3, which suggested that NK cells expressing TIGIT might also indirectly contribute to the exhaustion of CD8^{+} T cells [92]. Blockade of TIGIT inhibited tumor growth and prevented exhaustion of tumor-infiltrating NK cells in the CT26 colon carcinoma mouse model [92]. Mechanistically, tumor cells expressing CD155 impair NK cell functions by downregulating their CD226 expression [94, 95]. CD155-/- mice displayed reduced tumor growth and metastasis via CD226 upregulation and enhanced effector functions of NK cells [35]. Similarly, NK cell-specific TIGIT-deficiency resulted in a greater frequency of intra-tumoral NK cells expressing CD226 in the B16 melanoma mouse model [92]. Furthermore, antibody blockade of nectin-4 suppresses human tumor growth in SCID mice transplanted with human NK cells, while nectin-4 overexpression in human tumor

cells led to increased tumor growth in the presence of human NK cells [25]. However, whether TIGIT blockade synergizes with PD-1 blockade to improve NK cell cytotoxicity is as yet unknown. Notably, IL-15 can increase the expression of both CD226 and TIGIT by intra-tumoral NK cells [95], and combination therapy of IL-15 and TIGIT blockade increased cytotoxicity of NK cells against melanoma and suppressed lung metastasis in mouse melanoma models. The authors suggest the development of novel combinatorial immunotherapy with IL-15 and TIGIT blockade to promote NK cell-mediated destruction of MHC class I-deficient melanoma, which are refractory to CD8$^+$ T cell-mediated immunity [95].

In humans TIGIT was shown to have variable expression on NK cells, and high TIGIT expression correlated with reduced NK cell functions [96]. A TIGIT/CD226 dysbalance with high TIGIT and low CD226 expression on intra-tumoral NK cells been shown in multiple human tumors, e.g. colorectal cancer (CRC) [95], ovarian cancer[97] and HCC [98], and compromises intra-tumoral NK cell functions. *In vitro* blockade of the TIGIT pathway significantly increased functions of circulating NK-cells, particularly in NK cells with high levels of TIGIT expression [96]. TIGIT$^+$ NK cells from metastatic melanoma patients displayed a lower cytolytic activity than TIGIT$^-$ NK cells against CD155$^+$ MHC class I-deficient melanoma cells [95]. TIGIT blockade boosts *in vitro* functional responsiveness of ovarian cancer ascites-derived CD56^{dim} NK cells in patients with baseline reactivity against ovarian cancer tumor cells [97]. Blocking TIGIT was shown to increase circulating NK cell cytotoxicity against HCC cell lines, suggesting that targeting TIGIT may be a beneficial approach to improve NK cell function in HCC patients [98]. Gur C et al. showed that a CRC-associated bacterium (Fusobacterium nucleatum) inhibits human NK cells via TIGIT, which can be blocked by anti-TIGIT antibody [99], suggesting that NK-cell responses in CRC can be suppressed by the gut microbiome in a TIGIT-mediated fashion. Collectively, TIGIT blockade has convincingly been shown to enhance anti-tumor NK cell responses. The interaction of TIGIT on NK cells with its ligands and the effect of anti-TIGIT and IL-15 co-treatment on NK cells are illustrated in **Figure 4**.
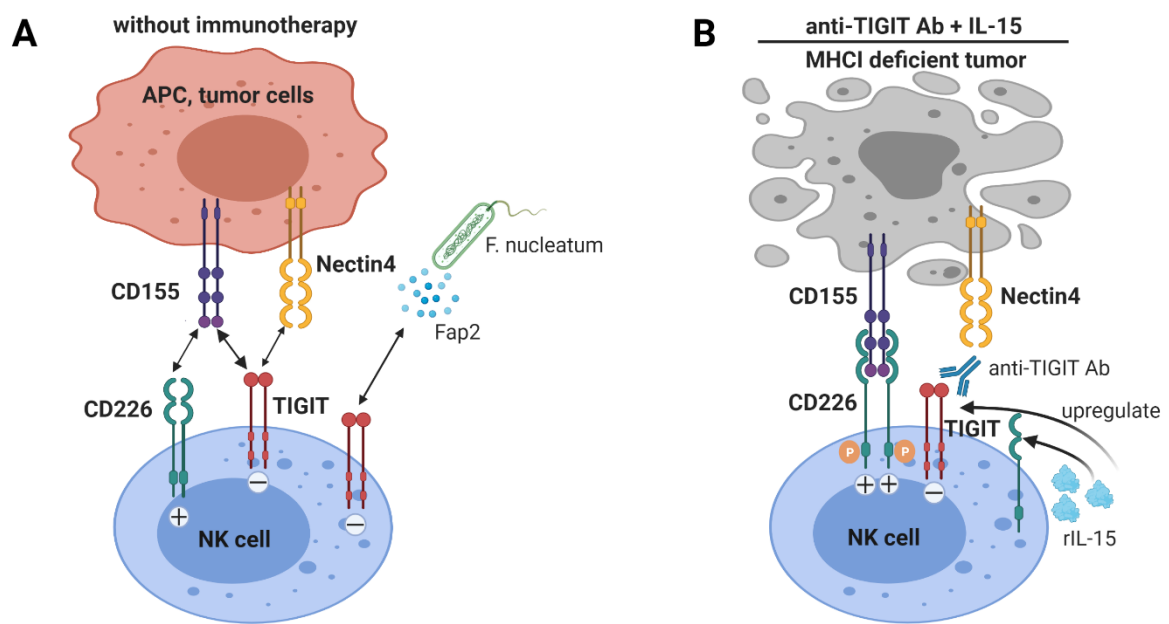
Figure 4. Blockade of TIGIT on NK cells augments anti-tumor immunity. (A) NK cells expressing TIGIT are functionally impaired by binding to CD155 and nectin-4, and in colorectal cancer to Fap2 protein produced by a gut bacterium. (B) TIGIT blockade not only interrupts inhibitory signaling by TIGIT in NK cells, but also allows interaction of the co-stimulatory receptor CD226 with CD155. IL-15 treatment increases TIGIT and CD226 expression on NK cells. Thus IL-15 combined with TIGIT blockade further enhanced NK cells anti-tumor functions, especially promoting NK cell-mediated destruction of MHC class I-deficient tumors.

TIGIT in clinical trials to treat cancer

Over last two years, the above mentioned immunomodulatory effects of TIGIT have attracted the attention from pharmaceutical companies worldwide. Currently, nine human anti-TIGIT mAbs are being tested in 43 phase 1/2/3 clinical trials either as a monotherapy or, in most studies, in combination with anti-PD-1/PD-L1 antibodies or chemotherapies for the treatment of advanced solid tumors, and in two trials in multiple myeloma (**Table 1**). Recently, the first data of its clinical efficacy have been reported. Interim data from an ongoing global phase II trial (CITYSCAPE) demonstrated the improved efficacy of an anti-TIGIT antibody tiragolumab in combination with anti-PD-L1 antibody atezolizumab compared to atezolizumab alone in PD-L1-positive metastatic NSCLC patients[100] in terms of overall response and progression free survival. Importantly, all grade 3-5 adverse events (AEs) were similar in both groups

(48% vs 44%) [100], in accordance with pre-clinical data showing limited immunotoxicity in TIGIT-deficiency in mice, as discussed earlier.

Concluding remarks

Therapeutic immune checkpoint inhibition has revolutionized cancer treatment, and recent experience has made clear that combination therapies that target multiple CPI are more effective than monotherapies. TIGIT has been shown to be expressed by dysfunctional CD8+ T cells and NK cells, as well as highly immunosuppressive regulatory T cells in mouse and human tumors. Its main ligand CD155 is over-expressed in several types of cancer and hampers immune surveillance by interacting with TIGIT on these immune cells. Preclinical studies have demonstrated that blocking TIGIT-signaling improves CD8+ T-cell and NK-cell responses and reduces suppressive functions of regulatory T cells. However, single TIGIT-blockade has minimal effects on tumor growth in most experimental tumor models, and is also insufficient to reinvigorate functions of human tumor-infiltrating CD8+ T cells. TIGIT-blockade synergizes with PD-1/PDL-1 blockade to enhance anti-tumor CD8+ T-cell immunity in pre-clinical models, and is even effective in mouse tumors models that are resistant of PD-1 blockade, thus providing hope for clinical efficacy in patients with anti-PD1 resistant tumors. A unique property of TIGIT among inhibitory immune checkpoints is that its blockade not only augments anti-tumor effector CD8+ T-cell responses, but also anti-tumor NK-cell responses, and reduces the suppressive capacity of regulatory T cells. Whether TIGIT blockade can enhance T-helper cell responses it largely unknown. The clinical proof of its efficacy, especially for cancers that are resistant against single anti-PD1 therapy, in ongoing clinical trials is eagerly awaited for.

Acknowledgements

Table 1. Currently ongoing clinical trials involving human anti-TIGIT mAbs

Agent	Trial sponsor	ClinicalTrials.gov identifier	Type of trial	Estimated enrollment	Tumor type	Combined therapy
BMS-986207	Bristol-Myers Squibb	NCT02913313	Phase 1/2	170	Advanced solid tumors	Monotherapy or combined with nivolumab (anti-PD-1 mAb)
	Multiple Myeloma Research Consortium	NCT04150965	Phase 1/2	104	Refractory multiple myeloma	Monotherapy or combined with pomalidomide and dexamethasone
	Compugen Ltd	NCT04570839	Phase 1/2	100	Advanced solid tumors	Combined with Nivo and COM701(inhibitor of poliovirus receptor)
Tiragolumab (MTIG7192A; RG6058)	Genentech/Roche	NCT03563716	Phase 2	135	Locally advanced or metastatic Non-small cell lung cancer (NSCLC)	Combined with atezolizumab (anti-PD-L1 mAb)
		NCT04294810	Phase 3	500	Locally advanced or metastatic PD-L1-selected NSCLC	Combined with atezolizumab
		NCT04513925	Phase 3	800	NSCLC stage III	Combined with atezolizumab compared with Durvalumab
		NCT04619797	Phase 2	200	Unresectable or metastatic NSCLC	Combined with atezolizumab and pemetrexed
		NCT04256421	Phase 3	400	Untreated extensive-stage small cell lung cancer (SCLC)	Combined with atezolizumab and carboplatin and etoposide (CE)
		NCT04308785	Phase 2	363	SCLC	Combined with atezolizumab VS atezolizumab
		NCT03281369	Phase 1b/2	410	Esophageal cancer	Combined with atezolizumab VS atezolizumab and chemotheraoy
		NCT04540211	Phase 3	450	Unresectable esophageal cancer	Combined with atezolizumab +paclitaxel and cisplatin (PC) VS placebo+PC
	Roche	NCT04543617	Phase 3	750	Unresectable esophageal squamous cell carcinoma	Combined with atezolizumab VS atezolizumab
		NCT04524871	Phase 1/2	100	Advanced liver cancers	Combined with Atezolizumab + Bevacizumab
		NCT04584112	Phase 1	80	Triple-negative breast cancer	Combined with atezolizumab + chemotherapy
		NCT04045028	Phase 1	52	Refractory multiple myeloma	Monotherapy or combined with daratumumab or rituximab
		NCT02794571	Phase 1	540	Locally advanced or metastatic tumors	Monotherapy or in combined with atezolizumab and/or other anti-cancer therapies
		NCT04300647	Phase 2	220	Cervical cancer (PD-L1-positive)	Combined with atezolizumab
		NCT03281369	Phase 1/2	410	Gastric and esophageal cancer	Combined with atezolizumab with/without cisplatin+5FU
		NCT03193190	Phase 1/2	290	Metastatic pancreatic ductal Adenocarcinoma	Combined with atezolizumab +chemotherapy
		NCT03869190	Phase 1/2	385	Locally advanced or metastatic urothelial carcinoma	Combined with atezolizumab

Drug	Company	NCT Number	Phase	Enrollment	Indication	Description
Tiragolumab (MTIG7192A; RG6058)	Roche	NCT04665843	Phase 2	120	PD-L1-positive squamous cell carcinoma of the head and neck	Combined with atezolizumab
		NCT03708224	Phase 2	55	Squamous cell carcinoma of the head and neck	Combined with atezolizumab VS atezolizumab
MK-7684	Merck	NCT02964013	Phase 1	492	Advanced solid tumors	Monotherapy or combined with pembrolizumab (anti-PD-1 mAb)
		NCT04305041	Phase 1/2	200	Melanoma	Combined with pembrolizumab VS pembrolizumab
		NCT04305054	Phase 1/2	135	Melanoma	Combined with pembrolizumab VS pembrolizumab
		NCT04738487	Phase 3	598	PD-L1 positive metastatic NSCLC	Combined with pembrolizumab VS pembrolizumab
		NCT04725188	Phase 2	240	Metastatic NSCLC	Combined with pembrolizumab +Docetaxel VS Docetaxel
		NCT04165070	Phase 2	90	Advanced NSCLC	Combined with pembrolizumab + Carboplatin + Paclitaxel
		NCT02861573	Phase 1	1000	Metastatic castrate resistant prostate cancer	Combined with pembrolizumab
		NCT04303169	Phase 1/2	65	Stage III melanoma	Combined with pembrolizumab VS pembrolizumab
AB154	Arcus Biosciences	NCT03628677	Phase 1	66	Advanced solid tumors	Monotherapy or combined with AB122 (anti-PD-1 mAb)
		NCT04262856	Phase 2	150	NSCLC	Combined with AB122 or AB122 and AB928 (dual adenosine receptor antagonist)
		NCT04656535	Phase 1	46	Recurrent glioblastoma	Combined with AB122
		NCT04736173	Phase 3	625	PD-L1 positive metastatic NSCLC	Combined with AB122 VS AB122
COM902	Compugen	NCT04354246	Phase 1	45	Advanced malignant tumors	Monotherapy
IBI939	Innovent Biologics	NCT04353830	Phase 1	270	Advanced malignant tumors	Monotherapy or combined with sintilimab (anti-PD-1 mAb)
		NCT04672356	Phase 1	20	Advanced lung cancer	Combined with sintilimab
		NCT04672369	Phase 1	42	Advanced NSCLC	Combined with sintilimab VS sintilimab
BGB-A1217	BeiGene	NCT04047862	Phase 1	39	Advanced solid tumors	Monotherapy or combined with tislelizumab (anti-PD-1 mAb)
		NCT04732494	Phase 2	280	Recurrent or metastatic Esophageal squamous cell carcinoma	Combined with tislelizumab VS tislelizumab +placebo
		NCT04746924	Phase 3	605	Locally advanced or metastatic NSCLC	Combined with tislelizumab VS pembrolizumab+placebo
		NCT04693234	Phase 2	167	Metastatic cervical cancer	Combined with tislelizumab VS tislelizumab
ASP8374	Astellas Pharma	NCT03260322	Phase 1	169	Advanced solid tumors	Monotherapy or combined with pembrolizumab (anti-PD-1 mAb)
		NCT03945253	Phase 1	6	Advanced solid tumors	Monotherapy
M6223	EMD Serono	NCT04457778	Phase 1	35	Advanced solid tumors	Monotherapy or combined with Bintrafusp alfa

References

1.   Zhang H. Advances of FDA Approved Drugs that Target PD-1 and PD-L1 for Cancer Immunotherapy. American Journal of Cancer Science 2019;7:18-31.
2.   Sanmamed MF, Chen L. A paradigm shift in cancer immunotherapy: from enhancement to normalization. Cell 2018;175:313-326.
3.   Le DT, Durham JN, Smith KN, Wang H, Bartlett BR, Aulakh LK, Lu S, Kemberling H, Wilt C, Luber BS, Wong F, Azad NS, Rucki AA, Laheru D, Donehower R, Zaheer A, Fisher GA, Crocenzi TS, Lee JJ, Greten TF, Duffy AG, Ciombor KK, Eyring AD, Lam BH, Joe A, Kang SP, Holdhoff M, Danilova L, Cope L, Meyer C, Zhou S, Goldberg RM, Armstrong DK, Bever KM, Fader AN, Taube J, Housseau F, Spetzler D, Xiao N, Pardoll DM, Papadopoulos N, Kinzler KW, Eshleman JR, Vogelstein B, Anders RA, Diaz LA. Mismatch repair deficiency predicts response of solid tumors to PD-1 blockade. Science 2017;357:409.
4.   El-Khoueiry AB, Sangro B, Yau T, Crocenzi TS, Kudo M, Hsu C, Kim T-Y, Choo S-P, Trojan J, Welling TH, Meyer T, Kang Y-K, Yeo W, Chopra A, Anderson J, dela Cruz C, Lang L, Neely J, Tang H, Dastani HB, Melero I. Nivolumab in patients with advanced hepatocellular carcinoma (CheckMate 040): an open-label, non-comparative, phase 1/2 dose escalation and expansion trial. The Lancet 2017;389:2492-2502.
5.   Larkin J, Minor D, D'Angelo S, Neyns B, Smylie M, Miller WH, Jr., Gutzmer R, Linette G, Chmielowski B, Lao CD, Lorigan P, Grossmann K, Hassel JC, Sznol M, Daud A, Sosman J, Khushalani N, Schadendorf D, Hoeller C, Walker D, Kong G, Horak C, Weber J. Overall Survival in Patients With Advanced Melanoma Who Received Nivolumab Versus Investigator's Choice Chemotherapy in CheckMate 037: A Randomized, Controlled, Open-Label Phase III Trial. J Clin Oncol 2018;36:383-390.
6.   Le DT, Uram JN, Wang H, Bartlett BR, Kemberling H, Eyring AD, Skora AD, Luber BS, Azad NS, Laheru D. PD-1 blockade in tumors with mismatch-repair deficiency. New England Journal of Medicine 2015;372:2509-2520.
7.   O'Neil BH, Wallmark JM, Lorente D, Elez E, Raimbourg J, Gomez-Roca C, Ejadi S, Piha-Paul SA, Stein MN, Abdul Razak AR. Safety and antitumor activity of the anti–PD-1 antibody pembrolizumab in patients with advanced colorectal carcinoma. PloS one 2017;12:e0189848.
8.   Popovic A, Jaffee EM, Zaidi N. Emerging strategies for combination checkpoint modulators in cancer immunotherapy. The Journal of clinical investigation 2018;128:3209-3218.
9.   Das M, Zhu C, Kuchroo VK. Tim-3 and its role in regulating anti-tumor immunity. Immunological Reviews 2017;276:97-111.
10.   Andrews LP, Marciscano AE, Drake CG, Vignali DAA. LAG3 (CD223) as a cancer immunotherapy target. Immunological Reviews 2017;276:80-96.
11.   Zhao Y, Yang W, Huang Y, Cui R, Li X, Li B. Evolving Roles for Targeting CTLA-4 in Cancer Immunotherapy. Cellular Physiology and Biochemistry 2018;47:721-734.
12.   Chauvin J-M, Zarour HM. TIGIT in cancer immunotherapy. Journal for immunotherapy of cancer 2020;8:e000957.
13.   Larkin J, Chiarion-Sileni V, Gonzalez R, Grob JJ, Cowey CL, Lao CD, Schadendorf D, Dummer R, Smylie M, Rutkowski P. Combined nivolumab and ipilimumab or monotherapy in untreated melanoma. New England journal of medicine 2015;373:23-34.
14.   Hellmann MD, Paz-Ares L, Bernabe Caro R, Zurawski B, Kim S-W, Carcereny Costa E, Park K, Alexandru A, Lupinacci L, de la Mora Jimenez E, Sakai H, Albert I, Vergnenegre A, Peters S, Syrigos K, Barlesi F, Reck M, Borghaei H, Brahmer JR, O'Byrne KJ, Geese WJ, Bhagavatheeswaran P, Rabindran SK, Kasinathan RS, Nathan FE, Ramalingam SS. Nivolumab plus Ipilimumab in Advanced Non-Small-Cell Lung Cancer. The New England journal of medicine 2019;381:2020-2031.
15.   Yau T, Kang Y-K, Kim T-Y, El-Khoueiry AB, Santoro A, Sangro B, Melero I, Kudo M, Hou M-M, Matilla A. Efficacy and safety of nivolumab plus ipilimumab in patients with advanced hepatocellular carcinoma previously treated with sorafenib: The CheckMate 040 randomized clinical trial. JAMA oncology 2020;6:e204564-e204564.
16.   De Velasco G, Je Y, Bossé D, Awad MM, Ott PA, Moreira RB, Schutz F, Bellmunt J, Sonpavde GP, Hodi FS, Choueiri TK. Comprehensive Meta-analysis of Key Immune-

Related Adverse Events from CTLA-4 and PD-1/PD-L1 Inhibitors in Cancer Patients. Cancer Immunol Res 2017;5:312-318.

17. Levin SD, Taft DW, Brandt CS, Bucher C, Howard ED, Chadwick EM, Johnston J, Hammond A, Bontadelli K, Ardourel D, Hebb L, Wolf A, Bukowski TR, Rixon MW, Kuijper JL, Ostrander CD, West JW, Bilsborough J, Fox B, Gao Z, Xu W, Ramsdell F, Blazar BR, Lewis KE. Vstm3 is a member of the CD28 family and an important modulator of T-cell function. Eur J Immunol 2011;41:902-15.

18. Joller N, Hafler JP, Brynedal B, Kassam N, Spoerl S, Levin SD, Sharpe AH, Kuchroo VK. Cutting edge: TIGIT has T cell-intrinsic inhibitory functions. J Immunol 2011;186:1338-42.

19. Khattri R, Auger JA, Griffin MD, Sharpe AH, Bluestone JA. Lymphoproliferative disorder in CTLA-4 knockout mice is characterized by CD28-regulated activation of Th2 responses. J Immunol 1999;162:5784-91.

20. Boles KS, Vermi W, Facchetti F, Fuchs A, Wilson TJ, Diacovo TG, Cella M, Colonna M. A novel molecular interaction for the adhesion of follicular CD4 T cells to follicular DC. Eur J Immunol 2009;39:695-703.

21. Yu X, Harden K, Gonzalez LC, Francesco M, Chiang E, Irving B, Tom I, Ivelja S, Refino CJ, Clark H, Eaton D, Grogan JL. The surface protein TIGIT suppresses T cell activation by promoting the generation of mature immunoregulatory dendritic cells. Nat Immunol 2009;10:48-57.

22. Stanietsky N, Simic H, Arapovic J, Toporik A, Levy O, Novik A, Levine Z, Beiman M, Dassa L, Achdout H, Stern-Ginossar N, Tsukerman P, Jonjic S, Mandelboim O. The interaction of TIGIT with PVR and PVRL2 inhibits human NK cell cytotoxicity. Proc Natl Acad Sci U S A 2009;106:17858-63.

23. Liu S, Zhang H, Li M, Hu D, Li C, Ge B, Jin B, Fan Z. Recruitment of Grb2 and SHIP1 by the ITT-like motif of TIGIT suppresses granule polarization and cytotoxicity of NK cells. Cell Death & Differentiation 2013;20:456-464.

24. Li M, Xia P, Du Y, Liu S, Huang G, Chen J, Zhang H, Hou N, Cheng X, Zhou L, Li P, Yang X, Fan Z. T-cell Immunoglobulin and ITIM Domain (TIGIT) Receptor/Poliovirus Receptor (PVR) Ligand Engagement Suppresses Interferon-γ Production of Natural Killer Cells via β-Arrestin 2-mediated Negative Signaling*. Journal of Biological Chemistry 2014;289:17647-17657.

25. Reches A, Ophir Y, Stein N, Kol I, Isaacson B, Charpak Amikam Y, Elnekave A, Tsukerman P, Kucan Brlic P, Lenac T, Seliger B, Jonjic S, Mandelboim O. Nectin4 is a novel TIGIT ligand which combines checkpoint inhibition and tumor specificity. J Immunother Cancer 2020;8.

26. Masson D, Jarry A, Baury B, Blanchardie P, Laboisse C, Lustenberger P, Denis MG. Overexpression of the CD155 gene in human colorectal carcinoma. Gut 2001;49:236-40.

27. Nakai R, Maniwa Y, Tanaka Y, Nishio W, Yoshimura M, Okita Y, Ohbayashi C, Satoh N, Ogita H, Takai Y, Hayashi Y. Overexpression of Necl-5 correlates with unfavorable prognosis in patients with lung adenocarcinoma. Cancer Sci 2010;101:1326-30.

28. Bevelacqua V, Bevelacqua Y, Candido S, Skarmoutsou E, Amoroso A, Guarneri C, Strazzanti A, Gangemi P, Mazzarino MC, D'Amico F, McCubrey JA, Libra M, Malaponte G. Nectin like-5 overexpression correlates with the malignant phenotype in cutaneous melanoma. Oncotarget 2012;3:882-92.

29. Nishiwada S, Sho M, Yasuda S, Shimada K, Yamato I, Akahori T, Kinoshita S, Nagai M, Konishi N, Nakajima Y. Clinical significance of CD155 expression in human pancreatic cancer. Anticancer Res 2015;35:2287-97.

30. Sloan KE, Eustace BK, Stewart JK, Zehetmeier C, Torella C, Simeone M, Roy JE, Unger C, Louis DN, Ilag LL, Jay DG. CD155/PVR plays a key role in cell motility during tumor cell invasion and migration. BMC Cancer 2004;4:73.

31. Ge Z, Zhou G, Carrascosa LC, Gausvik E, Boor PPC, Noordam L, Douka M, Polak WG, Terkivatan T, Pan Q, Takkenberg RB, Verheij J, Erdmann JI, Ijzerman JNM, Peppelenbosch M, Kraan J, Kwekkeboom J, Sprengers D. TIGIT and PD1 Co-blockade Restores ex vivo Functions of Human Tumor-Infiltrating CD8+ T Cells in Hepatocellular Carcinoma. Cellular and Molecular Gastroenterology and Hepatology 2021.

32. Lange R, Peng X, Wimmer E, Lipp M, Bernhardt G. The poliovirus receptor CD155 mediates cell-to-matrix contacts by specifically binding to vitronectin. Virology 2001;285:218-27.

33. Takai Y, Irie K, Shimizu K, Sakisaka T, Ikeda W. Nectins and nectin-like molecules: roles in cell adhesion, migration, and polarization. Cancer Sci 2003;94:655-67.

34. He Y, Bowman VD, Mueller S, Bator CM, Bella J, Peng X, Baker TS, Wimmer E, Kuhn RJ, Rossmann MG. Interaction of the poliovirus receptor with poliovirus. Proceedings of the National Academy of Sciences 2000;97:79.

35. Li X-Y, Das I, Lepletier A, Addala V, Bald T, Stannard K, Barkauskas D, Liu J, Aguilera AR, Takeda K. CD155 loss enhances tumor suppression via combined host and tumor-intrinsic mechanisms. The Journal of clinical investigation 2018;128:2613-2625.

36. Lepletier A, Madore J, O'Donnell JS, Johnston RL, Li X-Y, McDonald E, Ahern E, Kuchel A, Eastgate M, Pearson S-A. Tumor CD155 expression is associated with resistance to anti-PD1 immunotherapy in metastatic melanoma. Clinical Cancer Research 2020.

37. Chiu DK-C, Yuen VW-H, Cheu JW-S, Wei LL, Ting V, Fehlings M, Sumatoh H, Nardin A, Newell EW, Ng IO-L. Hepatocellular Carcinoma Cells Upregulate PVRL1, Stabilizing PVR and Inhibiting the Cytotoxic T-cell Response via TIGIT to Mediate Tumor Resistance to PD1 Inhibitors in Mice. Gastroenterology 2020.

38. Pende D, Castriconi R, Romagnani P, Spaggiari GM, Marcenaro S, Dondero A, Lazzeri E, Lasagni L, Martini S, Rivera P, Capobianco A, Moretta L, Moretta A, Bottino C. Expression of the DNAM-1 ligands, Nectin-2 (CD112) and poliovirus receptor (CD155), on dendritic cells: relevance for natural killer-dendritic cell interaction. Blood 2006;107:2030-2036.

39. Sanchez-Correa B, Gayoso I, Bergua JM, Casado JG, Morgado S, Solana R, Tarazona R. Decreased expression of DNAM-1 on NK cells from acute myeloid leukemia patients. Immunology and cell biology 2012;90:109-115.

40. El-Sherbiny YM, Meade JL, Holmes TD, McGonagle D, Mackie SL, Morgan AW, Cook G, Feyler S, Richards SJ, Davies FE, Morgan GJ, Cook GP. The requirement for DNAM-1, NKG2D, and NKp46 in the natural killer cell-mediated killing of myeloma cells. Cancer Res 2007;67:8444-9.

41. Lozano E, Mena MP, Díaz T, Martin-Antonio B, León S, Rodríguez-Lobato LG, Oliver-Caldés A, Cibeira MT, Bladé J, Prat A, Rosiñol L, Fernández de Larrea C. Nectin-2 Expression on Malignant Plasma Cells Is Associated with Better Response to TIGIT Blockade in Multiple Myeloma. Clin Cancer Res 2020;26:4688-4698.

42. Guillerey C, Harjunpää H, Carrié N, Kassem S, Teo T, Miles K, Krumeich S, Weulersse M, Cuisinier M, Stannard K, Yu Y, Minnie SA, Hill GR, Dougall WC, Avet-Loiseau H, Teng MWL, Nakamura K, Martinet L, Smyth MJ. TIGIT immune checkpoint blockade restores CD8(+) T-cell immunity against multiple myeloma. Blood 2018;132:1689-1694.

43. Casado JG, Pawelec G, Morgado S, Sanchez-Correa B, Delgado E, Gayoso I, Duran E, Solana R, Tarazona R. Expression of adhesion molecules and ligands for activating and costimulatory receptors involved in cell-mediated cytotoxicity in a large panel of human melanoma cell lines. Cancer immunology, immunotherapy 2009;58:1517-1526.

44. Miao X, Yang ZL, Xiong L, Zou Q, Yuan Y, Li J, Liang L, Chen M, Chen S. Nectin-2 and DDX3 are biomarkers for metastasis and poor prognosis of squamous cell/adenosquamous carcinomas and adenocarcinoma of gallbladder. Int J Clin Exp Pathol 2013;6:179-90.

45. Zhu Y, Paniccia A, Schulick AC, Chen W, Koenig MR, Byers JT, Yao S, Bevers S, Edil BH. Identification of CD112R as a novel checkpoint for human T cells. The Journal of experimental medicine 2016;213:167-176.

46. Murter B, Pan X, Ophir E, Alteber Z, Azulay M, Sen R, Levy O, Dassa L, Vaknin I, Fridman-Kfir T, Salomon R, Ravet A, Tam A, Levin D, Vaknin Y, Tatirovsky E, Machlenkin A, Pardoll D, Ganguly S. Mouse PVRIG Has CD8(+) T Cell-Specific Coinhibitory Functions and Dampens Antitumor Immunity. Cancer Immunol Res 2019;7:244-256.

47. Whelan S, Ophir E, Kotturi MF, Levy O, Ganguly S, Leung L, Vaknin I, Kumar S, Dassa L, Hansen K, Bernados D, Murter B, Soni A, Taube JM, Fader AN, Wang TL, Shih IM, White M, Pardoll DM, Liang SC. PVRIG and PVRL2 Are Induced in Cancer and Inhibit CD8(+) T-cell Function. Cancer Immunol Res 2019;7:257-268.

88

48. Parry RV, Chemnitz JM, Frauwirth KA, Lanfranco AR, Braunstein I, Kobayashi SV, Linsley PS, Thompson CB, Riley JL. CTLA-4 and PD-1 Receptors Inhibit T-Cell Activation by Distinct Mechanisms. Molecular and Cellular Biology 2005;25:9543.

49. Josefsson SE, Huse K, Kolstad A, Beiske K, Pende D, Steen CB, Inderberg EM, Lingjærde OC, Østenstad B, Smeland EB, Levy R, Irish JM, Myklebust JH. T Cells Expressing Checkpoint Receptor TIGIT Are Enriched in Follicular Lymphoma Tumors and Characterized by Reversible Suppression of T-cell Receptor Signaling. Clin Cancer Res 2018;24:870-881.

50. Lozano E, Dominguez-Villar M, Kuchroo V, Hafler DA. The TIGIT/CD226 axis regulates human T cell function. The Journal of Immunology 2012;188:3869-3875.

51. Johnston RJ, Comps-Agrar L, Hackney J, Yu X, Huseni M, Yang Y, Park S, Javinal V, Chiu H, Irving B, Eaton DL, Grogan JL. The immunoreceptor TIGIT regulates antitumor and antiviral CD8(+) T cell effector function. Cancer Cell 2014;26:923-937.

52. Chauvin JM, Pagliano O, Fourcade J, Sun Z, Wang H, Sander C, Kirkwood JM, Chen TH, Maurer M, Korman AJ, Zarour HM. TIGIT and PD-1 impair tumor antigen-specific CD8(+) T cells in melanoma patients. J Clin Invest 2015;125:2046-58.

53. Inozume T, Yaguchi T, Furuta J, Harada K, Kawakami Y, Shimada S. Melanoma Cells Control Antimelanoma CTL Responses via Interaction between TIGIT and CD155 in the Effector Phase. Journal of Investigative Dermatology 2016;136:255-263.

54. Hu F, Wang W, Fang C, Bai C. TIGIT presents earlier expression dynamic than PD-1 in activated CD8+ T cells and is upregulated in non-small cell lung cancer patients. Experimental Cell Research 2020;396:112260.

55. Thommen DS, Koelzer VH, Herzig P, Roller A, Trefny M, Dimeloe S, Kiialainen A, Hanhart J, Schill C, Hess C, Savic Prince S, Wiese M, Lardinois D, Ho P-C, Klein C, Karanikas V, Mertz KD, Schumacher TN, Zippelius A. A transcriptionally and functionally distinct PD-1+ CD8+ T cell pool with predictive potential in non-small-cell lung cancer treated with PD-1 blockade. Nature Medicine 2018;24:994-1004.

56. Ostroumov D, Duong S, Wingerath J, Woller N, Manns MP, Timrott K, Kleine M, Ramackers W, Roessler S, Nahnsen S. Transcriptome profiling identifies TIGIT as a marker of T cell exhaustion in liver cancer. Hepatology 2020.

57. Xu D, Zhao E, Zhu C, Zhao W, Wang C, Zhang Z, Zhao G. TIGIT and PD-1 may serve as potential prognostic biomarkers for gastric cancer. Immunobiology 2020;225:151915.

58. Lucca LE, Lerner BA, Park C, DeBartolo D, Harnett B, Kumar VP, Ponath G, Raddassi K, Huttner A, Hafler DA, Pitt D. Differential expression of the T-cell inhibitor TIGIT in glioblastoma and MS. Neurol Neuroimmunol Neuroinflamm 2020;7.

59. Yang ZZ, Kim HJ, Wu H, Jalali S, Tang X, Krull J, Ding W, Novak AJ, Ansell SM. TIGIT expression is associated with T-cell suppression and exhaustion and predicts clinical outcome and anti-PD-1 response in follicular lymphoma. Clin Cancer Res 2020.

60. Kong Y, Zhu L, Schell TD, Zhang J, Claxton DF, Ehmann WC, Rybka WB, George MR, Zeng H, Zheng H. T-Cell Immunoglobulin and ITIM Domain (TIGIT) Associates with CD8+ T-Cell Exhaustion and Poor Clinical Outcome in AML Patients. Clin Cancer Res 2016;22:3057-66.

61. Kong Y, Zhu L, Schell TD, Zhang J, Claxton DF, Ehmann WC, Rybka WB, George MR, Zeng H, Zheng H. T-cell immunoglobulin and ITIM domain (TIGIT) associates with CD8+ T-cell exhaustion and poor clinical outcome in AML patients. Clinical Cancer Research 2016;22:3057-3066.

62. Liu X, Li M, Wang X, Dang Z, Jiang Y, Wang X, Kong Y, Yang Z. PD-1+ TIGIT+ CD8+ T cells are associated with pathogenesis and progression of patients with hepatitis B virus-related hepatocellular carcinoma. Cancer Immunology, Immunotherapy 2019;68:2041-2054.

63. Hung AL, Maxwell R, Theodros D, Belcaid Z, Mathios D, Luksik AS, Kim E, Wu A, Xia Y, Garzon-Muvdi T, Jackson C, Ye X, Tyler B, Selby M, Korman A, Barnhart B, Park SM, Youn JI, Chowdhury T, Park CK, Brem H, Pardoll DM, Lim M. TIGIT and PD-1 dual checkpoint blockade enhances antitumor immunity and survival in GBM. Oncoimmunology 2018;7:e1466769.

64. Josefsson SE, Beiske K, Blaker YN, Førsund MS, Holte H, Østenstad B, Kimby E, Köksal H, Wälchli S, Bai B, Smeland EB, Levy R, Kolstad A, Huse K, Myklebust JH. TIGIT and PD-

1 Mark Intratumoral T Cells with Reduced Effector Function in B-cell Non-Hodgkin Lymphoma. Cancer Immunology Research 2019;7:355-362.

65. Wu L, Mao L, Liu J-F, Chen L, Yu G-T, Yang L-L, Wu H, Bu L-L, Kulkarni AB, Zhang W-F, Sun Z-J. Blockade of TIGIT/CD155 Signaling Reverses T-cell Exhaustion and Enhances Antitumor Capability in Head and Neck Squamous Cell Carcinoma. Cancer Immunology Research 2019;7:1700-1713.

66. Kurtulus S, Sakuishi K, Ngiow SF, Joller N, Tan DJ, Teng MW, Smyth MJ, Kuchroo VK, Anderson AC. TIGIT predominantly regulates the immune response via regulatory T cells. J Clin Invest 2015;125:4053-62.

67. Ma J, Zheng B, Goswami S, Meng L, Zhang D, Cao C, Li T, Zhu F, Ma L, Zhang Z, Zhang S, Duan M, Chen Q, Gao Q, Zhang X. PD1(Hi) CD8(+) T cells correlate with exhausted signature and poor clinical outcome in hepatocellular carcinoma. J Immunother Cancer 2019;7:331.

68. Dixon KO, Schorer M, Nevin J, Etminan Y, Amoozgar Z, Kondo T, Kurtulus S, Kassam N, Sobel RA, Fukumura D, Jain RK, Anderson AC, Kuchroo VK, Joller N. Functional Anti-TIGIT Antibodies Regulate Development of Autoimmunity and Antitumor Immunity. J Immunol 2018;200:3000-3007.

69. Wang B, Zhang W, Jankovic V, Golubov J, Poon P, Oswald EM, Gurer C, Wei J, Ramos I, Wu Q. Combination cancer immunotherapy targeting PD-1 and GITR can rescue CD8+ T cell dysfunction and maintain memory phenotype. Science immunology 2018;3.

70. Jin HS, Ko M, Choi DS, Kim JH, Lee DH, Kang SH, Kim I, Lee HJ, Choi EK, Kim KP, Yoo C, Park Y. CD226(hi)CD8(+) T Cells Are a Prerequisite for Anti-TIGIT Immunotherapy. Cancer Immunol Res 2020;8:912-925.

71. Gros A, Robbins PF, Yao X, Li YF, Turcotte S, Tran E, Wunderlich JR, Mixon A, Farid S, Dudley ME, Hanada K-i, Almeida JR, Darko S, Douek DC, Yang JC, Rosenberg SA. PD-1 identifies the patient-specific CD8+ tumor-reactive repertoire infiltrating human tumors. The Journal of Clinical Investigation 2014;124:2246-2259.

72. Joller N, Lozano E, Burkett PR, Patel B, Xiao S, Zhu C, Xia J, Tan TG, Sefik E, Yajnik V, Sharpe AH, Quintana FJ, Mathis D, Benoist C, Hafler DA, Kuchroo VK. Treg cells expressing the coinhibitory molecule TIGIT selectively inhibit proinflammatory Th1 and Th17 cell responses. Immunity 2014;40:569-81.

73. Fuhrman CA, Yeh W-I, Seay HR, Lakshmi PS, Chopra G, Zhang L, Perry DJ, McClymont SA, Yadav M, Lopez M-C. Divergent phenotypes of human regulatory T cells expressing the receptors TIGIT and CD226. The Journal of Immunology 2015;195:145-155.

74. Fourcade J, Sun Z, Chauvin J-M, Ka M, Davar D, Pagliano O, Wang H, Saada S, Menna C, Amin R. CD226 opposes TIGIT to disrupt Tregs in melanoma. JCI insight 2018;3.

75. Tan MC, Goedegebuure PS, Belt BA, Flaherty B, Sankpal N, Gillanders WE, Eberlein TJ, Hsieh CS, Linehan DC. Disruption of CCR5-dependent homing of regulatory T cells inhibits tumor growth in a murine model of pancreatic cancer. J Immunol 2009;182:1746-55.

76. Iellem A, Mariani M, Lang R, Recalde H, Panina-Bordignon P, Sinigaglia F, D'Ambrosio D. Unique chemotactic response profile and specific expression of chemokine receptors CCR4 and CCR8 by CD4(+)CD25(+) regulatory T cells. J Exp Med 2001;194:847-53.

77. De Simone M, Arrigoni A, Rossetti G, Gruarin P, Ranzani V, Politano C, Bonnal RJP, Provasi E, Sarnicola ML, Panzeri I. Transcriptional landscape of human tissue lymphocytes unveils uniqueness of tumor-infiltrating T regulatory cells. Immunity 2016;45:1135-1147.

78. Tan CL, Kuchroo JR, Sage PT, Liang D, Francisco LM, Buck J, Thaker YR, Zhang Q, McArdel SL, Juneja VR, Lee SJ, Lovitch SB, Lian C, Murphy GF, Blazar BR, Vignali DAA, Freeman GJ, Sharpe AH. PD-1 restraint of regulatory T cell suppressive activity is critical for immune tolerance. J Exp Med 2021;218.

79. Franceschini D, Paroli M, Francavilla V, Videtta M, Morrone S, Labbadia G, Cerino A, Mondelli MU, Barnaba V. PD-L1 negatively regulates CD4+CD25+Foxp3+ Tregs by limiting STAT-5 phosphorylation in patients chronically infected with HCV. J Clin Invest 2009;119:551-64.

80. Kumagai S, Togashi Y, Kamada T, Sugiyama E, Nishinakamura H, Takeuchi Y, Vitaly K, Itahashi K, Maeda Y, Matsui S, Shibahara T, Yamashita Y, Irie T, Tsuge A, Fukuoka S, Kawazoe A, Udagawa H, Kirita K, Aokage K, Ishii G, Kuwata T, Nakama K, Kawazu M, Ueno T, Yamazaki N, Goto K, Tsuboi M, Mano H, Doi T, Shitara K, Nishikawa H. The PD-

1 expression balance between effector and regulatory T cells predicts the clinical efficacy of PD-1 blockade therapies. Nat Immunol 2020;21:1346-1358.

81. Park HJ, Park JS, Jeong YH, Son J, Ban YH, Lee BH, Chen L, Chang J, Chung DH, Choi I, Ha SJ. PD-1 upregulated on regulatory T cells during chronic virus infection enhances the suppression of CD8+ T cell immune response via the interaction with PD-L1 expressed on CD8+ T cells. J Immunol 2015;194:5801-11.

82. Hung K, Hayashi R, Lafond-Walker A, Lowenstein C, Pardoll D, Levitsky H. The central role of CD4(+) T cells in the antitumor immune response. J Exp Med 1998;188:2357-68.

83. Miller JS, Lanier LL. Natural Killer Cells in Cancer Immunotherapy. Annual Review of Cancer Biology 2019;3:77-103.

84. Souza-Fonseca-Guimaraes F, Cursons J, Huntington ND. The Emergence of Natural Killer Cells as a Major Target in Cancer Immunotherapy. Trends in Immunology 2019;40:142-158.

85. Zaretsky JM, Garcia-Diaz A, Shin DS, Escuin-Ordinas H, Hugo W, Hu-Lieskovan S, Torrejon DY, Abril-Rodriguez G, Sandoval S, Barthly L, Saco J, Homet Moreno B, Mezzadra R, Chmielowski B, Ruchalski K, Shintaku IP, Sanchez PJ, Puig-Saus C, Cherry G, Seja E, Kong X, Pang J, Berent-Maoz B, Comin-Anduix B, Graeber TG, Tumeh PC, Schumacher TNM, Lo RS, Ribas A. Mutations Associated with Acquired Resistance to PD-1 Blockade in Melanoma. New England Journal of Medicine 2016;375:819-829.

86. Gettinger S, Choi J, Hastings K, Truini A, Datar I, Sowell R, Wurtz A, Dong W, Cai G, Melnick MA, Du VY, Schlessinger J, Goldberg SB, Chiang A, Sanmamed MF, Melero I, Agorreta J, Montuenga LM, Lifton R, Ferrone S, Kavathas P, Rimm DL, Kaech SM, Schalper K, Herbst RS, Politi K. Impaired HLA Class I Antigen Processing and Presentation as a Mechanism of Acquired Resistance to Immune Checkpoint Inhibitors in Lung Cancer. Cancer Discovery 2017;7:1420.

87. Torrejon DY, Abril-Rodriguez G, Champhekar AS, Tsoi J, Campbell KM, Kalbasi A, Parisi G, Zaretsky JM, Garcia-Diaz A, Puig-Saus C, Cheung-Lau G, Wohlwender T, Krystofinski P, Vega-Crespo A, Lee CM, Mascaro P, Grasso CS, Berent-Maoz B, Comin-Anduix B, Hu-Lieskovan S, Ribas A. Overcoming Genetically Based Resistance Mechanisms to PD-1 Blockade. Cancer Discovery 2020;10:1140.

88. Böttcher JP, Bonavita E, Chakravarty P, Blees H, Cabeza-Cabrerizo M, Sammicheli S, Rogers NC, Sahai E, Zelenay S, Reis ESC. NK Cells Stimulate Recruitment of cDC1 into the Tumor Microenvironment Promoting Cancer Immune Control. Cell 2018;172:1022-1037 e14.

89. Pallmer K, Oxenius A. Recognition and Regulation of T Cells by NK Cells. Front Immunol 2016;7:251.

90. Schuster IS, Coudert JD, Andoniou CE, Degli-Esposti MA. "Natural Regulators": NK Cells as Modulators of T Cell Immunity. Frontiers in immunology 2016;7:235-235.

91. Mocikat R, Braumüller H, Gumy A, Egeter O, Ziegler H, Reusch U, Bubeck A, Louis J, Mailhammer R, Riethmüller G, Koszinowski U, Röcken M. Natural killer cells activated by MHC class I(low) targets prime dendritic cells to induce protective CD8 T cell responses. Immunity 2003;19:561-9.

92. Zhang Q, Bi J, Zheng X, Chen Y, Wang H, Wu W, Wang Z, Wu Q, Peng H, Wei H. Blockade of the checkpoint receptor TIGIT prevents NK cell exhaustion and elicits potent anti-tumor immunity. Nature immunology 2018;19:723-732.

93. Sanchez-Correa B, Valhondo I, Hassouneh F, Lopez-Sejas N, Pera A, Bergua JM, Arcos MJ, Bañas H, Casas-Avilés I, Durán E, Alonso C, Solana R, Tarazona R. DNAM-1 and the TIGIT/PVRIG/TACTILE Axis: Novel Immune Checkpoints for Natural Killer Cell-Based Cancer Immunotherapy. Cancers (Basel) 2019;11.

94. Carlsten M, Norell H, Bryceson YT, Poschke I, Schedvins K, Ljunggren HG, Kiessling R, Malmberg KJ. Primary human tumor cells expressing CD155 impair tumor targeting by down-regulating DNAM-1 on NK cells. J Immunol 2009;183:4921-30.

95. Chauvin JM, Ka M, Pagliano O, Menna C, Ding Q, DeBlasio R, Sanders C, Hou J, Li XY, Ferrone S, Davar D, Kirkwood JM, Johnston RJ, Korman AJ, Smyth MJ, Zarour HM. IL15 Stimulation with TIGIT Blockade Reverses CD155-mediated NK-Cell Dysfunction in Melanoma. Clin Cancer Res 2020;26:5520-5533.

96. Wang F, Hou H, Wu S, Tang Q, Liu W, Huang M, Yin B, Huang J, Mao L, Lu Y, Sun Z. TIGIT expression levels on human NK cells correlate with functional heterogeneity among healthy individuals. Eur J Immunol 2015;45:2886-97.

97. Maas RJ, Hoogstad-van Evert JS, Van der Meer JM, Mekers V, Rezaeifard S, Korman AJ, de Jonge PK, Cany J, Woestenenk R, Schaap NP, Massuger LF, Jansen JH, Hobo W, Dolstra H. TIGIT blockade enhances functionality of peritoneal NK cells with altered expression of DNAM-1/TIGIT/CD96 checkpoint molecules in ovarian cancer. Oncoimmunology 2020;9:1843247.

98. Sun H, Huang Q, Huang M, Wen H, Lin R, Zheng M, Qu K, Li K, Wei H, Xiao W, Sun R, Tian Z, Sun C. Human CD96 Correlates to Natural Killer Cell Exhaustion and Predicts the Prognosis of Human Hepatocellular Carcinoma. Hepatology 2019;70:168-183.

99. Gur C, Ibrahim Y, Isaacson B, Yamin R, Abed J, Gamliel M, Enk J, Bar-On Y, Stanietsky-Kaynan N, Coppenhagen-Glazer S, Shussman N, Almogy G, Cuapio A, Hofer E, Mevorach D, Tabib A, Ortenberg R, Markel G, Miklić K, Jonjic S, Brennan CA, Garrett WS, Bachrach G, Mandelboim O. Binding of the Fap2 protein of Fusobacterium nucleatum to human inhibitory receptor TIGIT protects tumors from immune cell attack. Immunity 2015;42:344-355.

100. Rodriguez-Abreu D, Johnson ML, Hussein MA, Cobo M, Patel AJ, Secen NM, Lee KH, Massuti B, Hiret S, Yang JC-H, Barlesi F, Lee DH, Paz-Ares LG, Hsieh RW, Miller K, Patil N, Twomey P, Kapp AV, Meng R, Cho BC. Primary analysis of a randomized, double-blind, phase II study of the anti-TIGIT antibody tiragolumab (tira) plus atezolizumab (atezo) versus placebo plus atezo as first-line (1L) treatment in patients with PD-L1-selected NSCLC (CITYSCAPE). Journal of Clinical Oncology 2020;38:9503-9503.

101. Pauken KE, Wherry EJ. TIGIT and CD226: tipping the balance between costimulatory and coinhibitory molecules to augment the cancer immunotherapy toolkit. Cancer Cell 2014;26:785-787.

CHAPTER 5

TIGIT and PD-1 co-blockade restores *ex vivo* functions of human tumor-infiltrating CD8+ T cells in hepatocellular carcinoma

Zhouhong Ge[1], Guoying Zhou[1], Lucia Campos Carrascosa[1], Erik Gausvik[1], Patrick P.C.Boor[1], Lisanne Noordam[1], Michael Doukas[2], Wojciech G.Polak[3], Türkan Terkivatan[3], Qiuwei Pan[1], R.Bart Takkenberg[4], Joanne Verheij[5], Joris I. Erdmann[6], Jan N.M.IJzermans[3], Maikel Peppelenbosch[1], Jaco Kraan[7], Jaap Kwekkeboom*[1], Dave Sprengers*[1].

Departments of [1]Gastroenterology and Hepatology, [2]Pathology, and [3]Surgery, [7]Medical Oncology, Erasmus MC-University Medical Center, Rotterdam, the Netherlands; Departments of [4]Gastroenterology and Hepatology, [5]Pathology, and [6]Surgery, Academic Medical Center(AMC), Amsterdam, the Netherlands

Abstract

Background and aims: TIGIT is a co-inhibitory receptor and its suitability as a target for cancer immunotherapy in HCC is unknown. PD1 blockade is clinically effective in about 20% of advanced HCC patients. Here we aim to determine whether co-blockade of TIGIT/PD1 has added value to restore functionality of HCC tumor-infiltrating T cells (TILs).

Methods: Mononuclear leukocytes were isolated from tumors, paired tumor-free liver tissues (TFL) and peripheral blood of HCC patients, and used for flowcytometric phenotyping and functional assays. CD3/CD28 T-cell stimulation and antigen-specific assays were used to study the *ex vivo* effects of TIGIT/PD1 single or dual blockade on T-cell functions.

Results: TIGIT was enriched whereas its co-stimulatory counterpart CD226 was downregulated on PD1^{high}CD8$^+$ TILs. PD1^{high}TIGIT$^+$CD8$^+$ TILs co-expressed exhaustion markers TIM3 and LAG3, and demonstrated higher TOX expression. Furthermore, this subset showed decreased capacity to produce IFN-γ and TNF-α. Expression of TIGIT-ligand CD155 was upregulated on tumor cells compared to hepatocytes in TFL. Whereas single PD1 blockade preferentially enhanced *ex vivo* functions of CD8$^+$ TILs from tumors with PD1^{high}CD8$^+$ TILs (high PD1 expressers), co-blockade of TIGIT and PD1 improved proliferation and cytokine production of CD8$^+$ TILs from tumors enriched for PD1^{int} CD8$^+$ TILs (low PD1 expressers). Importantly, *ex vivo* co-blockade of TIGIT/PD1 improved proliferation, cytokine production and anti-tumor cytotoxicity of CD8$^+$ TILs compared to single PD1 blockade.

Conclusions: *Ex vivo,* co-blockade of TIGIT/PD1 improves functionality of CD8$^+$ TILs that do not respond to single PD1 blockade. Therefore co-blockade of TIGIT/PD1 could be a promising immune therapeutic strategy for HCC patients.

Key words: TIGIT; CD226; TOX; HCC; immunotherapy

Introduction

Liver cancer is the sixth most common cancer and the fourth most frequent cause of cancer-related death worldwide in 2018[1]. Hepatocellular carcinoma (HCC) comprises 75%-85% of all liver cancer cases[1]. Most patients are diagnosed at a late stage and their median survival is less than 2 years [2]. Efforts are underway to identify new therapies for the treatment of advanced HCC. Recently, cancer immunotherapies targeting the co-inhibitory PD1/PD-L1 pathway achieved survival benefit in multiple cancers, with the FDA approval of anti-PD1 antibody nivolumab for HCC treatment in 2017 [3], and pembrolizumab in 2018 [4].

Anti-PD1 therapy results in objective response rates of 16-20% in patients with advanced HCC[3, 4], but does not prolong survival in HCC patients previously treated with sorafenib[5]. In an effort to improve the response rate of anti-PD1 therapy, combination therapies with blockade of other inhibitory immune checkpoints are being investigated. Anti-PD1/PD-L1 treatment in combination with anti-cytotoxic T-lymphocyte associated protein 4 (CTLA-4) is highly efficacious in melanoma and advanced non-small-cell lung cancer [6-8]. The combination of anti-PD1 with anti-cell immunoglobulin and mucin domain 3 (TIM-3)[9, 10] have demonstrated promising results in pre-clinical studies. Our group previously found that the combined blockade of PD-L1 with TIM3, lymphocyte- activation gene 3 (LAG3), or CTLA-4 further restored responses of human HCC tumor-derived T cells to tumor associated antigens (TAAs) in *ex vivo* assays compared to single PD-L1 blockade[11].

T cell immune receptor with Ig and ITIM domains (TIGIT) is a novel co-inhibitory molecule in cancer immunotherapy. TIGIT has a co-stimulatory counterpart called CD226 (DNAM-1). Both are expressed on multiple immune cell subsets, including activated and memory T cells, regulatory T cells (Treg), and natural killer (NK) cells[12-15]. These two receptors share the same ligand CD155 (also known as PVR, poliovirus receptor), but TIGIT has higher affinity for CD155. CD155 is highly expressed on dendritic cells (DCs), fibroblasts, endothelial cells and some tumor cells[12, 16, 17]. It has been shown that TIGIT exerts immunosuppressive functions by inhibiting IL-12 and enhancing IL-10 production by DCs through CD155, thereby inhibiting CD4+ T cell proliferation and IFN-γ production[12]. Furthermore, TIGIT can directly suppress T cell functions by cell-intrinsic inhibitory signaling[18]. Finally, TIGIT can compete for ligand

binding with CD226 thereby reducing T-cell co-stimulation via CD226[19] and can prevent co-stimulatory signaling via CD226 by blocking CD226 homo-dimerization[20]. Interestingly, TIGIT is expressed on tumor-infiltrating T cells (TILs) in several types of human tumors, and its expression on TILs correlates with PD1 expression[20-22]. TIGIT and PD1 were also found to be co-expressed on tumor antigen (TA)-specific CD8$^+$ T cells from melanoma patients[23] and dual TIGIT/PD-L1 blockade synergistically elicits tumor rejection in mouse cancer models[20, 24] and increases *in vitro* proliferation and cytokine production of TA-specific CD8$^+$ T cells from melanoma patients[23]. Therefore, clinical trials on co-blockade of TIGIT with PD1/PD-L1 in multiple solid tumors are ongoing (BMS: NCT02913313, Genetech:NCT02794571, NCT03563716, Oncomed: NCT03119428).

To which extent TIGIT is expressed on TILs of HCC patients and whether TIGIT blockade alone or in combination with PD1 blockade can reinvigorate TILs of HCC patients is still unknown. Here, we compared expression of TIGIT and its co-stimulatory counterpart CD226 on T cells isolated from tumors, paired tumor free liver tissues (TFL) and peripheral blood (PB) of HCC patients, characterized TIGIT-expressing CD8$^+$ TIL, and studied the effects of single and combined TIGIT/PD1 blockade on *ex vivo* TIL responses.

Materials and methods

Patients

A total of 47 HCC-patients who were eligible for surgical tumor resection were enrolled in the study between June 2015 and Nov 2020. Paired fresh liver tumor and TFL tissues, cut out at a minimal distance of ≥1 cm from the tumor, were used for isolating TILs and intrahepatic lymphocytes. In addition, PB was collected on the day of resection. None of the patients received systemic anti-cancer therapy or immunosuppressive treatment at least 3 months before surgery. The clinical characteristics of the patients are summarized in **Table 1**. The study was approved by the local ethics committee, and all specimens were obtained after written informed consent.

Cell Preparation

Single cell suspensions from PB, tumors and TFLs were obtained as described previously[25]. Fresh tissue was cut into small pieces and digested in Hanks' Balanced Salt solution with Ca^{2+} and Mg^{2+} (Sigma, the Netherlands) with 0.125 mg/ml of collagenase IV (Sigma-Aldrich, USA) and 0.2 mg/mL of DNase I (Roche, USA) for 30 minutes at 37°C with magnetic bead stirring. Cell suspensions were filtered through 100 μm cell strainers (BD Biosciences, Belgium) and mononuclear cells (MNCs) were obtained by Ficoll density gradient centrifugation. $CD45^+DAPI^-$ leukocytes were quantified using a MACSQuant flow cytometer (Miltennyi Biotech, Germany) after being stained with a mixture of DAPI, CD3 and CD45 antibodies.

Polyclonal T cell stimulation

TILs of HCC patients were suspended in RPMI medium supplemented with 10% normal human serum, 2 mM L-glutamine, 50 mM Hepes buffer, 1% penicillin-streptomycin, 5 mM sodium pyruvate, and 1% minimum essential medium nonessential amino acids. 5×10^4 $CD45^+$ TILs were seeded in each well of a 96-well round-bottom culture plate and stimulated with a suboptimal amount of CD3/CD28 beads (beads to TILs ratio ranging from 1:10 to 1:800). Blocking mouse anti-human TIGIT antibody (clone MBSA43, eBioscience, USA) was chosen based on the referred article[26] and used at 10 and 20 μg/mL. Blocking human anti-human PD1 antibody (nivolumab, Bristol-Myers Squibb; provided by the Erasmus MC hospital pharmacy)

was used at 10 μg/mL, which was based on the referred article [27]. Blocking anti-CD226 antibody clone DX11 (BD Biosciences) was used at 20 μg/mL according to previous studies[19, 28, 29]. Isotype control antibodies mIgG1 (clone MOPC-21, Biolegend) and hIgG4 (clone QA16A15, Biolegend) were added at 20 μg/mL and 10 μg/mL respectively. T cell proliferation was determined after 4 days of culture based on Ki67-expression in CD3$^+$CD8$^+$ T cells on a FACSCanto II flow cytometer, and analyzed using FlowJo software Version 10 (Tree Star, USA). Dead cells were excluded by Aqua live/dead fixable dye (Thermo Fisher scientific) according to manufacturer's instructions. To measure intracellular IFN-γ produced by CD8$^+$ TILs, TILs were restimulated with anti-CD3/CD28 beads on day 3 after polyclonal stimulation and Golgistop (containing monensin) was added (1:1500 dilution, BD Biosciences). After additional 24 hours of incubation, TILs were harvested and subjected to intracellular cytokine staining.

Antigen specific stimulation

To test the effects of dual TIGIT/PD1 blockade on tumor-specific T-cell immunity, we used an antigen specific assay as described in our previous HCC-research[11, 30]. Briefly, autologous B-cell blasts served as APC, and were electroporated with mRNA encoding GPC3 or MAGEC2, two tumor antigens that are frequently expressed in HCC tumors[31]. Importantly, the sequences encoding the tumor antigens in the mRNA's are directly followed by a sequence encoding the transmembrane and luminal regions for DC-Lamp, which is a targeting signal for the endolysosomal compartment resulting in peptide loading in MHC class II as well as in MHC class I and thereby presentation to CD4$^+$ and CD8$^+$ T cells. TILs were stained with CFSE, and co-cultured with GPC3 mRNA- and/or MAGEC2 mRNA-, or eGFP (irrelevant control antigen) mRNA-transfected autologous B-cell blasts with a TIL:B cell ratio of 1:1, and proliferation of CD8$^+$ T cells was measured using flow cytometry on day 6.

***Ex vivo* cytotoxicity assay**

HepG2 HCC cells expressing RFP-H2B upon lentiviral transfection, were used as target cells. RFP-H2B transduced cells give fluorescence in the Percp channel, thus enabling better differentiation between CD45$^+$ leucocytes and HepG2 cells. CD3$^+$ TILs isolated using CD3 microbeads (Miltenyi Biotec, Germany) were used as effector cells. HepG2 cells were pre-treated with IFN-γ for 48 hours to induce PD-L1 expression.

CD3^{+} TILs were pre-activated for 3 days with anti-CD3/CD28 beads, and then co-cultured with IFN-γ-treated HepG2 cells in a ratio of 10:1 in absence or presence of nivolumab or nivolumab plus anti-TIGIT antibody, or corresponding isotype control antibodies (mentioned above). After 96 hours of co-culture, the remaining HepG2 cells were quantified using a MACSQuant flow cytometer.

Statistical analysis

The distribution of all data sets was analyzed for normality using the Shapiro-Wilk test. The differences between paired groups of data were analyzed according to their distribution via paired t test or Wilcoxon matched pairs test. Differences between different groups of patients were analyzed via t test or Mann-Whitney test. Spearman's rank correlation test for nonparametric data and Pearson's correlation test for parametric data were used to analyze the correlation between two factors. Statistical analysis was performed using GraphPad Prism 8.0. P value less than 0.05 was considered statistically significant (*$P < 0.05$; **$P < 0.01$; ***$P < 0.001$; ****$P < 0.0001$).

Table 1. Patient Characteristics

	HCC patients* (n=47)
Sex (male /female)	35/12
Age at surgery (years)**	67 ± 10
Race (Caucasian/Asian/African)	39/4/4
Cirrhosis (Yes/no)	17/30
Tumor size (cm)**	8.7 ± 5.5
Tumor number (1/2)	43/4
AFP level before resection (ug/L)	
<20/ 20-400/ >400/ unknown	26/8/12/1

*Etiology of liver disease: no known liver disease (n=19), Hepatitis B/C (n= 7/5), Alcohol-related liver disease (n= 1), non-alcoholic steatohepatitis (NASH)/non-alcoholic fatty liver disease(NAFLD) (n= 15)

** Median ± SD.

Results

TIGIT/CD226 ratio is increased on intratumoral CD8^{+} T and Treg cells

We compared the expression of TIGIT and CD226 on CD8^{+} T cells, CD4^{+}FOXP3^{+} Treg and CD4^{+}FOXP3^{-} Th cells in HCC tumors, paired TFL and blood. Gating strategy is shown in **Fig.S1A**. In all tissue compartments, TIGIT was expressed on CD8^{+} T cells and Th, whereas the highest expression was found on Treg (**Fig.1A-1D**). In contrast, compared to TFL and blood, significantly reduced proportions of CD8^{+} T and Treg cells in tumor expressed CD226 (**Fig.1A-1D and S1B**). In addition, the median fluorescent intensities (MFI) of TIGIT on CD8^{+}, Treg and Th cells in tumor and TFL did not differ much, whereas the MFI of CD226 was considerably decreased in tumor compared to TFL (**Fig.S1C and S1D**). As a result, ratios of TIGIT/CD226 frequencies and MFI of both CD8^{+} T and Treg cells were highest in the tumor (**Fig.1E and S1E**). We observed limited co-expression of TIGIT and CD226 on T cell subsets in all three tissue compartments (**Fig.1F**). Importantly, the TIGIT^{+}CD226^{-} T cell fractions were increased significantly in Treg and Th in the tumor compared to TFL (**Fig.S1F**).

These data suggest that tumor-infiltrating CD8^{+} T cells receive mainly co-inhibitory signals (via TIGIT) and less co-stimulatory signals (via CD226) from CD155-expressing cells. In addition, increased TIGIT/CD226 ratios on Treg may enable Treg to be highly sensitive to TIGIT signals that can enhance their suppressive function[32].
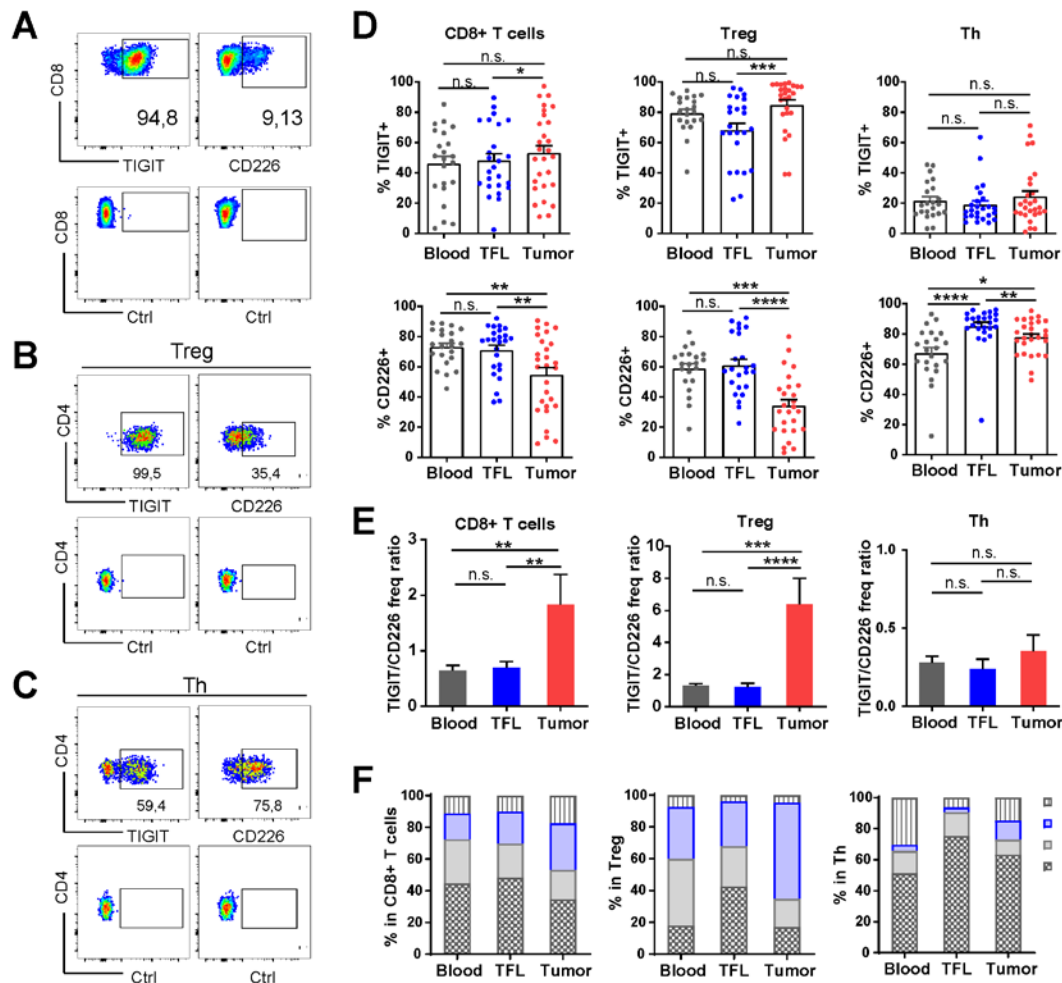
Figure 1. TIGIT/CD226 ratio is increased on intratumoral Treg and CD8$^+$ T cells. (A-C) Flow-cytometry plots of TIGIT and CD226 expression on tumor-infiltrating CD8$^+$ T, Treg and Th cells. (D) The percentages of TIGIT and CD226 positive cells among CD8$^+$ T, Treg and Th cells in blood, TFL and tumor (n=28). (E) The frequency ratio of TIGIT/CD226 in CD8$^+$ T, Treg and Th cells. (F) The mean percentage of co-expression of TIGIT and CD226 among CD8$^+$ T, Treg and Th cells in tumors, TFL and blood from HCC patients (n=16). Dots represent individual patients. Bars represent means ± SEM. *P < 0.05, **P < 0.01, ***P < 0.001.

TIGIT is enriched and CD226 is downregulated on intratumoral PD1^{high} CD8$^+$ TILs

Consistent with Kim et al [33] and Ma et al [34], we observed two subgroups of HCC patients based on the presence or absence of a distinct PD1^{high} subpopulation in tumor-derived CD8$^+$ T cells. HCC patients with a PD1^{high} CD8$^+$ TILs population were termed high PD1 expressers (**Fig.2A and S2A**), whereas patients with only PD1-intermediate CD8$^+$ TILs were called low PD1 expressers (**Fig.2A and S2B**). High PD1 expressers comprised 68% of the total analyzed population (**Fig.2A**). All tumor-derived PD1^{high} CD8$^+$ T cells expressed TIGIT (**Fig.2B**). The PD1^{high} TIGIT$^+$ fraction comprised on average 58% of the total CD8$^+$ TILs, and part of these cells co-expressed the co-

102

inhibitory receptors TIM3 and LAG3 (**Fig.2B and S2C**). Interestingly, in contrast to TIM3 and LAG3, TIGIT was also expressed on a subset of CD8$^+$PD1^{int} TILs in high PD1 expressers (**Fig.2B**). Moreover, this subset showed higher expression of CD226 than PD1^{high} CD8$^+$ TILs (**Fig.2B**). High PD1 expressers had significantly increased frequencies of TIGIT-expressing CD8$^+$ TILs, but in low PD1 expressers percentages of CD226-expressing CD8$^+$ TILs were enhanced. MFI of TIGIT and CD226 showed the same differences (**Fig.2C**). In high PD1 expressers, ratios of TIGIT/CD226 on CD8$^+$ T cells were upregulated in tumor compared to TFL and blood (**Fig.2D**) and correlated positively with the frequencies of PD1^{high} CD8$^+$ TILs (**Fig.S2D**). In low PD1 expressers, ratios of TIGIT/CD226 on CD8$^+$ T cells did not differ between tumor, TFL and blood (**Fig.S2E**). Within high PD1 expressers, both the frequencies and MFI of TIGIT increased step-wise according to the level of PD1 expression on CD8$^+$ T cells (**Fig.2E**), whereas CD226 frequency and MFI were negatively associated with PD1 expression (**Fig.2F**). Consequently, the ratio of TIGIT/CD226 was strongly enhanced in tumor-infiltrating PD1^{high} CD8$^+$ T cells, but only minimally on PD1^{int}CD8$^+$ compared to PD1$^-$ CD8$^+$ TILs (**Fig.2G**). In low PD1 expressers, TIGIT expression was minimally increased in PD1^{int} CD8$^+$ compared to PD1$^-$ CD8$^+$ TILs (**Fig.2H**) whereas CD226 did not show any difference (**Fig.2I**). The ratios of TIGIT/CD226 on PD1^{int} and PD1- CD8$^+$ TILs in low PD1 expressers were all below 1 (**Fig.2J**). Nevertheless, the PD1^{int}TIGIT$^+$ fraction of total CD8$^+$ TILs in low PD1 expressers was larger than in high PD1 expressers (on average 37% of total CD8$^+$ TILs (**Fig.S2F**) versus 14% (**Fig.2B**), respectively. The frequencies of PD1^{high}CD8$^+$, TIGIT$^+$ CD8$^+$ T cells and the ratios of TIGIT/CD226 on CD8$^+$ TILs correlated positively with serum AFP concentrations in individual patients (**Fig.S2G-S2I**).

Collectively, in high PD1 expressers TIGIT expression correlated with PD1 expression, and TIGIT/CD226 ratios were maximally increased on PD1^{high} CD8$^+$ TILs, whereas in low PD1 expressers CD8$^+$ TIL contain a larger proportion of PD1^{int} cells with TIGIT/CD226 ratios smaller than 1.
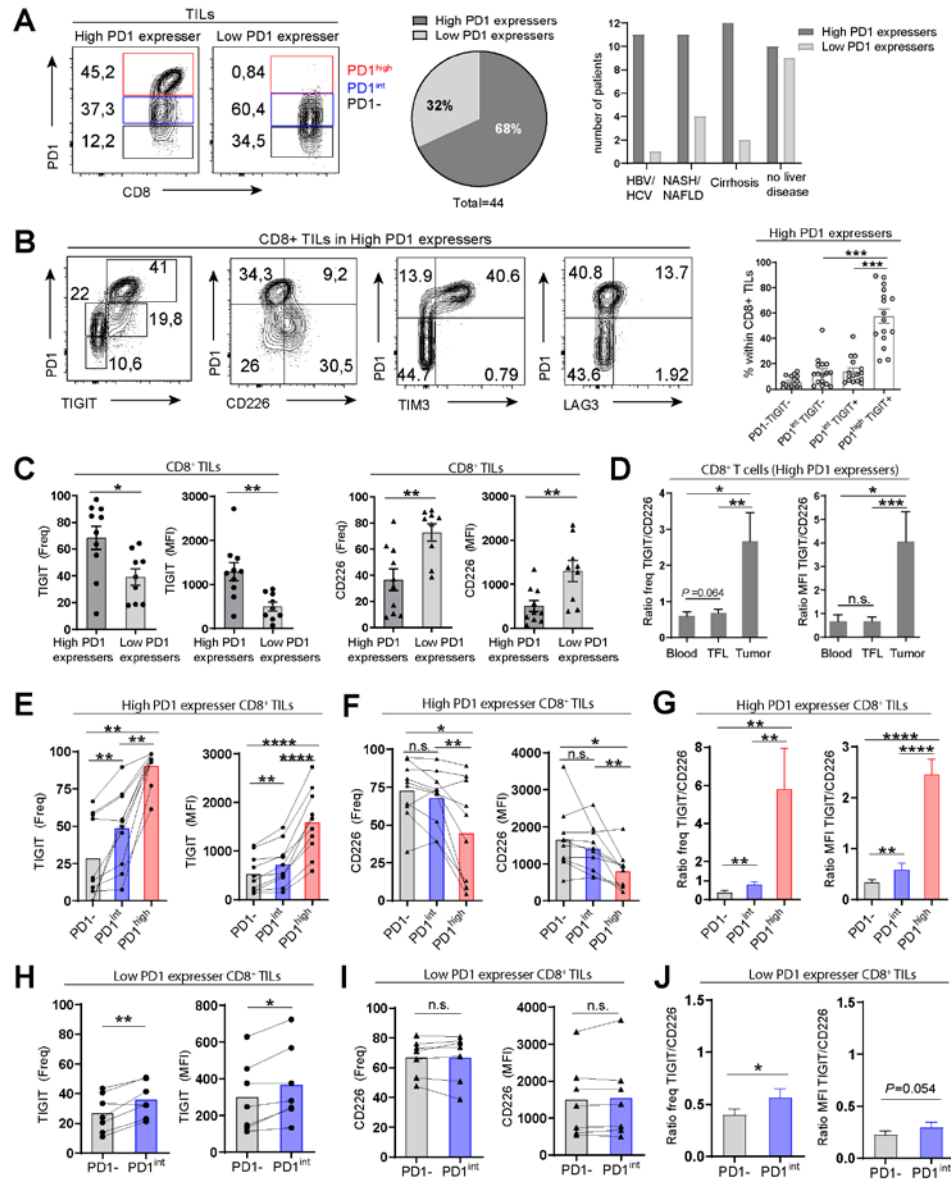
Figure 2. TIGIT is enriched and CD226 is down-regulated on intratumoral PD1^{high} CD8^{+} T cells. (A) Flow-cytometry plots revealed stratification of HCC patients based on differential PD1 expression on tumor-infiltrating CD8^{+} T cells. The gate to define the PD1^{high} subsets was set based on the intermediate PD1 expression of CD8^{+} TILs. The percentage of High PD1 expresser and its association with etiology are shown (n=44). (B) Flow-cytometry plots of co-expression of PD1 and TIGIT, CD226, TIM3 and LAG3 in High PD1 expressers. Percentages of coexpression of TIGIT and PD1 were shown (n=16). (C) Expression of TIGIT and CD226 on CD8^{+} TILs in high or low PD1 expressers. (D) Ratios of TIGIT/CD226 in blood, TFL and tumor. (E-F) Expression of TIGIT and CD226 in the PD1-, PD1^{int} and PD1^{high} subsets of CD8^{+} TILs in high PD1 expressers (n=10). (G) Ratios of TIGIT/CD226 in PD1-, PD1^{int} and PD1^{high} subsets of CD8^{+} TILs high PD1 expressers (n=10). (H-I) Expression of TIGIT and CD226 in the PD1- and PD1^{int} subsets of CD8^{+} TILs in High PD1 expressers (n=7). (J) Ratios of TIGIT/CD226 in PD1- and PD1^{int} subsets of CD8^{+} TILs in low PD1 expressers (n=7). Dots represent individual patients. Bars show mean or mean ± SEM.

PD1^{high}TIGIT$^+$ CD8$^+$ TILs are functionally exhausted with high TOX expression

TOX has been identified as a major driver of epigenetic changes associated with CD8+ T cell exhaustion and has a role in maintaining survival of exhausted T cells[35-37]. A TCF1$^+$ stem cell-like progenitor population exists with exhausted CD8$^+$ TILs that might be responsible for the proliferative and functional responses that occur following immune checkpoint blockade[38-40]. We therefore examined TOX and TCF1 expression in the different CD8$^+$ TIL subsets. In High PD1 expressers, the expression of TOX was specifically upregulated in PD1^{high}TIGIT$^+$ CD8$^+$ TILs, whereas TCF1 expression was downregulated in this subset (**Fig.3A-3C**). PD1^{high}TIGIT$^+$ CD8$^+$ TILs also expressed higher levels of activation markers Ki67, CD38 and HLA-DR (**Fig.3D-3F**). Co-expression of CD39 and CD103 identifies tumor-reactive CD8$^+$ T cells in multiple human solid tumors[41]. Here we found a higher frequency of CD39$^+$CD103$^+$ cells in PD1^{high}TIGIT$^+$ CD8$^+$ TIL subset compared to other subsets (**Fig.3G**).

Since dysfunctional production of cytotoxins is a feature of exhaustion, we analyzed their intracellular expression directly *ex vivo*. The expression of granzyme B (GzmB) and perforin was significantly reduced in the PD1^{high} TIGIT$^+$ fraction compared to PD1^{int} TIGIT$^+$ fraction (**Fig.3H**). Interestingly, the PD1^{int}TIGIT$^+$ CD8 TIL subset tended to contain the most cytotoxins (**Fig.3H**). Furthermore, we stimulated TILs with phorbol 12-myristate 13-acetate (PMA) and ionomycin to assess effector cytokine production by flow cytometry. The percentages of TNF-α-and IFN-γ-producing cells were lowest in PD1^{high}TIGIT$^+$ cells compared to the other CD8$^+$ TIL fractions (**Fig.3I**).

PD1^{high}TIGIT$^+$ CD8$^+$ T cells were also present in TFL of High PD1 expressers (**Fig.S3A**), and part of these cells expressed TIM3 but not LAG3 (**Fig. S3B-C**). However, although this subset showed a decreased TCF1 level, it did not upregulate TOX (**Fig.S3D-E**). Notably, CD226 was not down-regulated and the ratios of TIGIT/CD226 were only modestly increased in PD1^{high} CD8$^+$ T cells in TFL (**Fig.S3F-H**) compared to those ratios on PD1^{high} CD8$^+$ TILs (**Fig.2H**). The expression of perforin but not GzmB was significantly reduced in the PD1^{high} TIGIT$^+$ fraction compared to PD1^{int} TIGIT$^+$ fraction in TFL (**Fig.S3I**).

These data demonstrate that in contrast to PD1^{int} CD8$^+$ TIL, PD1^{high}TIGIT$^+$ CD8$^+$ TILs are highly activated, terminally differentiated dysfunctional T cells, characterized by high TOX expression.
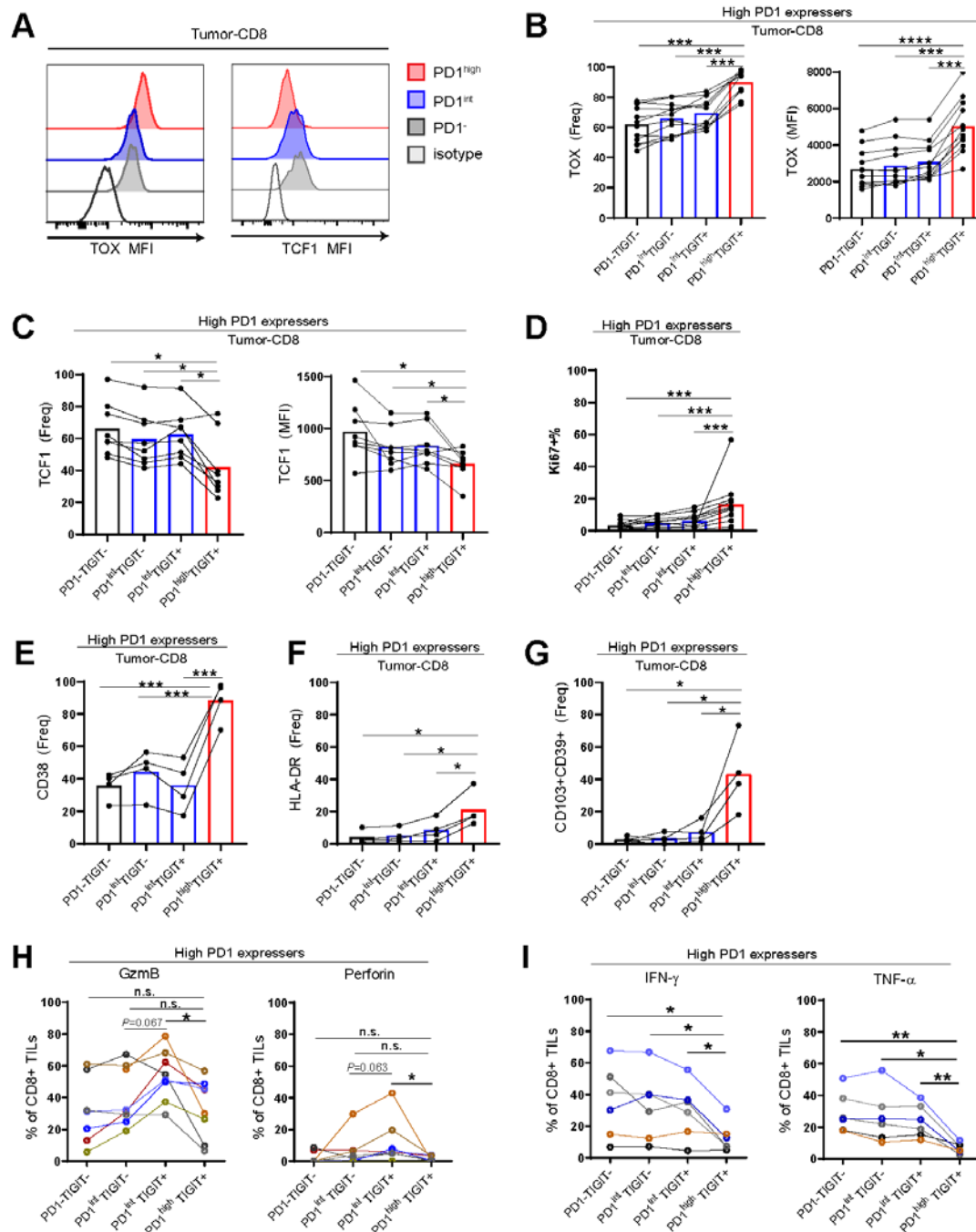
Figure 3. PD1^{high}TIGIT$^+$ CD8$^+$ TILs are functionally exhausted with high TOX expression. (A) Flow-cytometry plots of TOX and TCF1 expression in PD1$^-$, PD1^{int} and PD1^{high} CD8$^+$ TILs. (B-F) Expression of TOX, TCF1, Ki67, CD38 and HLA-DR in four subsets of CD8$^+$ TILs in High PD1 expressers. Dots represent individual patients and bars show mean. (G) Coexpression of CD39 and CD103 in four subsets of CD8$^+$ TILs in high PD1 expressers. (H) The percentages of intracellular granzyme B and perforin expression in four subsets of CD8$^+$ TILs in high PD1 expressers. (I) Production of IFN-γ and TNF-α by four subsets of CD8$^+$ TILs in high PD1 expressers after PMA/ionomycin stimulation.*$P < 0.05$, **$P < 0.01$, ***$P < 0.001$.

106

CD155 is present on tumor-infiltrating APCs and overexpressed on HCC tumor cells

As CD155 is the high affinity ligand for TIGIT and CD226, we analyzed CD155 expression on APC subsets in tumors . We focused on three major APC subsets, CD45^{+}BDCA1^{+}CD19^{-} conventional dendritic cells (cDC), CD45^{+}CD14^{+} monocytes/ macrophages, and CD45^{+}CD19^{+} B cells (**Fig.S4A**). The percentages of cDCs, monocytes /macrophages and B cells in tumor tissues did not significantly differ from those in TFL (**Fig.4A**). Prominent expression of CD155 was found on cDC and monocytes, and low expression on B cells (**Fig.4B-4C and S4B**). Both frequencies and MFI of CD155 expression on APCs in tumor did not differ with that in TFL and blood. We also examined CD155 protein expression on tumor cells using tissue microarrays with cores of tumors and tumor-free liver tissues from 97 HCC-patients by immunohistochemistry (described previously in[31, 42]). We found that most tumor cells express CD155 and that expression was significantly upregulated on tumor cells compared to hepatocytes in TFL tissue (**Fig.4D-4E**).

These data demonstrate that CD155 is highly expressed in the tumor microenvironment, suggesting that TIGIT^{+} TILs interact with CD155^{+} cells within the tumor which might result in T cell inhibition.
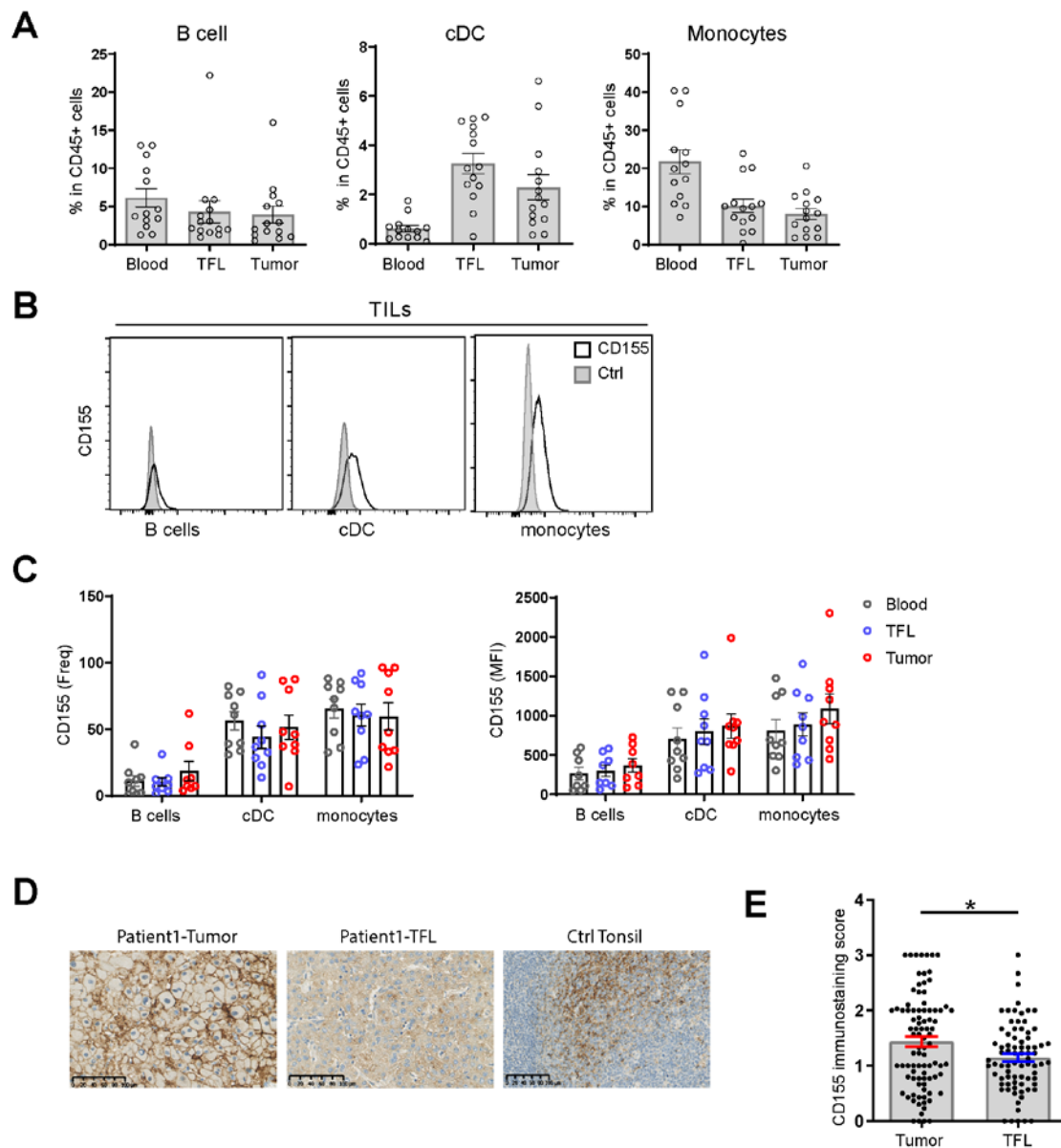
Figure 4. CD155 is present on tumor-infiltrating APCs and overexpressed on HCC tumor cells. (A)The percentages of B cells, cDC, and monocytes within CD45$^+$ cells from tumor, TFL and blood. Dots represent individual patients and bars show mean ± SEM. (B) Representative histograms of CD155 expression on tumor-infiltrating B cells, cDC and monocytes. (C) The percentages of CD155$^+$ cells within APC subsets and MFI of CD155 on APCs in tumor, TFL and blood. (D) Representative images of immunohistochemistry staining show CD155 expression in HCC tumor and paired TFL tissue. The immunostaining score for patient 1 was 3D in tumor, 1D in TFL. Tonsil served as both positive and negative control tissue. Scale bars are presented in each image. (E) The immunostaining score of CD155 in individual patients is presented (n=97). Significance was assessed by Wilcoxon matched-pairs signed rank test. Data are presented as mean ± SEM. *$P < 0.05$.

Combined TIGIT and PD1 blockade enhances *ex vivo* functionality of CD8+ TILs

We tested whether co-blocking TIGIT and PD1 can improve functionality of tumor-infiltrating T cells. We isolated on average 2.74×10^6 CD45+ leukocytes per gram of tumor (**Fig.S5A-S5B**). We stimulated TILs with a suboptimal amount of anti-CD3/CD28 beads, in the presence or absence of mouse anti-human TIGIT (10 µg/ml) and/or anti-PD1 (nivolumab,10 µg/ml), which completely blocked TIGIT and PD1 on CD8+ TILs until the end of the cultures (**Fig.S5C**), or isotype-matched control antibodies. After 4 days, T cell proliferation (**Fig.S5D**) and cytokine production were measured by flow cytometry. Single nivolumab treatment resulted in a minor increase in CD8+ TIL proliferation (**Fig.5A**) whereas single TIGIT blockade did not (**Fig.S5E**). But co-blockade of TIGIT and PD1 significantly enhanced the proliferation of CD8+ TILs compared to single PD1 blockade (**Fig.5A**). The stimulatory effect of co-blockade compared to single PD1 blockade was mainly observed in Low PD1 expressers and not observed in High PD1 expressers (**Fig.5B**). A higher concentration of TIGIT blocking antibody (20 µg/ml) in combination with nivolumab did not have added value to reinvigorate CD8+ TIL proliferation in High PD1 expressers (**Fig.S5F**). Combined blockade of TIGIT and PD1 also enhanced *ex vivo* proliferative responses of CD8+ TILs of HCC patients to tumor antigens GPC3 and/or MAGEC2 presented by autologous B cells (**Fig.5C and S5G-S5H**).

To compare the survival and proliferative ability of PD1^{high} and PD1$^{int \ \& \ -}$ CD8+ TILs, from high PD1 expressers we sorted PD1^{high} CD8+ and PD1^{int} plus PD1$^-$ CD8+ TILs and cultured each of those populations together with the remaining CD45+CD8- TILs in the presence of anti-CD3/CD28 beads. PD1^{high} CD8+ T cells showed limited expansion capacity compared to the PD1^{int} and PD1$^-$ subsets (**Fig. 5D**).

In addition, compared to single PD1 blockade, co-blockade of TIGIT/PD1 significantly enhanced IFN-γ production in CD8+ TIL of low PD1 expressers (**Fig.5E-5F**) and also in CD8+ TILs from some high PD1 expressers. Moreover, we used an HCC cell line (HepG2) to evaluate the effect of co-blockade on cytotoxicity of anti-CD3/CD28-stimulated purified CD3+ TIL. As HepG2 cells expressed high levels of CD155 but low levels of PD-L1, we induced PD-L1 expression on HepG2 by IFN-γ pre-treatment for 48h (**Fig.S6A**). CD155 expression did not change after IFN-γ treatment (**Fig.S6B**).

Combined PD1/TIGIT antibody blockade significantly enhanced cytotoxicity of CD3$^+$ TIL against HepG2 compared to single PD1 blockade (**Fig.5G and S6C**).

Collectively, these data demonstrate that compared to anti-PD1 monotherapy, co-blockade of TIGIT with PD1 improves *ex vivo* CD8$^+$ TIL proliferation, IFN-γ production and cytotoxicity as well as reactivity of CD8$^+$ TILs against tumor antigens.

Combined TIGIT and PD1 blockade enhances *ex vivo* functionality of CD8$^+$ TILs not responding to anti-PD1 single blockade

We next asked two questions: 1) whether combined blockade of TIGIT/PD1 can convert anti-PD1 non-responders to responders, 2) whether co-blockade can further enhance CD8$^+$ TIL function in anti-PD1 responders. We stratified HCC patient TILs into nivolumab (nivo) responders (11/22, 50%) and non-responders (11/22, 50%) based on CD8$^+$ TIL proliferation upon *ex vivo* single PD1 blockade (**Fig.6A**). Strikingly, compared to only blocking PD1, co-blockade of TIGIT/PD1 significantly enhanced the proliferation of CD8$^+$ TILs in nivo non-responders but not in nivo responders (**Fig.6B**). Similarly, nivo/anti-TIGIT treatment significantly improved IFN-γ production by CD8$^+$ TILs from nivo non-responders, although also enhanced IFN-γ production was observed in CD8$^+$ TILs of some nivo responders (**Fig.6C**). However, enhanced TIL cytotoxicity against HepG2 was observed in both groups upon co-blockade (**Fig.6D**). Interestingly, 73% of nivo responders were high PD1 expressers (**Fig.6F**), suggesting that high PD1 expressers tend to respond better to PD1 blockade.
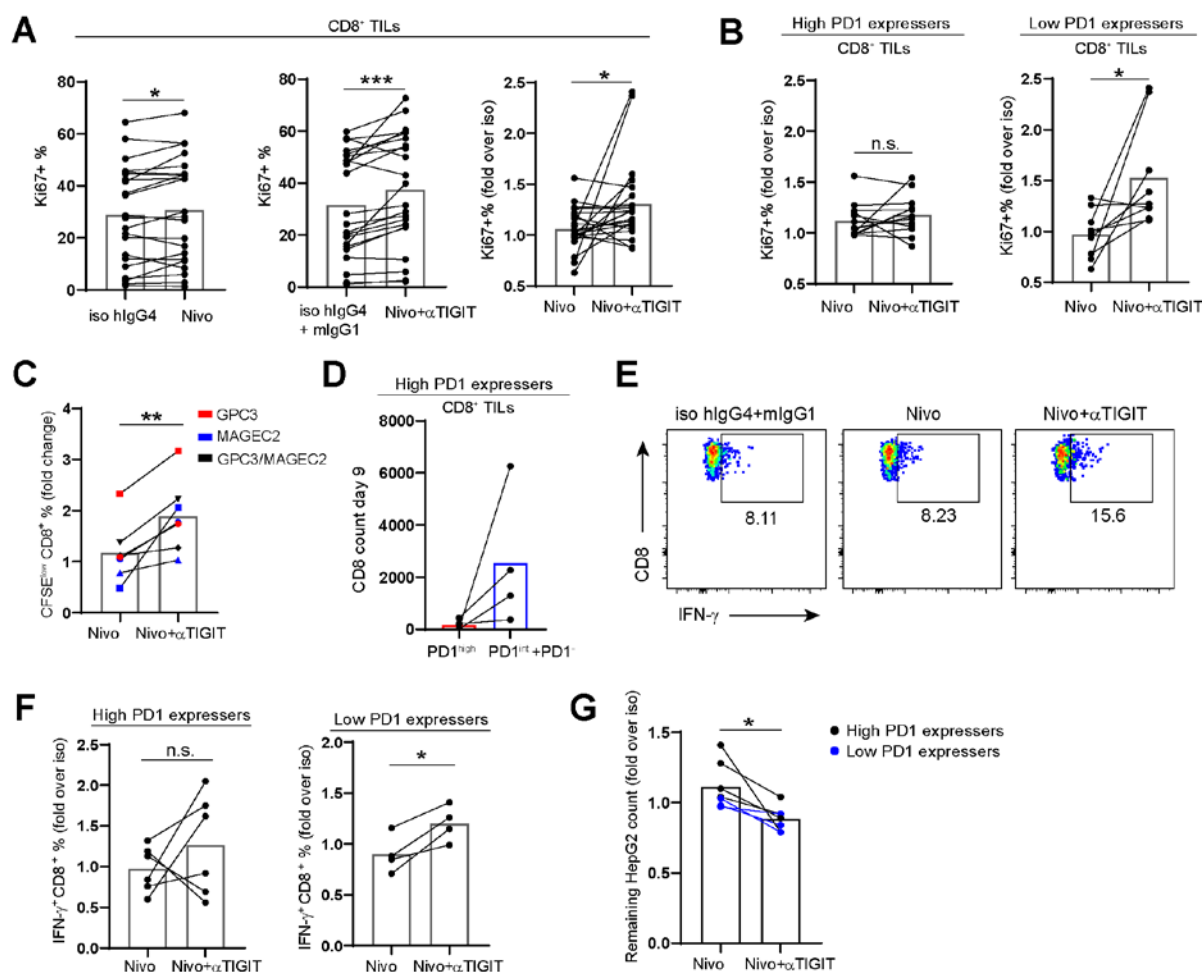
Figure 5. Combined TIGIT and PD1 blockade further enhances *ex vivo* functionality of CD8+ TILs (A) Effects of nivolumab single blockade and combined blockade with mouse anti-human TIGIT mAb on CD8+ TIL proliferation from individual patients upon anti-CD3/CD28 beads stimulation (n=22). (B) Effects of nivolumab blockade alone or combined with TIGIT blockade on CD8+ TIL proliferation in high or Low PD1 expressers. Data were normalized to each corresponding isotype. (C) Proliferation (CFSE-low) of CD8+ TILs of individual patients (2 high PD1 expressers and 3 low PD1 expressers) in response to GPC3 or/and MAGEC2 in the presence or absence of blocking antibodies. Shapes indicate different patients. Data were normalized to isotype and shown as fold change. (D) Total cell count of sorted PD1high and PD1int plus PD1- CD8+ TILs on day 9 with CD3/CD28 beads stimulation. Bars represent mean. (E) Flow cytometry plots of IFN-γ in CD8+ TILs after restimulated with anti-CD3/CD28 beads in polyclonal stimulation. (F) Production of IFN-γ by CD8+ TILs in high or low PD1 expressers after restimulated with anti-CD3/CD28 beads in polyclonal stimulation. (G) Percent of remaining HepG2 was calculated by HepG2 count in each condition divided by HepG2 count in TIL+HepG2 only then the killing ratio of Nivo or Nivo/anti-TIGIT was normalized to corresponding isotype (n=7) . *$P < 0.05$, **$P < 0.01$, ***$P < 0.001$.
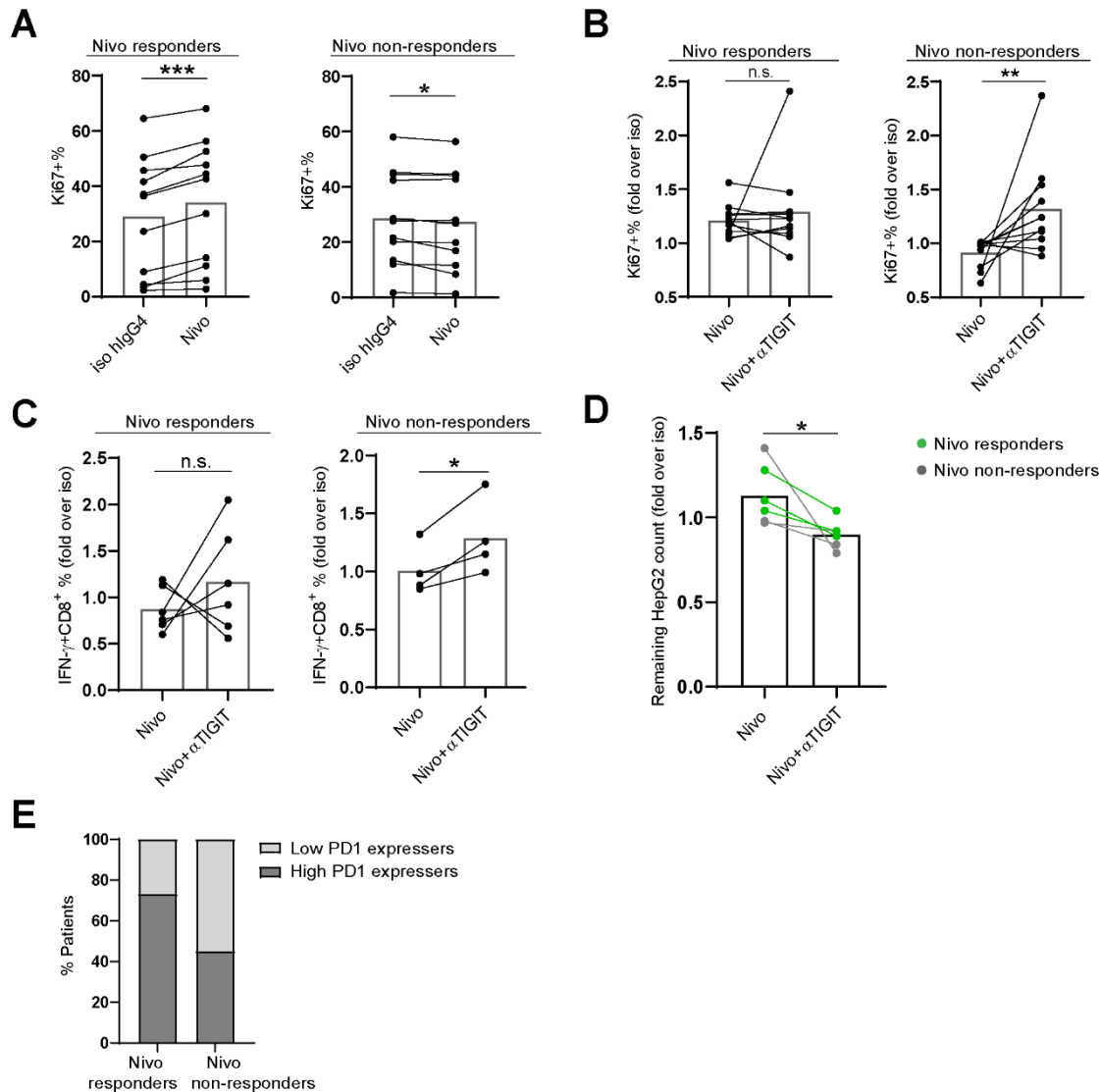
Figure 6. Combined TIGIT and PD1 blockade enhances *ex vivo* functionality of CD8^{+} TILs in nivolumab non-responders. (A) Stratification of nivolumab responders and non-responders based on CD8^{+} TIL proliferation. (B)Effects of nivolumab blockade alone or combined with TIGIT blockade on CD8^{+} TIL proliferation in nivolumab responders or non-responders. (C) Production of IFN-γ by CD8^{+} TILs in nivolumab responders or non-responders after restimulated with CD3/CD28 beads in polyclonal stimulation. (D) Percent of remaining HepG2 depicted as ratio of absolute HepG2 count in presence of TIL+ Nivo or Nivo/anti-TIGIT versus corresponding isotypes (n=6). (E) The distribution of high and low PD1 expressers in nivolumab responders and non-responders. Bars represent mean.

CD226 is required for the effect of TIGIT blockade

As CD226 is the co-stimulatory counterpart of TIGIT, we assessed whether CD226 expression is affected by TIGIT blockade and whether CD226 is required for the stimulatory effects of TIGIT blockade that we observed in TIL-cultures of some patients. In *ex vivo* polyclonal assays, we observed that TIGIT blockade significantly upregulated both CD226hi frequencies and CD226 MFI on day 4 (**Fig.7A and 7B**). Furthermore, the percentages of CD226hi CD8+ TILs correlated with the frequencies of Ki67+CD8+ TILs after TILs were used in *ex vivo* polyclonal assays with or without anti-TIGIT or dual blocking antibodies (**Fig.7C**). Notably, the addition of anti-CD226 blocking antibodies to TILs that responded to single TIGIT blockade abrogated the effect of TIGIT blockade partially (**Fig.7D-7E**).

Taken together, CD226 expression can be upregulated by TIGIT blockade and is partially required for the stimulatory effects of TIGIT blockade on CD8+ TILs.
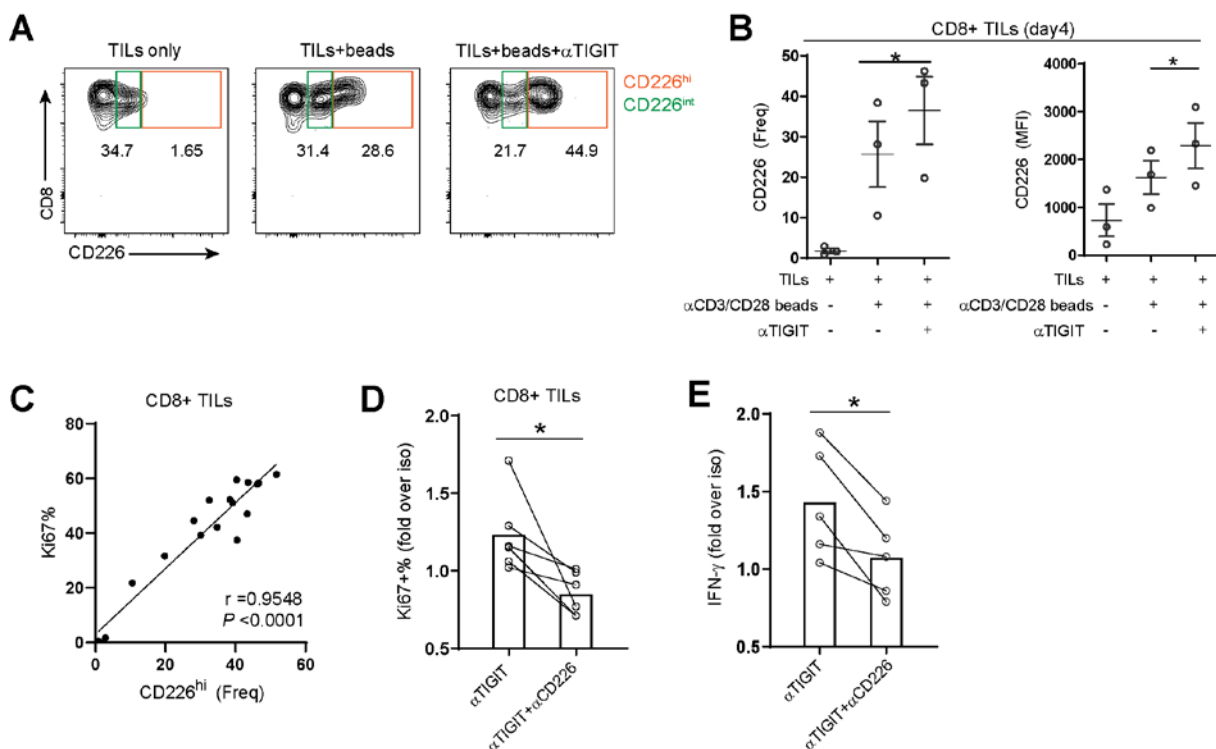

Figure 7. CD226 is required for the effect of TIGIT blockade. (A) Flow-cytometry plots of CD226 expression on CD8+ TILs after 4 days cultures with/without CD3/CD28 beads stimulation or anti-TIGIT antibody. (B) Expression of CD226 on CD8+ TILs after cultures with/without anti-CD3/CD28 beads stimulation or anti-TIGIT antibodies on day 4 (patients n=3). Data are presented as mean ± SEM. (C) Correlation of Ki67% and CD226hi frequencies in CD8+ TILs after *in vitro* stimulation with CD3/CD28 beads. Dots show data from TIL that were involved in *ex vivo* polyclonal assays, including data from TIL only, TIL+beads, TIL+anti-TIGIT

(10 and 20 μg/mL) or TIL+anti-PD1+ anti-TIGIT(10 and 20 μg/mL) (6 different conditions with n = 3 samples each, total 18). Significance was assessed by Pearson's correlation. (D) Proliferation of CD8^{+} TILs stimulated with anti-CD3/CD28 beads in the presence of anti-TIGIT or anti-TIGIT plus anti-CD226 antibodies (n=6). (E) Production of IFN-γ by TILs stimulated with anti-CD3/CD28 beads in the presence of anti-TIGIT or anti-TIGIT plus anti-CD226 antibodies (n=5). Data normalized to each isotype. *$P < 0.05$. Bars represent mean.

Discussion

The aims of this study were to characterize TIGIT-expressing TILs in HCC patients and to determine whether co-blockade of TIGIT and PD1 has added value over PD1 single blockade to restore functionality of HCC TILs. We observed elevated ratios of TIGIT/CD226 expression on intratumoral CD8^{+} T and Treg cells compared with their counterparts in TFL and blood. This allows more frequent interaction of TIGIT on these TIL subsets with its high affinity ligand CD155 expressed on APCs or tumor cells. This interaction may have different effects on CD8^{+} T cells and Treg. In CD8^{+} T cells, TIGIT signaling can directly or indirectly inhibit their cytotoxic/effector function[18, 20]; in Treg, TIGIT signaling can directly promote their suppressive functions[32, 43] or Treg can induce IL-10 production by DCs via TIGIT signaling, which also results in suppression of antitumor effector T cell responses[12].

Kim et al.[33] and Ma et al.[34] have shown that PD1 is differentially expressed on CD8^{+} TIL in about half of HCC patients, and that PD1^{high} CD8^{+} TILs are functionally the most exhausted subpopulation. Wang et al.[44] have shown that TOX is upregulated in functionally exhausted PD1^{high}CD8^{+} TILs in HCC. Here, we confirmed these observations, and we extended them by showing that the PD1^{high} CD8^{+} TIL subset has the lowest expression of the cytotoxins granzyme B and perforin, and co-expresses CD39 and CD103 suggesting enrichment with tumor-specific T cells. We further demonstrated that TIGIT expression was enriched whereas CD226 expression was downregulated on PD1^{high} CD8^{+} TILs compared to CD8^{+}PD1^{int} and CD8^{+}PD1^{-} TILs. Consequently, PD1^{high}TIGIT^{+} CD8^{+} TILs had the highest TIGIT/CD226 ratios compared to other CD8^{+} subsets. Since a large part of these cells also expressed the co-inhibitory receptors TIM3 and/or LAG3, our data suggest that the PD1^{high}TIGIT^{+} subset represents the terminally differentiated and exhausted CD8^{+} TIL subset in HCC tumors. In agreement with Kim et al.[33], we found that high PD1 expressers were mainly found among patients with high serum AFP levels. Ma et al.[34] reported recently that

114

the presence of CD8+PD1hi T cells in HCC tumors is associated with poor prognosis, and Liu et al.[45] found that elevated levels of peripheral PD1+TIGIT+ CD8+ T cells are associated with poor prognosis of patients with HBV-related HCC.

Interestingly, we demonstrate that the more PD1high TIGIT+ CD8+ T cells in tumor, the more PD1high TIGIT+ CD8+ T cells were found in TFL. PD1high TIGIT+ CD8+ T cells in TFL did not show increased levels of TOX, and neither reduced CD226 and granzyme B expression. Apparently, PD1high TIGIT+ CD8+ T cells in the tumors are in a further stage of exhaustion than their counterparts in TFL. This may be caused by chronic TCR stimulation in the tumor microenvironment. Several studies have shown that TOX expression was increased and remained high in exhausted CD8+ T cells by chronic TCR stimulation, whereas only low-level and transient TOX upregulation was seen in CD8+ T cells during acute infection[35-37]. TOX-expression in CD8+ TILs maybe further supported by tumor-derived factors, such as vascular endothelial growth factor-A (VEGF-A), that drive exhaustion in CD8+ TILs[46]. Further research is required to understand the specific factors in HCC tumor microenvironment that increase TOX levels on PD1high CD8+ TILs.

We performed polyclonal and tumor antigen-specific functional assays to test the effects of blocking PD1 and TIGIT on tumor-infiltrating CD8+ TILs *ex vivo*. Compared to single PD1 blockade, co-blockade of TIGIT/PD1 increased IFN-γ production by CD8+ TILs of some high PD1 expressers, but did not improve their proliferation. This might be caused by limited survival capacity and a terminally differentiated and exhausted state of CD8+ TILs. In contrast, CD8+ TIL of low PD1 expressers exhibited enhanced proliferation and cytokine production in response to co-blockade. CD8+ TIL of these patients are not terminally differentiated, and also express more CD226, thereby allowing better co-stimulation upon TIGIT blockade. Another hypothesis is that the PD1int TIGIT+ CD8+ subset, which was enriched in low PD1 expressers, may mediate the enhanced proliferative response. On average 60% of PD1int TIGIT+ CD8+ TILs expressed TCF1. TCF1 is a key transcription factor of progenitor exhausted CD8+ T cells (Tex), which express intermediate PD1, to produce differentiated effector T-cell progeny and to maintain themselves[38, 39]. This PD1int Tex cell subset mediates responses to PD1 checkpoint pathway blockade. Accordingly, PD1int TIGIT+ CD8+ TILs may be expanded after TIGIT/PD1 blockade to fill up the effector-type pool. Further

work is required to unravel the role of these PD1^{int} TIGIT^{+} TCF1^{+} CD8^{+} T cells in response to checkpoint blockade in HCC patients.

In HCC, the question still remains how to improve the response rate to anti-PD1 therapy. Here we found TIGIT/PD1 co-blockade could improve *ex vivo* proliferation, cytokine production, and cytotoxicity of CD8^{+} TILs which did not respond to nivolumab *ex vivo*. Interestingly, CD8^{+} TILs that *ex vivo* responded to single PD1 blockade were mainly derived from high PD1 expressers (**Fig.6E**). In contrast, the vast majority of combination-blockade responding CD8^{+} TILs were derived from low PD1 expressers (Fig.5B (78%) and 6B (73%)), suggesting that especially tumors with intermediate (and not high) PD1 expressing CD8^{+} TIL may display improved benefit from combined treatment with anti-PD1 and anti-TIGIT.

CD226 deficiency has been shown to impair antitumor T cell effector function[47]. Here we found that blocking TIGIT upregulated CD226 on CD3/CD28-stimulated CD8^{+} TILs, which enabled CD226 to interact more frequently with CD155. The linear correlation between CD226 and Ki67 expression after culture indicates the enhanced expression of CD226 might be responsible for the increased proliferation of CD8^{+} TILs. TIGIT may act directly to compete with CD226 for ligand binding[12, 19]. Johnston et al. showed that TIGIT directly interacts with CD226 and that this interaction impairs CD226 homodimerization and function[20]. Here we showed neutralizing CD226 on CD8^{+} TILs can counteract the effect of TIGIT blockade.

CD155 is the shared ligand for TIGIT and CD226. We found that CD155 is abundant on antigen presenting cells (cDC and monocytes) and present on HCC tumor and TFL tissues. We also found that the CD155 protein level was upregulated in HCC tumors compared to TFL. Duan et al. found that mRNA and protein levels of CD155 were higher in HCC cancer tissues than those in adjacent tumor-free tissues. The expression of CD155 gradually decreased as differentiation increased[48]. Sun et al. showed that higher intratumoral CD155 expression is correlated to a poorer prognosis of HCC patients[49]. The high expression of CD155 can contribute to the suppression of immune responses if TIGIT/CD226 ratios are elevated in the tumor microenvironment.

Our study has a few limitations: (1) checkpoint therapy is currently used to treat advanced HCC patients. However, the HCC cohort in this study is a representative cohort for resectable/early stage HCC patients in western countries; (2) considering

116

the predominant expression of TIGIT and increased TIGIT/CD226 ratios on tumor-infiltrating Treg, Treg may be involved in the observed effects of co-blockade. Although, after depletion of $CD4^+CD25^+$ Treg by magnetic sorting, combination treatment still enhanced $CD8^+$ TIL proliferation and IFN-γ production (data not shown), suggesting that T cells (non-Treg) are direct targets for co-blockade, further research is needed to unravel the role of TIGIT on Treg functions in HCC in more detail.

In summary, we conclude that TIGIT is enriched in PD1^{high} CD8$^+$ TILs and this subset represents the most dysfunctional and exhausted CD8$^+$ TIL fraction. Unlike TIM3 and LAG3, TIGIT is also expressed on the PD1^{int} CD8$^+$ subset which co-expresses CD226 and is prominent in tumors of HCC patients that do not have CD8$^+$PD1^{high} TILs. CD8$^+$ TILs of these patients preferentially respond *ex vivo* to dual TIGIT/PD1 blockade. Compared to single PD1 blockade, co-blockade of TIGIT/PD1 improved CD8$^+$ TIL cytotoxicity and converted CD8$^+$ TILs that *ex vivo* did not respond to PD1 blockade to responders. Therefore co-blocking TIGIT and PD1 could be a promising immune therapeutic strategy for HCC patients. The clinical proof of efficacy remains to be demonstrated and this will be the next challenge in future studies.

References

1.   Bray F, Ferlay J, Soerjomataram I, Siegel RL, Torre LA, Jemal A. Global cancer statistics 2018: GLOBOCAN estimates of incidence and mortality worldwide for 36 cancers in 185 countries. CA Cancer J Clin 2018;68:394-424.
2.   El-Serag HB, Marrero JA, Rudolph L, Reddy KR. Diagnosis and treatment of hepatocellular carcinoma. Gastroenterology 2008;134:1752-63.
3.   El-Khoueiry AB, Sangro B, Yau T, Crocenzi TS, Kudo M, Hsu C, Kim T-Y, Choo S-P, Trojan J, Welling TH, Meyer T, Kang Y-K, Yeo W, Chopra A, Anderson J, dela Cruz C, Lang L, Neely J, Tang H, Dastani HB, Melero I. Nivolumab in patients with advanced hepatocellular carcinoma (CheckMate 040): an open-label, non-comparative, phase 1/2 dose escalation and expansion trial. The Lancet 2017;389:2492-2502.
4.   Zhu AX, Finn RS, Edeline J, Cattan S, Ogasawara S, Palmer D, Verslype C, Zagonel V, Fartoux L, Vogel A, Sarker D, Verset G, Chan SL, Knox J, Daniele B, Webber AL, Ebbinghaus SW, Ma J, Siegel AB, Cheng AL, Kudo M, investigators K-. Pembrolizumab in patients with advanced hepatocellular carcinoma previously treated with sorafenib (KEYNOTE-224): a non-randomised, open-label phase 2 trial. Lancet Oncol 2018;19:940-952.
5.   Finn RS, Ryoo BY, Merle P, Kudo M, Bouattour M, Lim HY, Breder V, Edeline J, Chao Y, Ogasawara S, Yau T, Garrido M, Chan SL, Knox J, Daniele B, Ebbinghaus SW, Chen E, Siegel AB, Zhu AX, Cheng AL, investigators K-. Pembrolizumab As Second-Line Therapy in Patients With Advanced Hepatocellular Carcinoma in KEYNOTE-240: A Randomized, Double-Blind, Phase III Trial. J Clin Oncol 2020;38:193-202.
6.   Boutros C, Tarhini A, Routier E, Lambotte O, Ladurie FL, Carbonnel F, Izzeddine H, Marabelle A, Champiat S, Berdelou A. Safety profiles of anti-CTLA-4 and anti-PD-1 antibodies alone and in combination. Nature reviews Clinical oncology 2016;13:473.
7.   Larkin J, Chiarion-Sileni V, Gonzalez R, Grob JJ, Cowey CL, Lao CD, Schadendorf D, Dummer R, Smylie M, Rutkowski P. Combined nivolumab and ipilimumab or monotherapy in untreated melanoma. New England journal of medicine 2015;373:23-34.
8.   Hellmann MD, Paz-Ares L, Bernabe Caro R, Zurawski B, Kim S-W, Carcereny Costa E, Park K, Alexandru A, Lupinacci L, de la Mora Jimenez E, Sakai H, Albert I, Vergnenegre A, Peters S, Syrigos K, Barlesi F, Reck M, Borghaei H, Brahmer JR, O'Byrne KJ, Geese WJ, Bhagavatheeswaran P, Rabindran SK, Kasinathan RS, Nathan FE, Ramalingam SS. Nivolumab plus Ipilimumab in Advanced Non-Small-Cell Lung Cancer. The New England journal of medicine 2019;381:2020-2031.
9.   Kim JE, Patel MA, Mangraviti A, Kim ES, Theodros D, Velarde E, Liu A, Sankey EW, Tam A, Xu H, Mathios D, Jackson CM, Harris-Bookman S, Garzon-Muvdi T, Sheu M, Martin AM, Tyler BM, Tran PT, Ye X, Olivi A, Taube JM, Burger PC, Drake CG, Brem H, Pardoll DM, Lim M. Combination Therapy with Anti-PD-1, Anti-TIM-3, and Focal Radiation Results in Regression of Murine Gliomas. Clinical Cancer Research 2017;23:124.
10.   Sakuishi K, Apetoh L, Sullivan JM, Blazar BR, Kuchroo VK, Anderson AC. Targeting Tim-3 and PD-1 pathways to reverse T cell exhaustion and restore anti-tumor immunity. Journal of Experimental Medicine 2010;207:2187-2194.
11.   Zhou G, Sprengers D, Boor PPC, Doukas M, Schutz H, Mancham S, Pedroza-Gonzalez A, Polak WG, de Jonge J, Gaspersz M, Dong H, Thielemans K, Pan Q, JNM IJ, Bruno MJ, Kwekkeboom J. Antibodies Against Immune Checkpoint Molecules Restore Functions of Tumor-Infiltrating T Cells in Hepatocellular Carcinomas. Gastroenterology 2017;153:1107-1119 e10.
12.   Yu X, Harden K, Gonzalez LC, Francesco M, Chiang E, Irving B, Tom I, Ivelja S, Refino CJ, Clark H, Eaton D, Grogan JL. The surface protein TIGIT suppresses T cell activation by promoting the generation of mature immunoregulatory dendritic cells. Nat Immunol 2009;10:48-57.
13.   Stanietsky N, Simic H, Arapovic J, Toporik A, Levy O, Novik A, Levine Z, Beiman M, Dassa L, Achdout H, Stern-Ginossar N, Tsukerman P, Jonjic S, Mandelboim O. The interaction of TIGIT with PVR and PVRL2 inhibits human NK cell cytotoxicity. Proc Natl Acad Sci U S A 2009;106:17858-63.

14. Levin SD, Taft DW, Brandt CS, Bucher C, Howard ED, Chadwick EM, Johnston J, Hammond A, Bontadelli K, Ardourel D, Hebb L, Wolf A, Bukowski TR, Rixon MW, Kuijper JL, Ostrander CD, West JW, Bilsborough J, Fox B, Gao Z, Xu W, Ramsdell F, Blazar BR, Lewis KE. Vstm3 is a member of the CD28 family and an important modulator of T-cell function. Eur J Immunol 2011;41:902-15.
15. Boles KS, Vermi W, Facchetti F, Fuchs A, Wilson TJ, Diacovo TG, Cella M, Colonna M. A novel molecular interaction for the adhesion of follicular CD4 T cells to follicular DC. Eur J Immunol 2009;39:695-703.
16. Fuchs A, Cella M, Giurisato E, Shaw AS, Colonna M. Cutting Edge: CD96 (Tactile) Promotes NK Cell-Target Cell Adhesion by Interacting with the Poliovirus Receptor (CD155). The Journal of Immunology 2004;172:3994.
17. Sakisaka T, Takai Y. Biology and pathology of nectins and nectin-like molecules. Curr Opin Cell Biol 2004;16:513-21.
18. Joller N, Hafler JP, Brynedal B, Kassam N, Spoerl S, Levin SD, Sharpe AH, Kuchroo VK. Cutting edge: TIGIT has T cell-intrinsic inhibitory functions. J Immunol 2011;186:1338-42.
19. Lozano E, Dominguez-Villar M, Kuchroo V, Hafler DA. The TIGIT/CD226 axis regulates human T cell function. The Journal of Immunology 2012;188:3869-3875.
20. Johnston RJ, Comps-Agrar L, Hackney J, Yu X, Huseni M, Yang Y, Park S, Javinal V, Chiu H, Irving B, Eaton DL, Grogan JL. The immunoreceptor TIGIT regulates antitumor and antiviral CD8(+) T cell effector function. Cancer Cell 2014;26:923-937.
21. Josefsson SE, Huse K, Kolstad A, Beiske K, Pende D, Steen CB, Inderberg EM, Lingjærde OC, Østenstad B, Smeland EB, Levy R, Irish JM, Myklebust JH. T Cells Expressing Checkpoint Receptor TIGIT Are Enriched in Follicular Lymphoma Tumors and Characterized by Reversible Suppression of T-cell Receptor Signaling. Clinical cancer research : an official journal of the American Association for Cancer Research 2018;24:870-881.
22. Josefsson SE, Beiske K, Blaker YN, Førsund MS, Holte H, Østenstad B, Kimby E, Köksal H, Wälchli S, Bai B, Smeland EB, Levy R, Kolstad A, Huse K, Myklebust JH. TIGIT and PD-1 Mark Intratumoral T Cells with Reduced Effector Function in B-cell Non-Hodgkin Lymphoma. Cancer immunology research 2019;7:355-362.
23. Chauvin JM, Pagliano O, Fourcade J, Sun Z, Wang H, Sander C, Kirkwood JM, Chen TH, Maurer M, Korman AJ, Zarour HM. TIGIT and PD-1 impair tumor antigen-specific CD8(+) T cells in melanoma patients. J Clin Invest 2015;125:2046-58.
24. Dixon KO, Schorer M, Nevin J, Etminan Y, Amoozgar Z, Kondo T, Kurtulus S, Kassam N, Sobel RA, Fukumura D, Jain RK, Anderson AC, Kuchroo VK, Joller N. Functional Anti-TIGIT Antibodies Regulate Development of Autoimmunity and Antitumor Immunity. J Immunol 2018;200:3000-3007.
25. Kurtulus S, Sakuishi K, Ngiow SF, Joller N, Tan DJ, Teng MW, Smyth MJ, Kuchroo VK, Anderson AC. TIGIT predominantly regulates the immune response via regulatory T cells. J Clin Invest 2015;125:4053-62.
26. Kim HD, Song GW, Park S, Jung MK, Kim MH, Kang HJ, Yoo C, Yi K, Kim KH, Eo S, Moon DB, Hong SM, Ju YS, Shin EC, Hwang S, Park SH. Association Between Expression Level of PD1 by Tumor-Infiltrating CD8(+) T Cells and Features of Hepatocellular Carcinoma. Gastroenterology 2018;155:1936-1950 e17.
27. Ma J, Zheng B, Goswami S, Meng L, Zhang D, Cao C, Li T, Zhu F, Ma L, Zhang Z, Zhang S, Duan M, Chen Q, Gao Q, Zhang X. PD1(Hi) CD8(+) T cells correlate with exhausted signature and poor clinical outcome in hepatocellular carcinoma. J Immunother Cancer 2019;7:331.
28. Scott AC, Dundar F, Zumbo P, Chandran SS, Klebanoff CA, Shakiba M, Trivedi P, Menocal L, Appleby H, Camara S, Zamarin D, Walther T, Snyder A, Femia MR, Comen EA, Wen HY, Hellmann MD, Anandasabapathy N, Liu Y, Altorki NK, Lauer P, Levy O, Glickman MS, Kaye J, Betel D, Philip M, Schietinger A. TOX is a critical regulator of tumour-specific T cell differentiation. Nature 2019;571:270-274.
29. Alfei F, Kanev K, Hofmann M, Wu M, Ghoneim HE, Roelli P, Utzschneider DT, von Hoesslin M, Cullen JG, Fan Y, Eisenberg V, Wohlleber D, Steiger K, Merkler D, Delorenzi M, Knolle PA, Cohen CJ, Thimme R, Youngblood B, Zehn D. TOX reinforces the phenotype and longevity of exhausted T cells in chronic viral infection. Nature 2019;571:265-269.

30. Khan O, Giles JR, McDonald S, Manne S, Ngiow SF, Patel KP, Werner MT, Huang AC, Alexander KA, Wu JE, Attanasio J, Yan P, George SM, Bengsch B, Staupe RP, Donahue G, Xu W, Amaravadi RK, Xu X, Karakousis GC, Mitchell TC, Schuchter LM, Kaye J, Berger SL, Wherry EJ. TOX transcriptionally and epigenetically programs CD8(+) T cell exhaustion. Nature 2019;571:211-218.

31. Siddiqui I, Schaeuble K, Chennupati V, Fuertes Marraco SA, Calderon-Copete S, Pais Ferreira D, Carmona SJ, Scarpellino L, Gfeller D, Pradervand S, Luther SA, Speiser DE, Held W. Intratumoral Tcf1(+)PD-1(+)CD8(+) T Cells with Stem-like Properties Promote Tumor Control in Response to Vaccination and Checkpoint Blockade Immunotherapy. Immunity 2019;50:195-211.e10.

32. Chen Z, Ji Z, Ngiow SF, Manne S, Cai Z, Huang AC, Johnson J, Staupe RP, Bengsch B, Xu C, Yu S, Kurachi M, Herati RS, Vella LA, Baxter AE, Wu JE, Khan O, Beltra J-C, Giles JR, Stelekati E, McLane LM, Lau CW, Yang X, Berger SL, Vahedi G, Ji H, Wherry EJ. TCF-1-Centered Transcriptional Network Drives an Effector versus Exhausted CD8 T Cell-Fate Decision. Immunity 2019;51:840-855.e5.

33. Im SJ, Hashimoto M, Gerner MY, Lee J, Kissick HT, Burger MC, Shan Q, Hale JS, Lee J, Nasti TH, Sharpe AH, Freeman GJ, Germain RN, Nakaya HI, Xue HH, Ahmed R. Defining CD8+ T cells that provide the proliferative burst after PD-1 therapy. Nature 2016;537:417-421.

34. Duhen T, Duhen R, Montler R, Moses J, Moudgil T, de Miranda NF, Goodall CP, Blair TC, Fox BA, McDermott JE, Chang S-C, Grunkemeier G, Leidner R, Bell RB, Weinberg AD. Co-expression of CD39 and CD103 identifies tumor-reactive CD8 T cells in human solid tumors. Nature Communications 2018;9:2724.

35. Sideras K, Biermann K, Verheij J, Takkenberg BR, Mancham S, Hansen BE, Schutz HM, de Man RA, Sprengers D, Buschow SI, Verseput MC, Boor PP, Pan Q, van Gulik TM, Terkivatan T, Ijzermans JN, Beuers UH, Sleijfer S, Bruno MJ, Kwekkeboom J. PD-L1, Galectin-9 and CD8(+) tumor-infiltrating lymphocytes are associated with survival in hepatocellular carcinoma. Oncoimmunology 2017;6:e1273309.

36. Sideras K, Bots SJ, Biermann K, Sprengers D, Polak WG, JN IJ, de Man RA, Pan Q, Sleijfer S, Bruno MJ, Kwekkeboom J. Tumour antigen expression in hepatocellular carcinoma in a low-endemic western area. Br J Cancer 2015;112:1911-20.

37. Joller N, Lozano E, Burkett PR, Patel B, Xiao S, Zhu C, Xia J, Tan TG, Sefik E, Yajnik V, Sharpe AH, Quintana FJ, Mathis D, Benoist C, Hafler DA, Kuchroo VK. Treg cells expressing the coinhibitory molecule TIGIT selectively inhibit proinflammatory Th1 and Th17 cell responses. Immunity 2014;40:569-81.

38. Wang X, He Q, Shen H, Xia A, Tian W, Yu W, Sun B. TOX promotes the exhaustion of antitumor CD8+ T cells by preventing PD1 degradation in hepatocellular carcinoma. Journal of Hepatology 2019;71:731-741.

39. Liu X, Li M, Wang X, Dang Z, Jiang Y, Wang X, Kong Y, Yang Z. PD-1(+) TIGIT(+) CD8(+) T cells are associated with pathogenesis and progression of patients with hepatitis B virus-related hepatocellular carcinoma. Cancer Immunol Immunother 2019;68:2041-2054.

40. Kim CG, Jang M, Kim Y, Leem G, Kim KH, Lee H, Kim T-S, Choi SJ, Kim H-D, Han JW, Kwon M, Kim JH, Lee AJ, Nam SK, Bae S-J, Lee SB, Shin SJ, Park SH, Ahn JB, Jung I, Lee KY, Park S-H, Kim H, Min BS, Shin E-C. VEGF-A drives TOX-dependent T cell exhaustion in anti–PD-1–resistant microsatellite stable colorectal cancers. Science Immunology 2019;4:eaay0555.

41. Ramsbottom KM, Hawkins ED, Shimoni R, McGrath M, Chan CJ, Russell SM, Smyth MJ, Oliaro J. Cutting edge: DNAX accessory molecule 1-deficient CD8+ T cells display immunological synapse defects that impair antitumor immunity. Journal of immunology (Baltimore, Md : 1950) 2014;192:553-557.

42. Duan X, Liu J, Cui J, Ma B, Zhou Q, Yang X, Lu Z, Du Y, Su C. Expression of TIGIT/CD155 and correlations with clinical pathological features in human hepatocellular carcinoma. Molecular medicine reports 2019;20:3773-3781.

43. Sun H, Huang Q, Huang M, Wen H, Lin R, Zheng M, Qu K, Li K, Wei H, Xiao W, Sun R, Tian Z, Sun C. Human CD96 Correlates to Natural Killer Cell Exhaustion and Predicts the Prognosis of Human Hepatocellular Carcinoma. Hepatology 2019;70:168-183.

44. Pedroza-Gonzalez A, Verhoef C, Ijzermans JN, Peppelenbosch MP, Kwekkeboom J, Verheij J, Janssen HL, Sprengers D. Activated tumor-infiltrating CD4+ regulatory T cells restrain antitumor immunity in patients with primary or metastatic liver cancer. Hepatology 2013;57:183-94.

45. Inozume T, Yaguchi T, Furuta J, Harada K, Kawakami Y, Shimada S. Melanoma Cells Control Antimelanoma CTL Responses via Interaction between TIGIT and CD155 in the Effector Phase. Journal of Investigative Dermatology 2016;136:255-263.

46. Wang C, Thudium KB, Han M, Wang XT, Huang H, Feingersh D, Garcia C, Wu Y, Kuhne M, Srinivasan M, Singh S, Wong S, Garner N, Leblanc H, Bunch RT, Blanset D, Selby MJ, Korman AJ. In vitro characterization of the anti-PD-1 antibody nivolumab, BMS-936558, and in vivo toxicology in non-human primates. Cancer Immunol Res 2014;2:846-56.

47. Ayano M, Tsukamoto H, Kohno K, Ueda N, Tanaka A, Mitoma H, Akahoshi M, Arinobu Y, Niiro H, Horiuchi T, Akashi K. Increased CD226 Expression on CD8^{+} T Cells Is Associated with Upregulated Cytokine Production and Endothelial Cell Injury in Patients with Systemic Sclerosis. The Journal of Immunology 2015;195:892.

48. Boerman GH, van Ostaijen-ten Dam MM, Kraal KC, Santos SJ, Ball LM, Lankester AC, Schilham MW, Egeler RM, van Tol MJ. Role of NKG2D, DNAM-1 and natural cytotoxicity receptors in cytotoxicity toward rhabdomyosarcoma cell lines mediated by resting and IL-15-activated human natural killer cells. Cancer Immunol Immunother 2015;64:573-83.

49. van Beek AA, Zhou G, Doukas M, Boor PPC, Noordam L, Mancham S, Campos Carrascosa L, van der Heide-Mulder M, Polak WG, Ijzermans JNM, Pan Q, Heirman C, Mahne A, Bucktrout SL, Bruno MJ, Sprengers D, Kwekkeboom J. GITR ligation enhances functionality of tumor-infiltrating T cells in hepatocellular carcinoma. International journal of cancer 2019;145:1111-1124.

Supplemental data for:

TIGIT and PD-1 co-blockade restores ex vivo functions of human tumor-infiltrating CD8+ T cells in hepatocellular carcinoma

Table of contents

Supplemental materials and methods

Immunohistochemistry (IHC)

The construction of tissue microarrays (TMA) of tumor and tumor-free liver tissues has been described previously [1,2]. The TMAs were then immunohistochemically stained by the department of pathology of Erasmus MC, using rabbit anti-human monoclonal Ab CD155 (clone D3G7H, rabbit IgG, 1:400, Cell signaling), which is the clone recommended by Chandramohan et al. [3]. IHC was performed with an automated, validated and accredited staining system (Ventana Benchmark ULTRA, Ventana Medical Systems, Tucsen, AZ, USA) using Optiview universal DAB detection Kit (#760-700). In brief, following deparaffinization and heat-induced antigen retrieval the tissue samples were incubated according to their optimized time with CD155. Incubation was followed by hematoxylin II counter stain for 12 minutes and then a blue coloring reagent for 8 minutes according to the manufactures instructions (Ventana). The immunohistochemically stained TMAs were then scanned using NanoZoomer 2.0HT (Hamamatsu) and scored blindly by two researchers, based on the intensity of staining (0[none],1[low], 2[intermediate], 3[strong]) and the frequency of positive tumor cells or hepatocytes (A[<10%], B[10-50%], C[50-90%], D[>90%]). The score per core was calculated by multiplying the intensity by the frequency of positive cells (A=0.1, B=0.3, C=0.7 and D=1), and then the average score per tissue was calculated by taking the average of the three scores.

Flow cytometry analysis

PBMCs and MNCs isolated from TFL or tumor were analyzed for expression of surface and intracellular markers using the following anti-human antibodies: anti-TIGIT, anti-CD226, anti-PD1, anti-CD155, anti-perforin, anti-granzyme B, anti-CD8, anti-CD4, anti-CD56, anti-CD45, anti-TIM3, anti-LAG3, anti-TOX, anti-Ki67 and anti-TCF1 etc. (See supplemental table 1 for more antibody information). Viability of cells was assessed using Aqua LIVE/DEAD dye (Thermo Fisher Scientific). Fixation and permeabilization were performed using the Fixation/Permeabilization kit (eBioscience). For intracellular cytokine staining, cells were treated with 40 ng/mL PMA (Sigma, Zwijndrecht, the Netherlands) and 1μg/mL ionomycin (Sigma) at 37°C for 5 hours in the presence of GolgiStop at 1:1500 dilution (BD Biosciences), followed by staining of

IFN-γ and TNF-α on fixed cells. Cells were analyzed using FACSCanto II and Fortessa flow cytometers (BD Biosciences, San Diego, CA).

PMA/Ionomycin restimulation assay

TILs were stimulated with phorbol 12-myristate 13-acetate (PMA) and ionomycin to assess effector cytokine production. Golgistop (containing monensin) was added (1:1500 dilution, BD Biosciences). After exposure to PMA and ionomycin for 5 hours, intracellular interferon (IFN)-γ and tumor necrosis factor (TNF)-α were measured by flow cytometry.

Flow sorting

Frozen TILs were thawed and stained with anti-CD45-APC (clone HI30), anti-CD8-FITC (clone RPA-T8) and anti-PD1-PE (clone MIH4) antibodies. Dead cells were excluded by 7-AAD staining. PD1^{high} CD8$^+$ and PD1^{int} plus PD1$^-$ CD8$^+$ TILs were sorted separately into two FACS tubes. In addition, CD45$^+$CD8$^-$ leukocytes from TILs were sorted. Cells were sorted using Aria II sorter (BD Biosciences, San Diego, CA).

References

1. Sideras K, Bots SJ, Biermann K, et al. Tumour antigen expression in hepatocellular carcinoma in a low-endemic western area. Br J Cancer 2015;112:1911-20.
2. Sideras K, Biermann K, Verheij J, et al. PD-L1, Galectin-9 and CD8(+) tumor-infiltrating lymphocytes are associated with survival in hepatocellular carcinoma. Oncoimmunology 2017;6:e1273309.
3. Chandramohan V, Bryant JD, Piao H, et al. Validation of an Immunohistochemistry Assay for Detection of CD155, the Poliovirus Receptor, in Malignant Gliomas. Archives of pathology & laboratory medicine 2017;141:1697-1704.

Supplemental Table 1. Anti-human Antibodies Used in Flow Cytometry (FACS)

| Antibody	Clone	Supplier	Antibody	Clone	Supplier
TIGIT-PE	MBSA43	eBioscience	FOXP3-eFluor450	236A/E7	eBioscience
TIGIT-efluor450	MBSA43	eBioscience	Perforin-FITC	delta G9	eBioscience
CD226-APC	11A8	Biolegend	GranzymeB-V450	GB11	BD Biosciences
CD155-PE	2H7CD155	eBioscience	CD14-PerCPCy5.5	61D3	eBioscience
PD1-PECy7	J105	eBioscience	BDCA1-APC	AD5-8E7	Miltenyi
PD1-PE	MIH4	eBioscience	CD19-APCH7	SJ25C1	BD Biosciences
CD3-PE	UCHT1	eBioscience	CD45-APC	HI30	Biolegend
CD3-PECy7	UCHT1	eBioscience	CD45-eFluor450	HI30	eBioscience
CD3-PerCPCy5.5	SK7	BD Biosciences	LAG3-PerCPeF710	3DS223H	eBioscience
CD3-APCeFluor780	SK7	eBioscience	TIM3-PECF594	7D3	BD Biosciences
CD3-APCR700	UCHT1	BD Biosciences	IFN-γ-FITC	25723.11	BD Biosciences
CD3-Pacific blue	UCHT1	BD Pharmingen	TNF-α-PerCPCy5.5	Mab11	Biolegend
CD4-PE	13B8.2	Beckman	Ki67-FITC	20Raj1	eBioscience
CD4-APC	OKT4	Biolegend	Ki67-PECy7	20Raj1	eBioscience
CD4-APCeFluor780	OKT4	eBioscience	CD38-FITC	T16	Beckman
CD4-BV605	OKT4	Biolegend	HLA-DR-APC	LN3	eBioscience
CD4-eFluor450	OKT4	eBioscience	CD39-FITC	A1	Biolegend
CD8-PerCPCy5.5	RPA-T8	eBioscience	CD103-PECy7	Ber-ACT8	Biolegend
CD8-FITC	SK1	eBioscience	TOX-APC	REA473	Miltenyi
CD8-FITC	RPA-T8	eBioscience	TCF1-PE	7F11A10	Biolegend
CD8-APC	RPA-T8	Biolegend	hIgG1-APC	REA293	Miltenyi
CD8-eluor450	RPA-T8	eBioscience	mIgG1-PE	P3.6.2.8.1	eBioscience
CD56-FITC	TULY56	eBioscience	mIgG1-PECy7	MOPC-21	Biolegend
CD56-BV510	HCD56	Biolegend	mIgG2b-FITC	27-35	BD Pharmingen
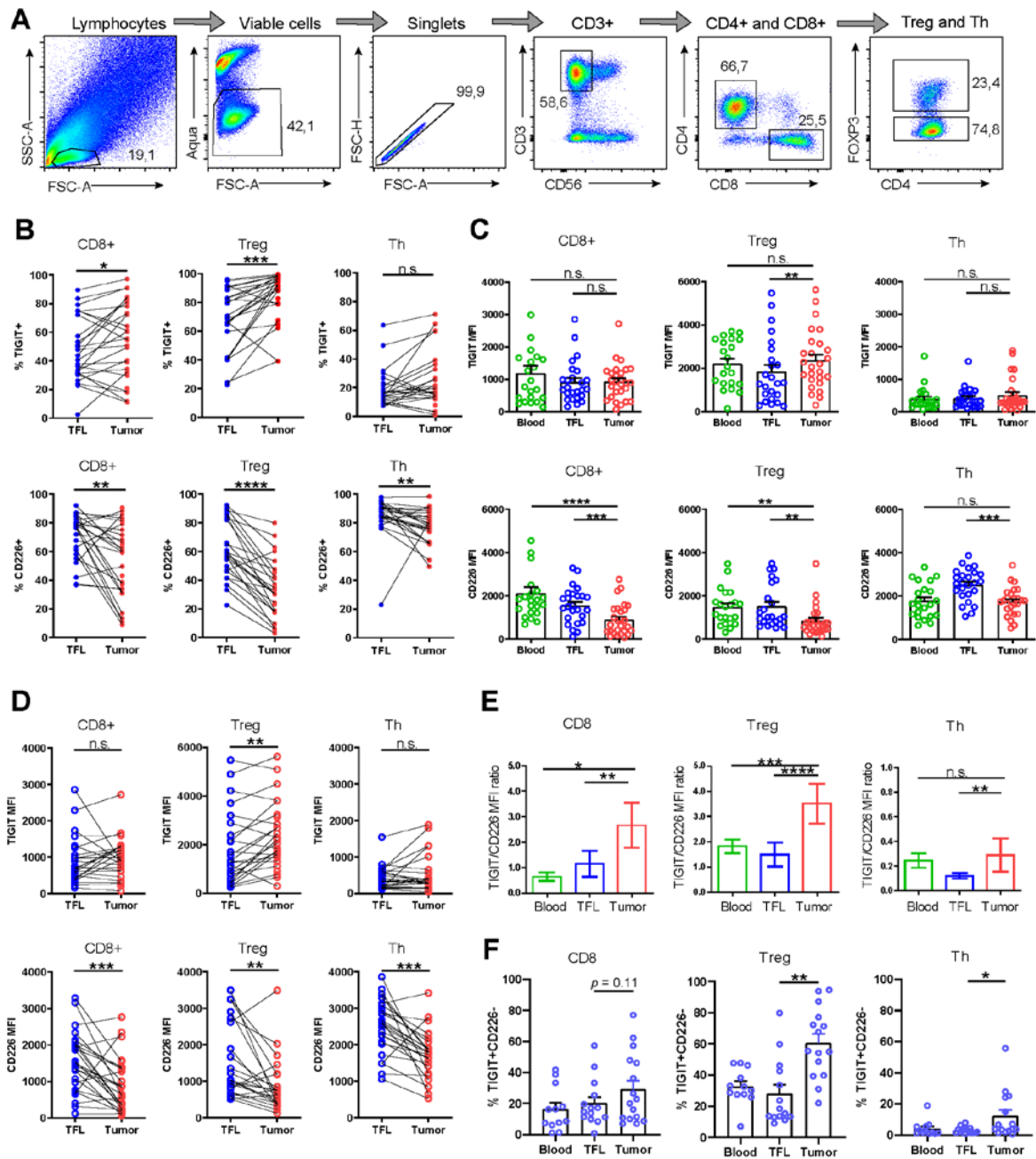
Supplemental Figure 1. (A) Gating strategy of CD8, Treg and Th. (B) The frequencies of TIGIT$^+$ and CD226$^+$ cells in T cell subsets in tumor and TFL of individual patients are shown. (C-D) The MFI of TIGIT and CD226 on CD8$^+$ T, Treg and Th cells in blood, TFL and tumor (n=28). (E) The MFI ratio of TIGIT/CD226 in CD8$^+$ T, Treg and Th cells. (F) The frequency of TIGIT$^+$CD226$^-$ subset in CD8, Treg and Th in blood, TFL and tumor (n=16). *$P < 0.05$, **$P < 0.01$, ***$P < 0.001$. Dots represent individual patients. Bars represent mean ± SEM.
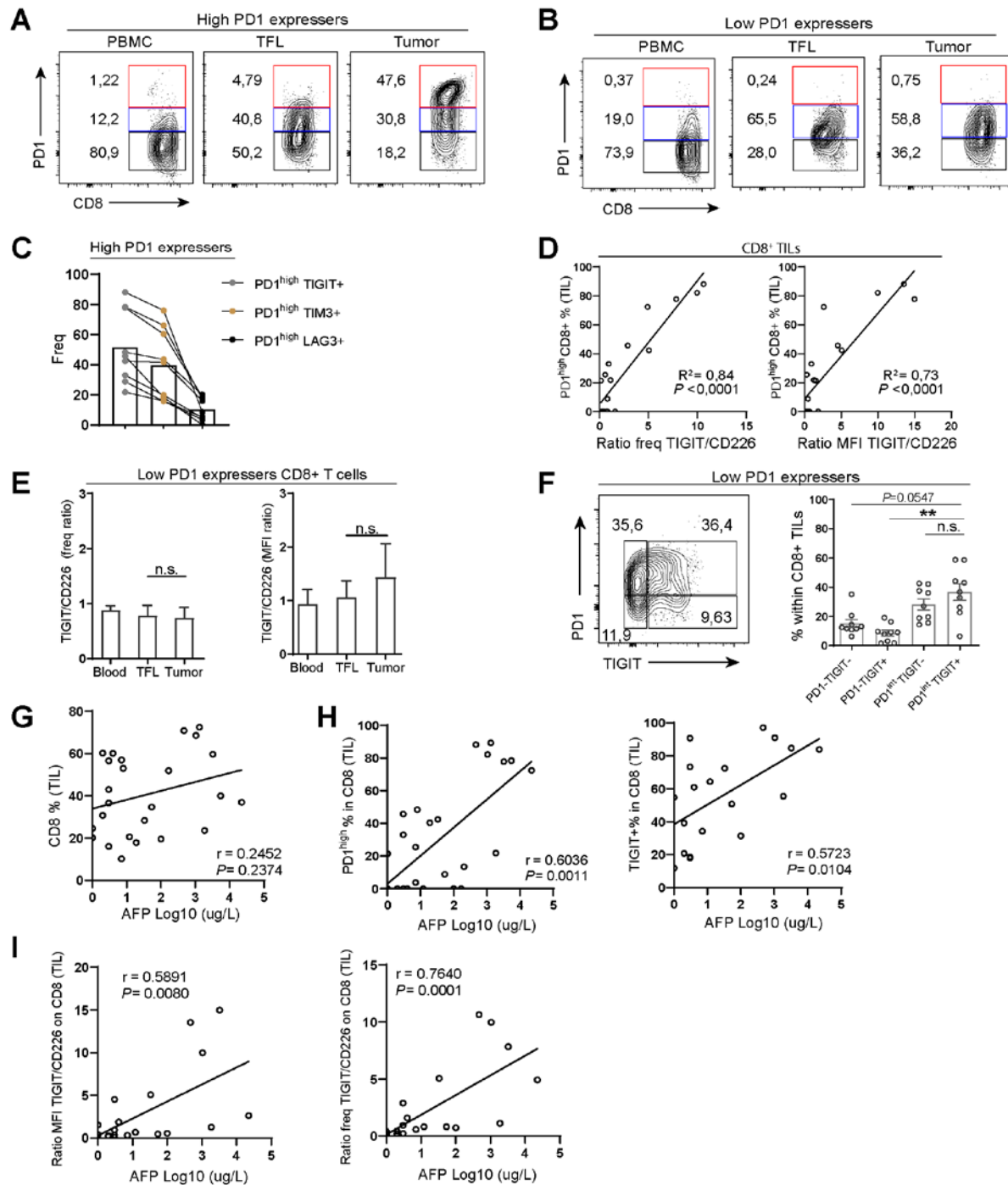
Supplemental Figure 2. (A-B) Gating strategy of PD1^{high}, PD1^{int} and PD1$^-$ in tumor, TFL and blood in High and Low PD1 expressers. (C) Percentages of PD1^{high}TIGIT$^+$, PD1^{high}TIM3$^+$ and PD1^{high}LAG3$^+$ in CD8$^+$ TILs from High PD1 expressers. Bars show means. (D) Correlation of PD1^{high}CD8$^+$ TILs with frequency and MFI ratios of TIGIT/CD226 in CD8$^+$ TILs (n=19). (E) Ratios of TIGIT/CD226 in CD8$^+$ T cells in blood, TFL and tumor from Low PD1 expressers. Bars show mean ± SEM (n=10). (F) Co-expression of TIGIT and PD1 on CD8$^+$ TILs from Low PD1 expressers (n=9). (G) Correlation between CD8$^+$ TIL frequency and serum AFP level from HCC patients. (H) Correlation between PD1^{high}CD8$^+$ TIL frequency and serum AFP level, TIGIT$^+$CD8$^+$ TIL frequency and serum AFP level from HCC patients. (I) Correlation between MFI or frequency ratios of TIGIT/CD226 and serum AFP level from HCC patients. *$P < 0.05$, **$P < 0.01$, ***$P < 0.001$.
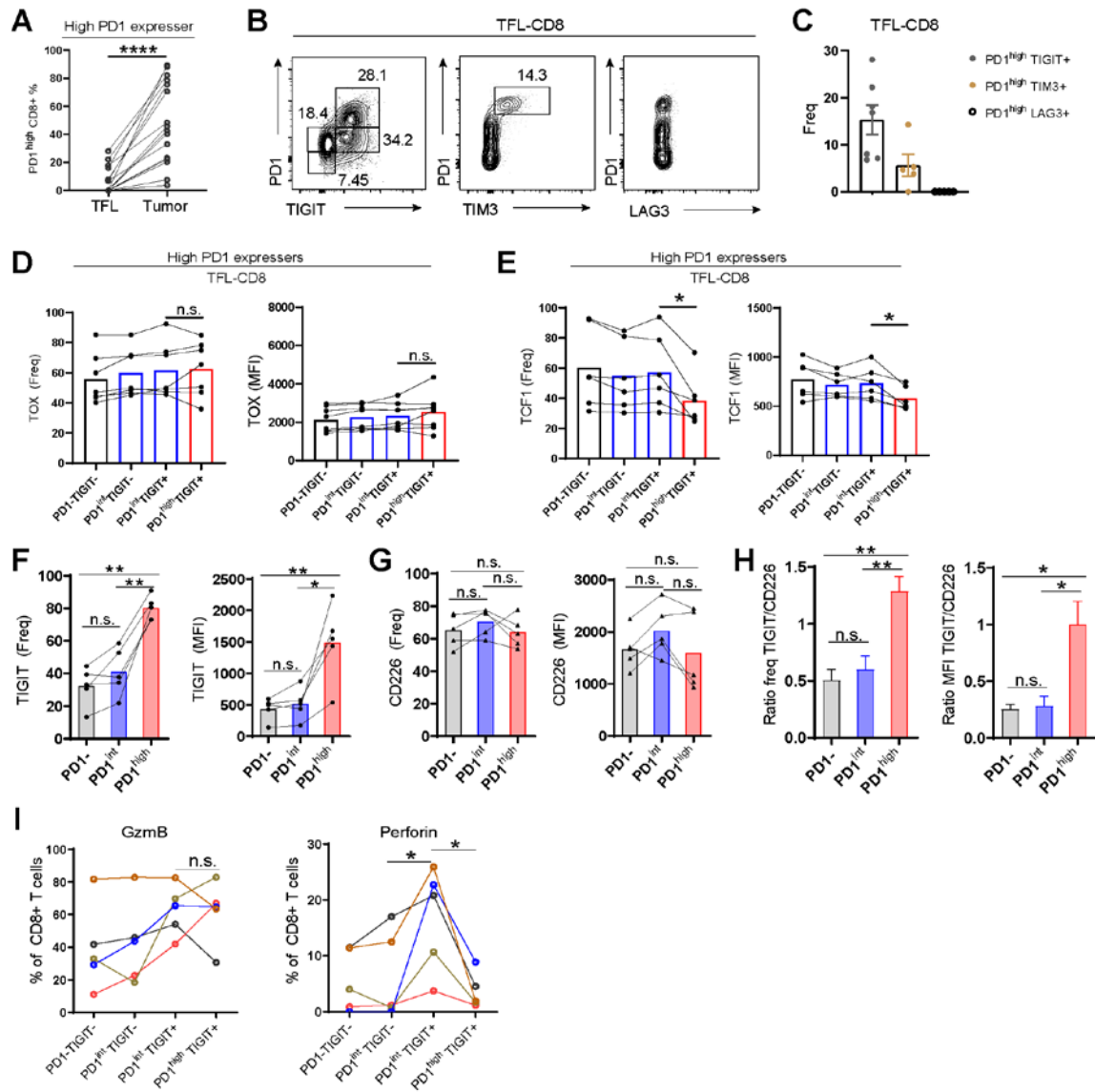
Supplemental Figure 3. (A) Frequencies of PD1^{high} CD8$^+$ T cells in TFL and tumor from High PD1 expressers (n=16). (B) FACS plots show co-expression of PD1 and TIGIT, TIM3, LAG3 on CD8$^+$ T cells in TFL containing PD1^{high} CD8$^+$ T cells. (C) Frequencies of PD1^{high} TIGIT$^+$, PD1^{high} TIM3$^+$ and PD1^{high} LAG3$^+$ within CD8$^+$ T cells in TFL. (D-E) Expression of TOX and TCF1 in four subsets of CD8$^+$ T cells in TFL. (F-G) Expression of TIGIT and CD226 in the PD1$^-$, PD1^{int} and PD1^{high} subsets of CD8$^+$ T cells in TFL (n=5). Dots represent individual patients and bars show mean. (H) Ratios of TIGIT/CD226 in PD1$^-$, PD1^{int} and PD1^{high} subsets of CD8$^+$ T cells in TFL. Bars show mean ± SEM. (I) The percentages of intracellular granzyme B and perforin expression in four subsets of CD8$^+$ T cells in TFL. *$P < 0.05$, **$P < 0.01$.
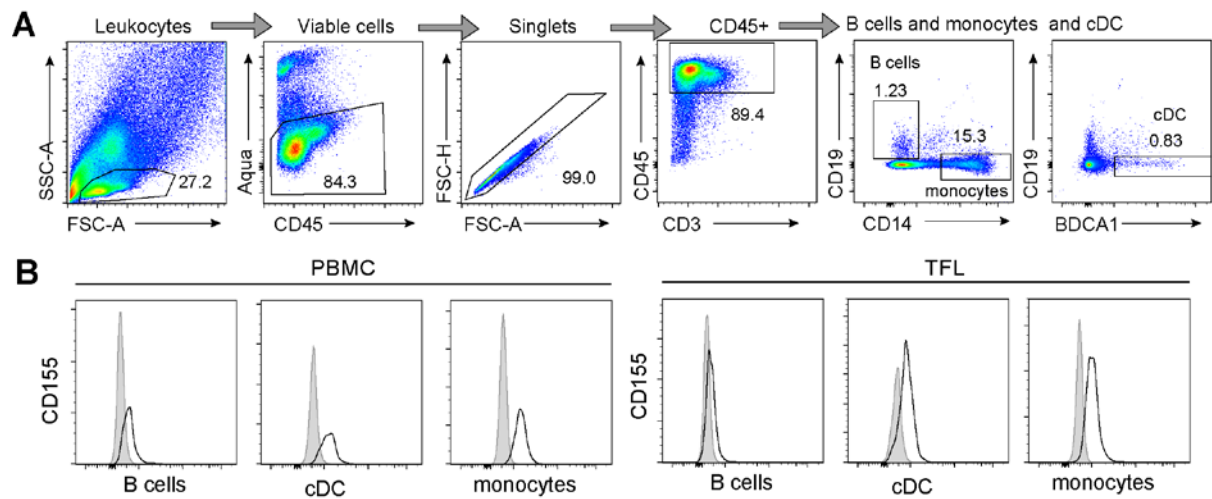
**Supplemental Figure 4.** (A) Gating strategy of CD19$^+$ B cells, CD14$^+$ monocytes and CD19$^-$ BDCA1$^+$ cDC was shown. (B) Representative flow-cytometry plots of CD155 expression on B cells, cDC and monocytes in PBMC and TFL.
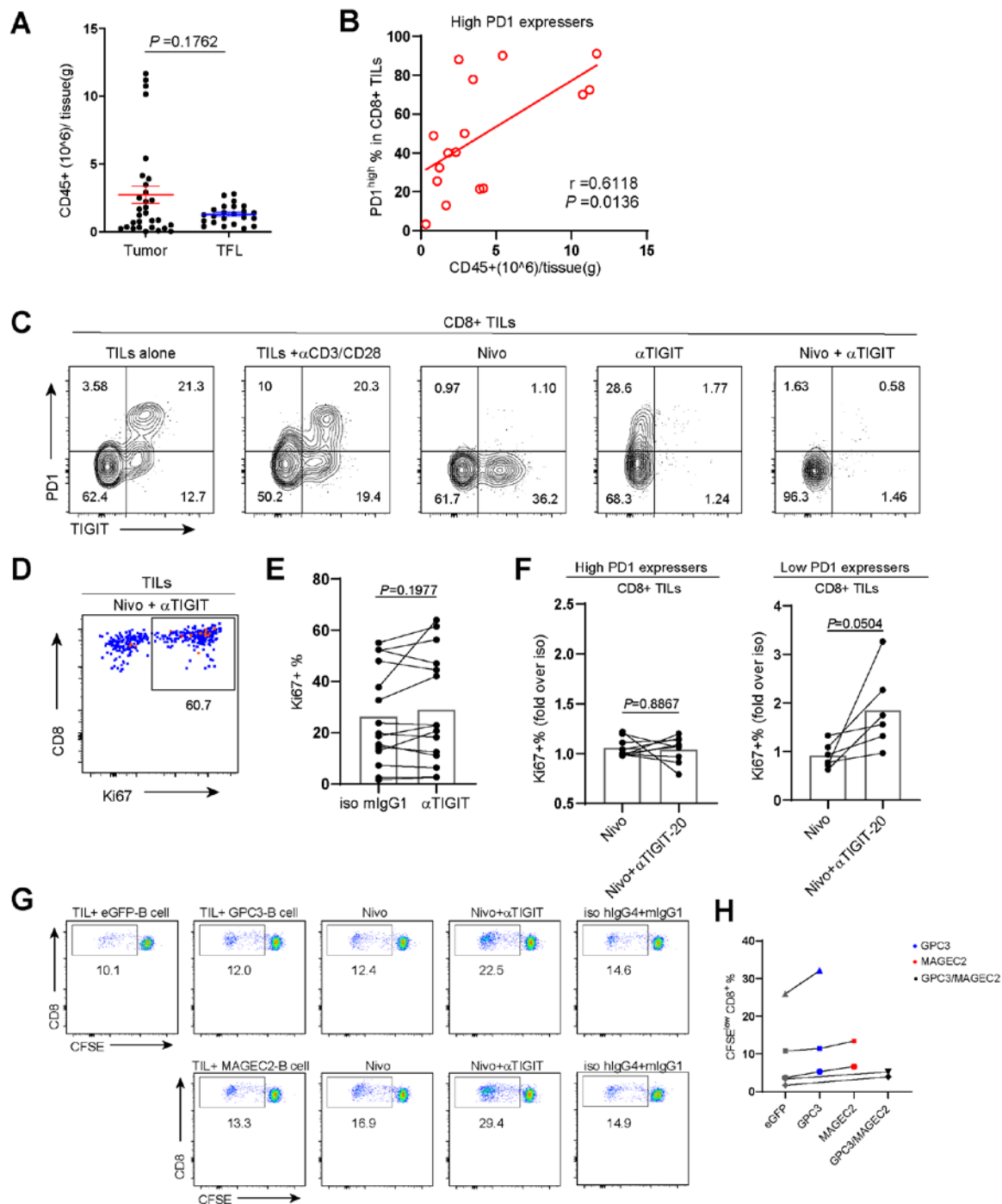
Supplemental Figure 5. (A) The number of CD45$^+$ cells isolated per gram of tissue from tumor and TFL. Dots show individual patients. (B) Correlation of PD1^{high} CD8$^+$ T cells frequency and CD45$^+$ cells per gram of tissue. (C) Flow-cytometry plots show the blockade of TIGIT and PD1 by anti-TIGIT and anti-PD1 antibodies after 4 days in culture. (D) Flow-cytometry plots show the proliferating (Ki67 positive) CD8$^+$ TILs after 4 days of stimulation by CD3/CD28 beads. (E) Effects of mouse anti-human TIGIT mAb (10 µg/ml) on CD8$^+$ TIL proliferation from individual patients upon anti-CD3/CD28 beads stimulation. (F) Effects of nivolumab blockade and combined blockade with mouse anti-human TIGIT mAb on proliferation of CD8$^+$ TILs from individual patients upon anti-CD3/CD28 beads stimulation. Percentages of Ki67 were normalized to cultures to which the corresponding isotype control antibodies had been added. (G) Flow-cytometry plots of CD8$^+$ TIL proliferation in response to MAGEC2, GPC3 or eGFP

mRNA-transfected autologous B-cell blasts in the presence or absence of blocking antibodies. (H) Proliferation (CFSE-low) of CD8^{+} TILs of individual patients in response to eGFP, GPC3 or/and MAGEC2.
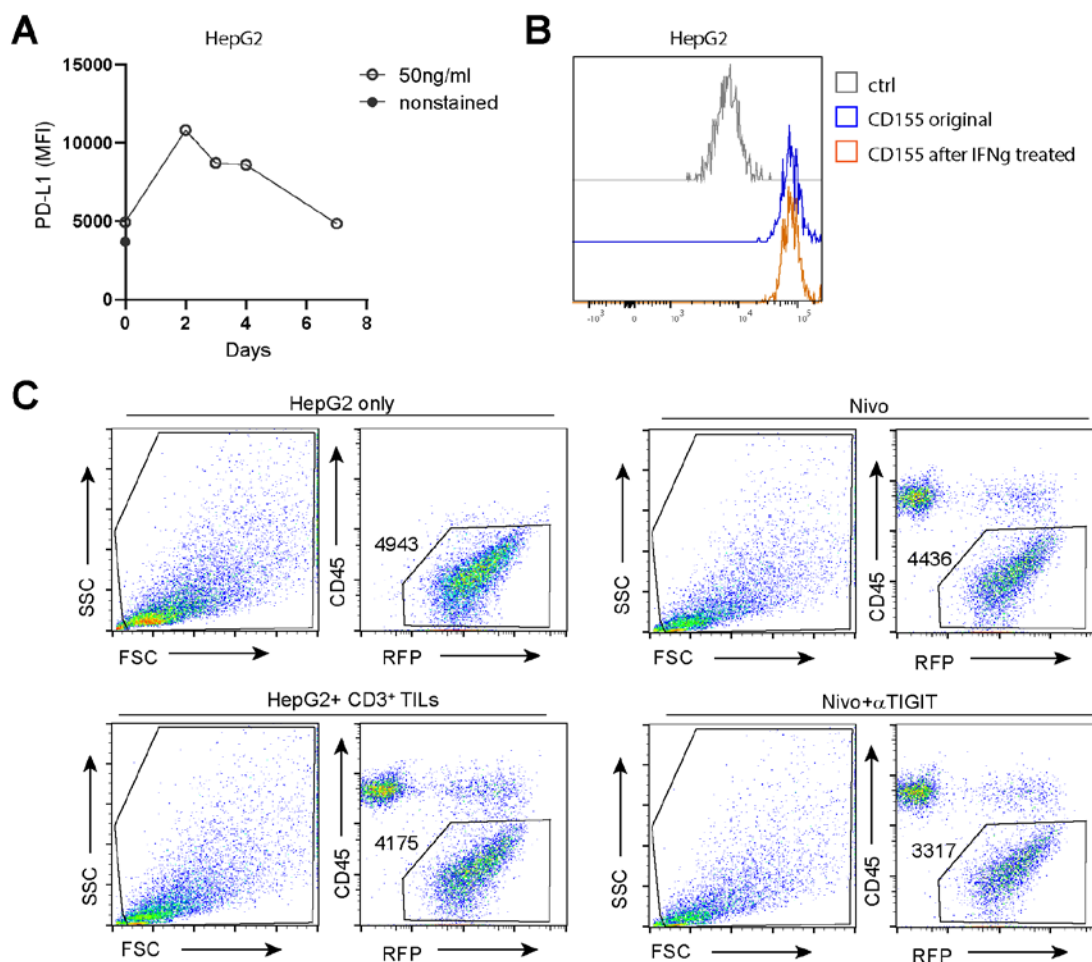
Supplemental Figure 6. (A) PD-L1 expression on HepG2 is shown over time after IFN-γ treatment. (B) Expression of CD155 on HepG2 without or with IFN-γ treatment is shown. (C) Flow cytometry plots of gating on HepG2 cells in *ex vivo* killing assay. Number means HepG2 (CD45^{-}RFP^{+}) absolute count

CHAPTER 6

Expression of cancer testis antigens in tumor-adjacent normal liver predicts post-resection recurrence of Hepatocellular Carcinoma

Lisanne Noordam[1], **Zhouhong Ge**[1], Hadiye Özturk[1], Michail Doukas[2], Shanta Mancham[1], Patrick P.C. Boor[1], Lucia Campos Carrascosa[1], Guoying Zhou[1], Thierry P.P. van den Bosch[2], Qiuwei Pan[1], Jan N.M. IJzermans[3], Marco J. Bruno[1], Dave Sprengers[1], Jaap Kwekkeboom[1]

[1]Department of Gastroenterology and Hepatology, Erasmus MC-University Medical Center, Rotterdam, the Netherlands. [2]Department of Pathology, Erasmus MC-University Medical Center, Rotterdam, the Netherlands. [3]Department of Surgery, Erasmus MC-University Medical Center

Abstract

Background: High recurrence rates after resection of hepatocellular carcinoma (HCC) with curative intent impair clinical outcomes of HCC. Cancer/testis antigens (CTAs) are suitable targets for cancer immunotherapy if selectively expressed in tumor cells. The aims were to identify CTAs that are frequently and selectively expressed in HCC-tumors, and to investigate whether CTAs could serve as biomarker for occult metastasis.

Methods: Tumor and paired TFL tissues of HCC-patients, and healthy tissues were assessed for mRNA expression of 49 CTAs by RT-qPCR and protein expression of 5 CTAs by immunohistochemistry.

Results: Twelve CTA-mRNAs were expressed in ≥10% of HCC-tumors and not in healthy tissues except testis. In tumors, mRNA and protein of ≥ 1 CTA was expressed in 78% and 71% of HCC-patients, respectively. In TFL, CTA mRNA and protein was found in 45% and 30% of HCC-patients, respectively. Interestingly, CTA-expression in TFL was an independent negative prognostic factor for post-resection HCC-recurrence and survival.

Conclusion: We established a panel of 12 testis-restricted CTAs expressed in tumors of most HCC-patients. The increased risk of HCC-recurrence in patients with CTA expression in TFL, suggests that CTA-expressing (pre-)malignant cells may be a source of HCC-recurrence and reflects the relevance of targeting these to prevent HCC-recurrence.

Keywords: liver neoplasms; cancer testis antigens; prognosis; neoplasm recurrence; immunotherapy

Introduction

Liver cancer is the fourth leading cause of cancer related death, with hepatocellular carcinoma (HCC) being the most common subtype.[1] HCC is often diagnosed at advanced stage and these patients can only be offered palliative therapies.[2, 3] However, with the help of intensive monitoring, at-risk-patients can be diagnosed at an early stage and can therefore be treated with curative intent; either by surgical resection or radiofrequency ablation. However, recurrence rates are high and currently no therapies are available to prevent recurrence. Patients experiencing early recurrence likely have occult multifocality at the time of resection, whereas late recurrences are more likely to represent de novo tumors.[4-6] Several clinicopathological factors, such as tumor size and vascular invasion, have been used to predict clinical outcome after surgery, but none have consequences for the management of HCC after surgical treatment.[7] It remains of great importance to identify occult metastasis at the time of resection to allow identification of patients at risk for recurrence, ideally by targetable tumor markers. Once occult micro-metastasis or de novo (pre-)malignant lesions can be characterized, therapeutic approaches targeting these markers may be developed to prevent tumor recurrence.

Cancer testis antigens (CTAs) are expressed in immune-privileged germ cells and are expressed in cancer cells of various histological subtypes.[8] Based on their expression profile in adult healthy tissues, they are classified into testis-restricted, testis/brain-restricted and testis-selective CTAs with the last group having additional expression in somatic tissues.[9] Since testis-restricted CTAs lack expression in healthy adult tissues, and have the potential to induce antitumor immune responses, they are considered ideal targets for cancer immunotherapy.[8, 10] Moreover, as testis-restricted CTAs are not expressed in healthy, tumor-free, tissues, sensitive techniques detecting these CTAs can potentially be used to recognize occult metastasis in surrounding macro- and microscopically tumor-free tissue.

The aims of this study were: 1) To establish a panel of CTAs that are frequently and selectively expressed in tumors of HCC patients; 2) To determine whether these CTAs are expressed in adjacent macroscopically tumor-free liver tissues of HCC-patients and whether they are an indication of occult metastasis, e.g. by being associated with early recurrence and/or worse HCC-specific survival.

Material and methods

This study followed the REMARK (Reporting Recommendations for Tumor Marker Prognostic Studies) guidelines.[11]

HCC patients and tissues

Ethical approval for this study was granted by the Ethics Committee at Erasmus MC, Rotterdam, the Netherlands, waiving the requirement for informed consent. For the discovery and validation cohorts 100 and 89, respectively, archived surgically-resected fresh frozen HCC-tumor and paired tumor-free liver (TFL) tissue samples (obtained at a distance of > 2 cm from the tumors) were collected after surgery or retrieved from the archives of the Department of Pathology, Erasmus Medical Center Rotterdam. For protein expression analysis 76 formalin-fixed paraffin-embedded (FFPE) paired HCC-tumor and TFL tissues were retrieved from the Dutch nationwide pathology archives (PALGA) respectively.

The HCC-patients included in the discovery cohort underwent hepatic resection (n=97 and n=73 for fresh frozen and FFPE samples respectively) or liver transplantation (n=3 for both fresh frozen and FFPE samples) for HCC in our center between February 1995 and September 2017, and diagnosis of HCC was confirmed by pathological examination. The patients included in the validation cohort underwent hepatic resection (n=89) for HCC in our center between December 2008 and August 2019, and diagnosis of HCC was confirmed by pathological examination.

Medical records were reviewed for clinicopathological variables (listed in **Supplementary Table S1**) and date of first recurrence, HCC-specific death and last follow-up. All patients were retrospectively included. Further details of these and other included tissues can be found in the supplementary materials and methods.

Selection of CTAs

A literature search to identify CTAs reported to be expressed in HCC was conducted in PubMed on October 4th, 2018. A summary of this search is provided in **Figure 1A** and the query in the Supplementary data. Papers written in English that described CTA expression in HCC patients and/or HCC cell lines were included. In addition, the CTA

database (http://www.cta.lncc.br/) was consulted to find additional CTAs expressed in HCC and one relevant paper was added.[12]

Quantitative real-time PCR

RNA was isolated from the frozen tissues and RT-qPCR was performed. The sequences, Tm-values and product lengths of the used primers are provided in **Supplementary Table S2**, and detailed methods can be found in the supplementary data file.

Immunohistochemistry

Protein expression was determined by immunohistochemistry (IHC) on tissue microarrays (TMA), that contained three 1 mm cores of each tumor and TFL tissue, as described in the supplementary data file. The stained TMAs were scored blindly by two researchers, based on the intensity of the staining (none, low, intermediate, strong) and the percentage of positive tumor cells or hepatocytes (<10%, 10-50%, 50-90%, >90%). If less than 5 positive cells per core were observed, the core was scored as 0, and cores smaller than 50% of the original surface were excluded. The final scores were the average scores of the three cores.

Statistical analysis

All statistical analyses were performed using Graphpad (Version 8.2.1 for Windows, San Diego, CA) and R Statistical software (Version 3.6.1 for Windows, Foundation for Statistical Computing, Vienna, Austria). The correlation analysis was performed in RStudio with the 'corplot' package, using Pearson's correlation coefficient. For creating heatmaps, RStudio was used with the 'gplots' and 'pheatmap' packages. Survival analysis was performed by the Kaplan-Meier method and the Cox proportional hazards model, using the 'survminer' and 'survival' packages. Time to event was calculated from the day of surgery. Used statistical tests are indicated in the figures. P-values < 0.05 were considered significant.

Results

Selection of 26 CTAs after literature study and exclusion of those expressed in healthy liver

To determine which CTAs are frequently expressed in HCC tumor tissue, a literature study was conducted. Using a query to identify publications on CTAs expressed in HCC tissue, 281 publication records were obtained through the PubMed search and one relevant paper[12] was added. After removal of non-English publications, 270 publications were screened on title and abstract, of which 231 papers were excluded. Full texts were screened of the remaining 39 studies, which all met the inclusion criteria **(Figure 1A)**. In these 39 studies, expression of 73 different CTAs in HCC was reported; mRNA expression of 51, protein expression of 1, and both mRNA and protein expression of 21 CTAs **(Supplementary Table S3)**. In addition, the CTA database (http://www.cta.lncc.br/) was consulted, which resulted in identification of 34 different CTAs expressed in HCC; 27 by mRNA, 4 by protein and 3 by protein and mRNA expression. Furthermore, 38 CTAs identified by the CTA database had already been identified in the literature search **(Figure 1B)**. Consequently, to exclude expression of these 107 CTAs in healthy tissues, studies using next-generation sequencing to quantify mRNA expression levels in samples obtained from a large array of healthy tissues and organs, provided by the FANTOM consortium,[13, 14] Human Protein Atlas (HPA) consortium,[15] and genome-based tissue expression (GTEx) consortium,[16] summarized on www.proteinatlas.org, and the genome-wide analysis of CTA mRNA expression by Hofmann *et al.*[9] were consulted, which led to the exclusion of 47 CTAs expressed in non-germline tissues **(Figure 1B)**.

To verify the absence of expression in healthy adult non-germline tissues, the expression of the remaining 60 CTAs was first determined in 21 healthy livers by RT-qPCR. For 11 CTAs it was not feasible to design specific primers, due to high sequence homology with other genes, and these were excluded. Of the 49 CTAs tested, 23 were expressed in healthy livers, with prevalence rates varying from 14 – 100%, and therefore also excluded from further analysis. Twenty-four CTAs showed undetectable mRNA expression levels in healthy livers. Two CTAs (*MAGEC1* and *RING finger protein 17* [*RNF17*]) were each found to be expressed in 1 out of 21 tested healthy livers (with very low relative expression levels of 0.005 and 0.002 respectively), and

therefore not excluded **(Figure 1C and Supplementary Table S4).** These 26 CTAs were selected for further study.

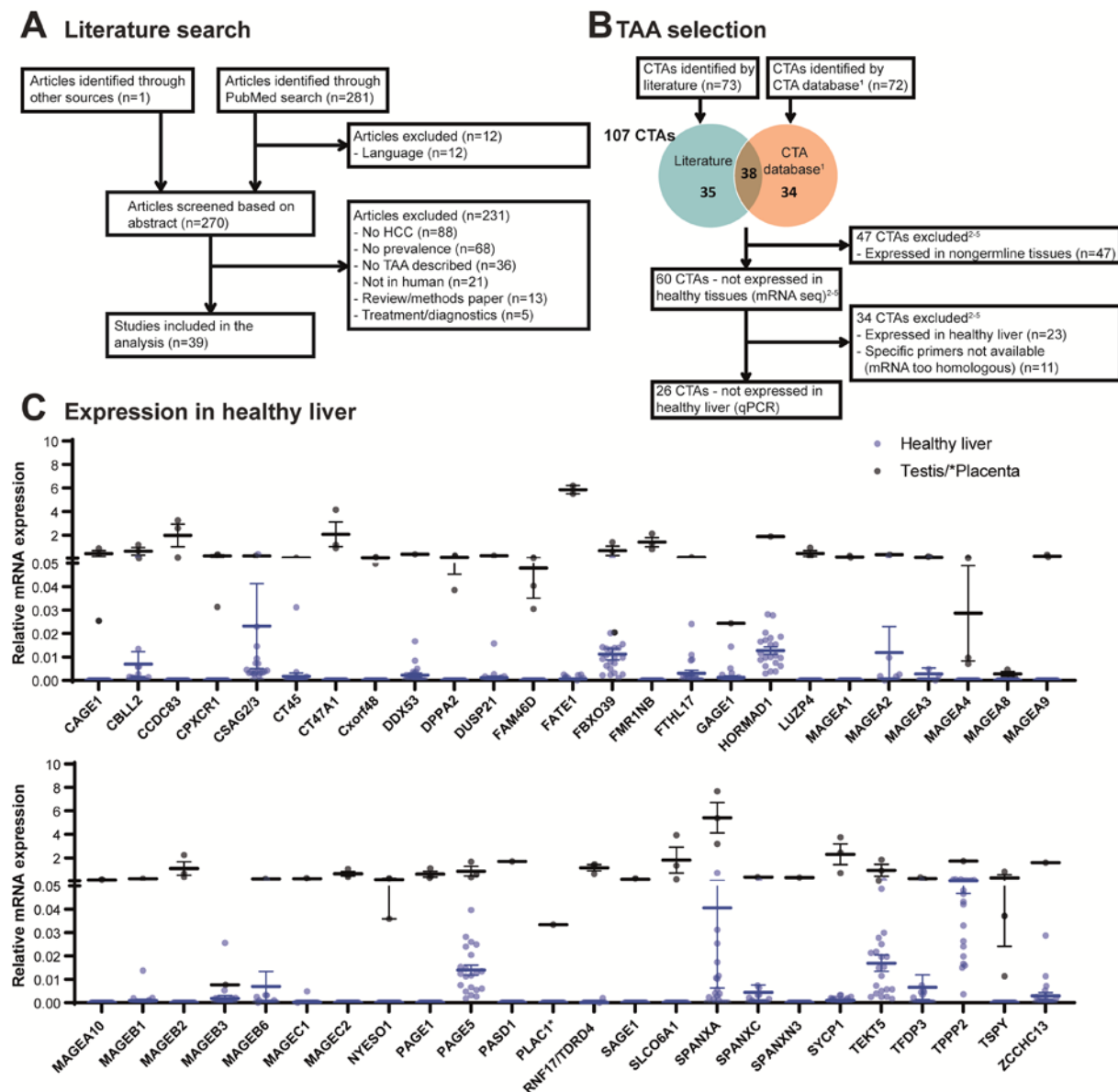**Figure 1. Selection of CTAs. A/B.** Study Flow Diagram. **C.** Relative mRNA expression of selected CTAs in healthy donor livers (n=21) in blue and in the respective positive control tissues in black. Control tissues were: placenta (for PLAC1; n=1) or testis (all other CTAs; n=1-3). [1]http://www.cta.lncc.br/, [2]Hofmann, et al. [3]FANTOM consortium, [4]HPA consortium, [5]GTEx consortium.[254, 259-261]

A panel of 12 CTAs is expressed in more than 10% of HCC tumors and not in healthy tissues

The mRNA expression of these 26 CTAs was determined in 100 paired HCC tumors and TFL and in 35 non-malignant cirrhotic liver tissues. Thirteen CTAs were expressed in tumors of >10% of HCC patients at variable expression levels (**Table 1, Figure 2A and Supplementary Table S5)** and selected for further study. To verify the absence of these 13 CTAs in healthy adult non-germline tissues, and to confirm they are targetable tumor markers, mRNA expression was determined in 23 types of healthy adult tissues other than liver **(Figure 2B)**. Most tissues did not express any CTA, except for ovary which expressed five CTAs. Four CTAs were expressed at very low relative expression levels in ovary (*MAGEB2* 0.002*, cancer/testis antigen family 47 member A1* [*CT47A1*] 0.002, *MAGEC1* 0.003 and *MAGEC2* 0.002). However, *RNF17* had a higher relative expression level (0.097) and was also expressed in other tissues (thyroid, adrenal gland, bladder, brain, throat, trachea, ovary and thymus), and was therefore excluded from further analysis.

Among the 12 remaining CTAs **(Table 1)** were 6 members of the MAGE gene family (*MAGEA1, MAGEA9, MAGEA10, MAGEB2, MAGEC1* and *MAGEC2*). *MAGEA1, MAGEC1* and *MAGEC2* were most frequently expressed, with expression rates between 48% and 59% of the tumors. Other CTAs that were expressed in more than 10% of tumors are *cancer antigen 1* (*CAGE1*; 14%), *CT47A1* (27%), *cancer/testis antigen 1B* (*CTAG1B*;10%), *PAGE family member 1* (*PAGE1*; 18%), *solute carrier organic anion transporter family member 6A1* (*SLCO6A1*; 26%) and *testis-specific Y-encoded protein 1* (*TSPY1*; in 21% of male HCC patients and 0% of female HCC patients, as expected from a gene located on the Y-chromosome).[17]

Thus, based on mRNA expression data, we identified a panel of 12 CTAs prevalently expressed in tumors of HCC-patients, but not in healthy adult tissues except testis. Seventy-eight percent of tumors expressed at least one of these 12 CTAs, 59% expressed at least 2 CTAs, 50% expressed at least 3 CTAs, and 40% expressed 4 or more CTAs (**Figure 2C and Supplementary Figure S1)**.

CTAs are expressed in tumor-free liver tissues of HCC patients

To investigate whether CTA expression in TFL could be an indication of occult metastasis, the expression of these CTAs was also determined in TFL. Despite the TFL being located at least 2 cm away from the tumor and being classified as tumor-free by a pathologist, all 12 CTAs were expressed in these tumor-free liver tissues of HCC patients, although at significantly lower levels **(Table 1, Figure 2A and Supplementary Table S5)**. Forty-five percent of patients expressed at least one CTA in TFL (**Supplementary Figure S1**). The CTAs most frequently expressed in TFL were *MAGEA1* (13% of patients), *MAGEC1* (32%) and *MAGEC2* (19%). The latter two were also found to be expressed in approximately 25% of cirrhotic liver tissues of HCC-patients without liver cancer, suggesting that their expression may be activated during early (pre-)malignant transformations in the liver. Interestingly, when a particular CTA was detected in TFL, it was often also present in the tumor (**Figure 2D**); 85% of patients that expressed any CTA in TFL, also had CTA expression in tumor. For example, LIHCC-064 expressed 7 CTAs in their tumor, of which 5 were also expressed in TFL, suggesting that CTA-expressing cells in TFL were derived from the primary tumor.

	mRNA-positive HCC (%)[1]	mean in mRNA-+ HCC (range)[2]	Relative expression HCC (compared to testis)[3]	mRNA-positive TFL (%)[4]	mean in mRNA-+ TFL (range)[5]	Relative expression TFL (compared to testis)[6]	mRNA-positive cirrhotic tissue[7]
CAGE1	14.4	0.082 (0.003-0.711)	0.188	2.0	0.009 (0.003-0.015)	0.020	0
CT47A1	26.8	1.311 (0.001-20.565)	0.632	6.1	0.255 (0.01-0.769)	0.123	0
MAGEA1	58.6	0.403 (0.003-1.926)	4.170	13.0	0.055 (0.005-0.188)	0.567	0
MAGEA9	14.1	0.41 (0.001-4.953)	2.848	1.0	0.035 (0.035-0.035)	0.243	0
MAGEA10	12.4	0.123 (0.002-0.518)	1.080	4.1	0.028 (0.004-0.088)	0.249	0
MAGEB2	24.2	0.395 (0.002-2.4)	0.761	6.0	0.053 (0.018-0.127)	0.102	0
MAGEC1	47.5	0.109 (0.001-0.841)	0.407	32.0	0.047 (0.002-0.466)	0.174	28.6
MAGEC2	55.6	0.692 (0.001-9.305)	1.542	19.0	0.041 (0.003-0.28)	0.091	25.7
NYESO1	10.1	0.13 (0.007-1.04)	0.525	1.0	0.018 (0.018-0.018)	0.071	0
PAGE1	18.2	0.37 (0.002-2.225)	1.001	5.0	0.059 (0.009-0.179)	0.159	2.9
SLCO6A1	25.8	0.095 (0.002-0.411)	0.053	4.1	0.011 (0.004-0.017)	0.006	2.9
TSPY*	21.0	0.827 (0.004-7.401)	34.135	4.8	0.218 (0.001-0.641)	9.012	4.2

Table 1. mRNA expression of CTAs in tumor and TFL of HCC-patients. [1]Percentage of hepatocellular carcinomas (HCC) expressing mRNA of the CTA – meaning a Ct-value <35 and relative expression > 0.001 (n=100); [2]Mean relative expression (relative to the geometric mean of the 3 household genes- GUSB, HPRT1, PMM1) level in HCCs expressing the CTA and range; [3]Mean relative expression of the CTA in HCC expressing the CTA, relative to the relative mean expression in 3 testis tissues; [4]Percentage of paired tumor-free liver (TFL) tissues expressing mRNA of the CTA (n=100); [5]Mean relative expression level in TFLs expressing the CTA and range; [6]Mean relative expression of the CTA in TFL expressing the CTA, relative to the relative mean expression in 3 testis tissues; [7]Percentage of non-cancerous/non-dysplastic cirrhotic liver tissues expressing the CTA (n=35); *% in male
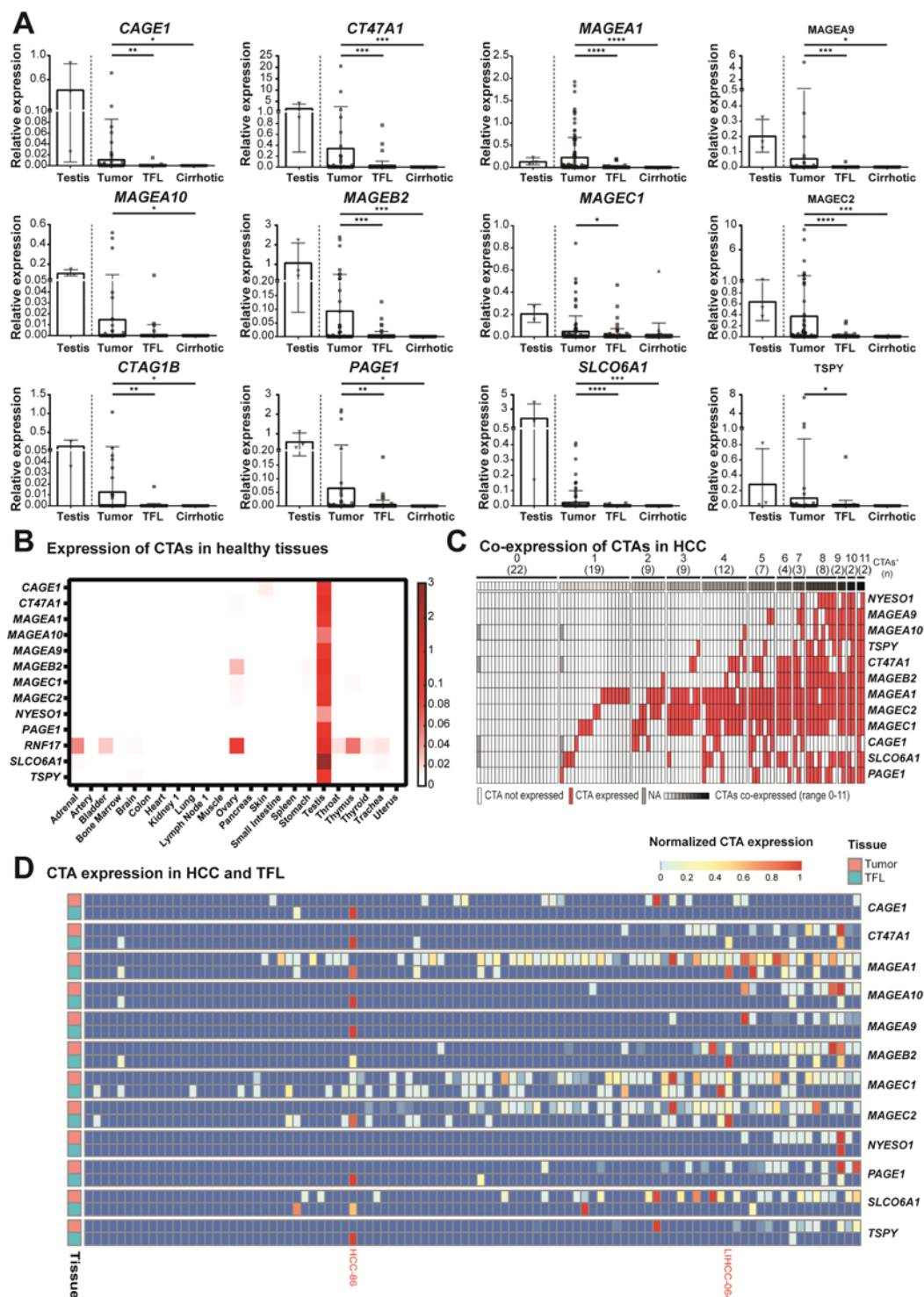
Figure 2. Panel of 12 CTAs expressed in >10% of HCC tumors, but not in healthy tissues. mRNA expression of 12 CTAs in 100 paired HCC and TFL tissues, 35 cirrhotic tissues and 22 different adult healthy tissues, as determined by RT-qPCR. **A.** mRNA expression of the 12 CTAs that are expressed in more than 10% of HCCs and not in healthy tissues. Dots show individual patient tissues, bars show the mean relative expression level, and error bars show the standard deviation. Wilcoxon signed-rank test, * p<0.05, **p<0.01, ***p<0.001. **B.** Heatmap indicating relative mRNA expression levels of all CTAs that are expressed in >10% of HCCs, in healthy adult tissues. **C.** Heatmap indicating co-expression of CTA mRNA in tumor tissue **D.**

Heatmap of mRNA expression of the 12 CTAs expressed in ≥ 10% of HCCs (rows), in HCC and TFL for every patient (columns). Patients were ordered by number of CTAs expressed in each individual tumor. The −ΔCt values were used and for normalization this data was scaled between 0 and 1 [((x-(min(x))/(max(x)-min(x)))]. Colors correspond to the value between 0 and 1 and patients LIHCC-064 and HCC-86 are highlighted in red. Heatmap was made in R, using the pheatmap package.

CTAs are expressed on protein level in HCC tumors and TFL

Consecutively, we examined protein expression of these CTAs in tumor and TFL tissues of 78 HCC-patients of which FFPE blocks were available (patient characteristics are shown in **Supplementary Table S6**). Protein expression of MAGEA1, MAGEA10, MAGEC1, MAGEC2 and NYESO1 in HCC tumors has previously been reported by our group [18]. For CAGE1 no suitable IHC antibodies (Ab) are available. The MAGEB2 IHC Ab showed reliable staining in testis tissue, however, we could not detect any positive cells in HCC and TFL tissues. TSPY1 and SCLO6A1 Abs demonstrated an unspecific staining pattern and a punctate staining that did not allow for quantification of positive cells, respectively, and were therefore discarded **(Supplementary Figure S2)**.[17]

CT47A1, PAGE1, MAGEA9, MAGEC2 and MAGEA1 were detected at protein level in tumor tissues (CT47A1 in 14%, PAGE1 in 23%, MAGEA9 in 11%, MAGEC2 in 59% and MAGEA1 in 34% of tumors; **Figure 3, Supplementary Figure S3**). These CTAs were exclusively expressed by tumor cells, similar to MAGEA10, MAGEC1 and CTAG1B proteins as demonstrated in our previous study.[18] Seventy-one percent of HCC tumor tissues expressed at least one of these CTAs on protein level **(Figure 3C)**. In the majority of patients, only part of the tumor cells expressed these CTAs. Proportions of tumor cells which expressed these CTAs were variable between different patients **(Figure 3B)**, similar to expression intensity (**Supplementary Figure S3**). MAGEA9 was not expressed in any TFL tissue, while we observed expression of CT47A1, PAGE1, MAGEC2 and MAGEA1 in hepatocytes in 1%, 3%, 17% and 9% of TFL tissues respectively, but at significantly lower expression levels than in tumors **(Figure 3B and Supplementary Figure S3)**. Thirty percent of patients expressed at least one CTA protein in their TFL tissue. Most CTA protein expression was focal, as illustrated by the observation that in most patients only part of the tumor cores included in the TMA showed protein expression (**Supplementary Figure S4)**.

In conclusion, the CTAs that were studied for protein expression, also showed protein expression in tumors and, except MAGEA9, also in TFL.
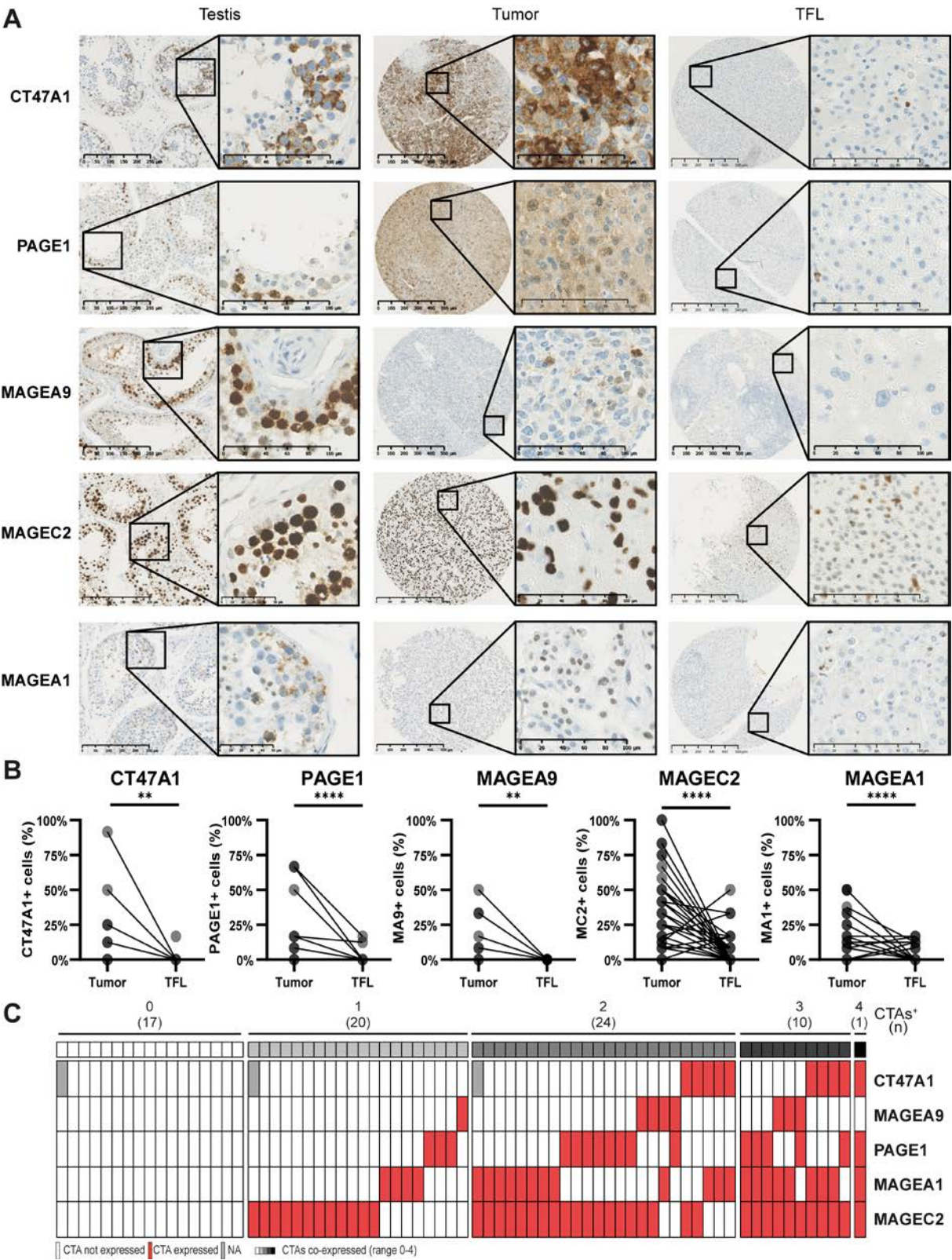
Figure 3. Proteins CT47A1, PAGE1, MAGEA9, MAGEC2 and MAGEA1 are expressed in HCC tumors and TFL. TMAs of tumor and TFL tissues were immunohistochemically stained to study the protein expression of aforementioned CTAs. **A.** Representative examples of immunohistochemical stains in testis, a positive HCC tumor tissue and the paired TFL tissue. **B.** Scores of percentages of tumor cells or hepatocytes expressing CT47A1, PAGE1, MAGEA9, MAGEC2 and MAGEA1 in tumors and paired TFL (n=78). Average scores of three tissue cores are shown. Wilcoxon signed-rank test, **p<0.01, ****p<0.0001. **C.** Heatmap indicating co-expression of CTA-proteins in tumor tissue. TMA slides were scanned by a Nanozoomer (Hamamatsu), and analyzed by NDP.view2 software (Hamamatsu).

CTA expression in TFL is correlated with early HCC recurrence and HCC-specific survival after surgical resection

To determine whether CTA expression in TFL could be an indication occult micrometastasis, we analyzed its association with early HCC recurrence, defined as HCC recurrence within 2 years, and HCC-specific survival. Expression of CTA mRNA in TFL (**Figure 4A**) was negatively associated with both early HCC recurrence and HCC-specific patient survival after surgical resection (**Figure 4B and Supplementary Figure S5**). Early recurrence was observed in 64% of patients with CTA expression in TFL versus 40% in those without. Two-year HCC-specific survival rates were 71% and 89% in patients with and without CTA expression in TFL, respectively. These results were confirmed in a validation cohort, also consisting of 100 HCC patients. In this cohort 29% of HCC patients expressed 1 or more CTAs in TFL, with a maximum of 4 CTAs. Early recurrence was observed in 54% of patients with CTA expression in TFL versus 38% in those without. Two-year HCC-specific survival rates were 69% and 94% in patients with and without CTA expression in TFL, respectively. In both cohorts Kaplan meier survival analysis showed a significant difference for both early HCC recurrence and HCC-specific survival based on CTA expression in TFL. Multivariate analysis mRNA expression in TFL was an independent prognostic factor for early HCC recurrence (hazard ratio [HR] 2.3 and 2.1, for the discovery and validation cohort respectively) and HCC-specific survival (HR 2.3 and 3.6, respectively) in both cohorts, as is shown in **Table 2**. CTA protein expression in TFL (**Figure 4C**) was associated with poor postsurgical outcome as well (**Figure 4D**). In multivariate analysis CTA protein expression in TFL was also an independent prognostic factor for HCC recurrence (HR 2.5) and HCC-specific survival (HR 3.8; **Supplementary Table S7**). An example of CTA protein expression in TFL is shown in **Figure 4E**, the MAGEC2

expressing cells were scattered across the TFL. All TFL tissues with CTA expression were reassessed by a medical pathologist to verify the absence of histologically detectable HCC metastasis. Except for extensive vascular invasion in one patient, which also expressed PAGE1 in TFL (**Supplementary Figure S6**), no histological indications for the presence of malignant cells in TFL were present. Both survival analysis and cox-regression analysis of CTA expression in tumor tissues did not show associations with postsurgical outcome (**Supplementary Table S8 and Supplementary Figure S7**), and neither did CTA protein expression (data not shown).

In conclusion, we found that CTA expression in TFL is an independent negative prognostic factor of both HCC recurrence and HCC-specific survival, and we validated these findings in a validation cohort. This may indicate that occult CTA-expressing (pre-)malignant cells are present in the remaining liver tissue after tumor resection and that these cells could be responsible for HCC recurrence after surgery.

Discovery cohort

| Variable	Early recurrence (<2 yr)				HCC-specific survival			
	Univariate analysis		Multivariate analysis		Univariate analysis		Multivariate analysis	
	HR (95% CI)	p-value	HR (95% CI)	p-value	HR (95% CI)	p-value	HR (95% CI)	p-value
≥1 CTA in TFL	2.3 (1.3-4.0)	**0.0034**	2.5 (1.47-4.5)	**0.003**	2.4 (1.1-5.4)	**0.03**	2.3 (1.0-5.3)	**0.044**
≥2 CTAs in TFL	2.1 (1.2-3.7)	**0.013**			1.7 (0.7-3.9)	0.22		
≥3 CTAs in TFL	4.2 (1.9-9.4)	**0.00053**			5.1 (1.9-14)	**0.0015**		
Number of CTAs in TFL (numeric)	1.3 (1.2-1.5)	**2.0E-05**			1.3 (1.1-1.5)	**0.0011**		
>1 tumor	1.2 (0.7-2.0)	0.56			1.1 (0.5-2.4)	0.83		
>2 tumors	2.6 (1.3-4.9)	**0.0042**	2.4 (1.2-4.7)	**0.02**	1.8 (0.7-4.9)	0.22		
Cirrhosis	1.6 (0.9-2.8)	0.12			1.5 (0.7-3.4)	0.33		
Chronic viral hepatitis	2.3 (1.3-4.0)	**0.0031**	2.7 (1.5-5.0)	**0.001**	3.3 (1.5-7.2)	**0.0032**	4.63 (2.0-10.8)	**0.0004**
Vascular invasion	1.3 (0.7-2.3)	0.41			2.2 (0.96-4.9)	0.063		
Tumor > 5 cm	1.3 (0.7-2.3)	0.37			2.3 (0.9-5.7)	0.081		
AFP > 200 ug/l	1.9 (1.0-3.4)	**0.034**			2.7 (1.2-6)	**0.013**		
AFP > 400 ug/l	2.4 (1.3-4.5)	**0.0051**	3.0 (1.5-5.8)	**0.001**	3.3 (1.5-7.3)	**0.0038**	4.0 (1.7-9.4)	**0.002**

Validation cohort

Variable	Early recurrence (<2 yr)				HCC-specific survival			
	Univariate analysis		Multivariate analysis		Univariate analysis		Multivariate analysis	
	HR (95% CI)	p-value	HR (95% CI)	p-value	HR (95% CI)	p-value	HR (95% CI)	p-value
≥1 CTA in TFL	2.2 (1.1-4.2)	**0.022**	2.1 (1.1-4.1)	**0.03**	3.3 (1.4-7.7)	**0.0074**	3.6 (1.5-8.8)	**0.004**
≥2 CTAs in TFL	1.5 (0.58-3.8)	0.41			2.3 (0.83-6.3)	0.11		
≥3 CTAs in TFL	1.1e-07 (0-Inf)	1			3.9e-08 (0-Inf)	1		
Number of CTAs in TFL (numeric)	1.2 (0.89-1.7)	0.21			1.4 (0.95-2)	0.095		
>1 tumor	2.1 (1-4.2)	**0.043**	2.2 (1.1-4.5)	**0.03**	0.9 (0.27-3.1)	0.87		
>2 tumors	1.7 (0.67-4.4)	0.26			0.96 (0.22-4.1)	0.96		
Cirrhosis	0.77 (0.39-1.5)	0.45			2.3 (0.97-5.5)	0.059	2.6 (1.1-6.3)	**0.03**
Chronic viral hepatitis	0.91 (0.42-2)	0.82			0.98 (0.36-2.7)	0.97		
Vascular invasion	2.1 (0.98-4.4)	0.055			1.5 (0.59-3.9)	0.38		
Tumor > 5 cm	2.5 (1.2-5)	**0.011**	2.6 (1.3-5.3)	**0.007**	1.5 (0.61-3.6)	0.38		
AFP > 200 ug/l	1.6 (0.8-3.3)	0.18			0.83 (0.28-2.5)	0.74		
AFP > 400 ug/l	1.3 (0.61-2.9)	0.46			0.65 (0.19-2.2)	0.5		

Table 2. CTA mRNA-expression in TFL is an independent prognostic factor of HCC recurrence and HCC-specific survival. Univariate and multivariate analyses of factors associated with recurrence and survival according to the cox proportional hazard model. Abbreviations: AFP, alphafoetoprotein; 95% CI, 95% confidence interval; CTA, cancer testis antigen; HR, hazard ratio; TFL, tumor-free liver.
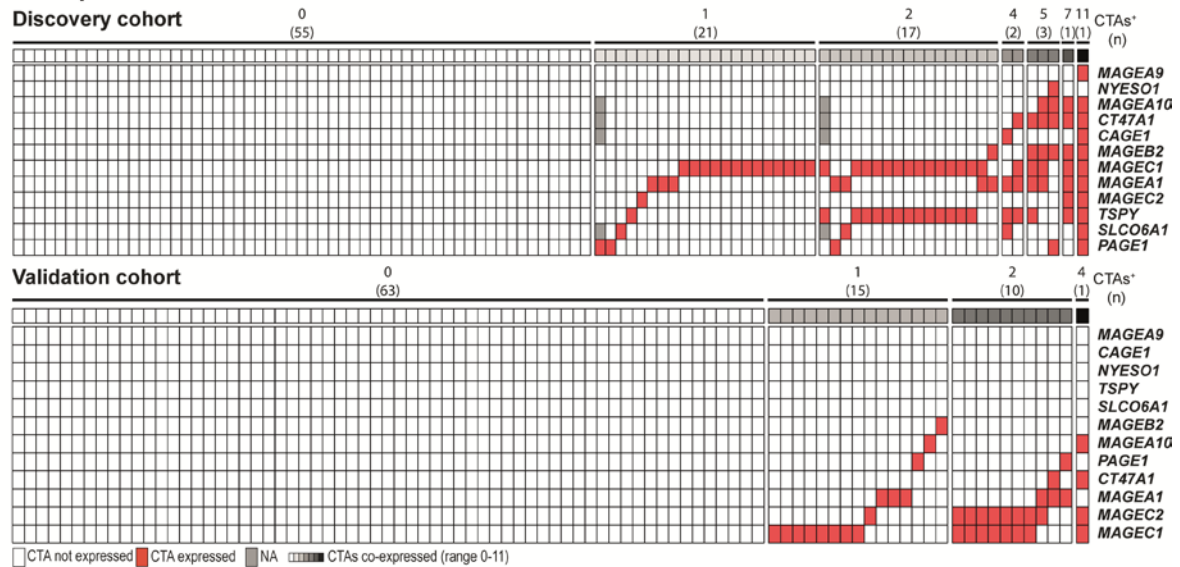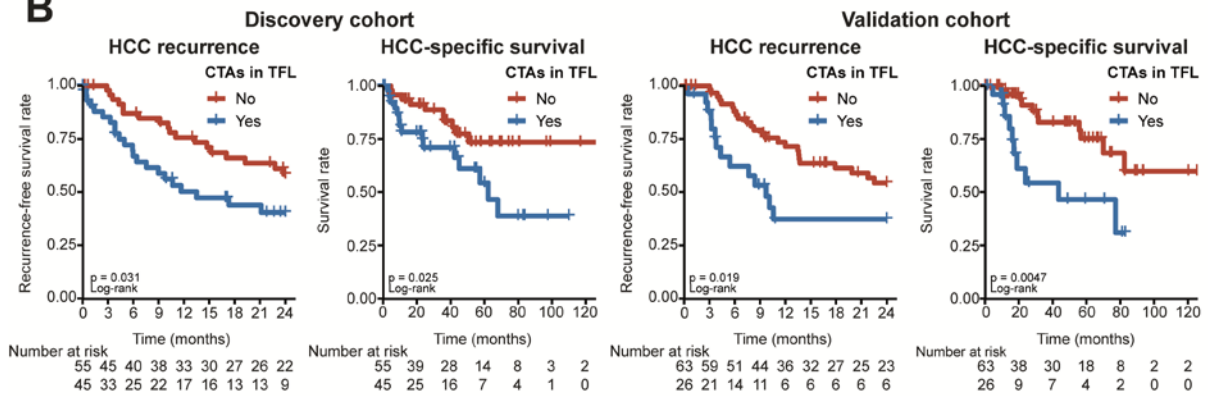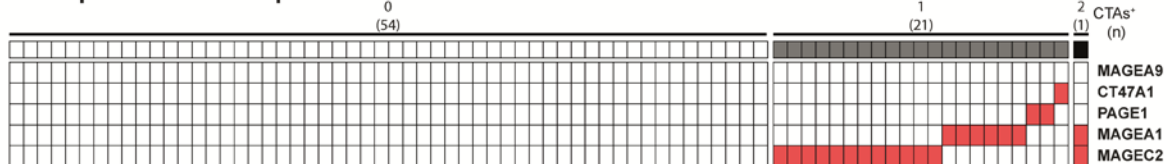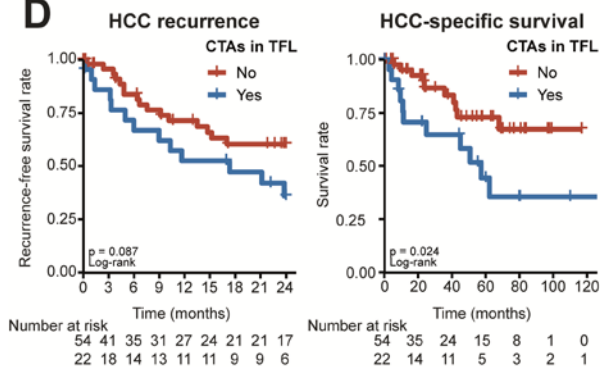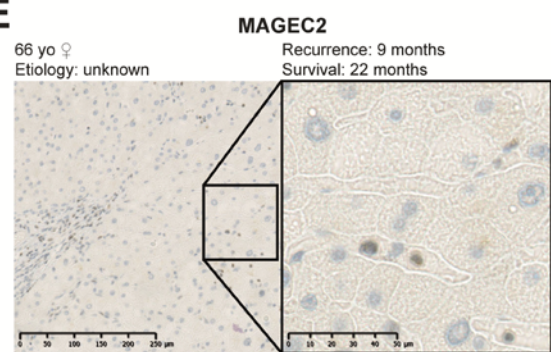
Figure 4. Both mRNA and protein expression of CTAs in TFL are associated with HCC recurrence and HCC-specific survival. **A.** Heatmap indicating co-expression of CTA mRNA in tumor-free liver tissue in the discovery and validation cohort. **B.** Early HCC recurrence and HCC-specific survival in HCC patients by CTA mRNA expression in TFL in the discovery and validation cohort. Plus-signs indicate censored data. Cox-Mantel log-rank test. **C.** Heatmap

indicating co-expression of CTA protein in tumor-free liver tissue. **D.** Early HCC recurrence and HCC-specific survival in HCC patients by CTA protein expression in TFL. Plus-signs indicate censored data. Cox-Mantel log-rank test. **E.** Representative example of IHC staining of MAGEC2 protein expression in TFL, and accompanying patient data. TMA slides were scanned by a Nanozoomer (Hamamatsu), and analyzed by NDP.view2 software (Hamamatsu).

Discussion

We established a novel panel of 12 CTAs, each expressed in at least 10% of HCC tumors and not in healthy tissues except immune-privileged testis. Based on mRNA analysis, approximately 80% of HCC-patients expressed one or more of these antigens in their tumor tissues, whereas protein expression of five of these CTAs was detected in approximately 70% of HCC tumors. In addition, we found that 45% of HCC-patients expressed one or more of the 12 CTAs of our panel in their histologically tumor-free liver tissue, which was associated with early HCC recurrence and worse patient survival after curative surgery. These associatoins were confirmed in a validation cohort, in which 29% of HCC patients expressed one or more CTAs in TFL.

High recurrence rates after surgery with curative intent worsens the survival of HCC patients. Aufhauser, et al.[19] hypothesized that early recurrence, defined as recurrence within 2 years after tumor resection, is due to occult metastasis rather than de novo tumor formation, but failed to find prognostic markers identifying patients with occult metastasis at the time of resection. Therefore, we aimed to find biomarkers detecting occult multifocality at the time of resection, in order for these patients to be selected for adjuvant treatment. We hypothesized that markers identifying occult multifocality should be abundantly and relatively frequently expressed in tumor tissues, to allow for higher sensitivity, and should be completely absent in healthy tissues, to allow for high specificity.

CTA expression in tumors of HCC-patients has been studied before, however, as demonstrated by the results of our literature study (**Supplementary Table S3**), most studies investigated only a few CTAs, determined either RNA or protein expression but not both, did not exclude CTAs expressed in healthy tissues, and most notably, did not look at or acknowledge CTA expression in tumor-free liver (**Figure 1B and C, Supplementary Table S5**). Thus, to assure we would determine the CTAs most likely to serve as markers for occult multifocality in TFL, we repeated CTA expression

analysis in tumor tissues and confirmed absence of the selected CTAs in healthy tissues. As far as we are aware, the present study is the most comprehensive investigation of CTA-expression in tumor and paired TFL tissues of HCC-patients performed. Another recent report used the GEPIA database to analyze CTA expression in tumors of HCC patients, but did not investigate CTA expression in non-cancerous liver tissues of HCC patients.[20] An additional benefit of excluding CTAs expressed in healthy tissues would be their suitability for therapeutic targeting, as targeting proteins exclusively expressed in the tumor will not lead to therapy-induced auto-immunity in potential future clinical applications.[8]

As the expression of CTAs in tumor-free liver tissues of HCC patients has barely been investigated before, the association between expression of CTAs in tumor-free tissue and prognosis has also not been investigated in HCC, nor any other types of cancer. Therefore it was unknown if it could serve as a biomarker for occult multifocality. The 2-year recurrence rate in the study of Aufhauser, et al[19] of 46% is comparable to the observed rate of 50% and 43% in the discovery and validation cohort of this study respectively, and therefore we expect the cohorts to be comparable. Unexpectedly, we observed mRNA expression of one or more of the 12 CTA tumormarkers of our panel in histologically tumor-free liver tissues in a substantial percentage of patients; 45% of tumor-free tissues included in the discovery cohort and in 29% of tumor-free tissues in the validation cohort. Protein expression of one or more of 4 of these CTAs was detected in non-cancerous liver tissues of 40% of patients of the discovery cohort. The 2-year recurrence rates in our cohorts were significantly higher in patients with CTA mRNA-expression in TFL compared to patients without CTA-expression in TFL; 64% vs 40% in the discovery cohort and 54% vs 38% in the validation cohort. Moreover, CTA mRNA expression profiles in TFL were similar to those in the corresponding tumors, and our preliminary immunohistochemical data show that CTA-expressing cells in TFL were either single cells or small foci. Based on these observations, we hypothesize that CTA-expressing cells in TFL of patients with early HCC recurrence indeed represent occult intra-hepatic micro-metastases, and are less likely to represent de novo tumors. This hypothesis is supported by a study performed in colorectal cancer patients with liver metastasis.[21] In TFL, they detected low frequencies of somatic mutations that were also observed in matched tumor samples, despite appearing normal histologically. Since these mutations were not found in the matched blood

samples, it was hypothesized that tumor DNA or tumor cells diffused or migrated into the surrounding normal tissue.[21] However, the authors did not correlate this to either cancer recurrence or survival. Similarly, a previous study detected MAGE-antigen expression in lung tissues of former smokers at risk for NSCLC development,[22] but also did not show any data regarding actual NSCLC development.

Determining lymph node involvement is a widely accepted method for staging a wide variety of cancers. The lymph node metastases themselves are not the cause of death in most patients, however, lymph node involvement is correlated with the spread to vital organs.[23] Therefore it is correlated with reduced patient survival and an important prognostic factor.[24, 25] Likewise, we showed that CTA expression in tumor-free tissue is correlated with recurrence of HCC after curative surgery, independent of other prognostic factors. Detection of occult metastasis in tumor-free tissue, by detection of CTA expression or other methods such as mutation analysis, could be used as a new concept to identify patients at risk for developing (local) metastasis and treatment could be adjusted accordingly, possibly by targeting the CTAs or other biomarkers used.

Most therapeutic cancer vaccination studies targeting CTAs have been performed in advanced cancer patients with high tumor load in which an immunosuppressive tumor microenvironment has been established, and showed modest clinical results.[26] Based on our data showing the presence of scattered single CTA-expressing cells and small foci of CTA-expressing cells in TFL of almost half of resected HCC-patients, therapeutic vaccination with CTA after tumor resection might be a promising approach to prevent HCC recurrence in such patients. Compared to vaccination in advanced cancer, we expect that the low tumor load remaining after resection of detectable tumors may enhance the probability of effective immunological eradication of CTA-expressing (pre-)malignant cells. A prerequisite for therapeutically targeting antigens by vaccination, is that they are immunogenic . Most of the CTAs included in our panel have previously been proven immunogenic in cancer patients.[27] More specifically in HCC patients, we and other research groups have demonstrated the presence of MAGEA1-, MAGEA10-, MAGEC2- and NY-ESO-1-specific T-cells, both in blood and in tumors.[28-32] In addition, NY-ESO-1 and TSPY-specific IgG have been detected in HCC-patients,[33, 34] while CT47A1-, PAGE1- and SLCO6A1-specific antibodies were recently detected in NSCLC patients.[35]

Several CTAs of our panel, such as the MAGE-family members, *CTAG1B*, *TSPY1* and *CAGE1*, are functionally involved in tumorigeneses and cancer progression by modulating gene expression, regulating mitosis and tumorigenic signaling.[8, 10, 36-38] More specifically, MAGE-A9 and TSPY have been shown to be involved in HCC tumor cell proliferation.[36, 38] Their role in cancer progression is further supported by data showing that CTA expression is more prevalent in advanced tumors.[39, 40] Importantly, the involvement of these CTAs in cancer progression may prevent antigen loss upon therapeutic targeting.[37]

We acknowledge several limitations of this study. First, since the etiologies of HCC differ geographically, this CTA-panel might not be applicable to non-Western HCC-populations. Secondly, future research is required to investigate whether CTA-expressing cells in TFL are really (pre-)malignant cells that can give rise to cancer recurrence. Moreover, as not all HCC tumors expressed the selected CTAs, occult micro-metastasis of the tumors not expressing CTAs may be missed. Finally, for the concept – detection of occult multifocality (and thereby prediction of recurrence) by detecting tumor markers in supposedly tumor-free tissue – to be widely applicable, it should be validated in other cancer types.

We established a panel of 12 testis-restricted CTAs that are expressed in almost 80% of HCC patients. In addition, we demonstrated expression of these CTAs in tumor-free liver tissues of 45% and 29% of HCC-patients in two different cohorts. The negative association between expression of these CTAs in TFL and HCC-recurrence and survival, combined with immunohistochemical data, suggests that CTA-expressing cells remain present in the liver after tumor resection, and are indicative for the potential relevance of therapeutic targeting of these antigens. To prevent tumor recurrence, HCC patients with CTA expression in TFL could be selected for adjuvant therapy, either by therapeutic targeting of these CTAs, other (immuno-) therapeutic strategies, or a combination of both.

References

1. Bray F, Ferlay J, Soerjomataram I, et al. Global cancer statistics 2018: GLOBOCAN estimates of incidence and mortality worldwide for 36 cancers in 185 countries. CA Cancer J Clin. 2018.
2. Llovet JM, Ricci S, Mazzaferro V, et al. Sorafenib in advanced hepatocellular carcinoma. N Engl J Med. 2008;359(4):378-90.
3. Bruix J, Qin S, Merle P, et al. Regorafenib for patients with hepatocellular carcinoma who progressed on sorafenib treatment (RESORCE): a randomised, double-blind, placebo-controlled, phase 3 trial. Lancet. 2017;389(10064):56-66.
4. Ulahannan SV, Duffy AG, McNeel TS, et al. Earlier presentation and application of curative treatments in hepatocellular carcinoma. Hepatology. 2014;60(5):1637-44.
5. Poon RT. Differentiating early and late recurrences after resection of HCC in cirrhotic patients: implications on surveillance, prevention, and treatment strategies. Ann Surg Oncol. 2009;16(4):792-4.
6. Finkelstein SD, Marsh W, Demetris AJ, et al. Microdissection-based allelotyping discriminates de novo tumor from intrahepatic spread in hepatocellular carcinoma. Hepatology. 2003;37(4):871-9.
7. Hoshida Y, Villanueva A, Kobayashi M, et al. Gene expression in fixed tissues and outcome in hepatocellular carcinoma. N Engl J Med. 2008;359(19):1995-2004.
8. Gjerstorff MF, Andersen MH, Ditzel HJ. Oncogenic cancer/testis antigens: prime candidates for immunotherapy. Oncotarget. 2015;6(18):15772-87.
9. Hofmann O, Caballero OL, Stevenson BJ, et al. Genome-wide analysis of cancer/testis gene expression. Proc Natl Acad Sci U S A. 2008;105(51):20422-7.
10. Whitehurst AW. Cause and consequence of cancer/testis antigen activation in cancer. Annu Rev Pharmacol Toxicol. 2014;54:251-72.
11. Altman DG, McShane LM, Sauerbrei W, et al. Reporting Recommendations for Tumor Marker Prognostic Studies (REMARK): explanation and elaboration. PLoS Med. 2012;9(5):e1001216.
12. Charoentong P, Finotello F, Angelova M, et al. Pan-cancer Immunogenomic Analyses Reveal Genotype-Immunophenotype Relationships and Predictors of Response to Checkpoint Blockade. Cell Rep. 2017;18(1):248-62.
13. Lizio M, Abugessaisa I, Noguchi S, et al. Update of the FANTOM web resource: expansion to provide additional transcriptome atlases. Nucleic Acids Res. 2019;47(D1):D752-D8.
14. Yu NY, Hallstrom BM, Fagerberg L, et al. Complementing tissue characterization by integrating transcriptome profiling from the Human Protein Atlas and from the FANTOM5 consortium. Nucleic Acids Res. 2015;43(14):6787-98.
15. Uhlen M, Fagerberg L, Hallstrom BM, et al. Proteomics. Tissue-based map of the human proteome. Science. 2015;347(6220):1260419.
16. Keen JC, Moore HM. The Genotype-Tissue Expression (GTEx) Project: Linking Clinical Data with Molecular Analysis to Advance Personalized Medicine. J Pers Med. 2015;5(1):22-9.
17. Schnieders F, Dork T, Arnemann J, et al. Testis-specific protein, Y-encoded (TSPY) expression in testicular tissues. Hum Mol Genet. 1996;5(11):1801-7.
18. Sideras K, Bots SJ, Biermann K, et al. Tumour antigen expression in hepatocellular carcinoma in a low-endemic western area. Br J Cancer. 2015;112(12):1911-20.
19. Aufhauser DD, Jr., Sadot E, Murken DR, et al. Incidence of Occult Intrahepatic Metastasis in Hepatocellular Carcinoma Treated With Transplantation Corresponds to Early Recurrence Rates After Partial Hepatectomy. Ann Surg. 2018;267(5):922-8.
20. Zhang YP, Bao ZW, Wu JB, et al. Cancer-Testis Gene Expression in Hepatocellular Carcinoma: Identification of Prognostic Markers and Potential Targets for Immunotherapy. Technol Cancer Res Treat. 2020;19:1533033820944274.
21. Beije N, Helmijr JC, Weerts MJA, et al. Somatic mutation detection using various targeted detection assays in paired samples of circulating tumor DNA, primary tumor and metastases from patients undergoing resection of colorectal liver metastases. Mol Oncol. 2016;10(10):1575-84.
22. Jang SJ, Soria JC, Wang L, et al. Activation of melanoma antigen tumor antigens occurs early in lung carcinogenesis. Cancer Res. 2001;61(21):7959-63.
23. Wong SY, Hynes RO. Lymphatic or hematogenous dissemination: how does a metastatic tumor cell decide? Cell Cycle. 2006;5(8):812-7.

154

24. Jones D, Pereira ER, Padera TP. Growth and Immune Evasion of Lymph Node Metastasis. Front Oncol. 2018;8:36.
25. Nathanson SD. Insights into the mechanisms of lymph node metastasis. Cancer. 2003;98(2):413-23.
26. Hollingsworth RE, Jansen K. Turning the corner on therapeutic cancer vaccines. NPJ Vaccines. 2019;4:7.
27. Andersen RS, Thrue CA, Junker N, et al. Dissection of T-cell antigen specificity in human melanoma. Cancer Res. 2012;72(7):1642-50.
28. Flecken T, Schmidt N, Hild S, et al. Immunodominance and functional alterations of tumor-associated antigen-specific CD8+ T-cell responses in hepatocellular carcinoma. Hepatology. 2014;59(4):1415-26.
29. Bricard G, Bouzourene H, Martinet O, et al. Naturally acquired MAGE-A10- and SSX-2-specific CD8+ T cell responses in patients with hepatocellular carcinoma. J Immunol. 2005;174(3):1709-16.
30. Zhou G, Sprengers D, Boor PPC, et al. Antibodies Against Immune Checkpoint Molecules Restore Functions of Tumor-Infiltrating T Cells in Hepatocellular Carcinomas. Gastroenterology. 2017;153(4):1107-19 e10.
31. Shang XY, Chen HS, Zhang HG, et al. The spontaneous CD8+ T-cell response to HLA-A2-restricted NY-ESO-1b peptide in hepatocellular carcinoma patients. Clin Cancer Res. 2004;10(20):6946-55.
32. Inada Y, Mizukoshi E, Seike T, et al. Characteristics of Immune Response to Tumor-Associated Antigens and Immune Cell Profile in Patients With Hepatocellular Carcinoma. Hepatology. 2019;69(2):653-65.
33. Yin YH, Li YY, Qiao H, et al. TSPY is a cancer testis antigen expressed in human hepatocellular carcinoma. Br J Cancer. 2005;93(4):458-63.
34. Korangy F, Ormandy LA, Bleck JS, et al. Spontaneous tumor-specific humoral and cellular immune responses to NY-ESO-1 in hepatocellular carcinoma. Clin Cancer Res. 2004;10(13):4332-41.
35. Djureinovic D, Dodig-Crnkovic T, Hellstrom C, et al. Detection of autoantibodies against cancer-testis antigens in non-small cell lung cancer. Lung Cancer. 2018;125:157-63.
36. Deng Q, Li KY, Chen H, et al. RNA interference against cancer/testis genes identifies dual specificity phosphatase 21 as a potential therapeutic target in human hepatocellular carcinoma. Hepatology. 2014;59(2):518-30.
37. Maxfield KE, Taus PJ, Corcoran K, et al. Comprehensive functional characterization of cancer-testis antigens defines obligate participation in multiple hallmarks of cancer. Nat Commun. 2015;6:8840.
38. Tu W, Yang B, Leng X, et al. Testis-specific protein, Y-linked 1 activates PI3K/AKT and RAS signaling pathways through suppressing IGFBP3 expression during tumor progression. Cancer Sci. 2019;110(5):1573-86.
39. Velazquez EF, Jungbluth AA, Yancovitz M, et al. Expression of the cancer/testis antigen NY-ESO-1 in primary and metastatic malignant melanoma (MM)--correlation with prognostic factors. Cancer Immun. 2007;7:11.
40. Barrow C, Browning J, MacGregor D, et al. Tumor antigen expression in melanoma varies according to antigen and stage. Clin Cancer Res. 2006;12(3 Pt 1):764-71.

Supplemental data for:

Expression of cancer testis antigens in tumor-adjacent normal liver predicts post-resection recurrence of Hepatocellular Carcinoma

Table of contents

Materials & Methods

Liver and healthy tissue samples

Freshly frozen healthy liver tissues (n=21) were obtained during liver transplantation from donor liver grafts at the end of cold ischemic storage. Archived freshly frozen tissue samples of non-cancerous cirrhotic livers (n=35) were retrieved from the tissue bank of the Department of Pathology, Erasmus Medical Center Rotterdam. The non-cancerous cirrhotic liver tissues had been retrieved from patients who underwent liver transplantation for liver cirrhosis in our center between May 2007 and June 2017. The etiology of the cirrhosis was determined by information from medical records, laboratory tests and pathological examination of the explanted livers. Cirrhotic livers with malignancies, diagnosed by pathological examination, were excluded.

RNA isolated from fresh frozen healthy adrenal gland (R1234004-50), artery (HR-810), brain (R1234035-50), colon (R1234090-50), heart (R1234122-50), lung (R1234152-50), muscle (R1234171-50), ovary (HR-406), pancreas (R1234188-50), skin (R1234218-50), small intestine (R1234226-50), stomach (HR-302), testis (R1234260-50), throat (R1234263-10), thymus (HR-702), thyroid (R1234265-50), trachea (R1234160-50), urinary bladder (R1234010-50) and uterus (R1234274-50) tissues were purchased from AMS Biotechnology Ltd, Abingdon, UK. Bone marrow derived from a healthy donor (Department of Hematology, Erasmus MC), healthy kidney tissue obtained from a donor kidney (Department of Internal Medicine, Erasmus MC) and RNA of healthy testis tissues (Department of Pathology, Erasmus MC) were kindly provided. Lymph node and spleen tissues were collected from samples retrieved during liver transplantation in our center in September 2019.

Quantitative real-time PCR

RNA was isolated using the NucleoSpin® RNA isolation kit of Macherey-Nagel (Dueren, Germany) according to manufacturer's instructions. RNA (4 ug) was reverse-transcribed into cDNA using PrimeScript™ RT master Mix (Perfect Real Time, Takara, cat# RR036A), according to the manufacturer's instructions. RT-qPCR was performed using SYBR™ Green PCR Master Mix (ThermoFisher) in a StepOnePlus™ Real-Time PCR System (Applied Biosystems), using 12.5 ng cDNA per reaction, with the following conditions: 50°C for 2 minutes, 95°C for 2 minutes,

then 38 cycles of 95°C for 15 seconds, 58-62°C for 15 seconds (according to the Tm of the primers), 72°C for 1 minute, and then finally for the Melt Curve stage 95°C for 15 seconds, 60°C for 1 minute and a 0.7°C step-wise increase until 95°C was reached. All Ct-values over 35 were considered negative. The level of target gene expression relative to the geometric mean of three control genes (HPRT1, GUSB, PMM1)[2] was calculated by $2^{-\Delta\Delta T}$ method, after which a cut-off of 0.001 was used to define expression. All amplifications were performed in at least two technical repeats. Means of technical replicates were used for analysis. Primers were designed with Primer Blast (NCBI), efficiency was determined by dilution of cDNA and product length was determined by gel electrophoresis.

Immunohistochemistry

The FFPE blocks of the HCC and TFL tissues were examined by a pathologist (MD) to mark tumor and tumor-free liver tissues. A TMA Grand Master (2.5; 3D Histech) was used to create tissue microarrays (TMA). Three tissue cores of 1 mm were taken of each tissue and placed in a recipient formalin block. Immunohistochemistry (IHC) was performed using an automated, validated and accredited staining system (Ventana Benchmark ULTRA, Ventana Medical Systems, Tucsen, AZ, USA) using the optiview universal DAB detection Kit (cat.760-700, Ventana Medical Systems). In brief, following deparaffinization and heat-induced antigen retrieval tissue sections were incubated with each of the primary antibodies according to their optimized incubation time and concentration **(Supplementary Table S9)**. The antibodies were titrated using testis as a positive control tissue and placenta and spleen as negative control tissues. Incubation was followed by hematoxylin II counter stain for 12 minutes and then a blue colouring reagent for 8 minutes according to the manufacturer's instructions (Ventana Medical Systems, Tucsen, AZ, USA). The stained TMAs were then scanned using a Nanozoomer (Hamamatsu), and analyzed using NDP.view2 software (Hamamatsu).

Search query:

(("cancer testis antigen"[All Fields] OR ((("cancer"[All Fields] OR "neoplas*"[All Fields]) AND ("testis"[All Fields] OR "testes"[All Fields]) AND ("Antigens, Neoplasm"[Majr] OR "antigen*"[All Fields] OR "Ags"[All Fields] OR "ag"[All Fields] OR "gene"[All Fields] OR "genes"[All Fields] OR "antigen*"[All Fields])))) AND (("Carcinoma, Hepatocellular"[Majr]) OR "Fibrolamellar hepatocellular carcinoma" [Supplementary Concept] OR "liver cell carcinoma"[All Fields] OR "liver cancer"[All Fields] OR "hepatocellular carcinoma cell line"[All Fields] OR (("liver"[All Fields] OR "hepat*"[All Fields]) AND ("carcinoma*"[All Fields] OR "ca"[All Fields] OR "cas"[All Fields] OR "cancer*"[All Fields]) OR "hepatocarcinom*"[All Fields])) AND "Humans"[Mesh]

Pubmed search 04-10-2018

Supplementary Table S1. Patient characteristics of HCC-patients in discovery and validation cohort based on CTA expression in TFL

Characteristic	Discovery cohort		Validation cohort	
	CTA in TFL- (n=55)	CTA in TFL+ (n=45)	CTA in TFL – (n=63)	CTA in TFL+ (n=26)
Age at surgery (years)				
Mean ± SD	60.0 ± 14.3	59.8 ± 15.0	65.9 ± 10.7	60.4 ± 11.0
Median (range)	63 (11-82)	64 (16-80)	67 (34-85)	61 (36-76)
Sex – no. (%)				
Male	36 (65.5)	27 (60)	49 (77.8)	15 (57.7)
Female	19 (34.5)	18 (40)	14 (22.2)	11 (42.3)
Race – no. (%)				
White	47 (85.5)	36 (80)	52 (82.5)	20 (76.9)
African	3 (5.5)	5 (11.1)	4 (6.3)	-
Asian	4 (7.3)	4 (8.9)	5 (7.9)	5 (19.2)
Not reported	1 (1.8)	-	2 (3.2)	1 (3.8)
Etiology – no. (%)				
No known liver disease	14 (25.5)	19 (42.2)	19 (30.2)	7 (26.9)
Alcohol	16 (29.1)	5 (11.1)	11 (17.5)	8 (30.8)
Hepatitis B	8 (14.5)	4 (8.9)	10 (15.9)	3 (11.5)
NASH	5 (9.1)	3 (6.7)	12 (19.0)	4 (15.4)
Hepatitis C + Alcohol	3 (5.5)	5 (11.1)	-	-
Hepatitis B + Alc/HepC/HepD/NASH	2 (3.6)	4 (8.9)	1 (1.6)	1 (3.8)
Hepatitis C	4 (7.3)	2 (4.4)	5 (7.9)	1 (3.8)
Fibrolamellar HCC	2 (3.6)	2 (4.4)	-	-
Hemochromatosis (+ NASH/Alcohol)	1 (1.8)	1 (2.2)	3 (4.8)	1 (3.8)
Autoimmune hepatitis	-	-	-	-
Primary sclerosing cholangitis	-	-	-	1 (3.8)
Other	-	-	2 (3.2)	-
Hepatitis status – no. (%)				
Hepatitis B or C positive	17 (30.9)	15 (33.3)	16 (25.4)	5 (19.2)
Chronic Hepatitis B	10 (18.2)	8 (17.8)	11 (17.5)	4 (15.4)
Chronic Hepatitis C	8 (14.5)	7 (15.6)	5 (7.9)	2 (7.7)
Cirrhosis – no. (%)				
Yes	22 (40)	12 (26.7)	24 (38.1)	10 (38.5)
No	33 (60)	33 (73.3)	39 (61.9)	16 (61.5)
Tumor differentiation – no. (%)				
Good	8 (14.5)	4 (8.9)	8 (12.7)	3 (11.5)
Moderate	30 (54.5)	22 (48.9)	36 (57.1)	15 (57.7)
Poor	9 (16.4)	9 (20)	14 (22.2)	5 (19.2)
Unknown	8 (14.5)	10 (22.2)	5 (7.9)	3 (11.5)
Vascular invasion – no. (%)				
Yes	23 (41.8)	26 (57.8)	41 (65.1)	18 (69.2)
No	27 (49.1)	15 (33.3)	22 (34.9)	6 (23.1)
Unknown	5 (9.1)	4 (8.9)	-	2 (7.7)
BCLC stage – no. (%)				
0	1 (1.8)	-	4 (6.3)	-
A	36 (65.5)	30 (66.7)	47 (74.6)	22 (84.6)
B	18	15 (33.3)	12 (19.0)	4 (15.4)
Number of lesions – no. (%)				
1	30 (54.5)	26 (57.8)	49 (77.8)	22 (84.6)
>1	25 (45.5)	19 (42.2)	14 (22.2)	4 (15.4)
Median (range)	1 (1-11)	1 (1-10)	1 (1-11)	1 (1-11)
Size of largest lesion (cm)				
Mean ± SD	6.2 ± 4.3	9.1 ± 6.9	7.0 ± 4.7	8.0 ± 4.7
Median (range)	5.2 (1.3-24)	7.5 (1-34)	5.7 (0.8-21.0)	7.15 (1.7-16.5)
AFP level before resection (ug/l)				
Mean ± SD	711 ± 2384	113360 ± 519877	1850 ± 6673	784 ± 1641
Median (range)	7 (1-10709)	12 (1-3118700)	9 (1-45803)	47 (1-4973)

160

Supplementary Table S2. Primer sequences and annealing temperatures (Tm) used for RT-qPCR.

Primer	Tm	Forward Primer	Reverse Primer	Product Length
CAGE1	60	TCATCCGAAGTCCATGACCA	GACTCTTCCTGGAGTGGTTG	118
CBLL2	62	TTCCACCAGAACAGCACACC	AACGGTTTCCCACTGGATGG	146
CCDC83	60	AGGAGGGCAGGCCTTTTTAATC	TCCATTGTGCTGGTTAGCTATGA	148
CPXCR1	60	CAGCCAGTCATACTATCCTC	CTACAGTCATTAGGAGGCTC	118
CSAG2/3	58	GGAGTGGGCCAACACTATCC	GGCTGTCCGAAGAGAGACTG	123
CT45	62	ATGCACATCACTCCCAGGTG	TTGTTTCCTTGCTGGAGGAGA	147
CT47A1	60	ACCTAGACGCAGCAGAGGT	AACTTGAACACTGTCACATACATCC	141
CTAG1A/B	60	GGCTTCAGGGCTGAATGGA	TGTTGCCGGACACAGTGAAC	191
Cxorf48	60	CTGGCAACGTGCCTCTAAAAG	AAGATGGCGAGGCACAACAT	110
DDX53	60	GTTGGTGTGGTCATTGGTTAC	CGCTTTGGCCTTTGCTTTCAT	144
DPPA2	62	CAATCTCCTTCCATCCCAGGGT	ACCAGTGTCAAAATCACACTTTCC	118
DUSP21	62	TTGTCAATGCCTCGGTGGAA	CGAGTCACGAGCATCGGTAA	86
FAM46D	60	AGCCTTAACGGATGAAGGAAAA	AAACTCCAGCTAGTGAAACTCC	92
FATE1	62	ATGGAGCTTGGATCTCGGTC	CTCAGCATTCTGGGCTTTGG	155
FBXO39	60	TGATAGATCTCCTGCCCACCT	CTCGTCGAGTGACTCATGGTT	83
FMR1NB	60	TCCTGCTGTTCGTGTGCTAC	TCAGCAAAGCTTCCAATGCG	147
FTHL17	60	ATCAACAGCCACATCACGCT	CATTTTGTCGTCCGACAGGC	132
GAGE1	60	ACCTGAGTCATCTTAAAACATGTGA	AGTAAACATGAAGCAGAGTGCC	80
GPC3	60	AACCATGTCTATGCCCAAAGGT	CCAGAGCCTCCAATGCACTC	108
GUSB	58	CAGGTGATGGAAGAAGTGG	GTTGCTCACAAGGTCACAG	171
HORMAD1	60	CAACGAATCTAGCATGTTGTC	CACAATCACCATCCTTAAAACC	188
HPRT1	58	GCTATAAATTCTTTGCTGACCTGCTG	AATTACTTTTATGTCCCCTGTTGACTGG	140
LUZP4	60	CTTCGTTTCGGAAGCTAACGC	CTCCGATGGCGATGTCTATGA	217
MAGEA1	60	AGAAGCGAGGTTTCCATTCTGA	GGAATCCTGTCCTCTGGGTTG	116
MAGEA2	62	CTCCAGCTTCTCGACTACCATC	GACTCCAGGTCGGGAAACATTC	148
MAGEA3	62	ATCTTCAGCAAAGCTTCCAGT	GGTGGCAAAGATGTACAAGTGG	93
MAGEA4	58	GAGCTTCTGCGTCTGACTCG	TGTCTGCTCAGAACCTTGTCTC	85
MAGEA8	60	GGTCGGCTTGAGATCGGCT	CCTCAGCTTGACTGCTACTACTG	150
MAGEA9B	60	GCTTGATACCGGTGGAGGAG	GGTTAGCCTGTCCCGAGAAC	124
MAGEA10	62	GAGATCGGCTGAAGAGAGCG	ACTCTTGTCAGATCCTGCGAC	140
MAGEB1	60	TGAAGTAGTGAGCAGCCAAGA	GCTGGCAGCACCAATAAATGT	172
MAGEB2	58	TCCTGACTTCCGCTTTGGAGGC	GCACGGAGCTTACTCTTCTGACC	135
MAGEB3	60	CTACCCAAACCTCTTCTCAGCC	AGACCCTGGATCCTCCCTCTA	144
MAGEB6	62	ACCCTTGTCAGCAAGCTAGG	GATCACAACCAGGAGCGACA	99
MAGEC1	62	GGCCATCTTGGGAGTCTGAA	TGGAGCACCTTGAAGACTGG	106
MAGEC2	62	GGAGTCAAGGCCTGTTGGAT	GGGAGGCATGACGACTTCTT	84
PAGE1	62	GGCTGAAGTTGTGAAATATGGGT	CTGCAGATGCTCCCTCATCC	177
PAGE5	62	TGATGTCAGGGAGGGGACTC	TGGTTTCAGTCTTCATTTGTCTTGG	105
PASD1	62	TGCAGAGGTTGAGCAGTATGG	GGATTCACCTCAGGCTCACC	153
PLAC1	60	ACACAGCAAGTTCCTTCTTCC	GAGGATTTCTTCTTCTGGCAGC	118
PMM1	58	CGAGTTCTCCGAACTGGAC	CTGTTTTCAGGGCTTCCAC	86

RNF17	60	GGACAATGCAGTGGTCCAAAG	AGGAGCACCAAGAGAATCGAA	137
SAGE1	58	CCTTAGCTGACTCTGGTGCTC	GACTCGTTTGAAGTGGAGAAGC	150
SLCO6A1	62	TGGCCTTGGGTGTAAGCTATG	ATCCAACAACGTCCTGTGTG	136
SPANXA	62	ATGATGCCGGAGACCCCAAC	GTGGTCATTCAGCAGTTCCTCT	144
SPANXC	60	CGCTACAGGAGGAACGTGAA	ATTCCTCCTCCTCCATTTGG	100
SPANXN3	62	ACCAGAATCATGGAACAGCCAA	TGTTTGGTACCTCTTGCATCTC	106
SYCP1	62	CTATCTGTGGACATCTGCCAA	TTGGTTTTGTTGGTGTCTTCAC	80
TEKT5	62	GGTCCATGACAACGTGGAGA	TGCTGAGCATCCCGGTTATC	126
TFDP3	60	TTGGAGGTGTGTTCACGACG	CTGAGATCCACCGGAGCTTG	113
TPPP2	60	GCAAAGTCAAGGCCAAGAACG	CTGGACTCTTCCCTTTGAAGC	99
TSPY	62	ACAAGATTGCTGAGTCCCCTG	TCAACAACTGGGAGTCCCCT	149
ZCCHC13	62	TGCTACAACTGTGGGAGAAGC	TGACGATCACAGTCACGAGC	122

Supplementary Table S3. Results of the literature search and overview of included articles.

Study	Gene(s)	Population	Detection method	Outcome
Wei Y, et al. Int J Oncol. 2018[4]	MAGEA9	HCC patients (n=90; China)	IHC	IHC: 40/90 (44%) MAGEA9+
Jiao Y, et al. PLoS One. 2017[5]	TFDP3	HCC cell line (HepG2) and normal human hepatocyte cell line (L-02) and HCC patients (China)	RT-qPCR and IHC	mRNA and IHC: HepG2 and L02 are both TFDP3+, expression is higher in HepG2. Also protein expression in HCC patients.
Liu, et al. Cancer Lett. 2017[6]	CTCFL	HCC cell lines (HepG2, SMMC-7721, Huh7, HCCLM3, PLC/PRF/5), normal human hepatocyte cell lines (L-02 and WRL68) and HCC patients (n=25; China)	RT-qPCR and IHC	RT-qPCR: all cell lines positive, expression higher in HCC cell lines than normal human hepatocyte cell lines IHC: 18/25 (72%) CTFCLhigh and 7/25 (28%) CTCFLlow
Xie, et al. Drug target. 2017[7]	TTK	Review	n.a.	Liu, Oncotarget 2015: 118/152 (77.63%) of HCC patients mRNA TTK+ – China
Charoentong, et al. Cell Rep. 2017[1]	BRDT, CAGE1, CCDC83, CPXCR1, CSAG2, CT45A1, DDX53, DPPA2, FMR1NB, FTHL17, GAGE1, LUZP4, MAGEA1, MAGEA2, MAGEA3, MAGEA4, MAGEA5, MAGEA9, FAM46D, MAGEB1, MAGEB2, MAGEB3, MAGEC1, PAGE1, PASD1, POTEA, POTEB, POTED, SLCO6A1, SPANXC, SPANXN3, SSX3, SSX5, SSX7, TSPY2, TSPY3, TSSK6, XAGE2, ZNF645,	The Cancer Genome Atlas (TCGA); including 363 HCC patients	RNA sequencing	Aforementioned genes are all correlated with CD4 and/or CD8 T cells in HCC
Kido, et al. J Genet Genomics. 2016[8]	TSPY	TCGA and refers to Kido, et al. 2014 IHC: male HCC patients (n=287; TMA purchased from US Biomax) and RT-qPCR: male HCC patients (n=32; China)	TCGA: RNA seq Kido, et al. 2014: RT-qPCR and IHC	This paper researches the TSPY co-expression network (TCN), which is activated in 30% of HCCs (TCGA). Kido, et al. 2014: RT-qPCR: 15/32 (46.9%) TSPY+ IHC: 55/287 (19.2%) TSPY+
Fu, et al. Int J Clin Exp Pathol. 2015[9]	ACRBP	HCC cell lines (Bel-7404[1], HepG2[2], QGY-7703[3], QGY-7701[4], BEL-7402[5], SMMC-7721[6])	RT-PCR[1-6], IHC[1,2] and WB[1,2]	RT-PCR: 6/6 cell lines IHC: 2/2 cell lines WB: 2/2 cell lines
Wang, et al. Int J Clin Exp Pathol. 2015[10]	MAGEA3, MAGEA4, MAGEC2, NY-ESO-1	HCC cell lines (LO2, HepG2, Hep3B, Huh7, SMMC-7721) and HCC patients (China; n=142)	RT-PCR and IHC	Cell lines: 4/5 cell lines for 4 TAAs. HCC patients: 112/142 (78.9%) MA3+, 48/142 (33.8%) MA4+, 106/142 (74.6%) MC2+, 20/142 (14.1%) NY-ESO-1+. No expression in TFL. IHC: 108/142 (76.1%) MA3+, 44/142 (31.0%) MA4+, 99/142 (69.7%) MC2+, 19/142 (13.4%) NY-ESO-1+
Sideras, et al. Br J Cancer. 2015[11]	MAGEA1, MAGEA3/4, MAGEA10, MAGEC1, MAGEC2, NY-ESO-1, SSX2, SP17	HCC patients (Netherlands; n=133)	IHC	9.8% MAGEA1+, 3.0% MAGEA3/4+, 7.5% MAGEA10+, 17.3% MAGEC1+, 19.5% MAGEC2+, 3.8% NY-ESO-1+, 0% SSX2+, 87% SP17+. No expression in TFL, except SP17 (88.0%)
Melis, et al. J Transl Med. 2014[12]	NUF2, TTK, MAGEA3, CEP55	HBV+ HCC patients (n=10; Italy)	RT-PCR	Expression of al 4 TAAs in 10 patients, both in HCC and TFL, but higher in HCC.

Li, et al. J Transl Med. 2014[13]	TSPY	HCC cell lines (HepG2, SMMC7721, Huh7, MHCC97L, MHCC97H, HCCLM3) and HCC patients (n= 52;China)	RT-PCR	6/6 cell lines and expression of TSPY in male HCC tissues, but not female HCC tissues
Deng, et al. Hepatology. 2014[14]	DUSP21, CT45, ZCCHC13, MAGEA9, MAGEB6, PIHD3, PNMA5, MPC1L, IL13RA1	HCC patients (n=24; China?)	RT-PCR	8/24 (33.3%) DUSP21+, 7/24 (29.2%) CT45+, 4/24 (16.7%) ZCCHC13+, 3/24 (12.5%) MAGEA9+, 3/24 (12.5%) MAGEB6+, 4/24 (16.7%) PIHD3+, 6/24 (25%) PNMA5+, 6/24 (25%) MPC1L+, 1/24 (4.2%) IL13RA1+
Xia, et al. Int J Clin Exp Pathol. 2013[15]	SP17, MAGEC1, NY-ESO-1	HCC patients (n=45; China)	IHC	16/45 (35.6%) MAGEC1+, 7/45 (15.6%) NY-ESO-1+, 36/45 (80%) SP17+
Zhou, et al. Oncol Rep. 2013[16]	FAM9C	HCC cell lines (SSMC-7721, QGY-7703, BEL-7404, BEL-7405, YY-8103, Huh7) and HCC patients (n=46; China)	RT-qPCR and IHC	RT-qPCR: 25/46 HCC patients have upregulation of FAM9C in T compared to TFL Cell lines: 2/6 FAM9C+ IHC showed nuclear staining (T>TFL)
Chen, et al. Genet Test Mol Biomarkers. 2013[17]	CTCFL	HCC cel lines (SMMC-7721, BEL-7402, Huh7, HepG2) and HCC patients (n=105; China)	RT-PCR, IHC and WB	Cell lines: 3/4 CTCFL+ (RT-PCR and WB) HCC patients: 58/105 (55.2%) CTCFL+ (IHC)
Song, et al. Oncol Rep. 2012[18]	AKAP3, CTp11	HCC cell lines (SNU-354, SNU-398, SNU-423, SNU-449, HepG2) and HCC patients (n= 10; Korea)	RT-PCR	5/10 (50%) AKAP3+, 1/9 (11.1%) CTp11+
Li, et al. Bull Cancer. 2012[19] – no full text	CABYR-c	HCC patients (n=20; China)	RT-PCR and WB	Both mRNA and protein expression are significantly higher in HCC compared to TFL
Yoon, et al. Tohoku J Exp Med. 2011[20]	RNF17	HCC patients (n=28; Korea), CCA patients (n=5) and combined HCC-CCA (n=8) – Korea	RT-qPCR	4/28 (14.3%) HCC RNF17+, 1/5 (20%) CCA RNF17+, 2/8 (25%) combined HCC/CCA RNF17+. No expression in TFL.
Tseng, et al. Oncol Rep. 2011[21]	CABYR-a/b, CABYR-c/d, CABYR-e	HCC cell lines (HepG2, Huh7) and HCC patients (n=16; Taiwan)	RT-PCR and WB	Cell lines: 2/2 expressed CABYR-a/b and CABYR-c/d HCC patients: 7/16 (43.8%) CABYR-a/b+, 14/16 (87.5%) CABYR-c/d+, 0/16 (0%) CABYR-e+
Wang, et al. Oncol Rep. 2009[21]	NY-ESO-1, CTAG2, SSX1	HCC patients (n=64; China)	RT-PCR	19/64 (29.7%) NY-ESO-1+, 29/64 (45.3%) CTAG2+, 24/64 (37.5%) SSX1+
Riener, et al. Int J Cancer. 2009[22]	MAGEA4, MAGEC1, MAGEC2, GAGE, NY-ESO-1	HCC patients (n=146; Switzerland), CCA (n=50), GBC (n=32)	IHC	HCC: 0/146 (0%) MAGEA4+, 17/146 (12%) MAGEC1+, 50/146 (34%) MAGEC2+, 16/146 (11%) GAGE+, 3/146 (2%) NY-ESO-1+. No expression in CCA. GBC: 4/32 (13%) MAGEC2+, 1/32 (3%) GAGE+, 1 (3%) NY-ESO-1+, 0/32 MAGEC1/MAGEA4+
Lu, et al. Chin Med J. 2007[23]	NY-ESO-1, SSX1	HCC patients (n=36; China)	RT-PCR	4/36 (11.1%) NY-ESO-1+, 22/36 (61.1%) SSX1+
Wu, et al. Life Sci. 2006[24]	SSX2, SSX5	HCC patients (n=36; China)	RT-PCR	13/36 (36.1%) SSX2, 17/36 (47.2%) SSX5
Watanabe, et al. Cancer Sci. 2005[25]	IGSF11	HCC cell line (Alexander, Huh7, HepG2, SNU475)	RT-PCR	HCC cell lines: 3/4 IGSF11+
Yin, et al. Br J Cancer. 2005[26]	TSPY	HCC cell lines (hep-hcc-1, hep-hcc-2, hep-hcc-HLE, Hep3B, COS7) and HCC patients (n= 57;China)	RT-PCR	20/57 (35%) TSPY+
Shi, et al. Br J Cancer. 2005[27]	DDX53	HCC patients (n=33; China)	RT-PCR	13/33 (39.4%) DDX53+
Peng, et al. Cancer Lett. 2005[28]	MAGEA1, MAGEA3, MAGEA4, MAGEA10, SSX1, SSX2, SSX4,	HCC patients (n=73; China)	RT-PCR	51/73 (69.9%) MAGEA1+, 35/73 (47.9%) MAGEA3+, 6/30 (20%) MAGEA4+, 11/30 (36.7%)

164

	SSX5, NY-ESO-1, MAGEB1, MAGEB2, MAGEC1, MAGEC2, SYCP1			MAGEA10+, 29/43 (67.4%) SSX1+, 26/73 (35.6%) SSX2+, 21/43 (48.8%) SSX4+, 13/43 (30.2%) SSX5+, 31/73 (42.5%) NY-ESO-1+, 13/25 (52%) MAGEB1+, 15/25 (60%) MAGEB2+, 12/25 (48%) MAGEC1+, 17/25 (68%) MAGEC2+, 10/30 (33.3%) SYCP1+
Sato, et al. Int J Oncol. 2005[29] – no full text	NY-ESO-1, CTAG2	HCC patients – Japan	RT-PCR and IHC	IHC: 3/10 (30%) NY-ESO-1+ - all 10 samples expressed NY-ESO-1 mRNA 1/6 (16.7%) CTAG2+ - all 6 samples expressed CTAG2 mRNA
Yang, et al. Lab Invest. 2005[30]	FATE	HCC patients (n=35; China)	RT-PCR and IHC	RT-PCR: 10/15 (66%) FATE+ IHC: 7/35 (20%) FATE+
Dong, et al. Biochem Cell Biol. 2004[31] – no full text	FATE	HCC patients (China)	RT-PCR	25% of HCC samples FATE+
Dong, et al. Br J Cancer. 2004[32]	ZNF165	HCC patients (n=42; China)	RT-PCR	22/42 (52%) ZNF165+
Zhao, et al. World J Gastroenterol. 2004[33]	MAGEA1, MAGEC2, SSX1, SPANXC	HCC patients (n=105; China)	RT-PCR	79/105 (75.2%) MAGEA1+, 59/105 (56.2%) MAGEC2+, 76/105 (72.4%) SSX1+, 66/105 (62.9%) SPANXC+
Li, et al. Lab Invest. 2003[34] – no full text	MAGEC2	HCC patients (n=70; China)	IHC	26/70 (37.1%) MAGEC2+
Dong, et al. Br J Cancer. 2003[35]	FATE, TPTE	HCC patients (n=62; China)	RT-PCR	41/62 (66%) FATE1+, 24/62 (39%) TPTE+
Luo, et al. Cancer Immun. 2002[36]	MAGEA1, MAGEA3, MAGEA4, GAGE, NY-ESO-1, SSX1, SSX2, SSX4, SYCP1, LUZP4	HCC patients (n=21; China)	RT-PCR	4/21 (19%) MAGEA1+, 5/21 (24%) MAGEA3+, 1/21 (4.8%) MAGEA4+, 8/21 (38%) GAGE+, 0/21 (0%) NY-ESO-1+, 8/21 (38%) SSX1+, 2/21 (9.5%) SSX2+, 2/21 (9.5%) SSX4+, 6/21 (29%) SYCP1+, 4/21 (19%) LUZP4+
Wang, et al. J Immunol. 2002[37]	MAGEC2, TFDP3	HCC patients (n=20; China)	RT-PCR	14/20 (70%) MAGEC2+, 5/17 (29.4%) TFDP3+
de Wit, et al. Int J Cancer. 2002[38]	DSCR8	HCC cell lines (Hep3B, HepG2, PLC/RPF/5, Huh7)	RT-PCR	1/4 cell lines DSCR8+
Ono, et al. Proc Natl Acad Sci U S A. 2001[39]	ACRBP	HCC patients (n=5; Japan)	RT-PCR	2/5 (40%) ACRBP+
Chen, et al. Cancer Lett. 2001[40]	SSX1, SSX2, SSX4, SSX5, SYCP1, NY-ESO-1	HCC patients (n=30; Taiwan)	RT-PCR	24/30 (80%) SSX1+, 14/30 (46.7%) SSX2+, 22/30 (73.3%) SSX4+, 10/30 (33.3%) SSX5+, 2/30 (6.7%) SYCP1+, 11/30 (36.7%) NY-ESO-1+

Supplementary Table S4. Frequency table of healthy liver tissues (n=21) expressing mRNA of the CTAs.

	mRNA+ healthy liver (%)		mRNA+ healthy liver (%)
CAGE1	0.0	MAGEA10	0.0
CBLL2	42.9	MAGEB1	19.0
CCDC83	0.0	MAGEB2	0.0
CPXCR1	0.0	MAGEB3	28.6
CSAG2/3	85.7	MAGEB6	28.6
CT45	14.3	MAGEC1	4.8
CT47A1	0.0	MAGEC2	0.0
Cxorf48	0.0	NYESO1	0.0
DDX53	47.6	PAGE1	0.0
DPPA2	0.0	PAGE5	100.0
DUSP21	23.8	PASD1	0.0
FAM46D	0.0	PLAC1	0.0
FATE1	33.3	RNF17	4.8
FBXO39	100.0	SAGE1	0.0
FMR1NB	0.0	SLCO6A1	0.0
FTHL17	42.9	SPANXA	66.7
GAGE1	23.8	SPANXC	38.1
HORMAD1	100.0	SPANXN3	0.0
LUZP4	0.0	SYCP1	47.6
MAGEA1	0.0	TEKT5	100.0
MAGEA2	23.8	TFDP3	33.3
MAGEA3	14.3	TPPP2	100.0
MAGEA4	0.0	TSPY	0.0
MAGEA8	0.0	ZCCHC13	38.1
MAGEA9	0.0		

Colors correlate to the percentage of positive healthy liver tissues.

Supplementary Table S5. Expression of excluded CTAs in HCC patients and in cirrhotic liver tissues without malignancy.

	mRNA-positive HCC (%)[1]	mean in mRNA-+ HCC (range)[2]	Relative expression HCC (compared to testis)[3]	mRNA-positive TFL (%)[4]	mean in mRNA-+ TFL (range)[5]	Relative expression TFL (compared to testis)[6]	mRNA-positive cirrhotic tissue[7]
CCDC83	0.00			0.00			0
CPXCR1	2.02	0.001 (0.001-0.001)	0.00378	0.00			0
Cxorf48	8.25	0.157 (0.002-0.991)	1.839	2.04	0.012 (0.001-0.023)	0.139	2.9
DPPA2	1.03	0.135 (0.135-0.135)	1.204	0.00			0
FAM46D	5.15	0.003 (0.002-0.004)	0.058	0.00			2.9
FMR1NB	6.19	0.031 (0.002-0.124)	0.022	1.02	0.088 (0.088-0.088)	0.062	0
LUZP4	6.19	0.106 (0.001-0.49)	0.242	1.02	0.279 (0.279-0.279)	0.636	0
MAGEA4	6.19	0.803 (0.001-2.559)	28.036	0.00			0
MAGEA8	3.09	0.014 (0.004-0.022)	5.115	0.00			0
PASD1	2.02	0.017 (0.007-0.026)	0.007	2.00	0.02 (0.019-0.021)	0.009	0
PLAC1	4.12	0.014 (0.001-0.041)	0.146	0.00			0
RNF17	21.65	0.053 (0.001-0.507)	0.04570	13.27	0.023 (0.002-0.134)	0.01964	5.7
SAGE1	4.12	0.086 (0.008-0.15)	0.505	3.06	0.19 (0.006-0.543)	1.117	0
SPANXN3	1.01	0.004 (0.004-0.004)	52.644	3.00	0.002 (0.001-0.003)	27.174	0.0

[1]Percentage of hepatocellular carcinomas (HCC) expressing mRNA of the excluded CTAs – meaning a Ct-value <35 and relative expression > 0.001 (n=100); [2]Mean relative expression (relative to the geometric mean of the 3 household genes- GUSB, HPRT1, PMM1) level in <u>HCCs expressing the CTA</u> and range; [3]Mean relative expression of the CTA in HCC expressing the CTA, relative to the relative mean expression in 3 testis tissues; [4]Percentage of paired tumor-free liver tissues (TFL) expressing mRNA of the excluded CTAs (n=100); [5]Mean relative expression level in <u>TFLs expressing the CTA</u> and range; [6]Mean relative expression of the CTA in TFL expressing the CTA, relative to the relative mean expression in 3 testis tissues; [7]Percentage of non-cancerous cirrhotic liver tissues expressing the CTA (n=35)

Supplementary Table S6. Patient characteristics of HCC-patients included in protein expression analysis.

Characteristic	HCC patients (n=76)
Age at surgery (years)	
Mean ± SD	60.4 ± 14.4
Median (range)	64 (16-82)
Sex – no. (%)	
Male	47 (61.8)
Female	29 (38.2)
Race – no. (%)	
White	64 (84.2)
African	6 (7.9)
Asian	5 (6.6)
Not reported	1 (1.3)
Etiology – no. (%)	
No known liver disease	21 (27.6)
Alcohol	17 (22.4)
Hepatitis B	9 (11.8)
NASH	8 (10.5)
Hepatitis C + Alcohol	6 (7.9)
Hepatitis B + Alc/HepC/HepD/NASH	6 (7.9)
Hepatitis C	5 (6.6)
Fibrolamellar HCC	3 (4.0)
Hemochromatosis + NASH	1 (1.3)
Autoimmune hepatitis	-
Primary sclerosing cholangitis	-
Hepatitis status – no. (%)	
Hepatitis B or C positive	26 (34.2)
Chronic Hepatitis B	15 (19.7)
Chronic Hepatitis C	12 (15.8)
Cirrhosis – no. (%)	
Yes	23 (30.3)
No	53 (69.7)
Tumor differentiation – no. (%)	
Good	8 (10.5)
Moderate	41 (54.0)
Poor	14 (18.4)
Unknown	13 (17.1)
Vascular invasion – no. (%)	
Yes	40 (52.6)
No	29 (38.2)
Unknown	7 (9.2)
Number of lesions – no. (%)	
1	40 (52.6)
>1	36 (47.4)
Median (range)	1 (1-11)
Size of largest lesion (cm)	
Mean ± SD	7.4 ± 5.2
Median (range)	6.1 (1-24)
AFP level before resection (ug/l)	
Mean ± SD	64965 ± 401956
Median (range)	9.5 (2-3118700)

168

Supplementary Table S7. Cox regression analysis of HCC recurrence and HCC-specific survival based on CTA protein expression in TFL

Variable	Early recurrence				HCC-specific survival			
	Univariate analysis		Multivariate analysis		Univariate analysis		Multivariate analysis	
	HR (95% CI)	p-value	HR (95% CI)	p-value	HR (95% CI)	p-value	HR (95% CI)	p-value
≥1 CTA in TFL	1.9 (0.9-3.9)	0.092	2.5 (1.2-5.2)	0.02	2.6 (1.1-6.1)	0.03	3.8 (1.5-9.6)	0.004
Number of CTAs in TFL (numeric)	1.9 (0.98-3.7)	0.058			2.7 (1.2-6)	0.012		
>2 tumors	4.7 (2-11)	0.00029	3.7 (1.5-8.9)	0.004	2.6 (0.9-7.2)	0.066		
Chronic viral hepatitis	3.4 (1.6-7.1)	0.0011	2.8 (1.3-6.2)	0.01	3.1 (1.3-7.3)	0.01	4.4 (1.8-11.1)	0.001
Vascular invasion	1.6 (0.73-3.7)	0.23			1.3 (0.5-3.1)	0.57		
Tumor > 5 cm	1.1 (0.49-2.3)	0.89			1.7 (0.7-4.5)	0.26		
AFP > 400 ug/l	1.9 (0.84-4.3)	0.12			2.2 (0.9-5.6)	0.083		

Abbreviations: HR, hazard ratio; CI, confidence interval; CTA, cancer-testis antigen; TFL, tumor-free liver; AFP , alphafetoprotein

Supplementary Table S8. Cox regression analysis of HCC recurrence and HCC-specific survival based on CTA mRNA expression in HCC tumors

Variable	HCC recurrence		HCC survival	
	Univariate analysis		Univariate analysis	
	HR (95% CI)	p-value	HR (95% CI)	p-value
≥1 CTA in tumor	1.8 (0.86-3.6)	0.12	1 (0.41-2.6)	0.94
≥2 CTAs in tumor	1.1 (0.65-1.9)	0.67	0.86 (0.39-1.9)	0.7
≥3 CTAs in tumor	1.1 (0.62-1.8)	0.85	0.74 (0.34-1.6)	0.47
Number of CTAs in tumor (numeric)	1 (0.96-1.1)	0.29	1 (0.87-1.1)	1
>1 tumor	1.2 (0.68-2)	0.56	1.1 (0.49-2.4)	0.83
>2 tumors	2.6 (1.3-4.9)	**0.0042**	1.8 (0.69-4.9)	0.22
Cirrhosis	1.6 (0.89-2.8)	0.12	1.5 (0.66-3.4)	0.33
Chronic viral hepatitis	2.3 (1.3-4)	**0.0031**	3.3 (1.5-7.2)	**0.0032**
Vascular invasion	1.3 (0.72-2.3)	0.41	2.2 (0.96-4.9)	0.063
Tumor > 5 cm	1.3 (0.74-2.3)	0.37	2.3 (0.9-5.7)	0.081
AFP > 200 ug/l	1.9 (1-3.4)	**0.034**	2.7 (1.2-6)	**0.013**
AFP > 400 ug/l	2.4 (1.3-4.5)	**0.0051**	3.3 (1.5-7.3)	**0.0038**

Abbreviations: HR, hazard ratio; CI, confidence interval; CTA, cancer-testis antigen; AFP , alphafetoprotein

170

Supplementary Table S9. Antibodies used for immunohistochemistry.

Antibody	Host Species	Dilution	Company	Clone	Lot number	Procedure	Ab incubation at 37˚C
PAGE1	Rabbit	1:1000	Sigma-Aldrich	Polyclonal	R04065	Optiview CC1 32'	32 minutes
TSPY	Rabbit	1:200	Sigma-Aldrich	Polyclonal	R59337	Optiview CC1 32'	32 minutes
MAGEA9	Mouse	1:50	Prof. Y. Fradet, Québec, Canada[317]	14A11	N/A	Optiview CC1 32'	32 minutes
MAGEC2	Rabbit	1:500	Sigma-Aldrich	Polyclonal	A115364	Optiview CC1 32'	32 minutes
CT47A1	Rabbit	1:8000	Sigma-Aldrich	Polyclonal	R39285	Optiview CC1 32'	32 minutes
MAGEA1	Mouse	1:50	Santa Cruz	MA454	B0507	Optiview CC1 32'	32 minutes
MAGEB2	Rabbit	1:500	Sigma-Aldrich	Polyclonal	R109336	Optiview CC1 32'	32 minutes
SLCO6A1	Rabbit	1:200	Sigma-Aldrich	Polyclonal	R72094	Optiview CC1 32'	32 minutes
MAGEC1	Mouse	1:3200	Santa Cruz	CT7-33	A1807	Optiview CC1 32'	32 minutes

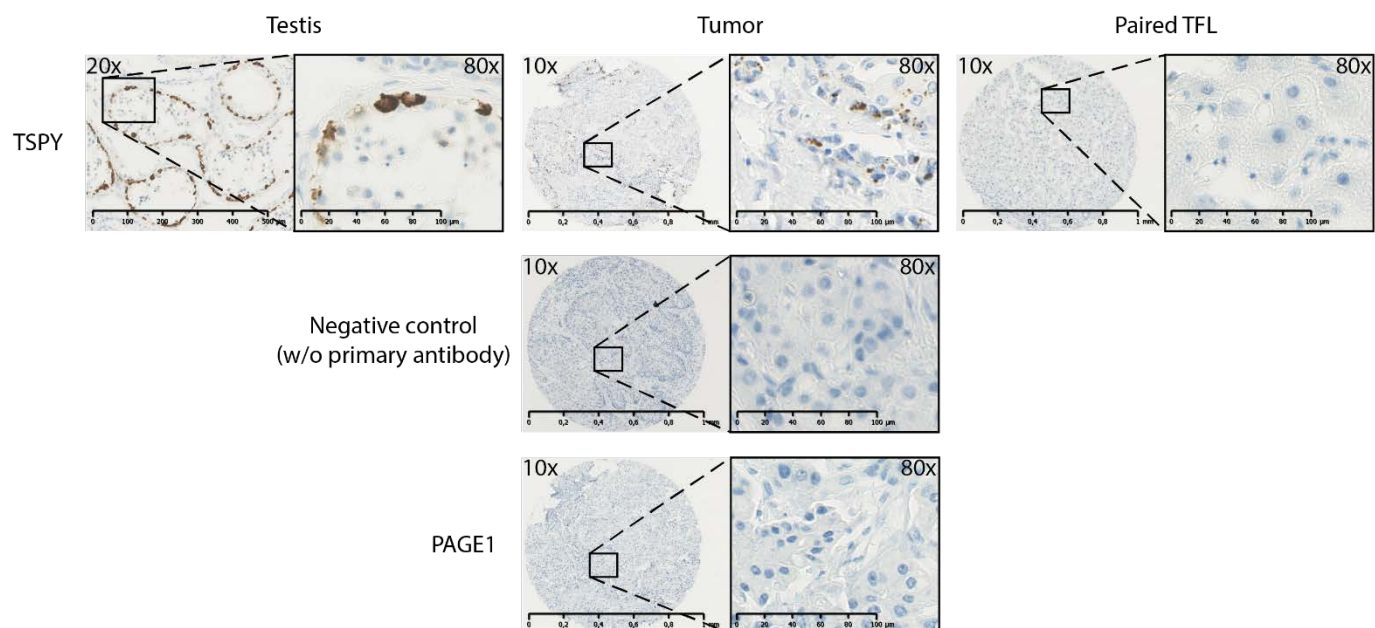**Supplementary Figure S1. Number of CTAs co-expressed in HCC tumors and TFL, based on mRNA expression.**
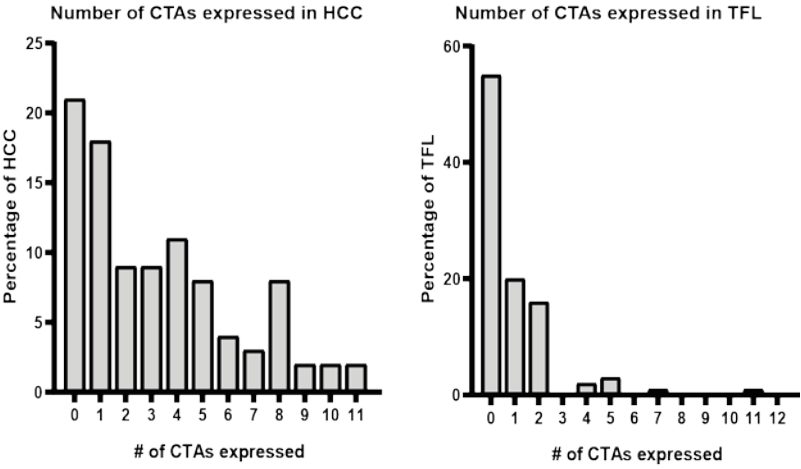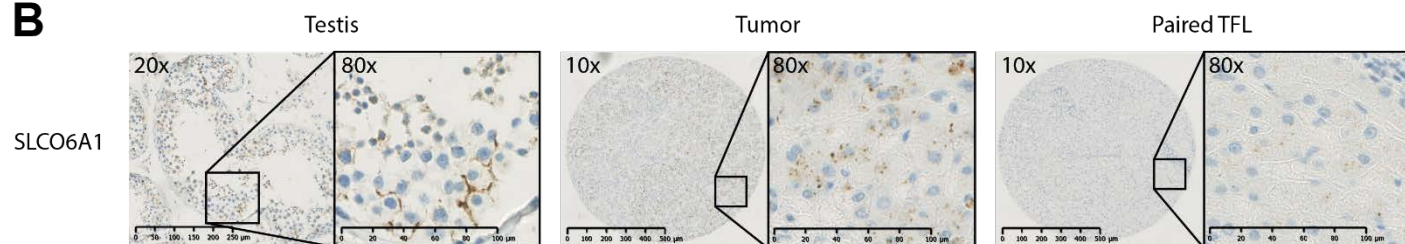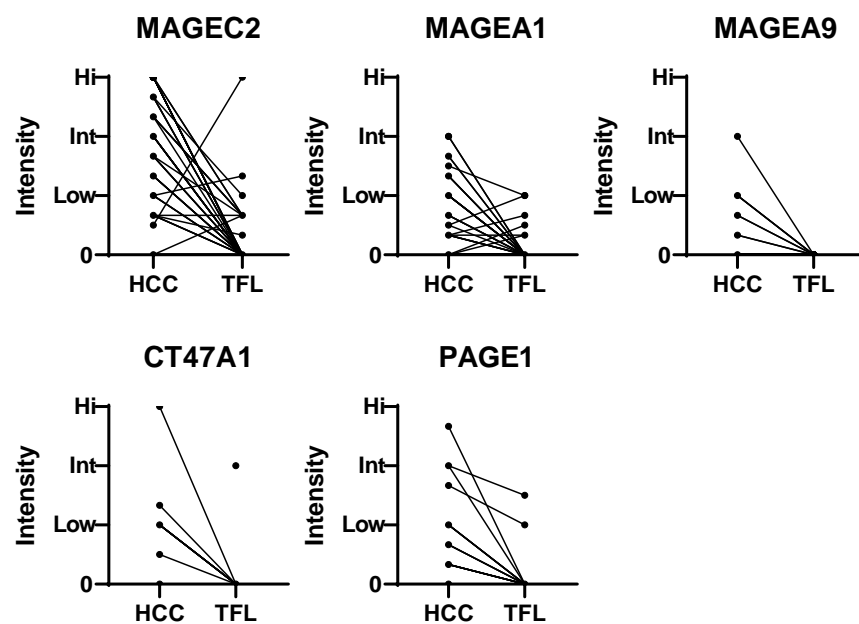
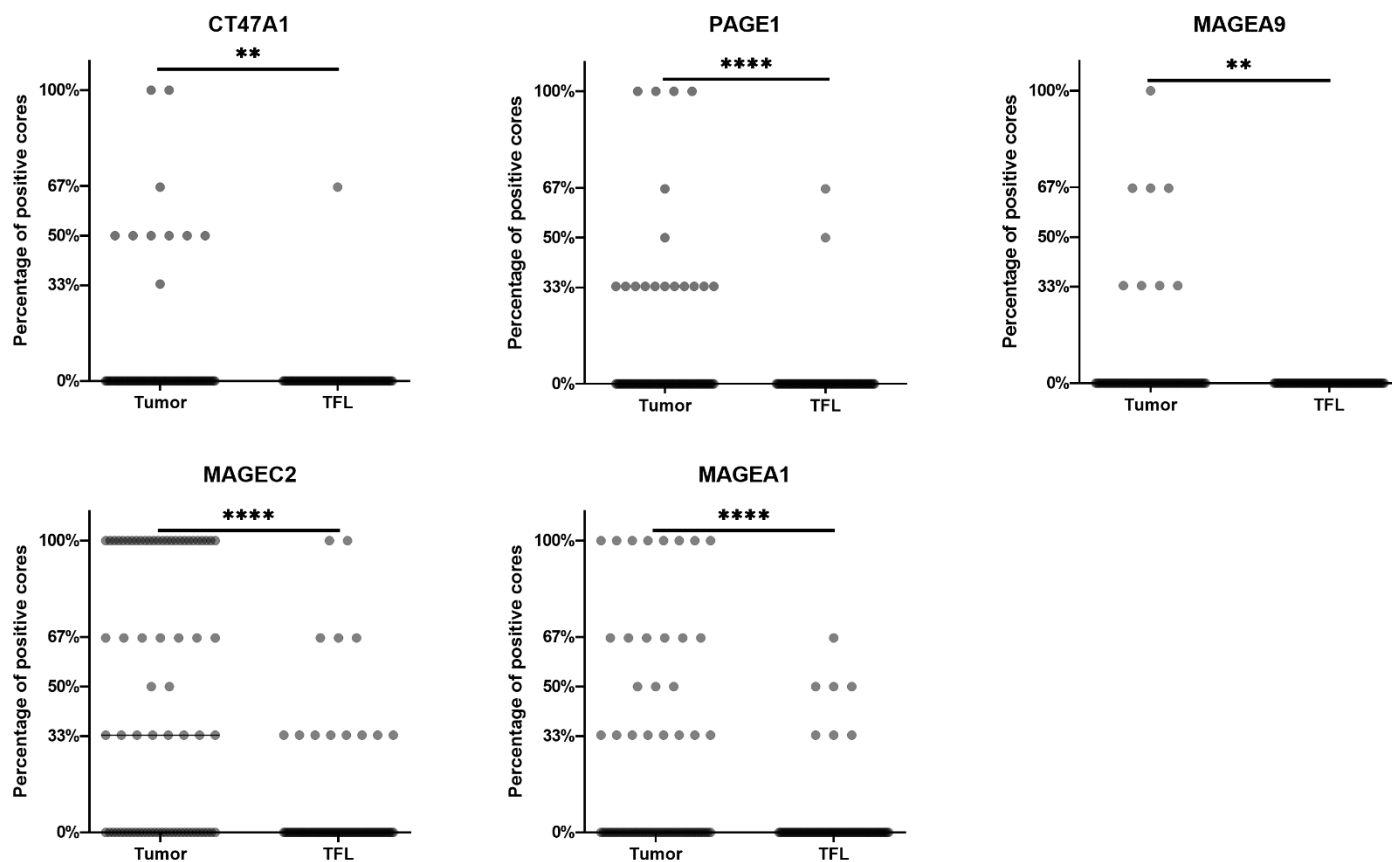**Supplementary Figure S2. TSPY expression in female HCC tumors and SLCO6A1 expression.**
A. TSPY protein expression was determined by IHC. TSPY is expressed in spermatogonia of normal testis, as expected.[41] However, TSPY protein expression was also found in two female HCC patients, of which one example is shown above. The staining is absent in the negative control and in the PAGE1 stained core. TSPY is encoded by the y-chromosome, expression in women is thus biologically impossible. **B.** Representative example of immunohistochemical stains of SLCO6A1 in testis, a positive HCC tumor tissue and the paired TFL tissue.
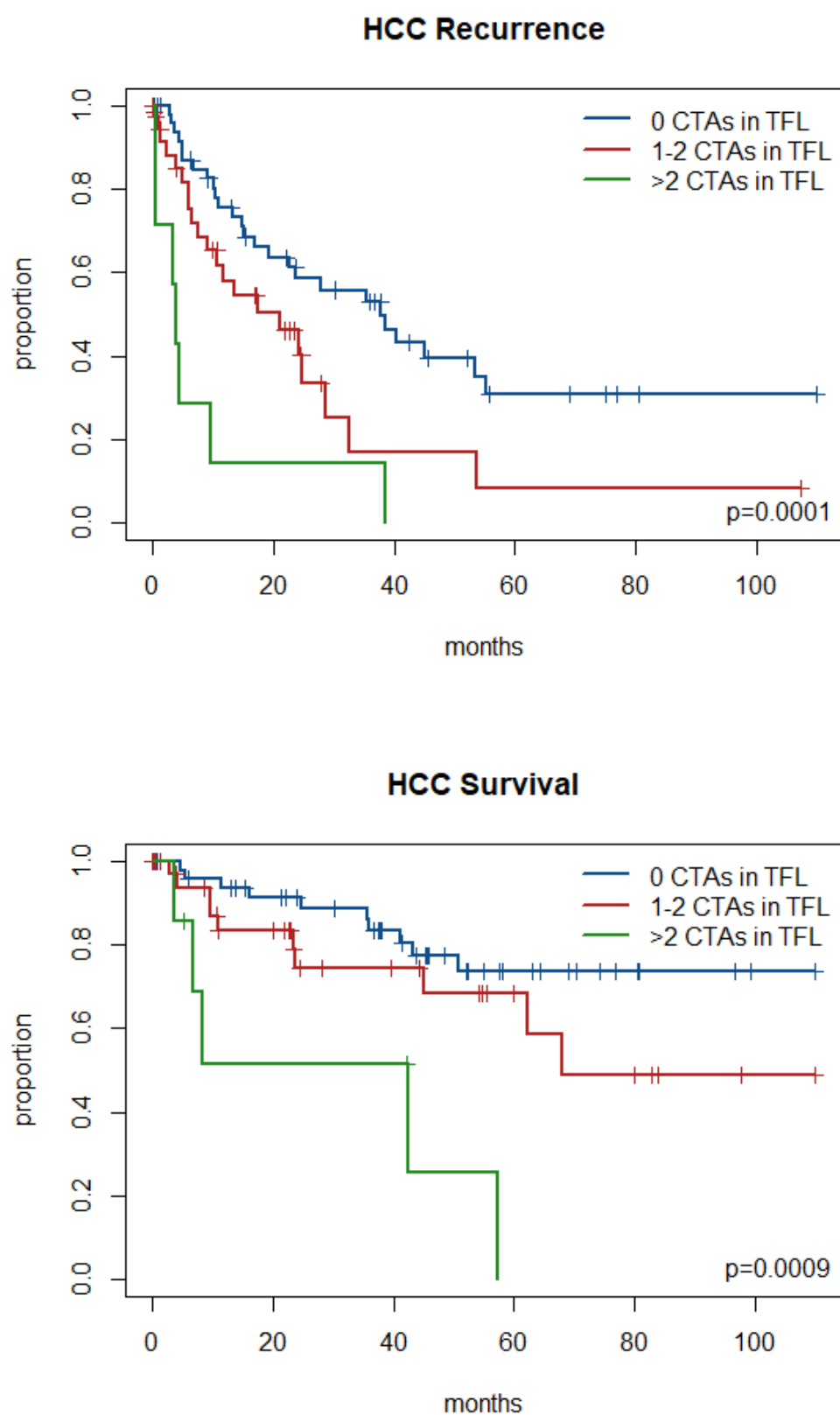
Supplementary Figure S3. Protein expression of CTAs in HCC tumors paired tumor free liver.
TMAs of tumor and TFL tissues were immunohistochemically stained to study the protein expression of aforementioned CTAs. The average intensity scores of three different tissue cores is depicted.
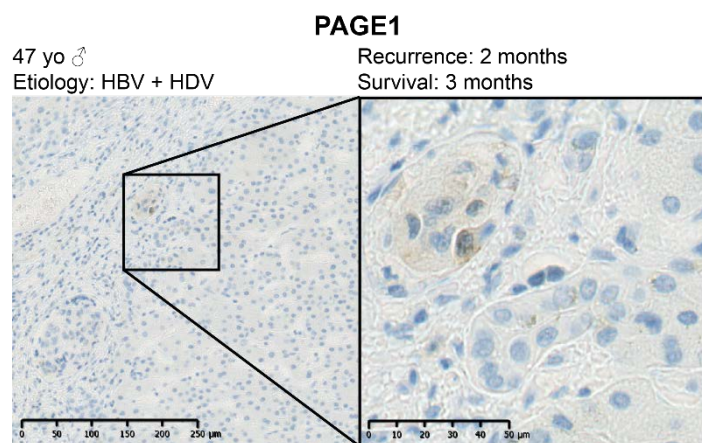
Supplementary Figure S4

Supplementary Figure S4. Proteins are focally expressed in most tumors. Protein expression was determined on TMAs, which had 3 cores of each tumor and TFL. The graphs display the percentage of cores containing protein-expressing cells (a score ≥1A). Most tumors and TFL express the proteins focally, illustrated by not all cores being positive. Wilcoxon signed-rank test. ** P<0.01, **** P<0.0001
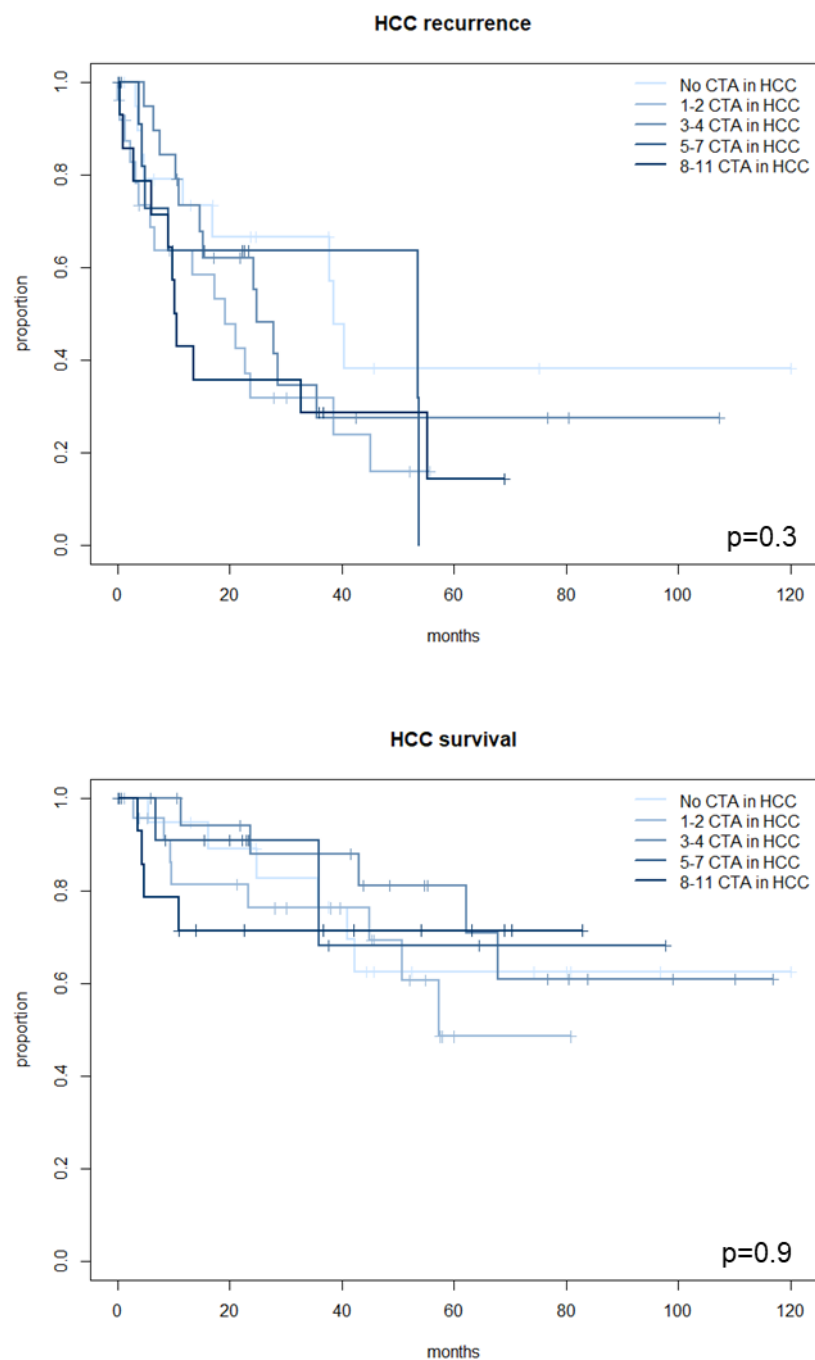
Supplementary Figure S5. HCC recurrence and HCC-specific survival by number of CTAs expressed in the discovery cohort (based on mRNA expression) in TFL. Log-rank test.

176

Supplementary Figure S6

PAGE1

47 yo ♂
Etiology: HBV + HDV

Recurrence: 2 months
Survival: 3 months

Supplementary Figure S6. PAGE1 expressing tumor nodule in TFL. Example of IHC staining of PAGE1 protein expression in an intravascular tumor nodule in TFL, and accompanying patient data.

Supplementary Figure S7.

Supplementary Figure S7. HCC recurrence and HCC-specific survival by CTA mRNA-expression in tumor tissue in the discovery cohort. Log-rank test.

178

References

1. Charoentong P, Finotello F, Angelova M, et al. Pan-cancer Immunogenomic Analyses Reveal Genotype-Immunophenotype Relationships and Predictors of Response to Checkpoint Blockade. Cell Rep 2017;18:248-262.
2. Sideras K, Biermann K, Verheij J, et al. PD-L1, Galectin-9 and CD8(+) tumor-infiltrating lymphocytes are associated with survival in hepatocellular carcinoma. Oncoimmunology 2017;6:e1273309.
3. Bergeron A, Picard V, LaRue H, et al. High frequency of MAGE-A4 and MAGE-A9 expression in high-risk bladder cancer. Int J Cancer 2009;125:1365-71.
4. Wei Y, Wang Y, Gong J, et al. High expression of MAGE-A9 contributes to stemness and malignancy of human hepatocellular carcinoma. Int J Oncol 2018;52:219-230.
5. Jiao Y, Ding L, Chu M, et al. Effects of cancer-testis antigen, TFDP3, on cell cycle regulation and its mechanism in L-02 and HepG2 cell lines in vitro. PLoS One 2017;12:e0182781.
6. Liu Q, Chen K, Liu Z, et al. BORIS up-regulates OCT4 via histone methylation to promote cancer stem cell-like properties in human liver cancer cells. Cancer Lett 2017;403:165-174.
7. Xie Y, Wang A, Lin J, et al. Mps1/TTK: a novel target and biomarker for cancer. J Drug Target 2017;25:112-118.
8. Kido T, Lau YC. Identification of a TSPY co-expression network associated with DNA hypomethylation and tumor gene expression in somatic cancers. J Genet Genomics 2016;43:577-585.
9. Fu J, Luo B, Guo WW, et al. Down-regulation of cancer/testis antigen OY-TES-1 attenuates malignant behaviors of hepatocellular carcinoma cells in vitro. Int J Clin Exp Pathol 2015;8:7786-97.
10. Wang M, Li J, Wang L, et al. Combined cancer testis antigens enhanced prediction accuracy for prognosis of patients with hepatocellular carcinoma. Int J Clin Exp Pathol 2015;8:3513-28.
11. Sideras K, Bots SJ, Biermann K, et al. Tumour antigen expression in hepatocellular carcinoma in a low-endemic western area. Br J Cancer 2015;112:1911-20.
12. Melis M, Diaz G, Kleiner DE, et al. Viral expression and molecular profiling in liver tissue versus microdissected hepatocytes in hepatitis B virus-associated hepatocellular carcinoma. J Transl Med 2014;12:230.
13. Li S, Mo C, Huang S, et al. Over-expressed Testis-specific Protein Y-encoded 1 as a novel biomarker for male hepatocellular carcinoma. PLoS One 2014;9:e89219.
14. Deng Q, Li KY, Chen H, et al. RNA interference against cancer/testis genes identifies dual specificity phosphatase 21 as a potential therapeutic target in human hepatocellular carcinoma. Hepatology 2014;59:518-30.
15. Xia QY, Liu S, Li FQ, et al. Sperm protein 17, MAGE-C1 and NY-ESO-1 in hepatocellular carcinoma: expression frequency and their correlation with clinical parameters. Int J Clin Exp Pathol 2013;6:1610-6.
16. Zhou JD, Shen F, Ji JS, et al. FAM9C plays an anti-apoptotic role through activation of the PI3K/Akt pathway in human hepatocellular carcinoma. Oncol Rep 2013;30:1275-84.
17. Chen K, Huang W, Huang B, et al. BORIS, brother of the regulator of imprinted sites, is aberrantly expressed in hepatocellular carcinoma. Genet Test Mol Biomarkers 2013;17:160-5.
18. Song MH, Choi KU, Shin DH, et al. Identification of the cancer/testis antigens AKAP3 and CTp11 by SEREX in hepatocellular carcinoma. Oncol Rep 2012;28:1792-8.
19. Li H, Fang L, Xiao X, et al. The expression and effects the CABYR-c transcript of CABYR gene in hepatocellular carcinoma. Bull Cancer 2012;99:E26-33.
20. Yoon H, Lee H, Kim HJ, et al. Tudor domain-containing protein 4 as a potential cancer/testis antigen in liver cancer. Tohoku J Exp Med 2011;224:41-6.
21. Wang XY, Chen HS, Luo S, et al. Comparisons for detecting NY-ESO-1 mRNA expression levels in hepatocellular carcinoma tissues. Oncol Rep 2009;21:713-9.
22. Riener MO, Wild PJ, Soll C, et al. Frequent expression of the novel cancer testis antigen MAGE-C2/CT-10 in hepatocellular carcinoma. Int J Cancer 2009;124:352-7.

23. Lu Y, Wu LQ, Lu ZH, et al. Expression of SSX-1 and NY-ESO-1 mRNA in tumor tissues and its corresponding peripheral blood expression in patients with hepatocellular carcinoma. Chin Med J (Engl) 2007;120:1042-6.
24. Wu LQ, Lu Y, Wang XF, et al. Expression of cancer-testis antigen (CTA) in tumor tissues and peripheral blood of Chinese patients with hepatocellular carcinoma. Life Sci 2006;79:744-8.
25. Watanabe T, Suda T, Tsunoda T, et al. Identification of immunoglobulin superfamily 11 (IGSF11) as a novel target for cancer immunotherapy of gastrointestinal and hepatocellular carcinomas. Cancer Sci 2005;96:498-506.
26. Yin YH, Li YY, Qiao H, et al. TSPY is a cancer testis antigen expressed in human hepatocellular carcinoma. Br J Cancer 2005;93:458-63.
27. Shi YY, Wang HC, Yin YH, et al. Identification and analysis of tumour-associated antigens in hepatocellular carcinoma. Br J Cancer 2005;92:929-34.
28. Peng JR, Chen HS, Mou DC, et al. Expression of cancer/testis (CT) antigens in Chinese hepatocellular carcinoma and its correlation with clinical parameters. Cancer Lett 2005;219:223-32.
29. Sato S, Noguchi Y, Wada H, et al. Quantitative real-time RT-PCR analysis of NY-ESO-1 and LAGE-1a mRNA expression in normal tissues and tumors, and correlation of the protein expression with the mRNA copy number. Int J Oncol 2005;26:57-63.
30. Yang XA, Dong XY, Qiao H, et al. Immunohistochemical analysis of the expression of FATE/BJ-HCC-2 antigen in normal and malignant tissues. Lab Invest 2005;85:205-13.
31. Dong XY, Li YY, Yang XA, et al. BJ-HCC-20, a potential novel cancer-testis antigen. Biochem Cell Biol 2004;82:577-82.
32. Dong XY, Yang XA, Wang YD, et al. Zinc-finger protein ZNF165 is a novel cancer-testis antigen capable of eliciting antibody response in hepatocellular carcinoma patients. Br J Cancer 2004;91:1566-70.
33. Zhao L, Mou DC, Leng XS, et al. Expression of cancer-testis antigens in hepatocellular carcinoma. World J Gastroenterol 2004;10:2034-8.
34. Li B, Qian XP, Pang XW, et al. HCA587 antigen expression in normal tissues and cancers: correlation with tumor differentiation in hepatocellular carcinoma. Lab Invest 2003;83:1185-92.
35. Dong XY, Su YR, Qian XP, et al. Identification of two novel CT antigens and their capacity to elicit antibody response in hepatocellular carcinoma patients. Br J Cancer 2003;89:291-7.
36. Luo G, Huang S, Xie X, et al. Expression of cancer-testis genes in human hepatocellular carcinomas. Cancer Immun 2002;2:11.
37. Wang Y, Han KJ, Pang XW, et al. Large scale identification of human hepatocellular carcinoma-associated antigens by autoantibodies. J Immunol 2002;169:1102-9.
38. de Wit NJ, Weidle UH, Ruiter DJ, et al. Expression profiling of MMA-1a and splice variant MMA-1b: new cancer/testis antigens identified in human melanoma. Int J Cancer 2002;98:547-53.
39. Ono T, Kurashige T, Harada N, et al. Identification of proacrosin binding protein sp32 precursor as a human cancer/testis antigen. Proc Natl Acad Sci U S A 2001;98:3282-7.
40. Chen CH, Chen GJ, Lee HS, et al. Expressions of cancer-testis antigens in human hepatocellular carcinomas. Cancer Lett 2001;164:189-95.
41. Schnieders F, Dork T, Arnemann J, et al. Testis-specific protein, Y-encoded (TSPY) expression in testicular tissues. Hum Mol Genet 1996;5:1801-7.

CHAPTER 7

General discussion and summary

Summary and discussion

Liver cancers are predicted to be the sixth most commonly diagnosed cancer and fourth leading cause of cancer death worldwide in 2018[1]. Hepatocellular carcinoma (HCC) comprises 75%-85% of all liver cancer cases[1]. More than 80% of HCC patients are diagnosed at advanced stage and their median survival is less than 2 years [2]. Tyrosine inhibitors (TKIs,), such as sorafenib[3] or lenvatinib[4], can only prolong overall survival time for 3 months and most patients will develop resistance to TKIs. Molecular profiling could contribute to the further understanding of tumor biology and the mechanism of primary resistance to treatments and facilitate better tailoring of therapeutic strategies. Although 20% of advanced HCC patients show response to immune checkpoint inhibitors targeting PD-1/PD-L1, around 80% of advanced HCC patients fail to respond to single checkpoint blockade. Currently, many studies are evaluating the combination of two immune checkpoint inhibitors in order to obtain an enhancement of efficacy through the modification of the tumor immune microenvironment.

Thus this thesis mainly focuses on two questions in hepatocellular carcinoma (HCC): 1) how to do better molecular diagnosis to facilitate targeted therapy; and 2) how to improve the efficacy of immune checkpoint blockade. Using tissue and blood from HCC patients, the research described in this thesis aimed to detect tumor mutations in two types of liquid biopsies: circulating tumor cells (CTCs) and circulating tumor DNA (ctDNA). In addition, the research aimed to demonstrate the potential added value of combined checkpoint blockade in HCC versus monotherapy with anti-PD1 antibodies, and to determine the expression of cancer testis antigens (CTAs), that may be potential therapeutic targets for improved immunotherapy in HCC.

1. Detection of oncogenic mutations in liquid biopsies in HCC

The classic biopsy is invasive and the limited tissue collected cannot represent the heterogeneity of the whole tumor. Compared with a classic biopsy, liquid biopsies are more convenient and present minimal procedural risk to the patient. Therefore, they can be performed on a serial basis. In theory, a̶ liquid biopsies may deliver more complete information regarding the patient's entire tumor burden. Moreover, analysis of therapeutic targets and drug resistance-conferring gene mutations from CTCs and ctDNA contributes to a better understanding and clinical management of drug

resistance in cancer patients. EpCAM$^+$ CTC count analysis using CellSearch has been approved by FDA for the monitoring of patients with metastatic breast, colorectal, or prostate cancer, with detection rate of 71% for metastatic breast cancer, 64% for colon cancer and 20% for prostate cancer [5]. ctDNA is found in both primary and metastatic cancer, with changing levels depending on the tumor burden. Some ctDNA assays have demonstrated clinical validity and utility with certain types of advanced cancer; however, there is insufficient evidence of clinical validity and utility for the majority of ctDNA assays [6]. With regards to early-stage cancer, there is no evidence of clinical utility and little evidence of clinical validity of ctDNA assays in treatment monitoring, or residual disease detection [6]. In HCC, current methods detect only a few CTCs in a single blood draw of 7.5 mL and CTCs can be detected using CellSearch in around 20% of advanced HCC patients, limiting their clinical utility. In contrast, ctDNA appears to be more readily detectable than CTCs.

Generally, capturing rare CTCs remains technically challenging and to authenticate whether cells are true CTCs is also challenging in cancer. Many studies have explored CTC detection methods, with some being based on cell size, cell density or cell markers or the combination of either two, such as filtration, centrifugation or fluorescent imaging. Most CTC isolation systems are not validated in clinic and only enrich a subgroup of cancer cells. The CanPatrol system which combines nanomembrane filtration technology and multiple RNA *in situ* analysis is reported to have a recovery of 80%, but it has only been tested by few research groups and not clinically validated [7, 8]. Marker-based systems such as CellSearch can only capture CTCs by single surface marker EpCAM which can easily be lost on CTCs during EMT transition, and most of HCC cells do not express EpCAM. **In chapter 2**, we sought to optimize a method to isolate as many CTCs as possible for mutational profiling. We analyzed several markers expressed in HCC and selected CK, ASGPR1, GPC3 and EpCAM for the detection of CTCs. We chose to combine RosetteSep negative selection for enrichment with multi-markers based fluorescence-activated cell sorting (FACS). However, despite including multiple markers, there is no clear CTC-events cluster detected in blood from 15 advanced HCC patients. Similarly, using FDA-approved CellSearch system, CTCs were found in only 27% of advanced HCC patients (**chapter 3**). Due to technical challenges, we failed to isolate sufficient DNA from few collected CTC events for downstream mutational analysis. These findings indicate that CTCs

184

are present in extremely low frequencies in HCC and can hardly be captured for further mutational analysis. We believe that, currently available methods can only detect very few CTCs in a single blood draw (<10ml), limiting their clinical utility.

Compared to CTCs, ctDNA appears to be more readily detectable. The main methods to detect ctDNA include droplet digital PCR (ddPCR) and next-generation sequencing (NGS). The use of assays that assess genomic variants in ctDNA is increasing in HCC. However, there is limited evidence of clinical validity of ctDNA analysis in HCC, and the clinical utility of these assays has not been established. **In Chapter 3**, we explored the feasibility of determining oncogenic mutations in paired ctDNA and CTCs in advanced HCC. Using a panel-based NGS and ddPCR techniques, mutations in ctDNA were identified in several genes, *TERT* promoter C228T, *TP53*, *CTNNB1*, *PIK3CA* and *NRAS*. Interestingly, the *TERT* C228T mutation was most prevalent (77% of HCC patients) and present in all patients with one or more ctDNA mutations, and in patients of which CTCs could be detectable in blood. We failed to collect enough CTCs for mutational analysis. These findings demonstrate that ctDNA is better suitable for molecular profiling of HCC than CTCs, and therefore ctDNA may potentially aid in treatment decisions.

CtDNA is reported to be strongly associated with tumors and patient outcomes. We found that the maximal variant allele frequency (VAF) of ctDNA was linearly correlated with tumor size and AFP level (log10). CtDNA positivity was associated with macrovascular invasion and correlated with poor patient survival. These findings indicate that ctDNA might potentially be used as a prognostic marker. Analyzing ctDNA, novel mutations associated with resistance to conventional and targeted therapy have been identified [9, 10]. These newly identified mutations might offer new avenues of treatment for cancer patients with advanced disease. Furthermore, additional studies combining ctDNA analysis with biomedical imaging or serum markers will determine the benefits of ctDNA in cancer surveillance as an adjunct diagnostic test.

2. Co-blockade of immune checkpoints in HCC

The success of immune checkpoint blockade in patients with a wide variety of malignancies has changed the treatment paradigm in oncology. Although PD-1/PD-L1 checkpoint blockade can result in dramatic therapeutic responses, this therapy is only effective in a subset of patients, and many patients are only partial responders to

therapy. Patients who do not respond to initial therapy with PD-1/PD-L1 blockade are referred to as having "primary resistance" to therapy, which can be caused by inadequate T cell infiltration due to lack of tumor immunogenicity, T cell exclusion and tumor cell resistance to interferon etc [11]. Furthermore, there is a growing subset of patients who, despite showing a robust initial response to therapy, go on to develop progressive disease. This phenomenon is known as "acquired resistance" to PD-1/PD-L1 blockade therapy which can be caused by loss of T cell function, disruption of antigen presentation and evolution of interferon resistance etc[11, 12]. Both phenomena are highly complex, as the mechanisms for both types of resistance can be overlapping and/or multifactorial [13]. To combat the loss of T cell function, one strategy is to apply dual checkpoint blockade therapy. For example, CTLA-4 and PD-1 are not functionally redundant, acting at different locations and times in the generation of effector T cells[14].This may mean that combination therapies may act in a complementary or even synergistic fashion. Blockade of both PD-1 and CTLA-4 showed improved clinical efficacy in patients with, amongst others, melanoma [15] and advanced non-small-cell lung cancer [16] and hepatocellular carcinoma [17]. However, PD-1 plus CTLA-4 blockade is hampered by a high frequency of severe immune-related systemic adverse effects[18], therefore other less toxic combinations are urgently needed.

Multiple lines of evidence support that TIGIT plays a critical role in limiting adaptive and innate immunity against tumors [19-22]. **In Chapter 4**, we summarize current knowledge and identify gaps in our current understanding of the role of TIGIT in cancer immunity and, based on these insights, provide recommendations for its positioning in cancer immunotherapy. We highlighted that TIGIT blockade can synergize with PD-1 blockade to enhance anti-tumor effects of CD8+ T cells. Unlike CTLA-4, PD-1 and TIM3, TIGIT is also expressed on NK cells. Thus TIGIT blockade does not only reinvigorate anti-tumor T cell responses but it also enhances anti-tumor NK cell responses. In addition, targeting TIGIT evokes less immunopathology compared to targeting CTLA-4 [22-24]. Co-blockade of TIGIT/PD-L1 induces similar adverse events compared to PD-L1 blockade alone in non-small cell lung cancer (NSCLC) patients [25]. TIGIT-blockade causes less toxicity compared to CTLA-4 blockade, because TIGIT knockout mice do not develop autoimmunity [22, 24], while CTLA-4 knockout mice die within 2-3 weeks due to severe autoimmunity [26]. **In Chapter 5,** we investigated the *ex vivo* efficacy of co-blockade of TIGIT/PD-1 in HCC. We reported that TIGIT was enriched whereas its co-

stimulatory counterpart CD226 was downregulated on PD-1^{high}CD8$^+$ TILs. PD-1^{high}CD8$^+$ TILs co-expressed exhaustion markers TIM3 and LAG3, and demonstrated higher TOX expression. This subset showed decreased capacity to produce IFN-γ and TNF-α. Expression of TIGIT-ligand CD155 was upregulated on tumor cells compared to hepatocytes in TFL. Co-blockade of TIGIT/PD-1 preferentially improved proliferation and cytokine production of CD8$^+$ TILs from tumors enriched for PD-1^{int}CD8$^+$ TILs (low PD-1 expressers) but not CD8$^+$ TILs enriched with PD-1^{high}CD8$^+$ TILs (high PD-1 expressers). Importantly, *ex vivo* co-blockade of TIGIT/PD-1 improved proliferation, IFN-γ production and anti-tumor cytotoxicity of CD8$^+$ TILs compared to single PD-1 blockade. Since only 20% of HCC patients responds to anti-PD-1 therapy [27, 28], a majority of patients are PD-1 non-responders. Our results demonstrate that *ex vivo*, co-blockade of TIGIT/PD-1 can convert CD8$^+$ TILs that did not respond to monotherapy with anti-PD-1 into therapy responders. Therefore co-blockade of TIGIT/PD-1 could be a promising immune therapeutic strategy for advanced HCC patients, especially for those patients that do not respond to anti-PD-1/PD-L1 therapy. Currently, the phase 1/2 clinical trial of TIGIT/PD-L1 combined blockade for the treatment of liver cancer is ongoing (NCT04524871). The results of the initial clinical trial will learn us whether co-blockade of TIGIT and PD-1/PD-L1 could improve the response rate of HCC patients and whether it can overcome the acquired resistance of single PD-1/PD-L1 blockade.

3. The prognostic value of cancer testis antigens expressed in tumor-adjacent liver

Recurrence rates are high and currently no therapies are available to prevent recurrence for HCC patients. Patients experiencing early recurrence likely have occult multifocality at the time of resection, whereas late recurrences are more likely to represent de novo tumors [29-31]. It remains of great importance to identify occult metastasis at the time of resection to allow identification of patients at risk for recurrence, ideally by targetable tumor markers. CTAs lack expression in healthy adult tissues, and have the potential to induce antitumor immune responses. Moreover, as testis-restricted CTAs are not expressed in healthy, tumor-free, tissues, sensitive techniques detecting these CTAs can potentially be used to recognize occult metastasis in surrounding macro- and microscopically tumor-free tissue.

In Chapter 6, we established a panel of 12 CTAs that are expressed in tumors of almost 80% of HCC patients. Interestingly, these CTAs are expressed in adjacent macroscopically tumor-adjacent liver tissues of 45% of HCC-patients. The negative association between expression of these CTAs in tumor-adjacent liver tissues and HCC-recurrence and survival, combined with immunohistochemical data, suggests that CTA-expressing cells remain present in the liver after tumor resection. These findings indicate that to prevent tumor recurrence, HCC patients with CTA expression in tumor-adjacent liver could be selected for adjuvant therapy, either by therapeutic targeting of these CTAs, other (immuno-) therapeutic strategies, or a combination of both.

Conclusion and future perspectives

- CtDNA assays might play a future role in facilitating treatment decision of advanced HCC patients. It is highly likely that evidence will emerge to enable better assessment of the clinical validity and utility of ctDNA assays in HCC.

- TIGIT is an attractive therapeutic candidate given that it plays a role in many of the steps that generate cancer immunity. Leveraging TIGIT in combination with other modalities such as PD-1/PD-L1 blockade may achieve even more robust clinical outcomes in HCC. Understanding how TIGIT functions, on what cells, and in what step(s) of the cancer immunity cycle will allow us to best design anti-TIGIT immunotherapies and target them to the patients who are most likely to respond.

- CTAs expressed in tumor-adjacent liver tissues might indicate HCC-recurrence and overall survival in post-resection HCC patients. Whether targeting CTAs is clinically effective remains to be proven.

References

1. Bray F, Ferlay J, Soerjomataram I, Siegel RL, Torre LA, Jemal A. Global cancer statistics 2018: GLOBOCAN estimates of incidence and mortality worldwide for 36 cancers in 185 countries. CA Cancer J Clin 2018;68:394-424.
2. European Association For The Study Of The L. EASL clinical practice guidelines: management of hepatocellular carcinoma. Journal of hepatology 2018;69:182-236.
3. Llovet JM, Ricci S, Mazzaferro V, Hilgard P, Gane E, Blanc J-F, de Oliveira AC, Santoro A, Raoul J-L, Forner A, Schwartz M, Porta C, Zeuzem S, Bolondi L, Greten TF, Galle PR, Seitz J-F, Borbath I, Häussinger D, Giannaris T, Shan M, Moscovici M, Voliotis D, Bruix J. Sorafenib in Advanced Hepatocellular Carcinoma. New England Journal of Medicine 2008;359:378-390.
4. Kudo M, Finn RS, Qin S, Han K-H, Ikeda K, Piscaglia F, Baron A, Park J-W, Han G, Jassem J. Lenvatinib versus sorafenib in first-line treatment of patients with unresectable hepatocellular carcinoma: a randomised phase 3 non-inferiority trial. The Lancet 2018;391:1163-1173.
5. Laget S, Broncy L, Hormigos K, Dhingra DM, BenMohamed F, Capiod T, Osteras M, Farinelli L, Jackson S, Paterlini-Brechot P. Technical insights into highly sensitive isolation and molecular characterization of fixed and live circulating tumor cells for early detection of tumor invasion. PloS one 2017;12:e0169427.
6. Merker JD, Oxnard GR, Compton C, Diehn M, Hurley P, Lazar AJ, Lindeman N, Lockwood CM, Rai AJ, Schilsky RL, Tsimberidou AM, Vasalos P, Billman BL, Oliver TK, Bruinooge SS, Hayes DF, Turner NC. Circulating Tumor DNA Analysis in Patients With Cancer: American Society of Clinical Oncology and College of American Pathologists Joint Review. J Clin Oncol 2018;36:1631-1641.
7. Wu S, Liu S, Liu Z, Huang J, Pu X, Li J, Yang D, Deng H, Yang N, Xu J. Classification of Circulating Tumor Cells by Epithelial-Mesenchymal Transition Markers. PLOS ONE 2015;10:e0123976.
8. Li J, Liao Y, Ran Y, Wang G, Wu W, Qiu Y, Liu J, Wen N, Jing T, Wang H, Zhang S. Evaluation of sensitivity and specificity of CanPatrol™ technology for detection of circulating tumor cells in patients with non-small cell lung cancer. BMC Pulmonary Medicine 2020;20:274.
9. Siravegna G, Mussolin B, Buscarino M, Corti G, Cassingena A, Crisafulli G, Ponzetti A, Cremolini C, Amatu A, Lauricella C. Clonal evolution and resistance to EGFR blockade in the blood of colorectal cancer patients. Nature medicine 2015;21:795-801.
10. Chabon JJ, Simmons AD, Lovejoy AF, Esfahani MS, Newman AM, Haringsma HJ, Kurtz DM, Stehr H, Scherer F, Karlovich CA. Corrigendum: circulating tumour DNA profiling reveals heterogeneity of EGFR inhibitor resistance mechanisms in lung cancer patients. Nature communications 2016;7.
11. Sharma P, Hu-Lieskovan S, Wargo JA, Ribas A. Primary, adaptive, and acquired resistance to cancer immunotherapy. Cell 2017;168:707-723.
12. O'Donnell JS, Smyth MJ, Teng MWL. Acquired resistance to anti-PD1 therapy: checkmate to checkpoint blockade? Genome medicine 2016;8:1-3.
13. Nowicki TS, Hu-Lieskovan S, Ribas A. Mechanisms of Resistance to PD-1 and PD-L1 Blockade. Cancer journal (Sudbury, Mass) 2018;24:47-53.
14. Wei SC, Levine JH, Cogdill AP, Zhao Y, Anang N-AAS, Andrews MC, Sharma P, Wang J, Wargo JA, Pe'er D. Distinct cellular mechanisms underlie anti-CTLA-4 and anti-PD-1 checkpoint blockade. Cell 2017;170:1120-1133. e17.
15. Larkin J, Chiarion-Sileni V, Gonzalez R, Grob JJ, Cowey CL, Lao CD, Schadendorf D, Dummer R, Smylie M, Rutkowski P, Ferrucci PF, Hill A, Wagstaff J, Carlino MS, Haanen JB, Maio M, Marquez-Rodas I, McArthur GA, Ascierto PA, Long GV, Callahan MK, Postow MA, Grossmann K, Sznol M, Dreno B, Bastholt L, Yang A, Rollin LM, Horak C, Hodi FS, Wolchok JD. Combined Nivolumab and Ipilimumab or Monotherapy in Untreated Melanoma. New England Journal of Medicine 2015;373:23-34.
16. Hellmann MD, Paz-Ares L, Bernabe Caro R, Zurawski B, Kim S-W, Carcereny Costa E, Park K, Alexandru A, Lupinacci L, de la Mora Jimenez E. Nivolumab plus ipilimumab in advanced non–small-cell lung cancer. New England Journal of Medicine 2019;381:2020-2031.
17. Yau T, Kang Y-K, Kim T-Y, El-Khoueiry AB, Santoro A, Sangro B, Melero I, Kudo M, Hou M-M, Matilla A. Efficacy and safety of nivolumab plus ipilimumab in patients with advanced

hepatocellular carcinoma previously treated with sorafenib: The CheckMate 040 randomized clinical trial. JAMA oncology 2020;6:e204564-e204564.

18. De Velasco G, Je Y, Bossé D, Awad MM, Ott PA, Moreira RB, Schutz F, Bellmunt J, Sonpavde GP, Hodi FS. Comprehensive meta-analysis of key immune-related adverse events from CTLA-4 and PD-1/PD-L1 inhibitors in cancer patients. Cancer immunology research 2017;5:312-318.

19. Boles KS, Vermi W, Facchetti F, Fuchs A, Wilson TJ, Diacovo TG, Cella M, Colonna M. A novel molecular interaction for the adhesion of follicular CD4 T cells to follicular DC. European journal of immunology 2009;39:695-703.

20. Stanietsky N, Simic H, Arapovic J, Toporik A, Levy O, Novik A, Levine Z, Beiman M, Dassa L, Achdout H, Stern-Ginossar N, Tsukerman P, Jonjic S, Mandelboim O. The interaction of TIGIT with PVR and PVRL2 inhibits human NK cell cytotoxicity. Proc Natl Acad Sci U S A 2009;106:17858-63.

21. Yu X, Harden K, Gonzalez LC, Francesco M, Chiang E, Irving B, Tom I, Ivelja S, Refino CJ, Clark H, Eaton D, Grogan JL. The surface protein TIGIT suppresses T cell activation by promoting the generation of mature immunoregulatory dendritic cells. Nat Immunol 2009;10:48-57.

22. Levin SD, Taft DW, Brandt CS, Bucher C, Howard ED, Chadwick EM, Johnston J, Hammond A, Bontadelli K, Ardourel D, Hebb L, Wolf A, Bukowski TR, Rixon MW, Kuijper JL, Ostrander CD, West JW, Bilsborough J, Fox B, Gao Z, Xu W, Ramsdell F, Blazar BR, Lewis KE. Vstm3 is a member of the CD28 family and an important modulator of T-cell function. Eur J Immunol 2011;41:902-15.

23. Khattri R, Auger JA, Griffin MD, Sharpe AH, Bluestone JA. Lymphoproliferative disorder in CTLA-4 knockout mice is characterized by CD28-regulated activation of Th2 responses. J Immunol 1999;162:5784-91.

24. Joller N, Hafler JP, Brynedal B, Kassam N, Spoerl S, Levin SD, Sharpe AH, Kuchroo VK. Cutting edge: TIGIT has T cell-intrinsic inhibitory functions. J Immunol 2011;186:1338-42.

25. Rodriguez-Abreu D, Johnson ML, Hussein MA, Cobo M, Patel AJ, Secen NM, Lee KH, Massuti B, Hiret S, Yang JC-H. Primary analysis of a randomized, double-blind, phase II study of the anti-TIGIT antibody tiragolumab (tira) plus atezolizumab (atezo) versus placebo plus atezo as first-line (1L) treatment in patients with PD-L1-selected NSCLC (CITYSCAPE): American Society of Clinical Oncology, 2020.

26. Khattri R, Auger JA, Griffin MD, Sharpe AH, Bluestone JA. Lymphoproliferative disorder in CTLA-4 knockout mice is characterized by CD28-regulated activation of Th2 responses. The Journal of Immunology 1999;162:5784-5791.

27. El-Khoueiry AB, Sangro B, Yau T, Crocenzi TS, Kudo M, Hsu C, Kim T-Y, Choo S-P, Trojan J, Welling TH, Meyer T, Kang Y-K, Yeo W, Chopra A, Anderson J, dela Cruz C, Lang L, Neely J, Tang H, Dastani HB, Melero I. Nivolumab in patients with advanced hepatocellular carcinoma (CheckMate 040): an open-label, non-comparative, phase 1/2 dose escalation and expansion trial. The Lancet 2017;389:2492-2502.

28. Zhu AX, Finn RS, Edeline J, Cattan S, Ogasawara S, Palmer D, Verslype C, Zagonel V, Fartoux L, Vogel A, Sarker D, Verset G, Chan SL, Knox J, Daniele B, Webber AL, Ebbinghaus SW, Ma J, Siegel AB, Cheng AL, Kudo M, investigators K-. Pembrolizumab in patients with advanced hepatocellular carcinoma previously treated with sorafenib (KEYNOTE-224): a non-randomised, open-label phase 2 trial. Lancet Oncol 2018;19:940-952.

29. Ulahannan SV, Duffy AG, McNeel TS, Kish JK, Dickie LA, Rahma OE, McGlynn KA, Greten TF, Altekruse SF. Earlier presentation and application of curative treatments in hepatocellular carcinoma. Hepatology (Baltimore, Md) 2014;60:1637-1644.

30. Poon RT. Differentiating early and late recurrences after resection of HCC in cirrhotic patients: implications on surveillance, prevention, and treatment strategies. Ann Surg Oncol 2009;16:792-4.

31. Finkelstein SD, Marsh W, Demetris AJ, Swalsky PA, Sasatomi E, Bonham A, Subotin M, Dvorchik I. Microdissection-based allelotyping discriminates de novo tumor from intrahepatic spread in hepatocellular carcinoma. Hepatology 2003;37:871-9.

CHAPTER 8

Nederlandse samenvatting

Dutch summary

194

Introductie

Hepatocellulair carcinoom (HCC) is de derde meest voorkomende oorzaak van aan kanker gerelateerde sterfgevallen. Leverchirurgie (hepatectomie en levertransplantatie) zijn momenteel de enige keuzes om een radicale genezing te bewerkstelligen. Echter, in de jaren na de operatie ontwikkelt ongeveer 50% van de patiënten terugkerende ziekte. Aangezien hematogene verspreiding de belangrijkste route van HCC-recidief is, heeft detectie van circulerende tumorcellen (CTC) in het bloed van HCC-patiënten ongetwijfeld een belangrijke klinische betekenis bij het voorspellen van herhaling en het bewaken van de therapeutische efficiëntie bij HCC-patiënten. Hoewel er verschillende pogingen zijn gedaan om CTC's van HCC-patiënten te detecteren, is onvoldoende aangetoond of daarbij de slecht gedifferentieerde en agressieve kankercellen zijn opgespoord.

Circulerend tumor-DNA (ctDNA) is de fractie celvrij DNA in het bloed die is afgeleid van primaire of uitgezaaide tumorcellen. De fractie circulerende mutante DNA-fragmenten is erg klein, vergeleken met circulerende wild-type DNA-fragmenten, waardoor het moeilijk is om te detecteren en te analyseren. De ontwikkeling van next generation sequencing (NGS), met name deep sequencing, en droplet digital PCR (ddPCR) hebben de identificatie van genetische varianten in ctDNA vergemakkelijkt.

De focus van ons HCC-onderzoek ligt op het ontwerpen van effectieve immunotherapie voor HCC-patiënten. We streven ernaar om tumorcellen efficiënt en selectief te vernietigen door een tumorspecifieke immuunrespons te induceren of te versterken.

De detectie van CTC's en ctDNA in het bloed van HCC-patiënten zal ons in staat stellen om biomarkers en tumorantigenen te definiëren, en moleculaire karakterisering van metastaserende tumorcellen uit te voeren. Een dergelijke "vloeibare" biopsie, die met behulp van een eenvoudige bloedafname kan worden uitgevoerd, en zodoende herhaaldelijk kan plaatsvinden zonder veel ongemak bij de patiënt, stelt ons bovendien in staat om moleculaire doelwitten voor gepersonaliseerde (immunotherapeutische) interventies te ontdekken en het effect ervan longitudinaal te vervolgen.

In hoofdstukken 2 en 3 van dit proefschrift beschrijven we achtereenvolgens de methode van CTC-detectie en de potentiële waarde van vloeibare biopsieën als diagnostische techniek bij HCC-patiënten.

In de daaropvolgende hoofdstukken focussen we ons op verbeterde behandeling van patiënten met gevorderd HCC. Therapeutische immune checkpoint remmers (ICR's) zijn medicijnen die zijn gericht op het herstellen van het vermogen van het immuunsysteem om kwaadaardige tumoren te bestrijden. De middelen zijn effectief gebleken bij veel soorten kanker. Specifiek zijn anti-PD-1 / PD-L1-therapieën goedgekeurd voor de behandeling van meer dan tien kankerentiteiten, waaronder melanoom, niet-kleincellig longcarcinoom en gevorderd HCC.

Helaas vertoont slechts een subgroep van HCC-patiënten een duurzame klinische respons, wat suggereert dat bij deze patiënten mechanismen aanwezig zijn die de effecten van anti-PD-1 / PD-L1-antilichamen beperken. T-cel-immunoreceptor met Ig- en ITIM-domeinen (TIGIT) is een remmende receptor die tot expressie wordt gebracht op lymfocyten. Hoge expressie zou de afweer tegen tumorcellen kunnen remmen, en blokkade van TIGIT zou deze remming mogelijk kunnen voorkomen waardoor therapeutische anti-PD1-antilichamen (langduriger) effectief kunnen zijn. We bestuderen deze mogelijkheid in de hoofdstukken 4 en 5.

De lymfocyten die zodoende worden gestimuleerd om tumorcellen te doden, dienen deze tumorcellen wel te herkennen. In hoofdstuk 6 beschrijven we de expressie van Kanker-Testis-antigenen (KTA's) in HCC. Dergelijke eiwitten zijn een aangrijpingspunt voor de afweer en zouden eventueel kunnen worden gebruikt in vaccinatie-strategieën met als doel om verdere immuunactivatie te bereiken, bijvoorbeeld in combinatie met therapeutische ICR's.

1. Detectie van oncogene mutaties in vloeibare biopsieën bij HCC

In vergelijking met een klassieke weefsel biopsie zijn vloeibare biopsieën gemakkelijker uitvoerbaar en minder risicovol voor de patiënt daar gebruik wordt gemaakt van perifeer bloed. Eenvoudige bloedafname voor analyse van tumorkarakteristieken kan frequenter worden uitgevoerd dan reguliere tumorbiopten, die een klein maar zeker risico hebben op inwendige bloedingen.

Dergelijke vloeibare biopsieën stellen ons in staat om de tumor serieel te bestuderen, bijvoorbeeld om tumor omvang te vervolgen. Bovendien kan analyse van CTC's of ctDNA ons helpen om de juiste therapie te kiezen en het effect ervan te vervolgen. Genmutaties in de tumor waarvan we weten dat deze een aangrijpingspunt zijn voor oncolytische therapie, kunnen in CTC's en/of ctDNA worden gedetecteerd. Genmutatie-analyse met behulp van ctDNA heeft in casuïstiek geleid tot aanpassingen in de behandeling: een HCC-patiënt met een CDKN2A-inactiverende en een CTNNB1-activerende mutatie in ctDNA ontving palbociclib (CDK4 / 6-remmer) en celecoxib (COX-2 / Wnt-remmer) als behandeling en er was een afname van het des-gamma-carboxy-protrombine (DCP) -niveau na 2 maanden behandeling. Een andere patiënt met een PTEN-inactiverende en een MET-activerende mutatie ontving sirolimus (mechanistisch doelwit van rapamycine-remmer) en cabozantinib (MET-remmer) en vertoonde tekenen van klinische werkzaamheid.

Het isoleren van zeldzame CTC's is technisch uitdagend en het is ook een uitdaging om te verifiëren of cellen echte CTC's zijn. Er zijn verschillende CTC-detectiemethoden onderzocht, gebruikmakend van celgrootte, celdichtheid, markers op het celoppervlak, of de combinatie van alle. De meeste CTC-isolatiesystemen zijn echter niet gevalideerd in de kliniek. Cellsearch dat CTC's uit het bloed isoleert op basis van Epithelial cell adhesion molecule (EPCAM) expressie op het oppervlak van cellen van verschillende kankertypen is als enige test gevalideerd voor gebruik in de kliniek. In **Hoofdstuk 2** hebben we geprobeerd een methode te optimaliseren om zoveel mogelijk CTC's te isoleren uit het bloed van HCC patiënten voor genmutatie-profilering. We gebruikten immunohistochemie om de expressie van verschillende eiwitten op het tumorceloppervlak te detecteren en selecteerden vervolgens CK, ASGPR1, GPC3 en EpCAM voor de detectie van CTC's. We kozen ervoor om de RosetteSep negatieve selectiemethode, voor verrijking van CTC's in bloedcellen, te combineren met op fluorescentie gebaseerde flowcytometrie-sortering. Ondanks het feit dat we meerdere oppervlaktemarkers gebruikte voor CTC-detectie werd er geen duidelijk cluster van CTC's geïdentificeerd in bloed van 15 gevorderde HCC-patiënten. Met het CellSearch-systeem werd bij slechts 27% van de gevorderde HCC-patiënten CTC's in het bloed gedetecteerd (**Hoofdstuk 3**). Vanwege technische uitdagingen slaagden we er niet in om voldoende DNA te isoleren uit enkele verzamelde CTC's voor mutatieanalyse. Deze teleurstellende bevindingen geven aan dat CTC's in extreem lage frequenties

aanwezig zijn in HCC en nauwelijks kunnen worden gebruikt voor verdere mutatieanalyse waardoor hun klinische bruikbaarheid wordt beperkt.

In vergelijking met CTC's lijkt ctDNA gemakkelijker detecteerbaar te zijn. De belangrijkste methoden om ctDNA te detecteren zijn digitale droplet-PCR (ddPCR) en next-generation sequencing (NGS). In **Hoofdstuk 3** vergelijken we de detectie van oncogene mutaties in gepaard ctDNA en CTC's van patiënten met gevorderd HCC. Met behulp van NGS- en ddPCR-technieken werden mutaties in ctDNA geïdentificeerd in verschillende genen; TERT-promotor C228T, TP53, CTNNB1, PIK3CA en NRAS. Interessant is dat de TERT C228T-mutatie het meest voorkomt (77% van de HCC-patiënten) en aanwezig is bij alle patiënten met een of meer ctDNA-mutaties of detecteerbare CTC's. We hebben niet genoeg CTC's verzameld voor mutatieanalyse. Deze bevinding toont aan dat ctDNA beter detecteerbaar is in vergelijking met CTC's. Analyse van ctDNA kan derhalve beter informatie verschaffen over de aanwezigheid van genmutaties die met medicatie zijn te benaderen. We ontdekten bovendien dat de maximale variante allelfrequentie (VAF) van ctDNA lineair gecorreleerd was met tumorgrootte en alpha-foetoproteine (AFP)-niveau (log10) in het bloed. CtDNA-positiviteit was geassocieerd met macrovasculaire invasie in de tumor en gecorreleerd met een slechte overleving van de patiënt. Deze associatie van ctDNA met klinische en histologische parameters suggereert dat analyse van ctDNA mogelijk als prognostische marker kan worden gebruikt.

We concluderen dat CTC's zeer moeilijk zijn te detecteren in bloed van HCC-patiënten. Daarentegen lijkt ctDNA geschikt voor genmutatieanalyse en draagt zodoende bij aan besluitvorming over behandelopties. Bovendien is associatie van ctDNA met klinische en pathologische parameters relevant voor prognosticatie.

2. De rol voor TIGIT bij immunotherapie voor HCC

Het succes van de ICR's bij patiënten met een grote verscheidenheid aan maligniteiten heeft het behandelingsparadigma in de oncologie veranderd. Recent werd de handeling van HCC-patienten met antilichamen tegen de PD1 en PD1L goedgekeurd. Bij een groep van ongeveer 20% van deze patiënten is er gedeeltelijke en soms zelfs complete respons op behandeling. Echter, de grootste groep patiënten reageert nauwelijks op deze therapie. Er is derhalve behoefte aan verbeterde immunotherapie en het lijkt logisch om te zoeken naar behandelingen waarbij meerder ICR's

tegelijkertijd worden benaderd, in plaats van alleen PD1/PDL1. TIGIT is een remmende receptor die tot expressie wordt gebracht op lymfocyten en de werkzaamheid ervan bij kankerimmunotherapie wordt momenteel uitgebreid bestudeerd. Bij meerdere typen kanker wordt TIGIT tot expressie gebracht op tumor-infiltrerende cytotoxische T-cellen, helper-T-cellen, regulerende T-cellen en NK-cellen, en het ligand CD155 wordt opgereguleerd op tumorcellen, wat bijdraagt aan lokale onderdrukking van immunosurveillance. Preklinische studies tonen dat co-blokkade van TIGIT en PD-1 / PD-L1 leidt tot tumorafstoting, zelfs in anti-PD-1-resistente tumormodellen. Een unieke eigenschap van TIGIT-blokkade is dat het niet alleen antitumor-effector-T-celresponsen versterkt, maar ook die van NK-cellen en bovendien de afweerremmende activiteit van regulatoire T cellen onderdrukt. Er zijn menselijke monoklonale anti-TIGIT-antilichamen ontwikkeld en recente klinische onderzoeken hebben veelbelovende resultaten getoond van gecombineerde TIGIT- en PD-L1-co-blokkade bij de behandeling van verschillende typen kanker, maar nog niet voor HCC. In **hoofdstuk 4** vatten we de huidige kennis samen en identificeren we de hiaten in ons huidige begrip van de rol van TIGIT bij kankerimmuniteit, en geven we, op basis van deze inzichten, aanbevelingen voor de positionering ervan bij kankerimmunotherapie.

In **Hoofdstuk 5** onderzoeken we de ex vivo werkzaamheid van co-blokkade van TIGIT en PD-1 bij patiënten met HCC. Daarbij maakten we gebruik van afweercellen die werden geïsoleerd uit tumoren van HCC-patiënten die een operatie ondergingen. We tonen aan dat TIGIT verhoogd tot expressie komt terwijl de co-stimulerende tegenhanger CD226 juist verlaagd tot expressie komt op hoog PD-1-positieve (PD1HI) CD8-positieve tumor-infiltrerende lymfocyten (TIL's). Deze cellen brengen ook TIM3 en LAG3 tot expressie, en vertonen een hogere TOX-expressie. Deze subset vertoond een verminderde capaciteit om de cytokinen IFN-gamma en TNF-alfa te produceren. Expressie van TIGIT-ligand CD155 is verhoogd op tumorcellen in vergelijking met hepatocyten in tumor-vrij leverweefsel (TVL). Co-blokkade van TIGIT / PD-1 verbetert preferentieel de proliferatie en cytokineproductie van CD8-positieve TIL's van tumoren verrijkt voor zwak-PD-1-positieve CD8-positieve TIL's (lage PD-1-expressers) maar niet CD8 + TIL's verrijkt met hoog-PD-1-positieve CD8-positieve TIL's (hoge PD-1-expressers). Belangrijk is dat ex vivo co-blokkade van TIGIT / PD-1 de proliferatie, IFN-gamma-productie en antitumorcytotoxiciteit van CD8-positieve TIL's verbeterde in

vergelijking met een alleen blokkade van PD-1. Aangezien slechts 20% van de HCC-patiënten reageert op behandeling met anti-PD-1-therapie en onze resultaten aantonen dat ex vivo co-blokkade van TIGIT en PD-1 ook in staat is om de functie van CD8-positieve TIL's die niet reageren op anti-PD1 te verbeteren, zou co-blokkade van TIGIT en PD-1 een veelbelovende immuuntherapeutische strategie kunnen zijn voor gevorderde HCC-patiënten, vooral voor die patiënten die niet reageren op anti-PD-1 / PD-L1-therapie.

Onze resultaten zouden derhalve de opstap kunnen zijn naar het evalueren van combinatie behandeling met anti-PD1 met anti-TIGIT voor patiënten met HCC in een klinische studie.

3. De prognostische waarde van de expressie van kanker-testisantigenen in tumor-aangrenzend leverweefsel

Zelfs als mensen een in-opzet genezende behandeling voor HCC ondergaan, is de kans op recidiverende ziekte met 50% in 5jr groot. Patiënten die een vroeg recidief ervaren, hebben waarschijnlijk occulte multifocaliteit op het moment van resectie, terwijl late recidieven eerder de novo tumoren vertegenwoordigen. Het is derhalve van groot belang om occulte metastasen op het moment van resectie te detecteren om patiënten met een hoog risico op recidief vroegtijdig te identificeren. Kanker-testisantigenen (CTA's) zijn eiwitten die niet tot expressie komen in gezonde volgroeide weefsels (behalve mannelijke kiemcellen), maar die wel kunnen worden gemaakt door kankercellen. De ontdekking ervan in normaal leverweefsel rondom de levertumor zou kunnen duiden op resterend kankerweefsel. Technieken voor het detecteren van deze CTA's zouden derhalve mogelijk kunnen worden gebruikt om occulte metastasen in omringend macro- en microscopisch tumorvrij weefsel te herkennen.

In **Hoofdstuk 6** beschrijven we dat van in totaal 49 onderzochte CTA's er 12 tot expressie komen in bijna 80% van de tumoren van HCC-patiënten. Interessant is dat deze CTA's ook tot expressie worden gebracht in tumor-aangrenzende leverweefsels bij 45% van de HCC-patiënten. De associatie CTA-expressie in tumor-aangrenzende leverweefsels met het optreden van HCC-recidief en verkorte overleving, suggereert dat CTA-positieve cellen aanwezig blijven in de lever na tumorresectie. Deze cellen zouden dus achtergebleven kankercellen kunnen zijn waaruit vervolgens een nieuwe

tumor zich ontwikkelt. Om tumorherhaling te voorkomen, zouden HCC-patiënten met CTA-expressie in tumor-aangrenzende lever kunnen worden geselecteerd voor adjuvante therapie na operatie. Daarbij kan worden gedacht aan CTA-doelgerichte immunotherapie al dan niet in combinatie met therapeutische ICR's.

Conclusie

• Een zogenaamd vloeibaar biopt voor detectie en moleculaire analyse van ctDNA kan in de nabije toekomst een belangrijke rol spelen bij therapie keuze bij behandeling van HCC-patiënten. Dergelijk onderzoek maakt belastende en risicovolle weefselbiopten grotendeels onnodig en seriële analyse van tumorkarakteristieken haalbaar.

• Immunotherapie met anti-PD1 antilichamen heeft tot op heden beperkte effectiviteit bij HCC-patiënten. Met blokkade van TIGIT in combinatie met anti-PD1 verbetert de functie van afweercellen tegen leverkanker en derhalve vormt deze combinatiebehandeling een potentiële verbetering van de therapie voor HCC-patiënten die het verdient om in klinische vervolgstudies te worden uitgewerkt.

• CTA's die tot expressie worden gebracht in tumor-aangrenzende leverweefsels kunnen duiden op resterend HCC en mogelijk een vroegtijdig recidief aankondigen. CTA-detectie in het resectiepreparaat na chirurgie voor HCC heeft dus potentiele consequenties voor post-operatieve behandeling en follow-up, en dient derhalve te worden uitgewerkt in aanvullend onderzoek.

APPENDIX

Acknowledgements

Publications

PhD Portfolio

Curriculum Vitae

Acknowledgements

I would like to thank the China Scholarship Council for providing me with the opportunity to pursue a PhD in Erasmus MC. The PhD journey is like finding a way in misty forest and I would like to thank those who helped me during this journey.

Maikel, thank you for your contribution on all my PhD projects. You rescued my ctDNA project by recommending oncomine sequencing provided by EMC diagnostic department. I'm grateful for the weekly talk with you in my last year and I really appreciate your understanding and encouragement.

Dave, thank you for your continuous support and help on my PhD projects. You are always prompt to reply to my emails and prompt to offer your help. You told me that there are bad or good PhDs but I would rather agree that a PhD is more often defined by the projects that he/she gets and does. There are high and low risky projects. We wasted 18 months on high risky projects without any publishable data. Luckily we made a balance among my PhD projects and the adventure finally ends after nearly 5 years.

Jaap, thank you for rescuing my PhD journey by providing TIGIT project to me. It turns out that I really enjoy the research on immune checkpoints although I started from zero basis on cancer immunotherapy. I always learn a lot from your professional comments on immunology and enjoy the collaboration with you.

Jaco, thank you for your contribution on CTCs and ctDNA projects. Although it is a pity that we can't bring this paper to higher journal, at least we made the first publication out of this collaboration between our group in MDL and your group in medical oncology department.

Leonie, thank you for making my PhD life easier. You are always so efficient and ready to help me.

Patrick, you are first one that I worked with when I started my PhD. You guided me through the first year and you are always warm-hearted and ready to help. You are the kindest and nicest person that I have ever met. Wish you all the best.

Lisanne, we had overlap for the whole 4 years. It is always nice and happy to work with you on the same project. We shared the good or bad results and complained together about the toughness during the PhD. We finally made it. Good luck with your career in pathology. Best wishes to you and Anton.

Lucia, you are such a special friend in my life. You are so talkative and warm up the atmosphere whenever. You bring happiness to everywhere. I remember we did fun games together. You are the one that brings everyone together. I also admire your ability to do science. Wish you a great great success in your career.

Aafka, you are quiet and careful. Thank for the comfort and companion that you bring to me. I still remember you cosplayed a ghost bride during 2019 Halloween party and when we had photos together you were so serious as a ghost bride can't smile:).

Bastiaan, you are so smart and always ready to offer comments and suggestion on research. You are always warm-hearted to share info about conferences or symposiums. Nice to have you as colleague.

Valeska, thank you for the help during my revision. I still remember we screamed and hided together during laser tag game. Thank you for always bringing cookies and chocolates which make office time sweeter.

Erik, my dear student. It's so nice to meet you in my third year. You surprised me by taking notes of each my word and it was always nice to discuss with you. Best wishes to your future doctor career.

Shanta, thank you for your help with my experiments. You are so organized for experiments and know those small tricks for doing experiments.

Suk Yee, I'm so lucky to meet you in my life. You are the angel that always bring comfort, warmness and happiness to others. You are the friend that I can fully trust and rely on, whenever and whatever. Best wishes to you! 祝你早日答辩，并找到一份自己喜欢的工作。

Sharida, it's nice to know you. You always have insightful thoughts. I like to join your lunch time and we went to Scheveningen together. Success with your PhD in EMC.

Yingying, thank you for your great support for my PhD life and job hunting. I still remember you suggested a very nice photography shop in Rotterdam for taking our wedding photo. During my job hunting, you are so kind to provide the practical info and encouraged me and it's normal to find a job after 1 year of searching.

Manzhi, another woman with strong power. I admire that you managed both baby and PhD work with strong will. You are dedicated to science and always works hard. I wish I could be as strong as you. Thank you for your support and help during my PhD study.

Shan, you always stay cheerful and bright. Thank you for your help during my PhD. See you in Chengdu in the future.

Jiaye and Sunrui, we came in the same year but you finished PhD ahead of me! Jiaye thank you for your support during my PhD. Wish you great success for your MD career.

Ling, you are always so warmhearted and ready to help others. Thank you for teaching me organoid techniques. Thank you for the companion. Good luck with your PhD.

Shaojun, we both came from Renji hospital. Wish you all the best with your cute baby girl and your wife.

Meng, thank you for picking me up in Schiphol when I arrived in NL the first time. You are always nice and kind. Thank you for the help during my PhD.

Wanlu, you are such a dedicated and hard-willed woman that I've had ever met. You will for sure achieve greatest success in your career.

Zhongli, we met in the Dutch course. I like your personality so much. I like to talk to you and share our life with each other. Wish all the best for you!

Jinluan, we know each other for already 5 years. 谢谢 5 年的陪伴和支持. You are like water (上善若水) and can always get along well with all others. 喜欢你说的，君子之交淡若水。Wish you all the luck and all the best with Changyuan.

Haopeng, 师父, you are so smart and you know clearly what you want to do in the future and you plan your life step by step. 希望你今后在 UK 的学术生活一切顺利(必须的)！

Shuang, we all agree that PhD is so hard (我们都遇到很烂的课题且没有很好的支持) and yet we have to survive. We have to make it through and I give my sincere blessings for you. Good luck!

Guannan, such a sensitive and kind girl. You pursue beauty in life and you cherish all the beautiful moments. I wish you live happily with Mr. Sun in Hangzhou, the city you choose to live for a life time.

Jun Liu, such a hard-working and optimistic girl. Thank you for guiding me to the alumni meeting where I met my husband. Wish you success in your career in UK!

Ann, we had one-year of overlap but we had so many memories together. We traveled to many places in Netherlands and it's always relaxing to be with you. We made appointments that we will travel together for sure again.

Utt, we met each other during TIP journal club. You are always friendly and cheerful. Thanks for the companion during PhD and I enjoyed talking with you. Wish you go higher and higher in your career! Maybe we meet someday in Thailand.

Do, you have special talent for talking and you know the art of communication, and with that you can easily connect to everyone. I'm grateful that you offered me great help during my job hunting. Have a great time and wish you success in Janssen!

Ron, you are so into science and so smart. Thank you for the support on science.

Monique, you are so sincere and thank you very much for the support for my PhD life. Good luck with your thesis and success with your job.

Gulce, such a warm girl. Wish you good luck with your postdoc in USA.

Mai, you are the only one that I can chat freely when I was doing experiments in your lab. Thank you for the companion and help that you offered during the time that I worked in your lab.

Priscilla, thank you for your help for sorting cells. It's amazing and so pleasant to work with you. You are so efficient and always take care of sorting.

Gertine, you are so kind and you care about people. I remember each talk with you and the support you give during my job hunting.

Jan, you have a golden heart. I was deeply touched that you adopted Chinese girls and you are always helpful in the lab.

Shanshan, Pengfei, Xiaopei, Yining and Bingting, nice to have you around in my last year. Thank you for the happiness that you bring to me. Wish you best luck during your PhD.

Shihao, Elisa, Alessandra, Katerina, Celio, Adriaan, Karlijn, Tijs, Steijn, Chunyan, Wenhui, Lei Xu, Buyun, Qin Yang, Ling Yan, Xumin, Yijin, Xinying, Yang Li, Zhijiang, Ruyi, Yunlong and Peifa, nice to meet you in MDL. Thanks for the wonderful time. Wish you all the best.

Qiuke, Raoul and Yini, nice to meet you in my last year. All the best wishes to you.

我由衷地感谢我的硕士导师覃文新，在他的指导下，我打下了扎实的科研基础。我也要感谢在 NKI 访学的王存老师和金浩杰师兄，对我学业和生活上的关照。

最后，我要感谢我的父母、奶奶和公公婆婆对我读博的莫大支持。一入博士深似海，从此难得把家还。感谢你们对我精神上的鼓励，生活上的嘘寒问暖，你们是我最坚实的后盾。

非常幸运，在荷兰遇到我的老公 Ruijie。感谢 Ruijie 对我的信任和支持，照顾和鼓励。没有你，我不知道怎么熬过这个博士生涯。你是我阴云般的博士生活中最灿烂的色彩。所有的喜怒哀乐，我们一一分享。我期待和你谱写人生的下一篇章。

Publications

1. **<u>Zhouhong Ge</u>**, Jean C.A. Helmijr, Maurice P.H.M. Jansen et al. Detection of oncogenic mutations in paired circulating tumor DNA and circulating tumor cells in in patients with hepatocellular carcinoma. (*Transl Oncol. 2021 Mar.*)

2. **<u>Zhouhong Ge</u>**, Guoying Zhou, Lucia Campos Carrascosa et al. TIGIT and PD1 co-blockade restores *ex vivo* functions of human tumor-infiltrating CD8$^+$ T cells in hepatocellular carcinoma. (*Cell Mol Gastroenterol Hepatol. 2021 Mar 26.*)

3. **<u>Zhouhong Ge</u>,** Maikel P.Peppelenbosch, Dave Sprengers, Jaap Kwekkeboom. TIGIT, the next step towards successful combination immune checkpoint therapy in cancer. (*Submitted*)

4. Lisanne Noordam, **<u>Zhouhong Ge</u>**, Hadiye Özturk et al. Expression of cancer testis antigens in tumor-adjacent normal liver predicts post-resection recurrence of hepatocellular carcinoma. (*Cancers. Revision submitted*)

5. Yuanming Xu, Lucia Campos Carrascosa, Yik Andy Yeung, Matthew Ling-Hon Chu, Wenjing Yang, Ivana Djuretic, Danielle Pappas, **<u>Zhouhong Ge</u>** et al. Improving anti-tumor immunity by delivering an engineered anti-PD1-IL15 fusion protein to PD-1 expressing T cells. (*Cancer Immunol Res. Under revision*)

6. Jiaye Liu, Pengfei Li, Ling Wang, Meng Li, **<u>Zhouhong Ge</u>** et al. Cancer-associated fibroblasts provide a stromal niche for liver cancer organoids that confers trophic effects and therapy resistance. *Cell Mol Gastroenterol Hepatol.*2021;11(2):407-431.

7. **<u>Zhouhong Ge</u>**, Zhuoan Chen, Xinrong Yang et al. Long noncoding RNA SchLAH suppresses metastasis of hepatocellular carcinoma through interacting with fused in sarcoma. *Cancer Sci.* 2017 Apr; 108(4): 653-662.

8. Jin Song*, **<u>Zhouhong Ge</u>***, Xinrong Yang et al. Hepatic stellate cells activated by acidic tumor microenvironment promote the metastasis of hepatocellular carcinoma via osteopontin. *Cancer Lett.* 2015 Jan 28; 356(2 Pt B):713-20.

  * These authors contribute equally as first authors.

PhD Portfolio

Name of PhD student	Zhouhong Ge
Department	Gastroenterology and Hepatology
PhD Period	Oct 2016 - Oct 2020
Promotor	Prof. Dr. Maikel P. Peppelenbosch
Copromotors	Dr. Dave Sprengers, Dr. Ing. Jaco Kraan

PhD training

General courses

- 2019, Basic and translational oncology (ECTS, 1.8)

- 2019, Biomedical English writing course (ECTS, 2.0)

- 2018, The advanced course on applications in flow cytometry (ECTS, 0.5)

- 2018, The Erasmus MC Cancer Institute Research Day (ECTS, 0.3)

- 2017, Advanced immunology course (ECTS, 0.5)

- 2017, The survival analysis course (ECTS, 0.6)

- 2017, Research integrity (ECTS, 0.3)

Seminars and meetings

2016-2020, Weekly MDL seminar program in experimental Gastroenterology and Hepatology
(attending, 42 weeks/year, ECTS: 9.0); (presenting, 1 times/year, ECTS: 2.3)

2016-2020, Weekly research group education
(attending, 42 weeks/year, ECTS: 9.0); (presenting, 8 times/year, ECTS: 1.7)

2016-2020, Weekly Tumor Immunotherapy Platform (TIP) meetings
(attending, 40 weeks/year, ECTS: 5.7); (presenting, 2 times/year, ECTS: 4.6)

2016-2018, Weekly Gastrointestinal Oncology (GIO) meetings

(attending, 42 weeks/year, ECTS: 3.0); (presenting, 2 times/year, ECTS: 2.3)

Teaching activities

2019 Feb-Jun, supervising master student: Erik Gausvik (ECTS, 2.0)

National and International Conferences

2021, 18th Digital Europe's Cancer Immunotherapy (CIMT) Meeting

2021, Digital Liver Cancer Summit by EASL.

2020, The Digital International Liver Congress (ILC) by EASL.

2019, Annual Day of the Molecular Medicine Postgraduate school, Rotterdam, the Netherlands.

2019, 17th Europe's Cancer Immunotherapy (CIMT) Meeting, Mainz, Germany

2018, 11th international symposium on minimal residual cancer (ISMRC), Montpellier, France

2017, Symposium: Current and future perspectives in primary liver tumors, Rotterdam, the Netherlands

Academic Awards

2016, China Scholarship Council (CSC) Scholarship (File No: 201606230253)

2020, Young Investigator Travel Awards (EASL International live congress 2020)

Curriculum Vitae

Zhouhong Ge was born on March 7, 1991, in Suzhou, Jiangsu Province, China. She grew up and attended primary, middle and high school in her hometown.

In 2009, she started her Bachelor's study in Nanjing Normal University. She majored in Biology (National Science Talent Training Base). She obtained her Bachelor's Degree of Science in 2013. During her bachelor study, she developed her interest in tumor biology. Afterwards, she started her master study in Shanghai Cancer Institute, affiliated to Renji hospital, Shanghai Jiaotong University. Under the supervision of Prof. Wenxin Qin, she focused on the role of long noncoding RNA in the progression of hepatocellular carcinoma and published her first research article in *Cancer Science*. She obtained the Master's Degree of Science in 2016. After her graduation, she aimed to conduct her PhD in a translational oncological setting.

In 2016, with the support of China Scholarship Council, she got an opportunity to start her PhD research at the department of Gastroenterology and Hepatology, Erasmus Medical Center Rotterdam, the Netherlands. Under the supervision of Prof. Dr. Maikel P. Peppelenbosch, co-supervised by Dr. Dave Sprengers, Dr. Jaap Kwekkeboom and Dr. Jaco Kraan, she mainly focused her research on liquid biopsy and immunotherapy in hepatocellular carcinoma (HCC).